

**Analyzing and modelling solute and sediment transport
at different spatial and temporal scales**

A case study of the catchment of the Wahnbach River, Germany

Dissertation

zur

Erlangung des Doktorgrades (Dr. rer. nat.)

der

Mathematisch-Naturwissenschaftlichen Fakultät

der

Rheinischen Friedrich-Wilhelms-Universität Bonn

vorgelegt von

Heye Bogena

aus

Norden

Bonn, Oktober 2001

Angefertigt mit Genehmigung der Mathematisch-Naturwissenschaftlichen Fakultät der
Rheinischen Friedrich-Wilhelms-Universität Bonn

1. Referent: Prof. B. Dieckrüger
2. Referent: Prof. J. Thein

Tag der Promotion: 14.12.2001

ACKNOWLEDGEMENTS

This work is supported by the German Research Foundation (Deutsche Forschungsgemeinschaft – DFG) in the frame of special collaboration program 350 ‘Interaction of continental systems of matter and their modelling‘ of the University of Bonn.

Prof. B. Diekkrüger, Head of the Hydrology Division at the University of Bonn, has given me scientific support and encouragement to do this research. His invaluable advice and insightful comments as well as his helpful hand with the modifications of OPUS provided me on the research.

All members of the Hydrological Group in Bonn (especially Michael Herbst and Klaus Stephan) are gratefully thanked for their support and fruitful discussions.

Klaus Jantos from the Institute of Geology in Bonn is acknowledged for providing sediment and water quality data.

Jens Lützen, Stefanie Uhrich, Simone Giertz, Juliane Dame, Katharina Lupp, Marc Lamers, Annette Schäfermeier and Mrs. Elfriede Mainz are gratefully acknowledged. Without their assistance in fieldwork, labour work and PC-work this study would have been impossible.

The author also thanks the association of the Wahnbach reservoir (WTV) for providing weather, runoff and landuse data for the Wahnbach catchment.

Last but not least I want to thank Birte Glüsing and Mr. Turlough Haughian for helping me to transform my draft into a readable form.

TABLE OF CONTENTS

1	INTRODUCTION.....	I
1.1	Statement of problem.....	1
1.2	The aim of this study	4
1.2.1	The analyzing methodology	4
1.2.2	The model concept.....	5
1.3	Structural overview.....	7
2	RESEARCH CONTEXT.....	8
2.1	Solute and sediment transport – processes and models.....	8
2.1.1	Processes determining hillslope runoff.....	8
2.1.1.1	Mechanisms producing surface flow	9
2.1.1.2	Mechanisms producing subsurface flow	9
2.1.1.3	Combination of runoff mechanisms	11
2.1.2	Transport of solutes from hillslopes	12
2.1.3	Soil erosion and sediment transport.....	13
2.1.4	Modelling nitrogen and sediment transport.....	14
2.1.4.1	Nitrogen transport models	14
2.1.4.2	Sediment transport models	16
2.2	Distributed models.....	17
2.2.1	Application possibilities of distributed models	17
2.2.2	The use of GIS in distributed hydrologic modelling	18
2.3	Scale issues in hydrologic modelling	20
2.3.1	Scales in hydrology	20
2.3.2	Scaling in hydrology.....	22
3	METHODS AND DATA.....	23
3.1	The research area	23
3.1.1	Geomorphology and soils.....	24
3.1.2	Climate.....	25
3.1.3	Landuse.....	29
3.1.4	The sub-catchments	30
3.1.5	The database for the simulations with OPUS.....	30
3.1.5.1	Sub-catchment scale simulations.....	30
3.1.5.2	Catchment scale simulations	31
3.1.5.3	Long-term simulations.....	32
3.1.6	Reconstruction of the soil erosion history	32
3.2	The model system OPUS.....	34
3.2.1	Water movement.....	34
3.2.2	Infiltration and overland flow.....	35
3.2.3	Erosion.....	36
3.2.4	Evapotranspiration.....	37
3.2.5	Nitrogen cycle.....	37
3.2.6	Solute transport.....	38
3.2.7	Plant growth.....	38
3.3	The weather generation model WGEN.....	39
3.3.1	Occurrence of rainfall.....	39
3.3.2	Amount of rainfall	39
3.3.3	Temperature and radiation.....	40
3.4	The HEC-6 model.....	40
3.4.1	Hydraulic calculations	41

3.4.2	Sediment calculations	42
3.4.2.1	The concept of active and passive layer	42
3.4.2.2	Bed material gradation.....	43
3.4.2.3	Vertical bed movement.....	44
3.5	Methods for model validation.....	44
4	ANALYZING THE FLUXES OF MATTER	46
4.1	Processes at the event scale	46
4.1.1	The research area Berrensiefen.....	46
4.1.2	Runoff generation	49
4.1.2.1	Convective rainfall events	50
4.1.2.2	Extreme rainstorm events	55
4.1.2.3	Comparison with other sub-catchments	58
4.1.3	Solute transport.....	63
4.1.4	Sediment transport.....	66
4.1.4.1	Bed Load.....	66
4.1.4.2	Suspended Load.....	67
4.2	Processes at the seasonal scale	70
4.2.1	Runoff.....	70
4.2.2	Anion concentrations.....	72
4.2.2.1	Chloride	72
4.2.2.2	Phosphate.....	75
4.2.2.3	Nitrate	76
4.2.2.4	Sulphate	77
4.2.3	Cation concentrations	77
4.2.3.1	Potassium.....	77
4.2.3.2	Sodium.....	79
4.2.3.3	Magnesium	80
4.2.3.4	Calcium.....	81
4.2.4	Suspensoid concentrations.....	82
4.3	Processes at the long-term scale	84
4.4	Development of a perceptual model	85
4.4.1	Runoff.....	85
4.4.2	Solute and sediment transport.....	88
5	APPLICATION SCHEME OF THE MODEL SYSTEM.....	90
5.1	The sub-catchment scale.....	90
5.1.1	Parameterization of the OPUS model.....	91
5.1.1.1	Parameterization of topography.....	91
5.1.1.2	Parameterization of soil horizons	94
5.1.1.3	Crop and management data	97
5.1.1.4	Sediment and erosion data.....	99
5.1.2	Modifications of the OPUS model	100
5.1.3	Sensitivity analysis	103
5.1.4	Calibration of the OPUS model.....	106
5.2	The catchment scale.....	110
5.2.1	Regionalization of the OPUS model	110
5.2.1.1	Spatial discretization of the Wahnbach catchment.....	110
5.2.1.2	Parameterization of the hillslopes.....	111
5.2.1.3	Generation of hillslopes and channel profiles	112
5.2.2	Parameterization of the HEC-6 model.....	112
5.2.2.1	Morphological parameter	112

5.2.2.2	Hydrological parameter	113
5.2.2.3	Sedimentological parameter	113
5.2.3	The long-term scale	115
5.2.3.1	Generation of long-term climate data	115
5.2.3.2	Parameterization of the historical landuse development	115
5.2.3.3	The daily option of the OPUS model	118
6	MODELLING THE FLUXES OF MATTER	119
6.1	The sub-catchment scale	119
6.1.1	Transport of water	119
6.1.1.1	Simulation of overland flow	119
6.1.1.2	Influence of rainfall data quality on overland flow simulation	121
6.1.1.3	Simulation of daily runoff	124
6.1.1.4	Influence of rainfall data resolution on the runoff simulation	127
6.1.2	Simulation of nitrate discharge	129
6.1.3	Simulation of sediment transport	132
6.1.3.1	Berrensiefen	132
6.1.3.2	Hellenkeutelsiefen	134
6.1.3.3	Steinersiefen	134
6.2	The catchment scale	137
6.2.1	Simulation of daily runoff	137
6.2.2	Simulation of soil erosion	138
6.2.3	Simulation of the fluvial sediment transport	140
6.2.4	OPUS simulations with daily rainfall data	143
6.2.4.1	Simulation of monthly runoff	143
6.2.4.2	Simulation of monthly nitrate discharge	144
6.2.4.3	Simulation of monthly soil erosion	145
6.3	The long-term scale	146
7	UNCERTAINTIES IN THE MODELLING PROCESS	148
7.1	Input data	148
7.1.1	Soil data	148
7.1.2	Landuse data	148
7.1.3	Spatial discretization	149
7.2	Model assumptions	150
7.3	Measurements for model validation	151
8	DISCUSSION	152
8.1	The analyzing concept	152
8.1.1	Processes determining the fluxes of matter	152
8.1.2	Influence of landuse on the fluxes of matter	153
8.1.3	The perceptual model	153
8.2	The modelling concept	154
8.2.1	Sub-catchment scale	154
8.2.2	Catchment scale	155
9	CONCLUSIONS	157
10	APPENDIX	160
11	LITERATURE	175

LIST OF FIGURES

Fig. 1: Applications of different model types depending on the required spatial and temporal scale (according to Schaub and Rolli, 1998).	2
Fig. 2: Concept for analyzing the fluxes of matter in the catchment of the Wahnbach River.	5
Fig. 3: Scheme of the various time scales in OPUS and associated processes simulated by the model (redrawn from Ferreira and Smith, 1992).	6
Fig. 4: A schematic outline of the modelling process in Chapt. 4, 5 and 6.	7
Fig. 5: Four different conceptual models to explaining fast subsurface runoff generation, redrawn from Anderson and Brooks (1996).	10
Fig. 6: Artificial hillslope displaying a sequence of runoff generation mechanism induced by a heavy rainfall event, adapted from Anderson and Burt (1990a).	11
Fig. 7: Flowchart indicating relations between sediment mobilization (erosion), production, deposition and sediment yield of a typical catchment (redrawn from Reid & Dunne, 1996).	14
Fig. 8: Organizational structure for linking, combining and integrating GIS and models (adapted from Hartkamp et al., 1999).	19
Fig. 9: Temporal and spatial extent of hydrological processes and natural phenomena with special consideration of soil erosion processes (redrawn from Renschler, 2000, with complements).....	21
Fig. 10: The catchments of the Wahnbach River and Wendbach River and the investigated sub-catchments.	23
Fig. 11: Minimum, maximum and weighted average of the annual regional precipitation amounts calculated from 10 stations located within or in the neighbourhood of the Wahnbach catchment and the calculated deviation factor, equation (1).	27
Fig. 12: The average monthly regional precipitation amount (squares) and the monthly minimum and maximum precipitation amounts (bars).	28
Fig. 13: The monthly maximum rainfall intensity and the monthly average rainfall intensity.	28
Fig. 14: Interpolated sediment thickness in the deposition basin; elevation data are provided by the Geological Institute Bonn and the WTV.	33
Fig. 15: The catchment of Berrensiefen with the installed gauging station and precipitation station. ...	46
Fig. 16: Landuse distribution and soil type distribution (scale of 1:5,000 and 1:50,000) of the Berrensiefen catchment.	47
Fig. 17: Sampling location of soil probes for K_s -measurement.	48
Fig. 18: The frequency distribution of the measured saturated soil hydraulic conductivity of the A_h -horizon and B_v -horizon (20 samples).	49
Fig. 19: Sequence of the continuously measured quantities precipitation, runoff, nitrate and conductivity in the sub-catchment Berrensiefen from 21.06.2000 until 22.06.2000.	50
Fig. 20: Sequence of the continuously measured quantities precipitation, runoff, nitrate and conductivity in the sub-catchment Berrensiefen from 24.07.2000 until 30.07.2000.	52
Fig. 21: Separation of the direct runoff from the total discharge using the measured conductivity and nitrate concentration.	54
Fig. 22: Runoff, conductivity, rainfall amount and rainfall intensity measured in September 1998.	55
Fig. 23: Separation of the direct runoff from the discharge hydrograph using the measured conductivity.	57
Fig. 24: Block diagrams of the sub-catchments Stucksiefen (above, right), Schlöbchensiefen (above, left) and Steinersiefen (below) displaying the slope distribution calculated from a digital elevation model with 5 m resolution; the bold lines mark the basin boundaries.	59
Fig. 25: Block diagrams of the sub-catchments Berrensiefen (above) and Hellenkeutelsiefen (below) displaying the slope distribution calculated from a digital elevation model with 5 m resolution; the bold lines mark the basin boundaries.	60
Fig. 26: Regional runoff responses of the sub-catchments Berrensiefen (Sub1), Hellenkeutelsiefen (Sub2) and Steinersiefen (Sub3) from 13.9.98 until 22.9.98.	61
Fig. 27: The course of the sum of base cations and anions during September 1998 (a) and the cation and anion concentrations as a function of discharge: (b) chloride and sulphate, (c) nitrate, (d) Ca^{2+} and K^+ and (e) Na^+ and Mg^{2+}	64

Fig. 28: Suspended load concentration, bed load discharge and runoff of the Berrensiefen during September 1998.....	66
Fig. 29: The grain-size distribution of the suspended load before (07.09.98 and 14.09.98) and after the rainstorm (28.09.98).....	68
Fig. 30: The monthly precipitation amounts measured of the rain gauges PEA and Berrensiefen, representing the southern and northern part of the Wahnbach catchment, respectively, and the monthly runoff amounts of all investigated sub-catchments.....	70
Fig. 31: The mean monthly concentrations of the base anions of all sub-catchments and the mean monthly discharge averaged over all sub-catchments from August 1998 until December 2000: a) chloride b) phosphate, c) nitrate, and d) sulphate.....	73
Fig. 32: R ² values of Tab. 7 plotted against the distance of sub-catchments.....	74
Fig. 33: The mean monthly concentrations of the base cations of all sub-catchments and the mean monthly discharge averaged over all sub-catchments from August 1998 until December 2000: a) phosphate, b) nitrate, c) chloride and d) sulphate.....	78
Fig. 34: Correlation of monthly magnesium and calcium concentrations of all sub-catchments.....	81
Fig. 35: R ² of calcium concentration plotted against the distance of sub-catchments.....	82
Fig. 36: The mean monthly concentrations of suspensoids of all sub-catchments and the mean monthly discharge averaged over all sub-catchments from August 1998 until November 2000.....	82
Fig. 37: Rainfall deviation from long-term average (above) and sediment discharge of the Wahnbach River (below).....	84
Fig. 38: Runoff generation in the research area with special consideration of the interflow process; a) cross-section of V-shaped valley, b) cross-section of a trough valley including an alluvial filling.....	87
Fig. 39: Application scheme for the simulations with the model system OPUS, including discretization, parameterization, calibration and presentation of results.....	90
Fig. 40: Generalised discretization scheme for the division of catchments into single planes for OPUS applications: 1) catchment delineation, 2) delineation of stream network and hillslopes, 3) allocation of input data and 4) connecting the hillslopes with a channel model.....	91
Fig. 41: Discretization of the sub-catchment Hellenkeutelsiefen into several planes; trenches along the roads are considered to have the same effect as the natural channel in respect of gathering overland flow.....	92
Fig. 42: Representative profiles for the sub-catchment Hellenkeutelsiefen.....	93
Fig. 43: The curvatures of the selected profiles for the sub-catchment Hellenkeutelsiefen.....	94
Fig. 44: The experimental variograms of sand and clay contents of the topsoil and subsoil, as well as the fitted variogram models for each scatter plot.....	95
Fig. 45: Discretization of the Berrensiefen sub-catchment into eight planes and interpolated sand content of the topsoil using ordinary kriging.....	96
Fig. 46: Simulated dry matter and LAI of corn, winter wheat and pasture by the OPUS model.....	97
Fig. 47: The modified model system OPUS with four different flow components: overland flow (1), interflow (2), quick groundwater flow (3) and slow groundwater flow (4).....	101
Fig. 48: Illustration of the equation used for the linking of unsaturated and saturated flow regions (redrawn from Smith, 1992).....	102
Fig. 49: The calculated IA-values displaying the quality of the runoff simulation results of the automatic calibration procedure; K _s -values in mmh ⁻¹	107
Fig. 50: The calculated IA-values displaying the goodness of the nitrate concentration-simulation results of the automatic calibration procedure; K _s -values in mmh ⁻¹	108
Fig. 51: Average IA-values of the automatic calibration procedure; the best fitting is obtained with a K _s -value of 1.0 mmh ⁻¹ and a Ma-value of 0.97.....	109
Fig. 52: Discretization of the Wahnbach catchment into sub-catchments; the enlarged sub-basin explains the subdivision into three single hillslopes.....	111
Fig. 53: Segmentation of the Wendbach River for the HEC-6 simulation and the assembled inflows of the OPUS simulation.....	113
Fig. 54: Measured and generated radiation of the year 1999.....	115
Fig. 55: Development of landuse in the catchment of the Wahnbach River since 1950 (percentage of area of pasture and arable land from the whole catchment area) and the division of the whole period of time into three sub-periods (triangle and squares denote measured values, whereas the lines are denoting polynomial interpolations).....	116

Fig. 56: Landuse and climate data used for the long-term simulation with OPUS; note that the different data quality from completely generated data in the fifties to data of high reliability in the nineties.	117
Fig. 57: Linear separation of the direct runoff of the rainfall event on the 25 th July 2000.	120
Fig. 58: Simulated and separated overland flow of the rainfall event on the 25 th of July 2000; the simulated overland flow was taken from a continuous OPUS simulation (1998 – 2000).	120
Fig. 59: The totalized precipitation of the 3 rd of May 2001 event measured with the radar of the Meteorological Institute at the University of Bonn.	121
Fig. 60: The totalized precipitation of the 3 rd of May 2001 event; the values of the Thiessen polygons are extracted from the radar measurement.	122
Fig. 61: Comparison of overland flow simulations using radar and tipped bucket data of the 3 rd of May 2001 event.	123
Fig. 62: Observed rainfall and simulated mean soil water content in three different depths of the Steinersiefen sub-catchment.	124
Fig. 63: Measured (dotted line) and simulated (solid line) mean daily runoff of Hellenkeutelsiefen, Steinersiefen and Berrensiefen and the measured daily precipitation amounts; note that the measured runoff data are not complete due to technical problems.	126
Fig. 64: The differences of the daily runoff simulations of Berrensiefen using the breakpoint and the daily option of OPUS; the positive values indicate that the breakpoint option produces more runoff than the daily option.	128
Fig. 65: Weekly measurements of the nitrate concentration at the outlet of the sub-catchments (solid line) and simulated nitrate concentration (dotted line).	130
Fig. 66: Monthly sediment discharge (solid line, calculated from measured runoff and sediment concentration) and the simulated monthly soil erosion (dotted line).	133
Fig. 67: Landuse distribution within the sub-catchment Steinersiefen as used during the whole simulation period.	135
Fig. 68: Mean soil erosion rates of the years 1999 and 2000 from the distributed OPUS simulation of the sub-catchment Steinersiefen.	135
Fig. 69: Measured daily runoff amount at the outlet of the upper Wahnbach catchment (54 km ²) (dotted line) and the mean daily runoff amounts (solid line) using the breakpoint option.	137
Fig. 70: Continuous simulation of soil erosion in the year 1998 using the modified OPUS model.	138
Fig. 71: Continuous simulation of soil erosion in the year 1998 with the AnnAgNPS model.	139
Fig. 72: Comparison of the model results of OPUS and AnnAgNPS; the correlation of the simulated soil erosion for the 890 planes; note that about 850 planes show erosion values near zero.	140
Fig. 73: Simulated runoff with OPUS and measured discharge of the Wendbach River.	140
Fig. 74: Measured and simulated concentrations of suspensoids of the Wendbach River.	141
Fig. 75: Temporal sediment storages and releases during the HEC-6 simulation of each channel segment; positive values indicate sediment accumulation and negative values indicate channel scour. Note that some segments show no dynamic at all, because the channel bed is artificially consolidated.	141
Fig. 76: Total amount of temporal sediment storages and releases during the HEC-6 simulation.	142
Fig. 77: Simulated and measured monthly runoff of the Wahnbach catchment (54km ²).	143
Fig. 78: Monthly nitrate discharge at the outlet of the Wahnbach catchment (dotted line, calculated from measured runoff and nitrate concentration) and mean monthly nitrate discharge of the simulated hillslopes (solid line).	144
Fig. 79: Monthly sediment discharge at the outlet of the Wahnbach catchment (dotted line, calculated from measured runoff and turbidity) and mean monthly soil erosion on the simulated hillslopes (solid line).	145
Fig. 80: Simulated soil erosion in the catchment of the Wahnbach River of the past 50 years with three landuse distributions, measured sediment discharge at the catchment outlet and the mean sediment yield calculated from the reservoir deposits.	147
Fig. 81: The digital elevation model of the Wahnbach catchment obtained by laser scanning.	161
Fig. 82: The digital geology map digitized on the basis of the following analog maps (1:25,000) from the regional geologic department of North Rhine Westphalia (5110 Ruppichteroth, 5109 Lohmar, 5010 Engelskirchen).	162

Fig. 83: The digital soil map of the Wahnbach catchment provided by the regional geologic department of North Rhine Westphalia.	163
Fig. 84: The digital landuse map of the Wahnbach catchment, own digitization on the basis of landuse mappings carried out by the association of the Wahnbach reservoir (WTV).....	164
Fig. 85: The rainfall stations in the Wahnbach catchment and mean annual precipitation amounts; rainfall data from the association of the Wahnbach reservoir (WTV).....	165

LIST OF TABLES

Tab. 1: The precipitation stations used for the calculation of the mean annual regional precipitation. 25	
Tab. 2: Matrix of correlation indices (R^2) calculated from the monthly precipitation amounts of each precipitation station; the bold numbers mark the chosen correlations and n denotes the number of months, which were available for the calculation (may not correspond to the recording duration due to data failures)	26
Tab. 3: The percentages of the main landuse types of the years 1989 and 2000 in the catchment of the Wahnbach reservoir (69,3 km ²) and the landuse changes.	29
Tab. 4: Some important characteristics of the five investigated sub-catchments within the Wahnbach catchment (see below for abbreviations).	30
Tab. 5: List of measured quantities in respect to the scale characteristics extent, spacing and support.	31
Tab. 6: Matrix of correlation indices (R^2) calculated from the monthly runoff amounts.	71
Tab. 7: Matrix of correlation indices (R^2) calculated from the monthly chloride concentrations.	74
Tab. 8: The average percentages of sand, clay, soil organic matter and nitrate-content of each plane. 96	
Tab. 9: Recommended fertilization amounts of nitrogen for several landuse types	98
Tab. 10: Sensitivity indices of variables effecting the simulation of overland flow, nitrate washout and nitrate content in surface runoff simulated by OPUS due to 10 % input changes	104
Tab. 11: Sensitivity indices of variables effecting the simulation of overland flow and soil erosion of Steinersiefen by the OPUS model due to 10 % input changes.	105
Tab. 12: Characteristics of the segment units; missing D_{50} -value indicates that the riverbed is mainly consolidated in the corresponding segment.	114
Tab. 13: Average percentage of area of pastureland and arable land of each period.	116
Tab. 14: The runoff curve numbers and Ma-values used for the daily option of OPUS.	118
Tab. 15: Performance indices reflecting the quality of the runoff simulation of the sub-catchments. 125	
Tab. 16: Measured and simulated water discharges between September 1998 and December 2000. 127	
Tab. 17: Simulated water discharges and the performance indices of both simulation methods.	128
Tab. 18: Indices reflecting the quality of the nitrate concentration simulation at the sub-catchment scale.	129
Tab. 19: Measured and simulated nitrate discharges between September 1998 and December 2000. 131	
Tab. 20: Measured and simulated sediment discharges between September 1998 and December 2000.	132
Tab. 21: Measured and simulated nitrate discharges between September 1998 and December 2000. 144	
Tab. 22: The percentages of the main landuse types in the Wahnbach catchment (54km ²) of the year 1998 before and after discretization.	149
Tab. 23: The percentages of the main landuse types in the upper Wahnbach catchment (54 km ²) of the year 1998 before and after discretization; redrawn from Giertz (2000).	150
Tab. 24: Weekly measured chloride concentrations [mg/l].	166
Tab. 25: Weekly measured nitrate-concentrations [mg/l].	167
Tab. 26: Weekly measured sulphate concentrations [mg/l].	168
Tab. 27: Weekly measured phosphate concentrations [μ g/l].	169
Tab. 28: Weekly measured calcium concentrations [mg/l].	170
Tab. 29: Weekly measured potassium concentrations [mg/l].	171
Tab. 30: Weekly measured sodium concentrations [mg/l].	172
Tab. 31: Weekly measured magnesium concentrations [mg/l].	173
Tab. 32: Weekly measured suspensoid concentrations [mg/l].	174

1 Introduction

1.1 Statement of problem

Today, there is a growing demand to predict natural processes, in order to address the environmental problems of the 21st century (Refsgaard and Abbott, 1996). This is clearly expressed in the introductory paragraph of the *Dublin statement on water and sustainable development* (ICWE, 1992):

“Scarcity and misuse of fresh water pose a serious and growing threat to sustainable development and protection of the environment. Human health and welfare, food security, industrial development and the ecosystems in which they depend, are all at risk, unless water and land resources are managed more effectively in the present decade and beyond than they have been in the past”.

The increased water resources problems require improved water resources management tools on sound scientific principles (Refsgaard and Abbott, 1996). In order to obtain useful management tools, the entire land phase of the hydrological cycle, which involves the description of water quantity, quality and ecology, has to be implemented into a model scheme. However, the application of such tools presupposes a sound understanding of the involved processes in the fluxes of matter. Processes determining the transport of solute and sediments occur at very different temporal and spatial scales. For example, sediment transport processes range from detachment of soil particles on hillslopes at very short and small scales (Fohrer, 1995) up to the incisions of valleys (Schumm, 1999) and the accumulation of lake sediments (Johnes, 1999).

Generally, there exist two main types of models, which are used depending on the required spatial and temporal scale (Fig. 1):

- Micro-scaled models for local sites or small catchments (<10 km²) suitable for simulation of fluxes of matter in a quantitative way;
- Macro-scaled models for regional assessments e.g. in order to determine soil erosion rates in a qualitative way.

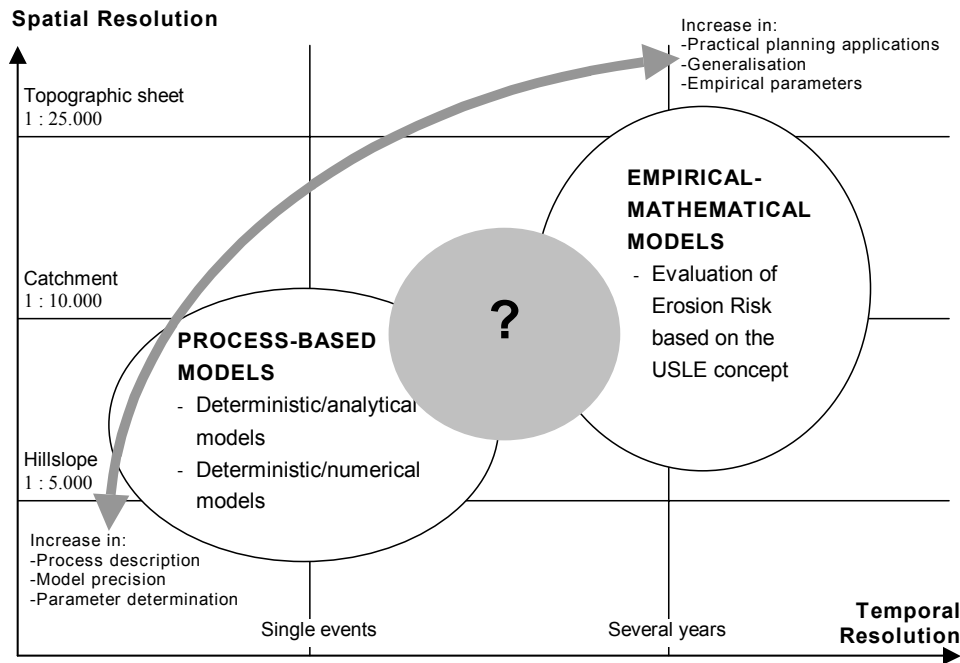


Fig. 1: Applications of different model types depending on the required spatial and temporal scale (according to Schaub and Rolli, 1998).

During the past decades numerous enthusiastic studies have been carried out with the aim of analyzing and modelling the natural systems in respect to the processes of runoff generation as well as the related transport of solutes and sediments. However, all these studies have different temporal and spatial scales from single events in micro-scaled sub-catchments (e.g. Bronstert and Plate, 1997; Merz and Bárdossy, 1998) or even plots (e.g. Smith, 1995; Bonilla, 1999; Esteves et al., 2000) up to macro-scaled catchments (e.g. Slutsky and Yen, 1997; Abdulla and Lettenmaier, 1997; Van de Witt, 2000) or even the whole globe (Panagoulia and Dimou, 1997; Kasper and Döll, 2000). The aim of these studies is mostly the same – to represent the natural system in a more or less sophisticated mathematical description in order to match the observed system outputs. The problem hereby is always to find the right model, which is appropriate for the particular scale and aim of the study.

There exists a distinct disagreement in the scientific community on which kind of model is more appropriate for the simulation of natural processes. It is widely recognized that the natural systems are extremely complex and the inherent processes are non-linearly connected and sometimes even characterized as being a chaotic system. To make things clearer these natural systems shall be named in the following as the ‘real world’ whereas the natural systems being described by any kind of model schemes shall be referred to as the ‘model world’.

On the one hand it is believed that ‘real world’ processes can only be simulated using simple and/or lumped models with a small amount of calibration parameters for adapting the model to the catchment of interest. This means that these models have only in part the possibility or even no opportunity at all for parameterisation with ‘real world’ data. Therefore measurements of the system output for an adequate period are a prerequisite for their application. However, lumped models have the disadvantage that the possibility of forecast simulations for ungauged sites is limited. In addition, in the case that not just the prediction of the runoff amount is demanded, simple models are then rapidly overtaxed. For example, the quantitative simulation of sediment transport involves a treatment of complex processes (e.g. soil detachment, surface runoff, sedimentation etc.). In the case that also a continuous simulation or even a long-term simulation is requested, the demands on the model are considerable. A further disadvantage is that no learning effect of the inherent processes of the catchment is achieved using simple models and the mechanism of runoff generation and transport of matter will remain a mystery, which cannot be the aim of a scientific study.

On the other hand, so-called ‘physically based’ models are used to offset the mentioned disadvantage of the simple models. The process description is derived from process studies at the micro-scale or even from the labour on mainly disturbed soil probes. Herewith the main assumption is often that the natural processes are relevant at all scales. Process studies are mainly undertaken under ‘ideal’ conditions and therefore under unnatural or only partly natural conditions, e.g. under water-saturated conditions. Therefore, one disadvantage is that processes of a larger scale may overlay small-scale processes in the ‘real world’ and the observed system output may be completely different although the inherent small-scale processes are well represented in the model.

Another problem is the need of many input parameters to run these models and the large heterogeneity of the ‘real world’ that has to be transferred into the ‘model world’. Especially concerning larger spatial as well as temporal scales, the problem of the availability of input data with the necessary quality is very difficult or often impossible to have with regard to financial or temporal constraints. Therefore, conceptual models with a small amount of parameters and an insignificant sensitivity to parameter uncertainty are generally used at these scales. Consequently, due to several advantages of conceptual models (e.g. simplicity, robustness, few parameters) they are still frequently used and regionalization schemes are developed in order to apply those models on ungauged sites (Schwarze, 1999).

1.2 The aim of this study

In this study the attempt is made to develop an analyzing and modelling concept, which is able to bridge the gap between several spatial and temporal scales. To reach this goal, measurement and process studies at different scales have been undertaken in the catchment of the Wahnbach River near Bonn, Germany. The acquired knowledge is then used to develop a model scheme, which is appropriate to satisfy the demands on the simulation of solute and sediment transport at different temporal and spatial scales using a ‘process-based’ model system as a kernel.

1.2.1 The analyzing methodology

This study is associated with the research project B14 ‘Balancing and modelling the flow of matter in the catchment of the Wahnbach River’ in the frame of the special collaboration program 350 ‘Interaction of continental systems of matter and their modelling’ of the University of Bonn. In collaboration with the Institute of Geology, Bonn, an analyzing methodology is developed for investigating the fluxes of matter within the catchment of the Wahnbach River. The concept takes several temporal and spatial scales into account (Fig. 2), covering small scaled measurements at the hillslope and sub-catchment scale as well as investigations of soil erosion deposits in the reservoir and in lakes, in order to determine the long-term sediment discharge at the catchment scale (54 km²).

In order to characterize the hydrological behaviour of catchment depending on factors like the geological situation or the landuse predominance, three sub-catchments were selected, which are distributed over the catchment area (Fig. 11, Chapt. 3.1). Their surface area ranges from 21 to 29 ha and the land use is predominated by forest (Hellenkeutelsiefen), pasture (Berrensiefen) and agriculture (Steinersiefen). Automatic gauging stations were installed for continuous measurements of quantities like rainfall, runoff, electric conductivity and temperature for a period of about three years. Furthermore anions and cations dissolved in stream and rainfall water were measured weekly and an intensive soil survey was carried out in the sub-catchment to provide the spatial variability of important soil hydraulic parameters. To capture the sediment discharge, sediment traps and suspended load samplers were installed in the channel beds. The measurements reveal a relationship between the different average concentrations of the material discharge (bed-load transport, suspended load and solution load) and the land use in the test catchments.

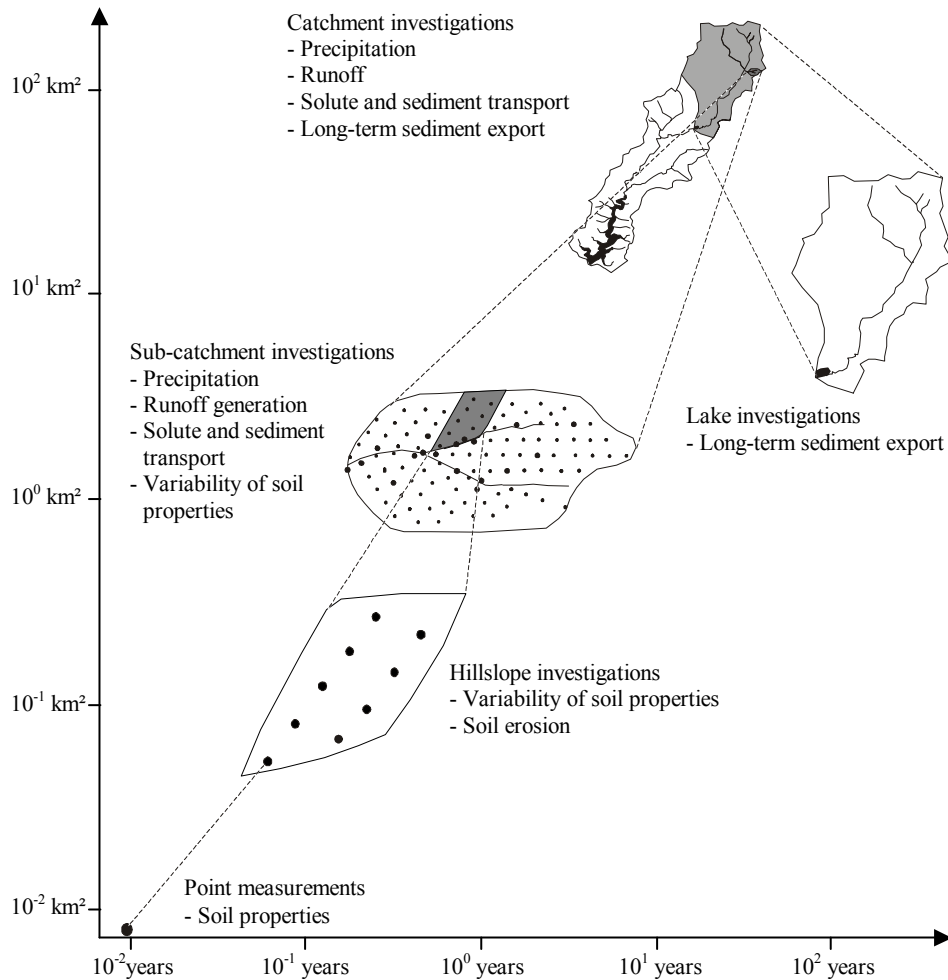


Fig. 2: Concept for analyzing the fluxes of matter in the catchment of the Wahnbach River.

Furthermore, water probes from the main rivers Wahnbach and Wendbach were taken to analyze the sediment transport processes at the catchment scale. Additionally, 20 years of runoff and solute data from Wahnbach and Wendbach were made available by the association of the Wahnbach reservoir (Wahnbachtalsperrenverband, WTV).

1.2.2 The model concept

In order to simulate short-term and long-term fluxes of matter, a model had to be chosen, which is able to simulate processes at very different temporal scales. Therefore, the OPUS model (Smith, 1992) was chosen, because it is able to simulate processes having a duration of only a few minutes to periods of many decades (Fig. 3).

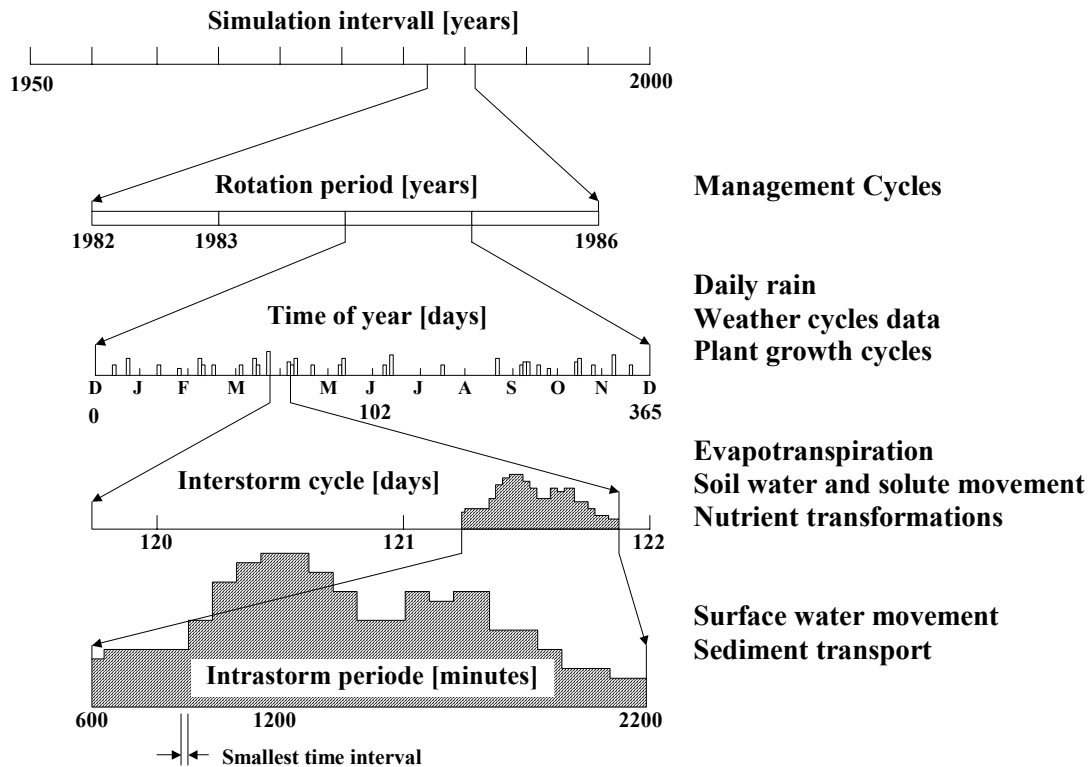


Fig. 3: Scheme of the various time scales in OPUS and associated processes simulated by the model (redrawn from Ferreira and Smith, 1992).

As OPUS belongs to the ‘physically-based’ models, a numerous amount of parameters is needed and therefore, as already mentioned above, the danger of model uncertainty is highly increased. This uncertainty has to be considered while judging the model results.

However, the applicability of OPUS is well acknowledged and the model is capable of simulating most of the necessary processes. Furthermore, it is possible to modify OPUS to the special conditions of the catchment because the source code is open and well documented.

The model has proven its usability in many investigations, e.g. Bonilla et al., 1999; Ma et al., 1999 and Diekkrüger et al., 1992. As OPUS is able to simulate the processes at single slopes, the catchment is discretized into a number of planes. This offers the advantage that all slopes existing in the catchment are directly reproduced in the model and therefore a validation of the model result within the watershed is possible. The weather generator WGEN is used to create a long-term climate data set. To ensure a validation of the sediment discharge from the research area a channel model links the slopes. Channel processes are simulated separately using the model HEC-6 (USACE, 1991), which is able to calculate sediment transport, deposition and scour in channels.

1.3 Structural overview

After a brief introduction to the aims and objectives of the dissertation, Chapt. 2 describes the past and present scientific status of the knowledge of processes determining the natural fluxes of matter and aspects of their modelling. In Chapt. 3 the research area and the available data are described and the applied models are explained.

The modelling process is explained in the Chapt. 4, 5 and 6. Chapt. 4 provides an analysis of the processes determining the fluxes of water, solutes and sediments in the study area, in order to develop a perceptual model of the processes in the catchment. Chapt. 5 describes the application scheme of the model system, containing aspects of model parameterization and modification at the sub-catchment scale as well as the regionalization methodology for the simulations at the catchment scale. The model results are presented in Chapt. 6.

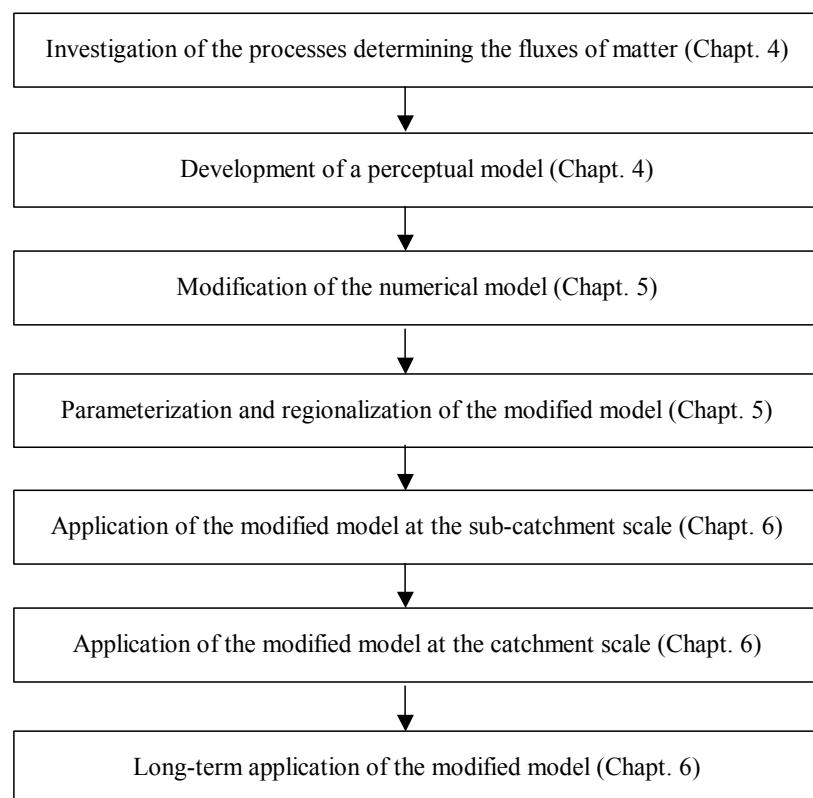


Fig. 4: A schematic outline of the modelling process in Chapt. 4, 5 and 6.

Fig. 4 displays a schematic outline of the different steps in the modelling process in this study. A discussion of the uncertainties involved in the modelling processes is presented in Chapt. 7 and a general discussion of the results is given in Chapt. 8. Finally general conclusions are presented in Chapt. 9.

2 Research context

2.1 Solute and sediment transport – processes and models

*Nature has not made it a priority to make it easy for us to discover its laws
(Einstein, 1901).*

In this chapter the most important processes transforming precipitation into runoff are presented. Precipitation is the main driving force for all processes related to solute and sediment transport. The first reason for this description is to provide a scientific basis for understanding the observed chemical and physical rainfall responses of the Wahnbach catchment.

The second reason is connected with the modelling aspect. One objective of hydrologic modelling is to calibrate a model in order to obtain a good correspondence of the observed and simulated quantities. However, a good correspondence is certainly no guarantee that the model results are produced for the right reason. In order to obtain a trustworthy application of a hydrologic model, an understanding of the involved processes to the greatest possible extent is indispensable.

2.1.1 Processes determining hillslope runoff

In general, hillslope hydrology is concerned with the partitioning of net precipitation passing through the vegetation coverage into several runoff components. In this respect, it is of great importance to know about the relevant mechanisms on the hillslopes conducting away the rainfall input, and thus delaying the runoff of a catchment more or less effectively. The correct description of the runoff components is a prerequisite for the correct quantification of solute and sediment fluxes, because in most cases water is the central transport medium of all relevant fluxes.

Commonly, the net precipitation is partitioned between overland flow and subsurface flow and the latter in further subdivisions e.g. interflow and groundwater flow. Subsurface flow is

the major runoff-generating mechanism, because both of its influence on surface runoff and as an important contributor to storm runoff in its own right (Anderson and Burt, 1990b).

2.1.1.1 Mechanisms producing surface flow

Hortonian overland flow, which is based on Horton's infiltration theory (Horton, 1933), is produced when the infiltration capacity of the soil is exceeded by the rainfall or snowmelt rate. Until the 1960s there was a wide agreement in the scientific community with Horton's infiltration theory, being the dominant process leading to flood flows (Kirkby, 1988).

In the following period several field studies revealed the great variety of possible runoff responses and the awareness grew that high flows could be produced by only a small fraction of the catchment generating overland flow (Kirkby, 1988). This mechanism is called **saturated overland flow**. It is produced when the storage capacity of the soils, which are typically located near the stream, is completely filled, and thus subsequent additions of water on the surface are forced to flow over the surface.

A further mechanism producing overland flow is called **return flow**, which can occur even after rainfall has ceased (Kirkby, 1985). This process occurs when subsurface flow is forced to exfiltrate out of the soil and is especially located in profile concavities and convergences or in the case of downslope decreasing permeability.

2.1.1.2 Mechanisms producing subsurface flow

During the 1960s and 1970s, increasing evidence of the complexity of flow generation and the impact of subsurface flow on storm hydrograph began to appear (Bryan and Jones, 1997). The field hydrologists realized that stormflows could take place where overland flow was completely absent, e.g. in forest catchments (Tani, 1998). They concluded that there had to be mechanisms in the subsurface involved, which lead to very rapid rainfall response.

For example, in catchments where impermeable bedrocks are overlaid by thin soils or where permeable soils become less permeable with depth, subsurface flow can account to a large extent for high flows (Anderson and Burt, 1990). This effect can occur at rainfall intensities well below those required for a Hortonian overland flow.

Fig. 5 displays four conceptual models of runoff generation in the presence of macropores and pipes. In **case 1**) rainfall water infiltrates through macropores into the mineral soil and

then directly through pipes into the stream, whereby two kinds of pipes can be differentiated: **by-pass pipes** which are located relatively near the surface and are fed through macropores carrying ponded water directly from the surface and **seepage pipes** which originate within the saturated zone, so that inflows occur under an appreciable pressure gradient (Kirkby, 1988).

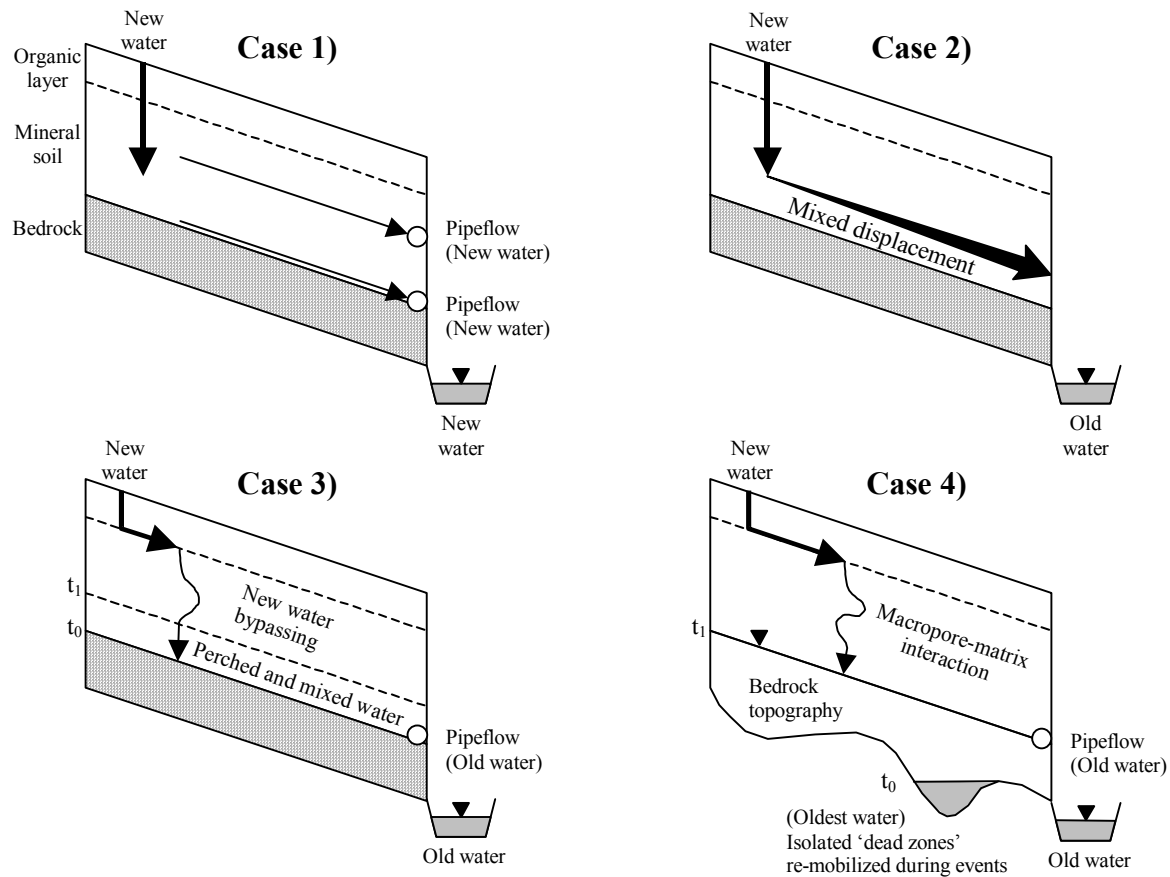


Fig. 5: Four different conceptual models to explaining fast subsurface runoff generation, redrawn from Anderson and Brooks (1996).

In the **first case** both pipes have only minimal contact with the soil matrix and consequently produce new water. The **second case** displays a hillslope, where an intensive interaction of infiltrated water and soil matrix is presumed to explain the displacement of old water. More complexity is introduced in the **third case**, where the groundwater system is initiated by vertical by-passing of the soil matrix through macropores.

In this context it is necessary to distinguish between a saturated hydraulic conductivity (K_s^*) of the soil matrix and a conductivity of the macroporous soil (K_{sat}), which is much greater than K_s^* . Therefore, if the flux density of rain is greater than the infiltration rate into the soil matrix, local ponding may occur, leading to vertical by-passing, although rain intensity may

be lower than K_{sat} . The invading new water perches at the soil-bedrock interface and interacts with the newly saturated matrix. Once free water exists, pipes in the lower soil zones transport the perched water downslope, producing a rapid through-flow response of well-mixed old water (McDonnell, 1990). The **fourth case** introduces the significant role played by the bedrock microtopography in storing water in isolated pockets for extended periods between events. When the water table rises during heavy rain events, these isolated systems will be connected again, enabling the release of stored water from the hillslope.

2.1.1.3 Combination of runoff mechanisms

Runoff is rarely generated by one single process. One exception may be the dry-weather flow, in which runoff is supplied by the delivery of deep groundwater sources. However, in the case of rainstorm events several runoff mechanisms may be involved, depending on rainfall and catchment characteristics.

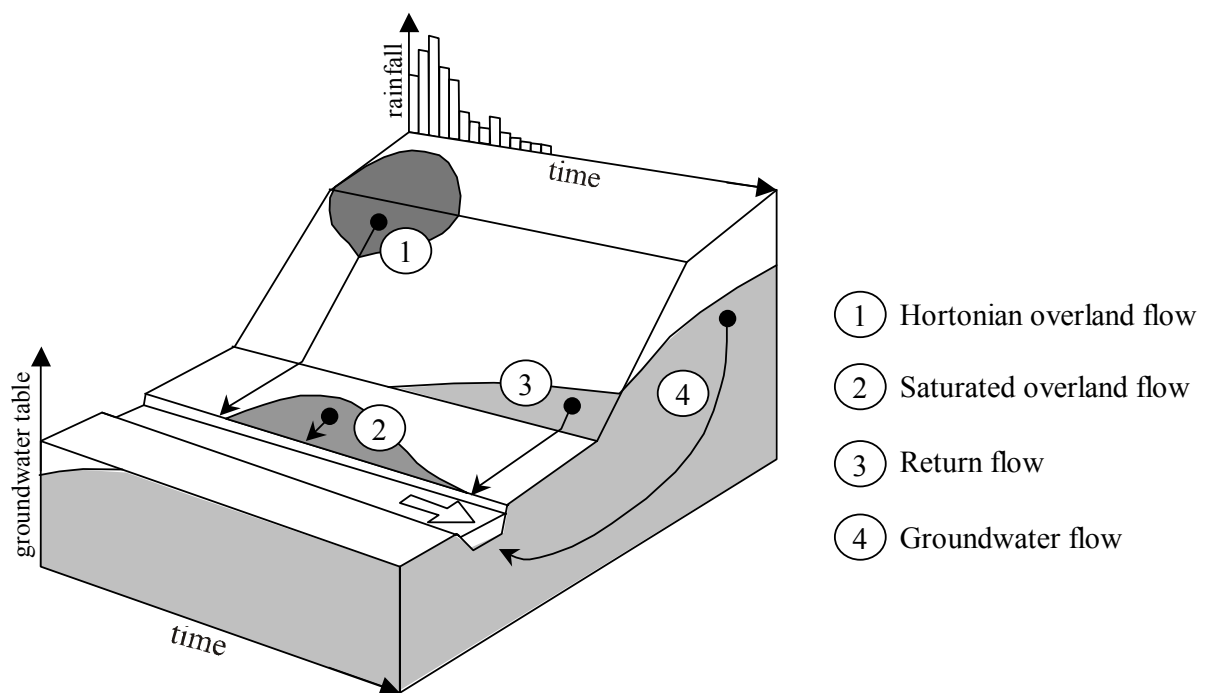


Fig. 6: Artificial hillslope displaying a sequence of runoff generation mechanism induced by a heavy rainfall event, adapted from Anderson and Burt (1990a).

In Fig. 6 an artificial hillslope is shown which displays four kinds of responses to a heavy rainfall event. During the highest rainfall intensities Hortonian overland flow is produced. Because of infiltrating water into the groundwater, the groundwater table rises, inducing saturated overland flow in the valley plain. Later on, in the case of the groundwater rising

additionally, return flow is produced. The last runoff component is the groundwater flow producing a long tailing of the hydrograph. As a simplification, it is assumed that pipe flow is absent on the artificial hillslope, but it may be conceivable that return flow is accelerated by pipe flow.

According to Jones (1997), runoff in the Maesnant catchment (Great Britain) is comprised of both Hortonian overland flow and ephemeral and perennial pipeflow. The Hortonian overland flow and the ephemeral pipeflow are significantly faster than perennial pipeflow, producing a very sharp peak. Botschek (1999) has observed that digging tunnels of small animals play an important role as flow paths for providing ephemeral pipeflow with the necessary water quantity. The runoff generation in perennial pipes is slower because their initiation depends on the rising of the groundwater table.

2.1.2 Transport of solutes from hillslopes

The processes determining the transport of solutes are much more complex than the runoff generation process. The most simple case of solute transport is given when a substance does not show any transformation processes (e.g. mineralization, volatilisation) and no interaction with the soil matrix (e.g. adsorption, desorption). Furthermore, it should not be subject to a selective uptake of the vegetation. In this case, the substance could be perfectly used to trace the flow of water. Because some substances have characteristics similar to such an ideal tracer, it is possible by applying them once with a well-known quantity, to visualize flow paths or to separate runoff components (Sklash, 1990).

In the case of nutrients, e.g. nitrate or phosphate, many of the restrictions mentioned above do not apply and several additional processes have to be taken into account. For example, the major process removing nitrogen from the soil profile is plant uptake (Thorsen et al., 1996). Some evidence exists that nonconservative constituents such as nitrate exhibit characteristic concentration patterns, which can be related to the dominating runoff mechanisms. At sites affected by large point-source inputs, nitrate concentration decreases with flow volume (Brown, 1986). Brown concluded that estimated concentrations of indirect runoff highly agree with typical measured values of concentration in groundwater. In contrast, at sites not being affected by point sources, nitrate concentrations do not correlate with streamflow, but exhibit seasonal variations due to factors like plant uptake.

2.1.3 Soil erosion and sediment transport

Despite the fact that many erosional processes are active on hillslopes, only those involving rainsplash and runoff are considered, because these processes are the major factors determining the sediment input into the stream system in temperate climates (Bryan, 2000). Rainsplash and runoff produce five more or less distinct sub-processes: splash erosion, sheetwash, rainflow, rill erosion and piping or tunnel erosion, which can either act sequentially or simultaneously. Generally, these sub-processes are classified in interrill processes in which entrainment is primarily caused by rainsplash and rill erosion or piping are caused by runoff (Morgan, 1999).

Soil loss by **interrill erosion** is closely linked to rainfall properties because raindrops are the major driving forces for the detachment. According to Salles and Poesen (2000), drop momentum and drop diameter describe best the detachment by raindrop impact. Interrill processes act intermittently over most parts of the hillslope (Bryan, 2000).

Rill erosion consists of small, ephemeral concentrated flow paths which either function as sediment source and sediment delivery systems for erosion on hillslopes. Rills actively erode and thus evolve morphologically over short timescales (Nearing et al., 1997). Head cuts and sidewall sloughing are sources of sediment, and during runoff recession plunge pools become sediment traps, which can turn into sediment sources if runoff increases again.

If the **sediment transport** within a certain catchment is of interest, additional processes have to be taken into account in order to obtain a complete sediment budget. Generally, sediment budget is defined as an accounting of the sources and disposition of sediment as it travels from its point of origin to its eventual exit from a drainage basin (Reid and Dunne, 1996). Fig. 7 shows a flowchart in which the most important processes are presented. Sediment is mobilized on the hillslopes by the erosion processes described above, but a certain part is redeposited on the slopes. The net mobilization of sediment is called sediment production, of which a certain percentage is temporally stored in floodplains and channels by aggradation. However, it is possible that these deposits are removed once more due to erosion processes. In the example of Fig. 3, a lower quantity is exported from the catchment than mobilized on the hillslopes.

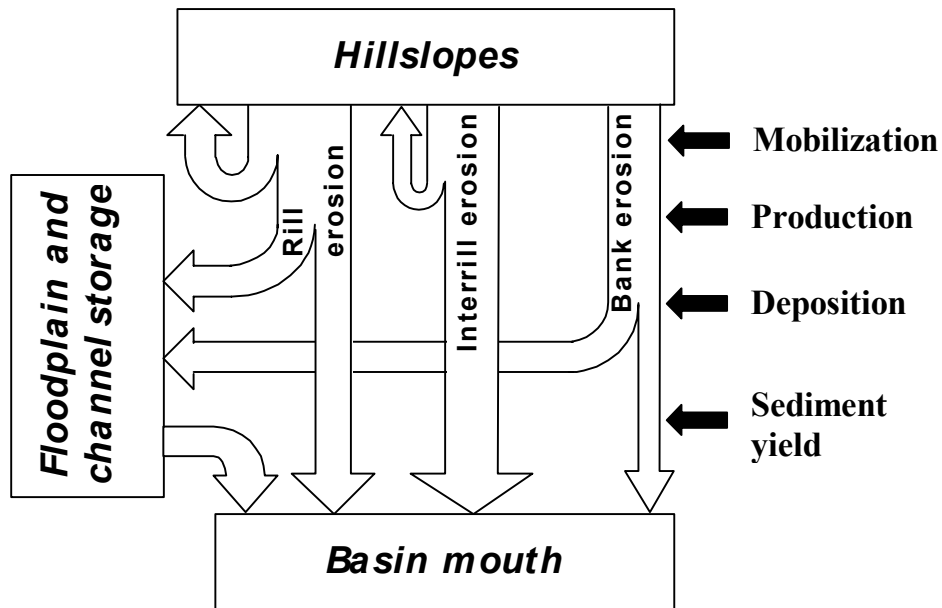


Fig. 7: Flowchart indicating relations between sediment mobilization (erosion), production, deposition and sediment yield of a typical catchment (redrawn from Reid & Dunne, 1996).

Temporal discontinuities in sediment transportation may introduce further complexity into the relationship between mobilization and sediment yield. The amount of sediment transported out of a catchment may reflect the recent history of erosion and sediment delivery, rather than contemporary erosion within its catchment (Walling, 1990). For example, it is conceivable that, due to landuse changes within a catchment, mobilization is effectively reduced, but sediment yield is still high because of unchanged or even increased sediment releases from floodplain and channel storages. Thus in evaluating the ‘off-farm’ impacts of soil erosion, such as channel and reservoir sedimentation, an understanding of sediment delivery and transfer mechanism is of great importance (Foster et al., 1990).

2.1.4 Modelling nitrogen and sediment transport

2.1.4.1 Nitrogen transport models

Losses of nitrogen as well as agricultural crop production are determined by a number of physical, chemical and biological processes. These include complex series of transformation and transport mechanisms, which are affected by external factors. A large number of models have been developed in the past years to simulate the transport of solutes, ranging from simple empirical formulas to distributed physically-/chemically-based descriptions (Thorsen et al., 1996).

Generally, leaching models which are confined to one-dimensional processes, e.g. WAVE (Vanclooster et al., 1994), have to be distinguished from catchment models, e.g. SWIM (Krysanova et al., 1998), sometimes incorporating a three-dimensional realisation of solute transport, e.g. SHETRAN (Birkinshaw, S.J. et al., 2000 and Ewen, J. et al., 2000). Several models exclude a water movement description, e.g. ANIMO (Rijtema et al., 1991) and hence require an external water flow model. However, most process-based models have incorporated a water transport model in which water movement is simulated often with a solution of the Richard's equation, e.g. OPUS (Smith, 1992) and SIMULAT (Diekkrüger, 1996).

Furthermore, a few models consider preferential flow paths in order to simulate water transport through macropores at a fast rate from surface layer to the bottom layer, e.g. SIMULAT and MACRO (Jarvis, 1994). The representation of mineralization, nitrification, denitrification and plant uptake varies considerably among the models. For example, the WAVE model works only with three organic matter pools, whereas the RZWQM model (DeCoursey et al., 1992) uses five organic matter pools and three biomass pools. The crop N-uptake and the crop production may be either simulated by a plant module accounting for gross photosynthesis, respiration etc., as for instance in DAISY (Hansen et al., 1993), or estimated indirectly by predefined curves (Thorsen et al., 1996).

Recently, nitrogen budget simulations were conducted using the GLUE methodology (Schulz et al., 1999). The GLUE concept is based on the assumption that often a wide range of parameter sets reproduces the available data in an acceptable way (Beven and Binley, 1992). This methodology requires a large number of model runs parameterised with random sets of parameter sets that are chosen from uniform distributions across the expected range of each parameter. Schulz et al. (1999) applied a simplified nitrogen budget model with average infiltration and nitrogen mineralization rates on this methodology and concluded that because of the equifinality of different parameter sets, their model structure may still be overparameterized.

The GLUE method may be very attractive in evaluating uncertainties in the parameter sets, but through the model calibration involved, effective parameters are obtained which may be only suitable for the calibration period. For example, in case of long-term nitrate predictions a process-based model may be preferable, because temporal discontinuities may exist. Under

these circumstances, a certain model complexity is necessary in order to account for the interaction of the main processes involved in the transport of nitrate. For instance, a conversion of the agricultural management from intensive to extensive agricultural land use may result in a change of the dominant runoff mechanism, and therefore would make the calibration of a simple model useless in supporting the forecast of nitrate discharge.

2.1.4.2 Sediment transport models

For the simulation of erosion, transport and sedimentation numerous models are available. While the USLE model is able to simulate long-term erosion at single slopes without considering sedimentation (Wischmeier, 1984), other approaches calculate all processes. One has to differentiate between models applicable to single events and for continuous simulations and between models for simulating single slopes and whole catchments of different sizes. Most of the simulation models are designed for single events, e.g. EROSION3D (Schmidt et al., 1999), EUROSEM (Folly et al., 1999), KINEROS2 (Smith et al., 1999), ANSWERS (De Roo, 1993) and AgNPSm (Grunwald and Frede, 1999). The main problem of this type of model is the correct determination of the initial conditions. Therefore these models are often used to simulate design storms in order to study the effects of e.g. management practices on erosion.

Continuous simulation models, e.g. WEPP (Lane and Nearing, 1989), AnnAgNPS (Cronshey and Theurer, 1998) and OPUS, are more complex because they are also able to simulate other processes like soil water dynamics and plant growth which determine the interstorm processes. The advantage is that the initial condition for a storm is automatically provided and that series of storms can be calculated without difficulty.

Continuous erosion models are mostly designed for single slope models and have to be differentiated from catchment models, which require a spatial discretization and parameterisation. On this scale two different concepts can be found. The standard method is a grid-based discretization (EROSION3D, ANSWERS, AgNPSm). Since the grid size does significantly influence the simulation results (Renschler et al., 1999), the maximum number of grids determines the maximum catchment size. In the second concept the catchment is discretized into a number of representative slopes (KINEROS2, EUROSEM, AnnAgNPS). These slopes are linked via a channel, which allows simulating erosion, transport and sedimentation in a catchment.

The validation of erosion models is a complicated task. As the results of different model comparisons show (e.g. Jetten et al., 1999 and Favis-Mortlock, 1998), erosion models may be calibrated to simulate the hydrographs and sedigraphs in an acceptable quality. The main problem is the transferability of model parameters and initial conditions to unobserved sites and the applicability for long-term simulations. Validation at the large catchment scale is difficult because distributed data are rare. For long-term analysis it is necessary to investigate the age of deposited sediments in order to compare the results of long-term simulations with measurements.

2.2 Distributed models

In general, distributed models can either be conceptual in their model structure or physically based. For example, a GIS-supported and grid-based calculation of soil erosion with the simple regression equations (e.g. USLE) can, in principle, be described as a distributed model. However, Beven (1985) appreciates only physically-based models consisting of equations that involve more than one space coordinate as distributed models. These kind of models are capable of calculating not only the spatial pattern of environmental quantities in a qualitative way, and thus producing e.g. erosion risk maps or perhaps just ‘colourful pictures’; but also quantities which can be measured in the ‘real world’, e.g. the spatial distribution of the soil moisture-content. Besides the opportunity to forecast distributed quantities, this feature also enables the possibility of a distributed model validation.

2.2.1 Application possibilities of distributed models

The application of distributed models involves a substantial expenditure in terms of programming, computer resources, data preparation, and field experiment (Beven, 1985). This leads to the questions in which case this expenditure is justified. Refsgaard and Abbott (1996) listed some aspects of environmental problems, which provide application possibilities of distributed models:

- Water resources assessment
- Irrigation
- Soil erosion
- Surface water pollution
- Groundwater pollution

- Effects of landuse change
- Aquatic ecology
- Analyzing of the effects of climate change
- Historical reconstructions of the impacts of human activity

They concluded that there is a growing need for advanced distributed models especially concerning man-induced impacts on the environment and hence for their application as a management tool.

2.2.2 The use of GIS in distributed hydrologic modelling

The application possibilities mentioned above lead to the requirement of taking data sets from different fields of expertise and different sources into consideration. This results in a very complex and increased data volume involved in the modelling process (Deckers and Te Stroet, 1996). Furthermore, the complexity of model outputs is growing simultaneously, demanding graphical tools for a fast and accurate visualisation of the model results in respect to validation and interpretation. Therefore a combination of databases with geographical information systems (GIS) may be an appropriate way for solving the problem of handling the increasing amount of spatial and temporal input and output data. Beside the possibility of visualising spatial data, GIS have been extended with a powerful set of spatial analysis functionalities (Deckers and Te Stroet, 1996). These extensions facilitate for example the option of a catchment discretization using digital elevation models (DEM).

With regard to a comfortable use of distributed models, it may be furthermore desirable to interface the GIS with the model of interest. Models have been interfaced since the mid-1980s (Hartkamp et al., 1999), but owing to commercial considerations process-based models have not been taken into account at the early stages. Therefore GIS-model interfaces are often a kind of an ad-hoc solution, developed for various research disciplines. As a result, standards for terminology, formats and procedures for interfacing models with GIS are still missing (Hartkamp et al., 1999). To elucidate this situation, Hartkamp et al. suggested the differentiation of three strategies for interfacing model and GIS (Fig. 8).

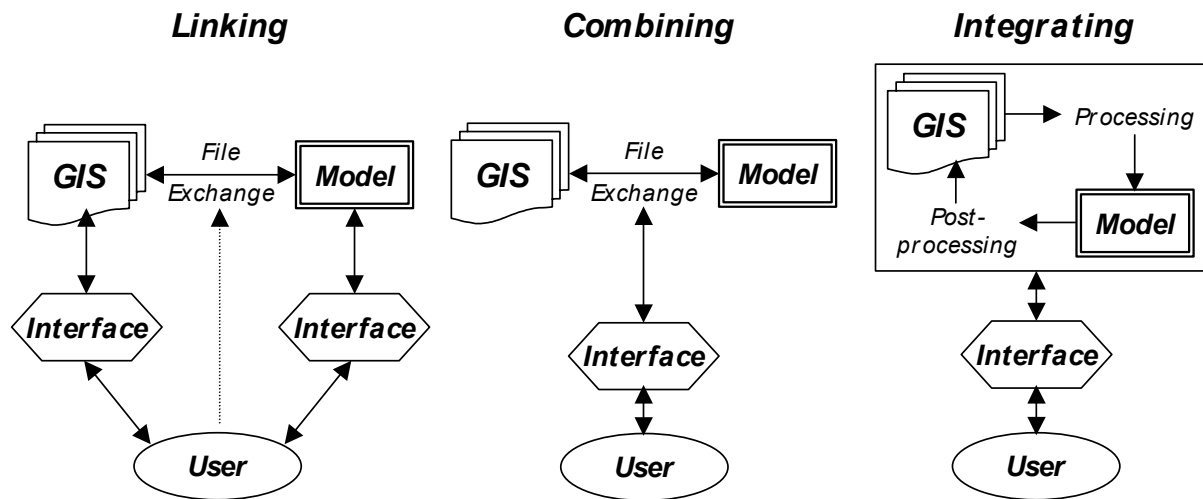


Fig. 8: Organizational structure for linking, combining and integrating GIS and models (adapted from Hartkamp et al., 1999).

Linking strategies involve the use of GIS functions such as interpolation, overlay and slope calculation to produce input data for the model as well as the spatial display of the model output. Because GIS and model are completely separated, a simple file transfer does the communication. The disadvantages may include awkwardness in data handling, incompatibility of the different software packages, and the failure to take full advantage of the functional capabilities of the GIS (Tim, 1996).

Combining involves the same features like linking and some further features like an automatic data transfer and interactive tools creating a better exploitation of the full potential of the GIS. This involves an increased programming effort and data management than simple linking does (Tim, 1996).

Integrating implies the incorporation of either the GIS in the model system or the model into the GIS-environment. Usually this involves the automatic use of relational databases, expert systems and statistical packages (Hartkamp et al., 1999). For the development of these systems a considerable programming effort is needed and, because of the involved complexities of process-based models, until now only conceptual models have been integrated into a GIS to the full extent.

De Roo (1989) developed a GIS-interfaced version of the ANSWERS model. He found that simulations with this version calculated 46% more runoff and 36% more erosion than with the

original model. This example suggests that GIS-interfacing has to be carried out carefully and error propagation caused by up- and down-scaling effects has to be considered, as elucidated in detail in the next chapter.

2.3 Scale issues in hydrologic modelling

And, indeed, if you believe there exists a single universal relationship underlying hydrologic processes at many scales it is hard not to fly off to cloud-cuckoo land with this idea (Blöschl, 2001).

According to Blöschl and Sivapalan (1995), the transfer of information across scales is called *scaling* and the problems associated with it are *scale issues*. The problems arise predominantly from an absence of scaling invariance, since runoff production is strongly influenced by natural heterogeneity, for instance geology, soils, vegetation, precipitation or geomorphological form of the catchment (Beven, 1995). After an introduction of the term *scale* in the context of hydrology, some problems associated with *scaling* are presented.

2.3.1 Scales in hydrology

Hydrological processes occur on a wide range of temporal and spatial scales, as it is indicated in Fig. 9. Fig. 9 illustrates the coexistence of dynamic changes of properties (e.g. texture) and processes (e.g. rill erosion) within a spatial and temporal framework. Phenomena and properties are important for the hydrological processes at the indicated scale.

For example, certain runoff mechanisms (Fig. 7, Chapt. 2.1.1.3) can have different length scales. Hortonian overland flow can be considered as a ‘point phenomenon’ and thus can be defined at a very small scale. Saturated overland flow is an integrating process and needs a certain area to be effective, because processes like lateral flow and groundwater rising are involved. Thus saturated overland flow has a greater scale length than Hortonian overland flow.

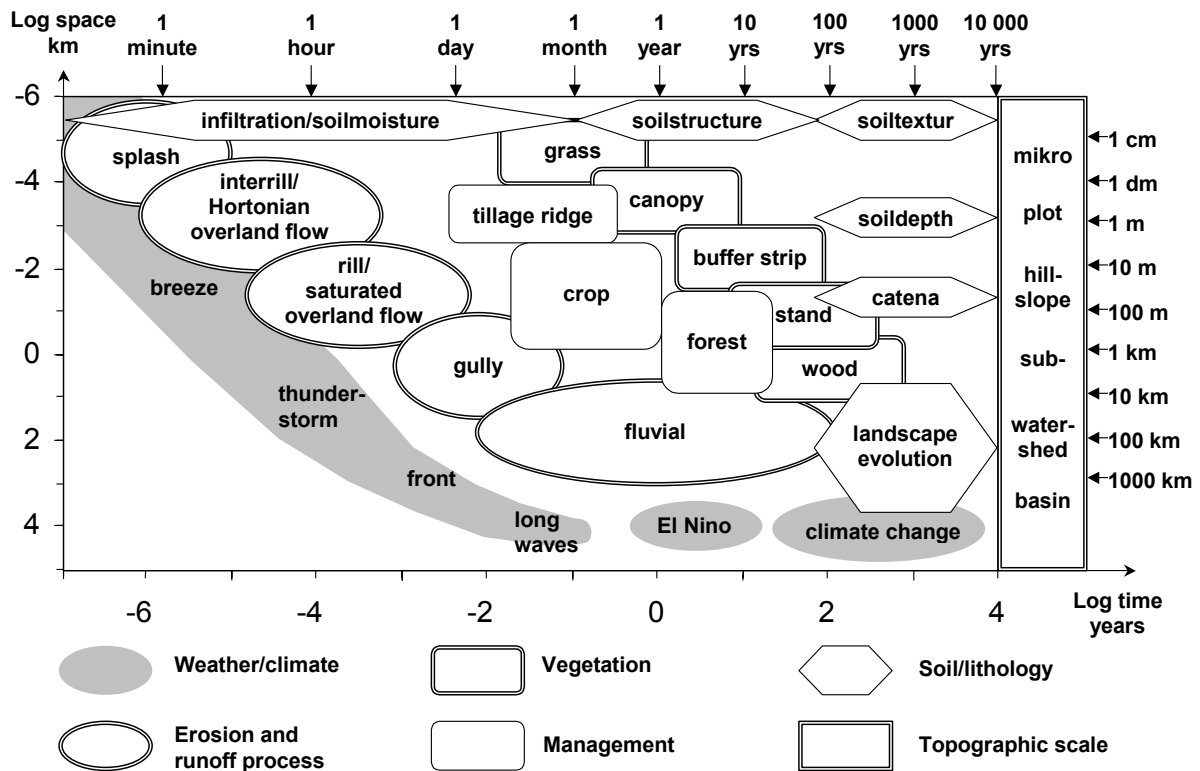


Fig. 9: Temporal and spatial extent of hydrological processes and natural phenomena with special consideration of soil erosion processes (redrawn from Renschler, 2000, with complements)

Blöschl and Sivapalan (1995) differentiate between the observation and process scale that are defined by the extent, spacing and support of the samples and the modelling scale. Typical modelling scales are the local scale (1m), the hillslope scale (100 m), the catchment scale (10 km) and the regional scale (1000 km), and in time the event scale (1 day), the seasonal scale (1 yr) and the long-term scale (100 yrs). They argue that the modelling scale often differs from the process scale, which necessitates an upscaling, downscaling or regionalization scheme. These methodologies are described more detailed in the next chapter.

In this context it has to be mentioned that the variability of the landscape leads to a contradictory problem: an increasing scale leads to an increase of variability and a decrease of knowledge about this variability (Diekkrüger, 2001). This problem is especially important in respect to hydrologic modelling. For example, Merz and Bardossy (1998) were able to show the effect of the spatial variability of soil distribution on runoff simulation results.

2.3.2 Scaling in hydrology

Following a description of Blöschl (1996), the term *scaling* denotes a change in scale, either in time or in space. Furthermore, he differentiated between a specific definition in which scaling is interpreted as the change in area or volume, and a broader definition in which scaling refers to all aspects of changing a scale including extrapolation, interpolation, aggregation and disaggregation.

The *aggregation approach* can be expressed in terms of the question of how to use measurements and process understanding at small scales in order to improve predictions of hydrological responses at larger scales (Beven, 2001). For example, Sivapalan and Wood (1995) developed a concept for finding an averaging scale - by means of analyzing runoff and topographic data of high resolution - where the variability between catchments is sufficiently small for using a simplified rainfall-runoff model. Furthermore, methodologies have been developed in order to find the optimal degree of aggregation. For instance, Grunwald (1997) applied a methodology where entropy is used as a measure for explaining the heterogeneity of spatial data for minimizing the uncertainty involved in the aggregation of spatial data.

In contrast, the *disaggregation approach* involves the question of how to use measurements and process understanding at larger catchment scales in order to predict local scale responses (Beven, 2001). If processes like solute and sediment transport are to be simulated, the inherent variability of properties like soil, relief or vegetation cannot be neglected (Diekkrüger, 2001). On the other hand, one may not be interested in the variability of a certain area but in its mean response behaviour. In this case, appropriate effective parameters have to be found, which requires the definition of an objective criterion, like water fluxes, soil water content or solute concentration. Several methodologies exist for the derivation of effective parameters, e.g. the Latin Hypercube approach (Diekkrüger, 2001) or the inverse modelling methodology (Feddes et al., 1993).

Unfortunately, these methods are not valid when lateral processes like runoff generation are considered. Diekkrüger (2001) showed that calculated effective parameters of the soil hydraulic conductivity are a function of rainfall intensity, and thus the concept of effective parameters fails in this case.

3 Methods and data

3.1 The research area

The Wahnbach River drains into a reservoir (Fig. 1), whose catchment is situated about 25 km east of Bonn, Germany, on the border of the Rhenish Massif. Therefore, it belongs to the ‘Bergische Land’, which is part of the German low-mountain range. The catchment of the reservoir covers an area of about 69.3 km² and has an extension of about 22 km in length, but only about 3 km in width.

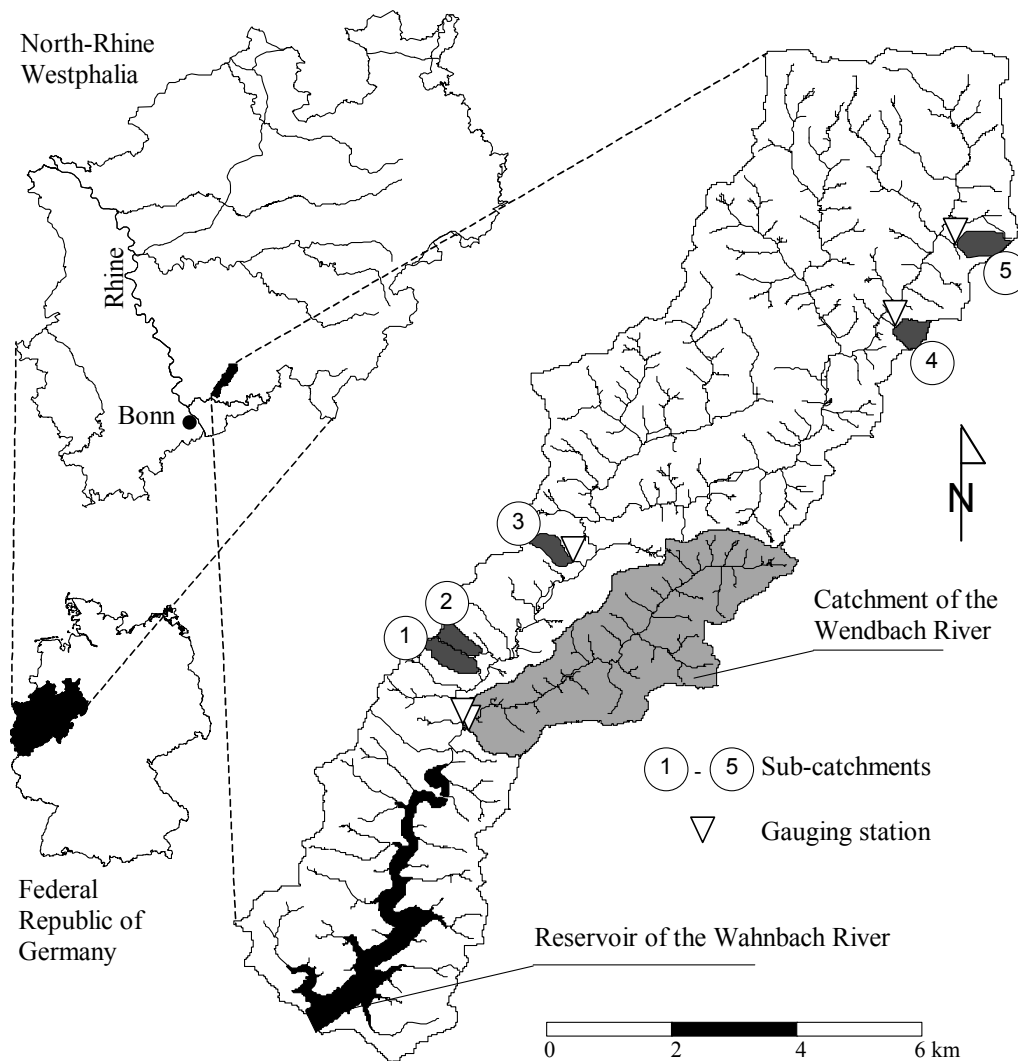


Fig. 10: The catchments of the Wahnbach River and Wendbach River and the investigated sub-catchments.

The elevation rises from 78 m at the barrage in the SW to about 383 m in the NE (Fig. 81, Appendix). On account of deep valley cuts, the research area is very structured. Excluding the region which drains directly into the reservoir, the Wahnbach catchment is restricted to an area of 54,0 km². The largest tributary of the Wahnbach River is the Wendbach River. The catchment of the Wendbach River covers an area of 8,92 km².

The reservoir was built from 1954 to 1958 in order to guarantee the supply of drinking water to the inhabitants of the Rhein-Sieg-Kreis. Today about 720.000 people are provided with drinking water by this reservoir. Owing to the intensive agricultural landuse, a heavy water pollution with phosphate takes place (Klingel et al., 1997). Phosphates enter the rivers both indirectly through soil erosion and directly via cattle faeces in the surroundings of drinking troughs. To protect the reservoir against eutrophication, a phosphate elimination system was installed in the seventies which assimilates the whole discharge and reduces effectively the phosphate concentration. Nevertheless, many other pollutants may reach the reservoir through improper agricultural activities. A careful management of the catchment is therefore essential to keep the reservoir clean.

3.1.1 Geomorphology and soils

The bedrock of the research area is built of clay-, silt- and sandstone, which were developed in the Palaeozoic period and were often heavily weathered throughout the Tertiary period (Jux, 1983). In the southern part of the catchment, these Devonian sediment rocks are overlaid by an up to 5 m thick loessial cover in which predominantly para-brown earth soils have developed (Fig. 82, Appendix). In the northern part, where a complete loess cover is missing and the surface is mainly formed by solifluction, brown earth soils are common. Furthermore, the soil map of the research area (Fig. 83, Appendix) reveals that gley soils have developed in the alluvial deposits situated in most valley plains.

However, in the deep valley cuts of many headwater catchments alluvial deposits are completely missing or restricted to minor extension, demonstrating that fluvial incision is the dominating alluviation. These valleys are called “Siefen”, which are gorge-like types of valley heads frequently occurring in the northeast of the Rhenish Massif (Nicke, 1989). These latest geomorphological features are natural erosional deepening comparable to gully forms, and subject to intensive recent formation processes.

In the upland areas of the catchment similigleys are common, indicating internal stagnant water due to the damming effect of the bedrock. Recent soil surveys of lower scale (1:5,000) reveal a wide occurrence of colluvial soils associated with a loess subsoil especially in the southern part of the research area. These features are often situated in prolongation of the headwater brooks, proving that soil erosion is common in this area.

3.1.2 Climate

The region ‘Bergische Land’ is characterized by oceanic climate conditions and can be assigned to the upstream mountain type. The region belongs to the low mountain ranges of Europe with the highest rainfall amount, where precipitation due to rising air masses is common. Due to the distinct elevation gradient within the Wahnbach catchment, a decrease of the annual mean temperature from 10 to 8.7°C and an increase of the annual rainfall from 850 to 1130 mm from SW to NE are observed.

The precipitation data of several stations located within the Wahnbach catchment or in its vicinity are used for the simulates at the catchment scale (Tab. 2). In order to create a complete data set, correlation indices (R^2) are calculated from the monthly precipitation amounts (Tab. 3). Subsequently, the missing rainfall data are completed by choosing the most appropriate correlations.

Tab. 1: The precipitation stations used for the calculation of the mean annual regional precipitation.

Name of station	Start of recording	Resolution	Mean annual rainfall
Seligental (P_sel)	10.07.58	daily	874.6 mm
Siegelsknippen (P_sie)	01.06.91	daily	877.9 mm
Braschoss (P_bra)	01.05.94	daily	883.3 mm
Phosphate elimination plant (P_pea)	01.08.79	daily	945.3 mm
	05.01.92	bp	
Neuenkirchen (P_neun)	01.11.67	daily	952.8 mm
Krawinkel (P_kra)	01.09.92	daily	966.1 mm
Hillesheim (P_hill)	10.08.94	bp	977.5 mm
Hochbehälter Much (P_hm)	01.08.94	daily	988.3 mm
Much (P_much)	01.05.69	daily	1056.7 mm
Bueddelhagen (P_bued)	01.08.94	daily	1094.6 mm

bp: breakpoint data

Tab. 2: Matrix of correlation indices (R^2) calculated from the monthly precipitation amounts of each precipitation station; the bold numbers mark the chosen correlations and n denotes the number of months, which were available for the calculation (may not correspond to the recording duration due to data failures).

	P_sel	P_wp	P_bra	P_pea	P_neun	P_kra	P_hill	P_hm	P_much	P_bued
P_sel		0.970	0.951	0.911	0.911	0.877	0.932	0.844	0.792	0.841
P_wp			0.956	0.893	0.871	0.821	0.883	0.707	0.730	0.661
P_bra				0.921	0.902	0.866	0.917	0.764	0.750	0.728
P_pea					0.940	0.958	0.956	0.877	0.901	0.846
P_neun						0.967	0.952	0.862	0.855	0.811
P_kra							0.967	0.893	0.916	0.863
P_hill								0.943	0.935	0.923
P_hm									0.960	0.977
P_much										0.943
n	471	111	111	222	362	65	34	38	347	35

The annual mean regional-precipitation amounts are calculated from the 10 rainfall stations, using the Thiessen polygons methodology (Fig. 85, Appendix). Fig. 11 shows the calculated mean annual regional-precipitation amounts and the spatial weighted averages as well as the minimum and maximum values.

Additionally, a deviation factor (DF) is introduced in Fig. 11, which is an expression showing the annual deviation of the rainfall at the stations from the calculated regional precipitation and is calculated as follows:

$$DF = \left((P_{\max} - P_{\min}) / P_{\text{regional}} \right) \cdot 100 \quad (1)$$

where P_{\max} is the maximum, P_{\min} the minimum and P_{regional} the regional-precipitation amount.

The factor DF reveals the problem of the methodology used for completing the missing data. For example, for the first eight years only one station was available, which results in a constant deviation factor. In the following time the factors dynamic is increasing because the number of stations increases.

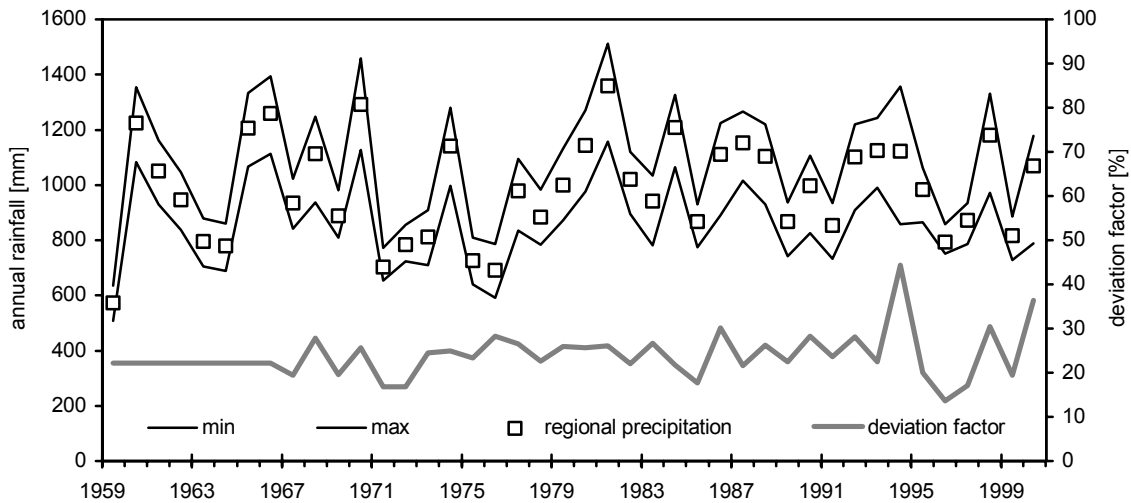


Fig. 11: Minimum, maximum and weighted average of the annual regional precipitation amounts calculated from 10 stations located within or in the neighbourhood of the Wahnbach catchment and the calculated deviation factor, equation (1).

Furthermore, the diagram reveals that the annual precipitation varies considerably (from 574 mm in 1959 up to 1360 mm in 1981) and the deviation factor fluctuates significantly within the catchment from year to year (from 13.6 in 1996 up to 44.4 in 1994), too. This implies that long-term soil water balance, soil erosion and sediment transport have been very differentiated over the last 50 years. Consequently, the use of e.g. the USLE concept for the prediction of an annual soil erosion amount, which only considers a mean precipitation characteristic, will lead to considerable under- or overestimations. For long-term simulation purposes where an annual resolution of the sediment export is demanded, a process-based model is therefore preferable. Furthermore, the uneven rainfall distribution within the Wahnbach catchment has to be considered for which a distributed model system is indispensable.

Fig. 12 shows the monthly average precipitation amount as well as the monthly minimum and maximum values. The average values exhibit a considerable fluctuation throughout the year. Smallest precipitation amounts can be expected in February with an average rainfall amount of about 58 mm, whereas July shows the highest value with approx. 96 mm of rainfall. A further increase of precipitation can be recognized in the winter season with a peak in December (93 mm). The minimum values fluctuate between 5 and 20 mm. The maximum values differ considerably during the year from 133 mm in November up to 218 mm in July.

Four months show a total precipitation of over 200 mm, which indicates enormous erosional potential in the catchment of the Wahnbach River.

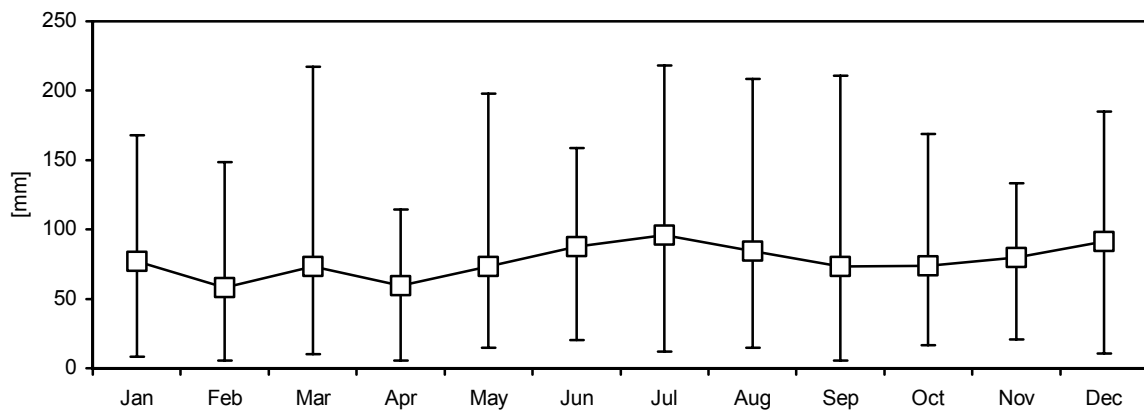


Fig. 12: The average monthly regional precipitation amount (squares) and the monthly minimum and maximum precipitation amounts (bars).

However, a better indicator for erosion potential is the rainfall intensity, which is presented in Fig. 13 with monthly values of maximum and average rainfall intensity. As data basis a nine-year record of rainfall intensities recorded within the catchment is used (P_{pea}, Tab. 3).

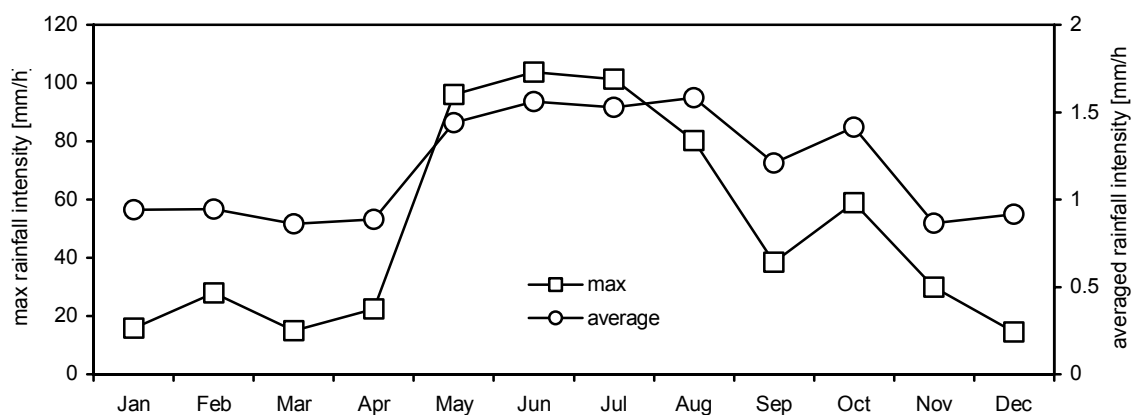


Fig. 13: The monthly maximum rainfall intensity and the monthly average rainfall intensity.

Fig. 13 reveals a distinct shaped form of the maximum values with highest values for May (96 mm/h), June (103.8 mm/h) and July (101.4 mm/h). Lowest rainfall intensities are observed in December with 13.4 mm/h. The course of the average values shows a similar but smoother shape, indicating that the maximum values cannot be generalized without reservations. But from this data it can be concluded that most erosional risks can be expected during late spring and summer due to convective rainfall events, whereas the high monthly

rainfall amounts in the winter season are of low intensity and thus of lower erosional potential.

3.1.3 Landuse

The landuse distribution is annually mapped out by the association of the Wahnbach reservoir. In combination with the ‘German topographic base map’, having a scale of 1:5,000, digital landuse maps of the period from 1989 until 2000 were produced (Fig. 84, Appendix). The forests are concentrated in the direct surroundings of the reservoir, in the steep hillslopes of the Siefen and on the upland areas, where they are often associated with similigley soils. Tab. 4 shows the landuse types and their percentages of surface area of the years 1989 and 2000.

Tab. 3: The percentages of the main landuse types of the years 1989 and 2000 in the catchment of the Wahnbach reservoir (69,3 km²) and the landuse changes.

Landuse type	Landuse 1989	Landuse 2000	Landuse changes	
	[%]	[%]	[ha]	[%]
Forest	22,24	22,16	-5,48	-0,35
Fields with individual trees	4,43	4,53	+6,83	+2,11
Cereals	2,63	2,30	-23,79	-14,45
Corn	3,45	3,97	+37,56	+13,20
Sugar beets	0,51	0,44	-4,84	-15,26
Leguminous plants	0,01	0,16	+10,39	+91,78
Potatoes	0,05	0,04	-0,65	-22,49
Golf course	0,92	0,92	0	0
Pasture	47,22	46,95	-19,12	-0,57
Settlement (up to 25 % sealed)	6,65	6,60	-3,28	-0,69
Settlement (25 -50 % sealed)	1,85	1,85	0	0
Settlement (more than 50 % sealed)	0,33	0,36	+2,64	+10,15
Roads	6,15	6,15	0	0
Surface water	3,56	3,56	-0,26	-0,10

Compared to other drinking water reservoirs, the catchment of the Wahnbach reservoir shows a relative high percentage of productive land, occupying place 10 from 43 German reservoirs (Krämer, 2000). About 53,9 % of the catchment is productive land. However, arable land takes up only about 7 % of the catchment area. Forests and settlements inclusive roads occupy about 26.2 % and 15 %, respectively, of the catchment area.

Most of the landuse types remain relatively constant during this period with a maximal change of corn (+37, 56 ha). Probably, the additional corn fields are mainly converted from cereal fields (-23,79 ha) and sugar beet fields (-4,84 ha). Worth mentioning is also the significant increase of fields being covered by leguminous plants (+91,78 %).

3.1.4 The sub-catchments

In order to characterize the hydrological behaviour of the sub-catchment, five sub-catchments were selected depending on factors like the geological situation or the landuse predominance (Fig. 11, Chapt. 3.1). The five sub-catchments are covering a wide range of landuse and geology types (Tab. 5).

Tab. 4: Some important characteristics of the five investigated sub-catchments within the Wahnbach catchment (see below for abbreviations).

Sub-catchment	Area [ha]	Mean slope [%]	Mean elevation [m]	Landuse [%]				Geology [%]		
				P	A	F	S	Al	L	D
Berrensiefen	28.9	11.6	272.4	80	-	18.4	1.6	3.5	-	96.6
Hellenkeutelsiefen	21.4	15.4	269.5	39	-	61	-	-	-	100
Steinersiefen	21.8	14.6	202.3	42	39	13.7	5.3	1.3	50	48.7
Schlößchensiefen	28.2	15.5	188.7	61	14	11	14	6.8	84.4	8.8
Stucksiefen	22.1	13.3	194.3	71	-	19	10	3.7	83.2	13.1

P: Pasture, A: Arable land, F: Forest, S: Settlements, Al: Alluvial fills, L: Loess, D: Devonian bedrock

3.1.5 The database for the simulations with OPUS

Several quantities were measured within the research project B14 during the period from 1998 until 2001. These measurements are carried out to improve general process understanding and for simulation applications in which they serve both as input data and for validation purposes.

3.1.5.1 Sub-catchment scale simulations

In three sub-catchments (Berrensiefen, Hellenkeutelsiefen, Stucksiefen) automatic gauging stations were installed for continuous measurements of quantities like rainfall, runoff, electric conductivity and temperature for a period of about three years.

Tab. 5 lists the measured quantities in respect to the scale-characteristics extent, spacing and support, according to the recommendation of Blöschl and Sivalpalan (1996):

Tab. 5: List of measured quantities in respect to the scale characteristics extent, spacing and support.

Measured quantity	Extent	Spacing	Support
Precipitation amount	5 minutes	5 minutes	2.5 years
Runoff amount	5 seconds	15 minutes	2.5 years
Physical quantities of stream water (e.g. conductivity, temperature etc.)	One second up to 5 minutes	15 min up to one week	2.5 up to 3.5 years
Chemical quantities of stream water (e.g. anions, cations etc.)	Punctual	One week	3.5 years
Physical quantities of soils and sediments (e.g. particle-size distribution, hydraulic conductivity etc.)	Punctual and continuous*	One week, singular measurements	2.5 years

*probe collectors have been weekly emptied

Most quantities are the basis for simulations at different temporal and spatial scales. Some aspects of these measurements and their usefulness for the simulations are mentioned in the following sections.

Precipitation is the driving force for all hydrological processes and therefore has to be considered as exactly as possible. Two subcatchments were instrumented with rainfall stations recording precipitation amounts with a temporal resolution of 5 minutes, in order to correctly reproduce advective precipitation as well as convective rainfall events. For the parameterisation of the soil module of OPUS, a soil survey was undertaken with a spatial resolution of 50 m and soil properties such as grain-size distribution and organic-carbon content were measured. For detailed information the reader is referred to Uhrich (1999). To facilitate the calibration of the model validation of the simulation results, runoff was recorded with 15 minutes resolution, whereas solute and sediment concentrations were measured with a weekly resolution.

3.1.5.2 Catchment scale simulations

To apply a process-based model at the catchment scale, a large database of distributed information has to be created. As mentioned above, the landuse distribution is reproduced in a reasonably good resolution. Other aspects may not be represented in a sufficient manner. For

example, the soil distribution is based on the digital soil map with a scale of 1:50,000, which involves some uncertainty because of its relatively low resolution. However, the variation of the soil properties is relatively invariable within the catchment of the Wahnbach River (Lützen, 1999), for which reason it can be assumed that the soil map is acceptable.

The resolution of the digital elevation model (DEM) may have significant influence on the model results (Renschler, 1999; Lützen, 1999). Therefore in this study a high resolution DEM with a grid spacing of 5 m was applied for the parameterization of the topographic features. To facilitate a validation of the model results, runoff and solute concentration data from the association of the Wahnbach reservoir were obtained. Furthermore, water probes were taken from the main rivers to validate sediment transport simulations (Giertz, 2000).

3.1.5.3 Long-term simulations

Long-term simulations with process-based models require a lot of input data, especially concerning climate data. However, climate data are often limited and methods have to be applied to cope with the problem of insufficient input data. In this study the weather generator WGEN (described in Chapt. 3.3) is used to create continuous climate-data set on the basis of the information available.

3.1.6 Reconstruction of the soil erosion history

The reservoir of the Wahnbach River is acting as an efficient sediment trap making a quantification of the sediment export from the catchment feasible. Generally the sediment deposition takes place in a small sedimentation basin in the front of the reservoir (Fig. 14). The water flows into the main reservoir via an outlet funnel, reducing the sediment outflow.

Before the inauguration of the reservoir (1958), the elevation in the area of the settling basin was measured by the WTV and a further levelling was carried out in 1994. By means of ordinary kriging, interpolations of the digitized elevation data were carried out. Through overlaying the two surfaces, a sediment volume of 33090 m³ could be calculated (Fig. 14).

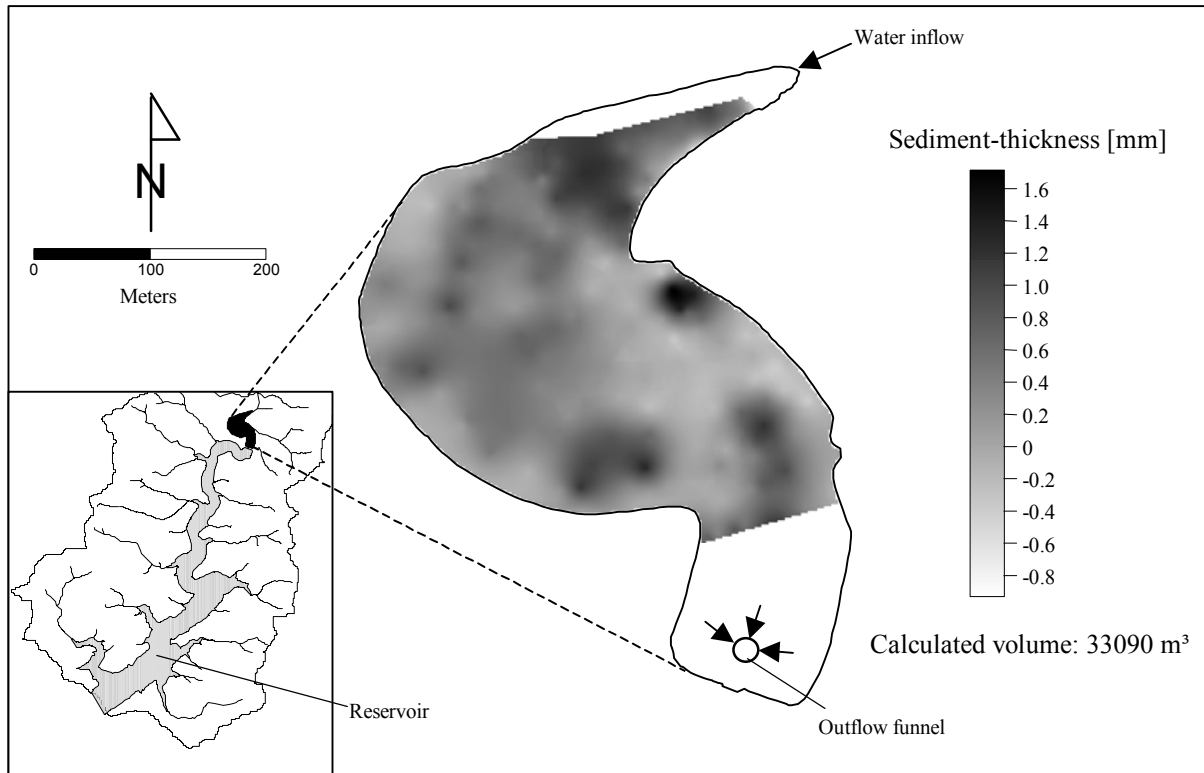


Fig. 14: Interpolated sediment thickness in the deposition basin; elevation data are provided by the Geological Institute Bonn and the WTV.

However, the levelling does not cover the whole sedimentation basis. The missing data result in an area of about 20 percent of the basin (white areas in Fig. 14) being unconsidered. By extrapolating the two surfaces the sediment volume of the missing areas is assessed, resulting in a total sediment volume of about 40.000 m³. With an average density value of the sediments of 1.2 gcm⁻³, an average sedimentation rate of about 1330 tonnes per year can be assumed. Of course, this value represents only the net output from the catchment, and other sediment sinks like ponds and valley plains have to be considered in evaluating the whole erosion amount.

3.2 The model system OPUS

The model system OPUS combines a one-dimensional simulation of the soil processes with a one-dimensional simulation of the processes of the soil surface. As OPUS was designed for agricultural ecosystems, the model can simultaneously simulate several interactive processes when hydrologic processes are computed, including erosion and sediment transport, nutrient cycling, plant growth and management practices. The model is designed to take into account the balanced precision of its components to guarantee congruence of the simulation outcome.

In the following sections the main components of the model are described; however, for a full description of all components and equations of OPUS the reader is referred to the model's manual (Smith, 1992).

3.2.1 Water movement

Water movement is simulated with a numerical solution of the well-known Richards' equation, in the one-dimensional form expressed as

$$\frac{\partial \theta}{\partial t} + \frac{\partial q}{\partial z} = q_e \quad (2)$$

where θ is the volumetric water content, t is time [min], z is the depth from surface [mm], q is the flux [mm/min] and q_e is the local inflow [min^{-1}] (Smith, 1992).

The soil water retention curve and the unsaturated hydraulic conductivity function are described by a modified version of the Brooks & Corey – function (Brooks and Cory, 1964) with an additional corresponding parameter (α):

$$\frac{(\theta - \theta_r)}{(\theta_s - \theta_r)} = \left[1 + \left(\frac{\Psi}{\Psi_b} \right)^\alpha \right]^{-\frac{\lambda}{\alpha}} \quad (3)$$

with λ is a pore-size distribution parameter, θ_r is the residual water, θ_s the water content at saturation, α is a fitting factor and Ψ_b is the bubbling pressure (Smith, 1992).

3.2.2 Infiltration and overland flow

The infiltration can be calculated in two different ways, depending on the resolution of the rainfall data. In the case that breakpoint data are available, an analytical solution of the Richards' equation can be chosen to calculate water infiltration (Smith and Parlange, 1976):

$$I(f) = \int_{\theta_i}^{\theta_s} (\theta - \theta_i) \frac{D(\theta)}{f - K_s} d\theta \quad (4)$$

in which $D(\theta)$ is diffusivity, defined as $K(\theta)d\psi/d\theta$ [mm²/min], I is the depth of infiltration from start of rainfall and f is the rate of infiltration [mm/min] (Smith, 1992).

Additionally, a simple approach for the simulation of surface crusting is implemented, reducing the infiltration capacity in relationship to clay content and rainfall energy.

The infiltration model is accompanied by an unsteady routing of the surface water using a kinematic wave simplification of de Saint-Venant's equations in the case when assuming that the slope of the surface water equals the bed slope. For very low slopes, the diffusive wave simplification of de Saint-Venant's equations is used instead. In both cases it is assumed that Hortonian overland flow is generated uniformly over the slope length leading to a direct proportionality of total and peak flow to slope length.

In the case that only daily rainfall data are available, the Soil Conservation Service (SCS) Curve Number (CN) runoff-estimation method (USDA-SCS, 1972) has been included.

$$Q = \frac{(P - I_a)^2}{P + s_w - I_a} \quad (5)$$

$$I_a = 0.2s_w \quad (6)$$

$$s_w = 254 \cdot \left(\frac{100}{CN} - 1 \right) \quad (7)$$

This method relates the runoff amount (Q) conceptually to the precipitation amount (P), a soil water storage value (s_w) and an initial abstraction (I_a) (all values expressed in millimetres).

The water storage is estimated from the soil water content and the initial abstraction is related to the Curve Number, an empirically-derived parameter.

3.2.3 Erosion

The routing model is connected with a distributed calculation of sediment transport following the continuous equation developed by Bennett (1974):

$$\frac{\partial}{\partial t}(aC_{sk}) + \frac{\partial}{\partial x}(qC_{sk}) - d(x,t)_k = q_s(x,t)_k \quad (8)$$

in which C_s is the sediment concentration, a is the cross-sectional area of flow [m^2], q is the water discharge per unit width [m^2/min], d is the rate of erosion or deposition at the bed [m/min], q_s is the local input of sediment [$m^3/m^2/min$] and k is a subscript referring to a particle size class (Smith, 1992).

Soil detachment is computed using the empirically-derived relations of Foster (1982). The equations relate the interrill detachment rate to rain intensity, surface coverage, surface angle and surface water depth and also represent the effects of management on the erosion process.

Rill detachment rates are related to local hydraulic shear:

$$d_{pr} = 139K_u\phi_u\phi_r\tau_s^{3/2} \quad (9)$$

in which d_{pr} is the potential rill detachment rate [$kg/m^3/min$], K_u is the soil erodibility factor [$kg/hr/N/m^2$], ϕ_u and ϕ_r are surface-soil residue factors and τ_s is the shear at the bed of surface flow [N/m^2] (Smith, 1992).

The Curve Number method is accompanied by an empirically-based calculation of erosion and sediment transport using the MUSLE approach (Williams, 1975):

$$Q_s = R_u \cdot K_u \cdot L_u \cdot S_u \cdot \phi \cdot P_u \quad (10)$$

in which Q_s is the net storm or daily soil loss [kg/m^2], R_u is the storm or daily erosivity [N/hr], K_u (see above), L_u is the slope length factor, S_u is the slope steepness factor, ϕ is a coefficient for cover and management and P_u is a factor for effects of supporting management practices (Smith, 1992).

3.2.4 Evapotranspiration

Potential evaporation (ET_p) is computed with a model of Ritchie (1972) which relates ET_p to mean daily temperature (T_K [°K]) and daily solar radiation (R_i [ly/day]):

$$ET_p = \frac{(1 + c_w)\Delta H_o}{\Delta + 0.68} \quad (11)$$

$$\Delta = 5304 \cdot \exp(21.255 - 5304/T_K) / T_K^2 \quad (12)$$

$$H_o = R_i(1 - \xi) / 58.3 \quad (13)$$

where c_w is a coefficient expressing effects of wind and humidity and ξ is the albedo of the field surface (Smith, 1992).

3.2.5 Nitrogen cycle

The nitrogen cycling is simulated in OPUS using the CENTURY organic residue decomposition model of Parton et al. (1988), which includes three pools of carbon material with different turnover rates. The CENTURY model has recently shown its applicability for a wide range of climates and soils (Gilmanov et al., 1997). The decomposition of each fraction is calculated using the following Equation:

$$\frac{d(m_{rC})_i}{dt} = k_i \cdot f_w \cdot f_T \cdot (m_{rC})_i \quad (13)$$

in which $d(m_{rC})_i$ is the carbon in the respective pools [gm/m²], i is the pool index, k_i is a parameter of maximum daily decomposition rate. The parameters f_w and f_T reflect the effects of soil water content and daily mean soil temperature on decomposition rate (Smith, 1992). The nitrogen model is coupled with the carbon model assuming that most nitrogen is bonded to carbon. The nitrogen model includes fixation by air and plant processes as well as nitrification and denitrification, which are related to water content, temperature and concentrations of ammonium and nitrogen.

3.2.6 Solute transport

A convective transport model operating in parallel with the water movement model simulates the movement of solutes. The solute transport is modelled with the following differential mass-conservation equation assuming equilibrium adsorption:

$$\frac{d}{dt}C_w(V + c_h K_d M_s) = C_i Q_i - C_o q_o \quad (14)$$

where C_w is the solute concentration [kg/l], K_d is an adsorption coefficient [kg/l], M_s is the mass of soil layer [kg/ha], c_h is a conversion factor, q and C are the flow and the concentration, respectively, in or out of a layer with the subscripts i and o representing inflow and outflow (Smith, 1992).

3.2.7 Plant growth

The mechanistic plant-growth model integrated in OPUS relates daily dry matter production to four major factors related to plant development:

$$\Delta pm = c_e \cdot f_e \cdot f_a \cdot f_m \cdot \tau \cdot R_i \Delta t \quad (15)$$

in which c_e is a conversion coefficient, f_e , f_a and f_m are factors for energy-conversion efficiency, for plant age and plant size, respectively, τ is a stress factor, taking into account water, nutrients and temperature stresses, R_i is the daily radiation [ly] and Δt is the time increment [day] (Smith, 1992).

3.3 The weather generation model WGEN

Climate data are a prerequisite to drive a physically-based continuous simulation model. As soon as one wants to perform a simulation over several decades, the lack of long time series of climate data is often a problem. For this reason, OPUS comprises the weather generation model WGEN (Richardson and Wright, 1984). However, for this study it is decided to use the WGEN model external because in this case we have the opportunity to create a combined data set of generated and measured data.

The fundamental idea of the WGEN model is that temperature and radiation changing from day to day are related to each other and to the occurrence of rainfall. The model calculates the statistical features of observed time series and the generally observed correlations between physically-related variables.

3.3.1 Occurrence of rainfall

The daily occurrence of rainfall is simulated as a Markov chain process, calculating the binary sequence of wet days and dry days using transition probabilities:

$$\begin{aligned} P_i(D/W) &= 1 - P_i(W/W) \\ P_i(D/D) &= 1 - P_i(W/D) \end{aligned} \quad (16)$$

where $P_i(D/W)$ and $P_i(D/D)$ are the probabilities of a dry day given a wet day on day $i-1$ and the probability of a dry day given dry day on day $i-1$, respectively. These probabilities change with seasonal climatic variations, so that a time series of at least five years is needed to calibrate the model sufficiently.

3.3.2 Amount of rainfall

The likely amount of rain for each occurrence is estimated by a two-parameter function for the gamma probability density, which is modified by a stochastic component generating seasonal variation:

$$f(p) = \frac{p^{\alpha-1} \cdot e^{-p/\beta}}{\beta^\alpha \cdot \Gamma(\alpha)}, p, \alpha, \beta > 0 \quad (17)$$

where $f(p)$ is the density function of p , α and β are distribution parameters, and $\Gamma(\alpha)$ is the gamma function of α . The shape of the distribution function is appropriate for precipitation amounts since small amounts occur more frequently than larger amounts (Richardson and Wright, 1984). To achieve variations during the year, the four precipitation parameters are varied from month to month.

3.3.3 Temperature and radiation

The model, assuming that daily values of temperature and radiation are autoregressively-related, calculates these quantities with the following equation:

$$x_i(j) = A_{x_{i-1}}(j) + B_{\varepsilon_i}(j) \quad (18)$$

where $x_i(j)$ is a 3x1 matrix for day i whose elements are residuals of maximum temperature ($j=1$), minimum temperature ($j=2$), and radiation ($j=3$), ε_i is a 3x1 matrix of independent random components, and A and B are 3x3 matrices whose elements are defined in a way that the new sequences have the desired serial-correlation and cross-correlation coefficients. Using two sets of correlations for either dry or wet days, the values are calculated with a Fourier model.

3.4 The HEC-6 model

The HEC-6 model is able to simulate a discharge hydrograph as a sequence of steady flows of variable duration (USACE, 1991). Based on the continuity equation of mass, changes in sediment transport are one-dimensionally calculated with respect to time and distance along the study reach. For the simulation, the whole reach is subdivided into several sub-reaches, each having specified cross-sections. Simulated processes include total sediment load, volume and gradation of sediment that is scoured or deposited, armouring of the bed surface, and the cross section elevations. In addition, sediment outflow at the downstream end of the study reach is calculated.

3.4.1 Hydraulic calculations

The calculation of flow hydraulics (e.g. width, depth, energy slope, and flow velocity) is indispensable for the sediment transport simulation. Water surface profiles are calculated for each flow using a standard-step method to solve the energy and continuity equations (USACE, 1991). The continuity equation can be formulated as follows:

$$\frac{\partial Q}{\partial x} + \frac{\partial A}{\partial t} = 0 \quad (19)$$

where Q is the runoff [m³/sec], A is the cross section area [m²], x is the length of a sub-reach [m] and t is the time [sec]. The one-dimensional energy equation is used for the unsteady routing of the reach water:

$$Se = \frac{\partial WE}{\partial x} + \frac{\partial}{\partial x} \left(\frac{\alpha v^2}{2g} \right) \quad (20)$$

where Se is the energy slope [-], g is the acceleration of gravity [m/sec²], WE is the water surface elevation [m], v is the velocity [m/sec], x is the length of a sub-reach [m] and α the velocity distribution coefficient [-]. According to the standard step method, the hydraulic parameters are calculated at each cross-section for each successive discharge solving the energy equation as follows:

$$WS_2 + \frac{\alpha_2 v_2^2}{2g} = WS_1 + \frac{\alpha_1 v_1^2}{2g} + h_f + h_o \quad (21)$$

with the indices 1 and 2 denoting two cross sections, whereas h_f and h_o represent energy losses due to friction and hydraulic contractions and expansions [-], respectively. Friction loss is calculated by Manning's equation:

$$h_f = \left(\frac{2nQL^{1/2}}{1.49(A_2 + A_1) \cdot ((R_2 + R_1)/2)^{2/3}} \right)^2 \quad (22)$$

where R_1 and R_2 are the downstream and upstream hydraulic radius [m], respectively, L is the length of reach section [m] and n is Manning's roughness coefficient [-]. Thus the total hydraulic roughness - including effects of grain roughness, bends, junctions, ripples, bank irregularities and vegetation - is described by a single Manning's n for each cross-section. Energy losses due to contractions and expansions are computed by the following equation:

$$h_o = C_L \left| \frac{a_2 V_2^2}{2g} + \frac{a_1 V_1^2}{2g} \right| \quad (23)$$

with C_L being a loss coefficient for expansion or contraction [-].

3.4.2 Sediment calculations

3.4.2.1 The concept of active and passive layer

The primary restrictions on rate of scour are the thickness of erodible bed material and the amount of surface area armoured. HEC-6 implements the concept of an active and an inactive bed layer. The active layer denotes the bed material between the bed surface and a hypothetical depth where no transport occurs for the given gradation and flow conditions. The active layer is assumed to be continually mixed by the flow, but it can have a surface of slow moving particles that shield the finer particles from being entrained in the flow (armouring). Exchange of sediment particles can occur between the bed sediment particles and the fluid-sediment mixture due to the energy in the moving fluid or between the active layer and the inactive layer due to the movement of the bed surface.

The minimum energy condition for negligible sediment transport for a particular grain size and thus the depth of the active layer ("equilibrium depth") D_e [m] for a particular grain size class d [mm] is calculated by a combination of Manning's, Strickler's and Einstein's equations (USACE, 1991):

$$D_e = \left[\frac{q}{10.21d^{1/3}} \right]^{6/7} \quad (24)$$

with q being the water discharge per unit width.

3.4.2.2 Bed material gradation

The changes in composition of the bed material (gradation) can be computed by two methods. The first method calculates the depth of scour within the active layer accumulating a sufficient amount of coarse surface material to armour the bed as follows (USACE, 1991):

$$D_{SE} = \left(\frac{2}{3}\right) \cdot \left[\frac{SAE \cdot d_a}{PC} \right] \quad (25)$$

where D_{se} is the depth of bed material which must be removed to reach equilibrium, SAE is the ratio of surface area of potential scour to total surface area, d_a is the smallest stable grain size in armour layer and PC is the fraction of material coarser than d_a . When all material is removed from the active layer, the bed is completely armoured for that hydraulic condition. If in the next time-step the calculated depth of the active layer is greater than the existing depth, sediment is added to the active layer from the inactive layer. In the reverse case sediment is removed from the active layer and added to the inactive layer.

If an armoured layer overlies fine bed material dominated by coarser grain sizes, their rate of movement is constrained by their availability and thus cannot be calculated from the flow hydraulics. In this case the stability of the armoured layer is computed using a normal probability function (USACE, 1991):

$$BSF = \frac{\sum_{i=1}^{NGS} PROB^2 \cdot P_i \cdot d_{mi}}{\sum_{i=1}^{NGS} PROB \cdot P_i \cdot d_{mi}} \quad (26)$$

where BSF is the bed stability coefficient [-], d_{mi} is the median grain diameter for grain size class i [m], NGS is the number of grain sizes present, P is the fraction of bed composed of a grain size class and PROB is the probability that grains will stay in the bed. If a partially armoured bed is stable for a given hydraulic condition, material is taken from the active layer until enough stable grains are left to cover the bed to the depth of a stable grain size. Otherwise, the layer is destroyed and a completely new active layer is calculated.

The second method introduces a subdivision of the active layer into a cover layer and a sub-surface layer. It is presumed that during the progress towards an equilibrium condition the thin cover layer is getting coarser and thus regulates the entrainment of finer particles from below. Both methods have disadvantages and the user is challenged to find out which one is the best for his particular case.

3.4.2.3 Vertical bed movement

The basis for the simulation of vertical movement of the bed is the Exner sediment continuity equation (USACE, 1991):

$$\frac{\partial G}{\partial x} + B_o \cdot \frac{\partial Y_s}{\partial t} = 0 \quad (27)$$

where B_o is the width of the movable bed, G is the average sediment discharge [m^3/sec], x is the distance along the channel and Y_s is the depth of sediment. Sediment transport potential is calculated for each grain size class in the bed. If transport capacity is greater than the load entering a control volume, available sediment is removed from the bed to satisfy continuity.

3.5 Methods for model validation

Many statistical measures have been developed for an objective validation of model results. One of the most frequently used indices is the Pearson product-moment correlation coefficient, which is often the basis for other indices:

$$r_{qq'} = \frac{N \sum_{i=1}^N q_i \cdot q'_i - \left(\sum_{i=1}^N q_i \right) \cdot \left(\sum_{i=1}^N q'_i \right)}{\sqrt{N \cdot \sum_{i=1}^N q_i^2 - \left(\sum_{i=1}^N q_i \right)^2} \cdot \sqrt{N \cdot \sum_{i=1}^N q_i'^2 - \left(\sum_{i=1}^N q'_i \right)^2}} \quad (28)$$

where q is the measured discharge, q' is the simulated discharge, N is the number of comparisons and $r_{qq'}$ is the Pearson correlation coefficient. Willmott (1981) provided arguments against its use as a comparative measure of performance because of the possibilities of obtaining higher values of $r_{qq'}$ which may even be statistically significant

despite the possibility that both the magnitude and the distribution of residuals can be unacceptable.

In order to improve r_{qq} , McCuen & Snyder (1975) combined the Pearson correlation coefficient with the ratio of the standard deviations of the two hydrographs resulting in the following term:

$$r_{mqq'} = r_{qq'} \cdot \sqrt{\frac{\sum q^2}{\sum (q')^2}} \quad (29)$$

The modified Pearson correlation coefficient is more demanding as it takes into account the differences in the size of the compared hydrographs.

Another coefficient is the index of agreement (IA) (Willmott, 1981), which is bounded between zero and one, relative, and capable of measuring the degree to which model predictions are error-free :

$$IA = 1 - \frac{\sum (q - q')^2}{\sum (|q - \bar{q}| + |q' - \bar{q}|)^2} \quad (30)$$

A further widely accepted criteria is the coefficient of model efficiency (CME) (Nash and Sutcliffe, 1970):

$$CME = \frac{\sum (q - \bar{q})^2 - \sum (q' - q)^2}{\sum (q - \bar{q})^2} \quad (31)$$

The values of CME ranges between 1, indicating a perfect reproduction of the measured data, and negative values, indicating that the mean value is a better predictor than the model used (Imam, 1994).

The validation of a model should always be a multi-criteria analysis, which means that not only one model output, e.g. the runoff amount at the catchment outlet, should be a criterion for judging the quality of a model. However, in most cases, only time series of measured state variables are available for validation.

4 Analyzing the fluxes of matter

The aim of this chapter is to present certain quantities that were measured within the research project B14 in the catchment of the Wahnbach River, and to analyze the underlying processes determining the fluxes of matter. Process understanding is essential for a subsequent modelling because it is necessary to adjust a model to local peculiarities in order to obtain realistic simulation results.

4.1 Processes at the event scale

In the following sections the measurements in the Berrensiefen basin are taken into consideration in order to analyze the processes determining solute and sediment transport at the sub-catchment scale. This sub-catchment is chosen because it represents the Wahnbach catchment very well; since pasture is predominate in both basins. Furthermore, it is the best-investigated sub-catchment of the Wahnbach catchment.

4.1.1 The research area Berrensiefen

Fig. 15 shows the Berrensiefen basin and the location of the installed instruments (gauging station and precipitation gauge).

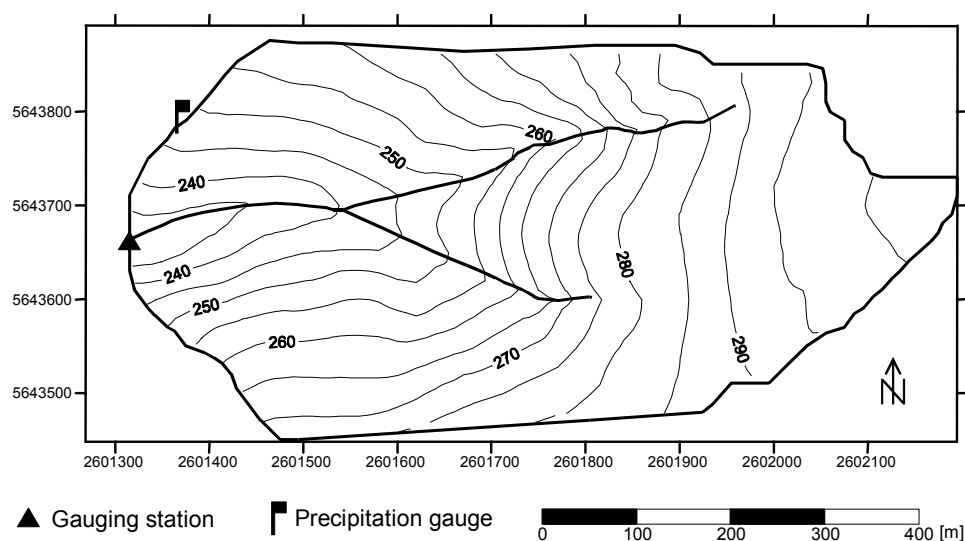


Fig. 15: The catchment of Berrensiefen with the installed gauging station and precipitation station.

The altitude in the sub-catchment rises from about 235 m at the outlet up to about 300 m at the eastern boundary of the catchment. In the western part, a small valley plane is located along the brook course. East of the junction, wooded deep valley cuts have developed.

The landuse of the Berrensiefen catchment (Fig. 16) covering an area of about 0.29 km² is dominated by pasture (ca. 79 %) and forest/bush (ca. 18.4 %). Settlements and roads cover the remaining area (approx. 7800 m²).

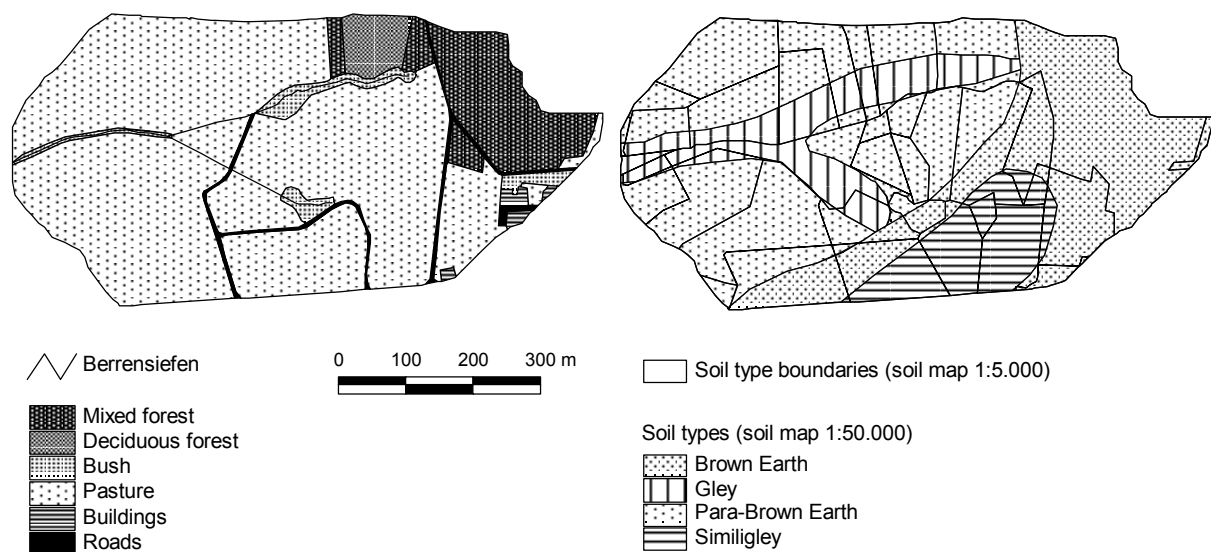


Fig. 16: Landuse distribution and soil type distribution (scale of 1:5,000 and 1:50,000) of the Berrensiefen catchment.

The small-scale soil map (1:50,000) reveals four kinds of soil types (Fig. 16). Gley soils can be found in the valleys, whereas brown earth and similigley soils are located in the flat upland areas. The steeper hillslopes are mainly covered by para-brown earth soils.

Due to the small scale of the soil map, both a generalisation and a distortion result in comparison to the large-scale soil map (1:5,000), which can effect solute transport calculations. For example, gley soils are a potential sink for nitrogen because they are often water saturated, which causes an increased denitrification rate. For that reason, a correct description of the extent of gley soils may be important in calculating nitrogen transport. In the small-scale map the area of the gley soils is three times larger than in the soil map with a scale of 1:5,000. Furthermore, field studies of soil type distribution have shown that even the extent of Gley soils in the large-scale map may be overrated.

In August 1998 the catchment of the Berrensiefen (Fig. 1) was instrumented with a gauging station and a precipitation gauge for the continuous measurement of rainfall, discharge rate as well as conductivity and temperature of runoff water.

For a better reproduction of solute transport processes, an additional probe has been installed for the continuous measurement of nitrate concentration. The gauging of nitrate is facilitated through an ion-selective probe, which can be connected with the logger through an additional amplifier unit. To compensate for the ageing of the probe, a new calibration has to be carried out every week. The probe has an exactness of about 5-15 % depending on the nitrate concentration, and its lifespan is given as being one year.

To provide the chemical and physical properties of the soils and their variability a detailed soil survey in the test area Berrensiefen was undertaken. About 180 soil samples were taken from two horizons (A_h - and B_v -horizon) covering the whole test area. Among other properties texture, soil organic matter and contents of nitrate and phosphate have been measured. Furthermore, an intensive soil survey was carried out on one hillslope to provide the spatial variability of important soil hydraulic parameters (Herbst and Diekkrüger, 2001). The location of the 20 samples taken from the A_h - and B_v -horizons is shown in Fig. 17.

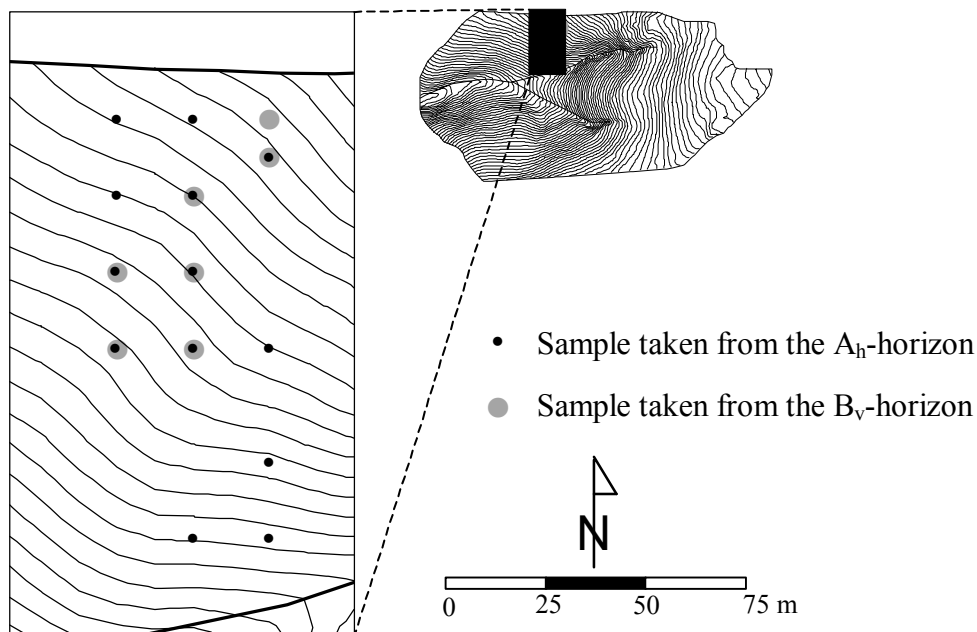


Fig. 17: Sampling location of soil probes for K_s -measurement.

The frequency distribution of the measured saturated soil-hydraulic conductivity (K_s -values) of the samples is displayed in Fig. 18.

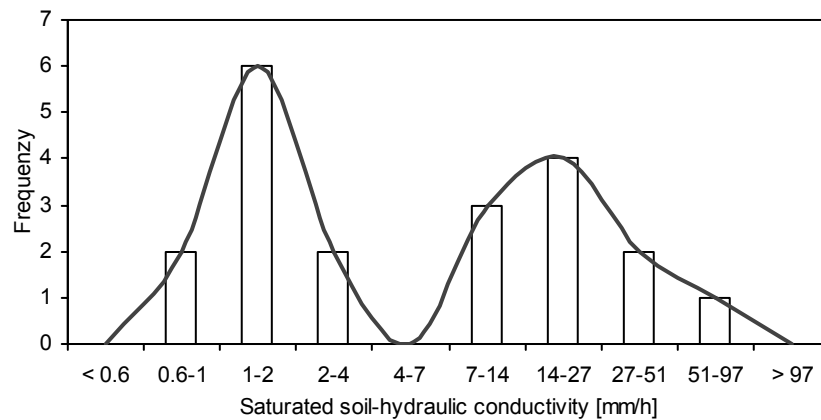


Fig. 18: The frequency distribution of the measured saturated soil hydraulic conductivity of the A_h -horizon and B_v -horizon (20 samples).

Fig. 18 reveals the strong influence of macropores on the value of K_s leading to a bimodal frequency distribution with a first K_s -maximum between 1 and 2 mmh^{-1} and a second K_s -maximum between 14 and 27 mmh^{-1} . The first maximum represents the K_s -value of the soil matrix and the second one is the result of the macropore system, which is mainly formed by earthworms. Therefore it is convenient to distinguish between a saturated hydraulic conductivity (K_s^*) of the soil matrix and of the macroporous soils (K_{sat}), which is much greater than K_s^* (McDonnell, 1990).

In addition, a large number of field voles have formed a dense network of channels on the slopes that are capable of draining large amounts of the infiltration excess into the soil-bedrock interface. Once free water exists in this area, pipes in the lower soil zones transport the perched water downslope, producing a rapid through-flow response that is called interflow.

4.1.2 Runoff generation

In this chapter some rainfall occurrences inducing a certain discharge response of Berrensiefen are analyzed in order to examine the underlying processes. Additionally, the evolution of the dissolved chemicals is used to confirm process theory.

In this context, chemical evolution is defined by the changes in concentration of chemical constituents that occur as water moves along flow paths and interacts with biological and geological media (Burns et al., 1998).

4.1.2.1 Convective rainfall events

Fig. 19 shows the measured quantities runoff, nitrate and conductivity from 21.06.00 at 12:00 until next day at 12:00.

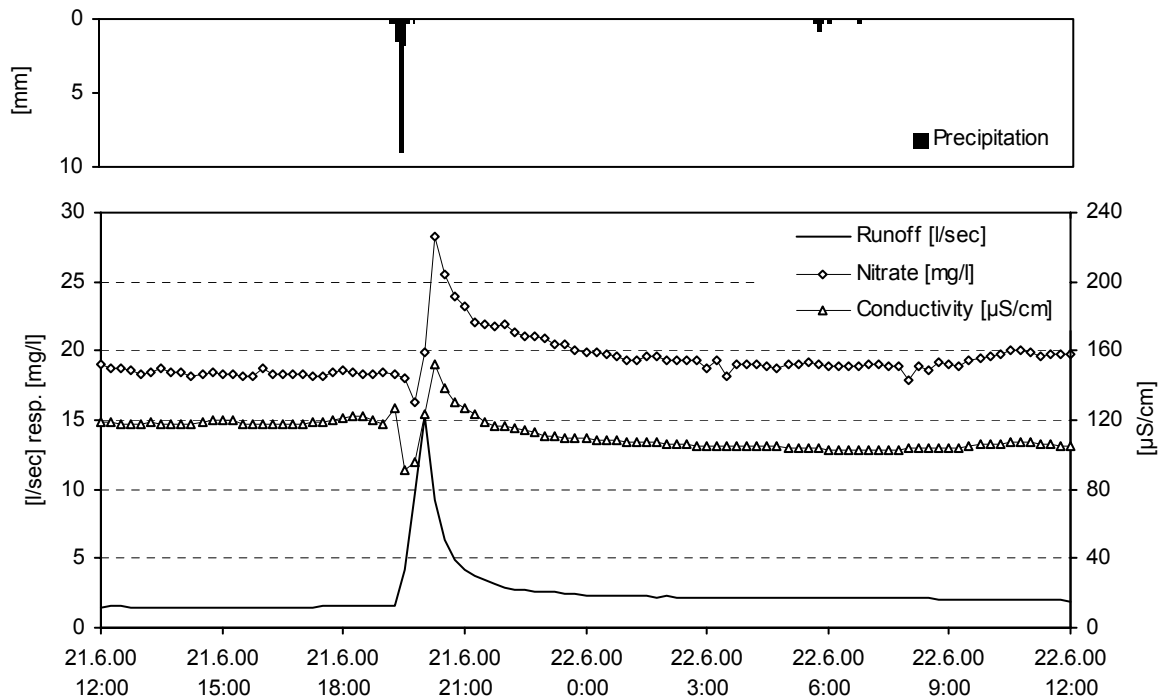


Fig. 19: Sequence of the continuously measured quantities precipitation, runoff, nitrate and conductivity in the sub-catchment Berrensielen from 21.06.2000 until 22.06.2000.

During the previous two weeks a total rainfall amount of only 6.25 mm and a daily average air temperature of 15.7 °C was measured; thus it can be expected that the soils have been significantly dried up. As a result the discharge rate was at a very low level (1.48 l/sec), just slightly below the lowest runoff rate ever gauged in the whole measuring period (1.10 l/sec) on 3.6.2000. Fig. 19 reveals the response of the catchment after a convective rainfall event, which had a total rainfall amount of 13.25 mm and a peak intensity of 108 mm/h. The relatively low runoff rate (about 1.5 l/sec), which is predominantly comprised of deep groundwater discharge, rises immediately after the rainfall has started. This can be explained to some extent by direct runoff from the roads going through the sub-catchment and draining directly into the Berrensielen. Using a linear baseflow-separation enables a total volume of overland flow of about 42.9 m³ to be calculated.

Making use of the relation of direct runoff volume and precipitation amount, which falls simultaneously relative to the occurrence of direct runoff, it is possible to calculate the maximal area producing direct runoff:

$$A_d = \frac{V_d}{P} \quad (32)$$

where A_d [m²] is the area affected by direct runoff, V_d [l] is the volume of calculated direct runoff and P [mm] is the precipitation amount producing direct runoff.

Therefore the necessary area to produce this direct-runoff volume has to be 3250 m² at maximum. The asphalted roads, which most likely produce direct-runoff, cover an area of approx. 1560 m². This is less than half of the calculated direct-runoff area, indicating that Hortonian overland flow on the hillslopes has occurred to a certain extent.

This assumption is also confirmed by the course of the conductivity and the nitrate concentration. During the rise of the runoff both the conductivity, reflecting the total dissolved load of matter in the surface water, as well as the nitrate concentration display a S-shaped curvature. This behaviour can be used for a conceptual consideration of the sequence of the involved processes.

The decrease of both quantities immediately after the rise in the discharge can be explained with a dilution effect induced by direct runoff water of low solute concentration from the sealed areas. After about 30 minutes both quantities rise considerably, especially the nitrate concentration (from 16.4 mg/l up to 28.3 mg/l). The reason for this increase can be interpreted as evidence of the occurrence of Hortonian overland flow on the hillslopes. The hillslopes are mainly used as pastureland, and therefore fertilizing with inorganic and organic manure is common. Additionally, faeces of livestock are observed especially in the area of the valley plains. Some of this matter may be washed out by the Hortonian overland flow, increasing the nitrate concentration of the stream water. Peter (1988) also observed this effect in the catchment Eschbachsiefen, which is located in the Wahnbach catchment as well.

The chemical response reaches the highest point 15 minutes after the runoff peak. This hysteresis effect reflects the different velocities of the involved processes, thus direct runoff from the roads being earlier than the Hortonian overland flow from the hillslopes. The direct runoff is faster because the roughness of the road surface is lower than the overgrown surface of the hillslopes. Furthermore, the initiation of the Hortonian overland flow may be somewhat delayed through extensive infiltration into the dry soils.

About 5 hours after the rainfall event, the discharge reaches a relatively constant rate of about 2.2 l/sec; thus being about 32 % higher than before the rainfall event. Therefore it can be concluded that the soils of the catchment were not able to absorb the rainfall water, inducing considerable subsurface flow with fast water flow through macropores being perhaps involved. Consequently, water from the hillslopes may be transported quickly to the surface-near groundwater body in the valley plain, and this leads to an increased discharge rate.

Also nitrate concentration and conductivity reach relatively constant values that are both different from the values before the rainfall event. The new level of nitrate concentration is slightly higher than before, whereas the conductivity is about 13 % lower. It can be concluded that the subsurface flow causes a change of the chemism of the stream water with percentage distribution of nitrate being increased. This may be caused by the discharge of the surface-near groundwater body into the valley plain, which gathers nitrate coming from the surrounding hillslopes by interflow, and therefore has higher nitrate concentration than the deeper groundwater.

Fig. 20 shows a section of the recorded quantities beginning on 24.07.00 and ending on 30.07.00, thus about one month later than the above-described event.

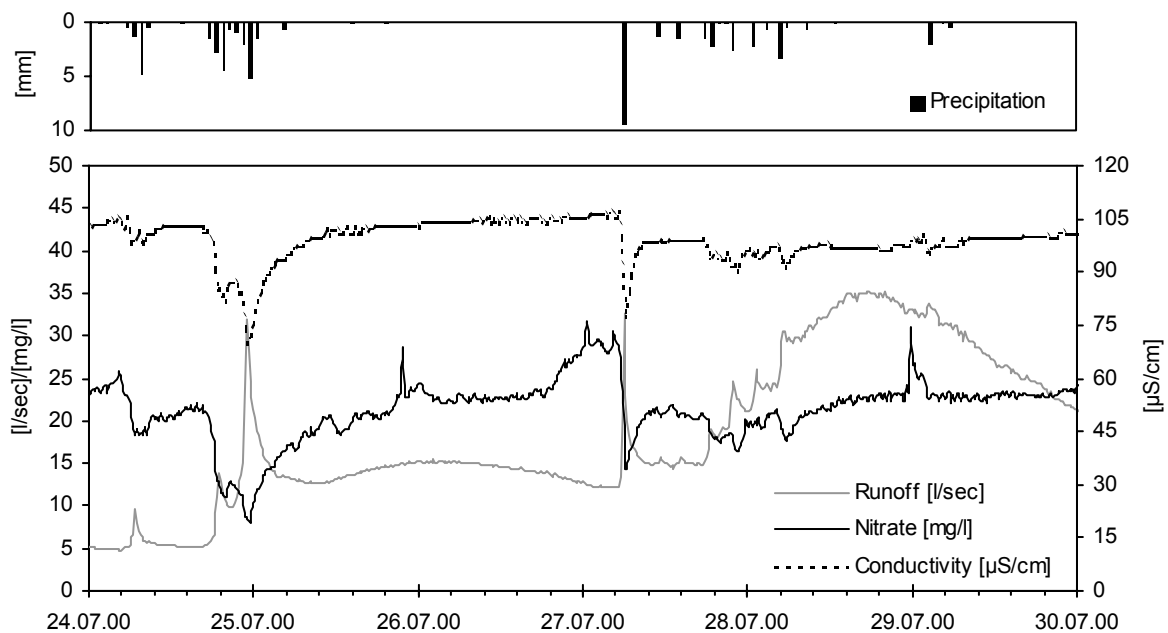


Fig. 20: Sequence of the continuously measured quantities precipitation, runoff, nitrate and conductivity in the sub-catchment Berrensiefen from 24.07.2000 until 30.07.2000.

During the previous two weeks a total precipitation amount of 74.75 mm was recorded, indicating that the soils are significantly wetter than in the previous case. This period is characterized by a relative high rainfall amount of totally 58.75 mm, concentrated at the beginning and in the middle of the sequence. The highest rainfall intensity was measured on 27.07.01 at 17:05 with a peak rainfall intensity of about 66 mm/h.

Two main precipitation events with a duration of about one day can be distinguished, each leading to a characteristic runoff response behaviour. Sharp peaks can be recognised in the hydrograph corresponding to the highest rainfall intensities, again indicating the contribution of direct runoff from the sealed area. During these events both nitrate concentration and conductivity are decreasing, thus Hortonian overland flow appears to be insignificant because rainfall intensities are not high enough. Furthermore, in both cases a smooth peak can be recognized about one day after rainfall has ceased. This phenomenon is a result of the interflow process, which can contribute up to 70 % of the total runoff amount from hillslopes used as grazing land (Flügel and Schwarz 1988).

The first peak is not so distinct as the second one although both rainfall events have equal rainfall amounts (28.25 mm and 30.5 mm) and rainfall intensities are also similar.

The change of the chemical properties of the stream water can be used for the calculation of the direct runoff volume using the following equation:

$$q_d = \frac{(C_m - C_b) \cdot q_m}{C_p - C_b} \quad (33)$$

where q_d is the direct runoff, C_m is the measured conductivity and nitrate concentration, C_b is the conductivity and nitrate concentration of the baseflow, respectively, q_m is the measured discharge and C_p is the conductivity and nitrate concentration of the precipitation, respectively.

By using the measured conductivity as well as measured nitrate concentration, a hydrograph separation of the direct runoff of the 25.07.00 event from the total discharge is carried out (Fig. 21).

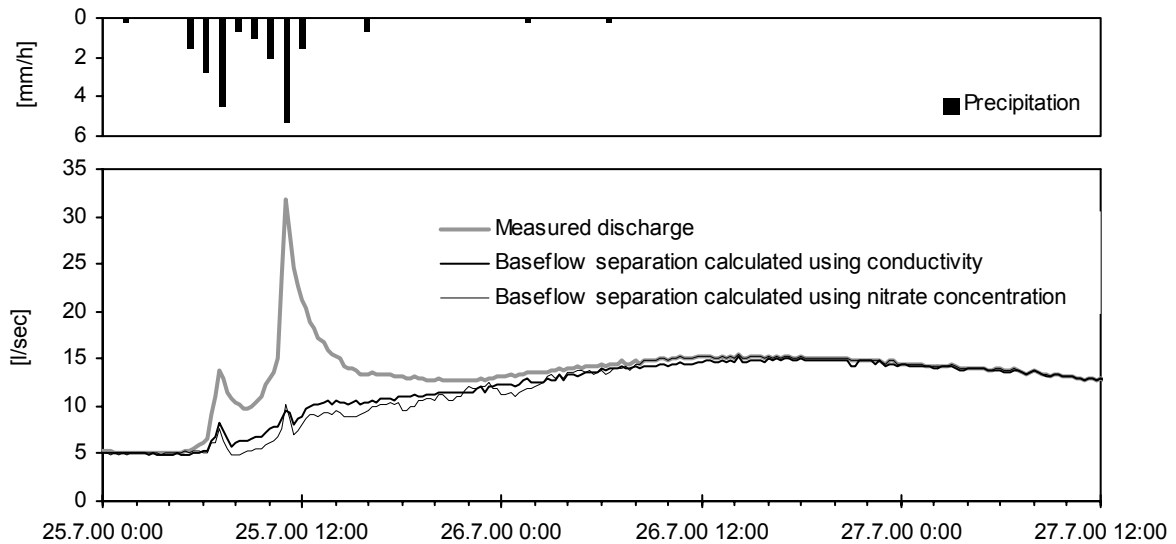


Fig. 21: Separation of the direct runoff from the total discharge using the measured conductivity and nitrate concentration.

To solve equation (33), conductivity and nitrate concentration of the rainfall water were set to $55 \mu\text{S}/\text{cm}$ and $2.5 \text{ mg}/\text{l}$, respectively. The direct runoff volume calculated from conductivity is about 349 m^3 , whereas the calculation using the nitrate concentration results in a value of about 379 m^3 . Hence the comparison indicated an accuracy of this methodology for hydrograph separation of about 10 %.

The calculated direct runoff contributing area using equation (32) is 1.74 ha and 1.89 ha, respectively. Thus, although no increase of conductivity or nitrate concentration is observed, like during the event described above, Hortonian overland flow may be produced on a proportion of the hillslopes. Two reasons may explain this finding. On the one hand fertilizer may be dissolved and washed out into the soils during previous rainfall events. On the other hand, the quantity of overland flow might have been high enough to compensate for additional chemicals from fertilizations. Furthermore, it has to be taken into account that some dilution effect may result from lower concentrated subsurface flow water and therefore the methodology may be somewhat improper in separating direct runoff.

The first interflow peak is less distinct with a peak discharge rate of about 15 l/sec than the second one with a peak discharge rate of about 35 l/sec (Fig. 21), although produced by more or less the same rainfall amount. One reason is the fact that the rainfall events are relatively close together, thus the discharge rate was still increased when the second event started. But this effect explains only approx. 25 % of the total difference. The main reason for the

sharpened course of the second peak is the increased water content of the soils. Interflow is mainly produced by the presence of macropores accelerating the water movement through the soil layer (e.g. Germann, 1990). Assuming that the soils are dry, some of the water draining through these macropores will be infiltrating in the surrounding soil matrix; thus interflow rate will be low. On the other hand, in the case that the soil matrix is saturated to some extent through a previous rainfall event, infiltration into the soil matrix will be reduced or absent and thus interflow rate will be significantly lower. Consequently, during dry conditions, the effect of an absorbing matrix should be taken into account in calculating the interflow discharge rate.

4.1.2.2 Extreme rainstorm events

Fig. 22 shows the courses of runoff, conductivity as well as rainfall amount and intensity in September 1998. During this month a precipitation amount of 239 mm in total was observed at the rainfall gauge within the Berrensiefen catchment, which is more than the threefold of the average regional precipitation amount (see Fig. 12, Chapt. 3.1.2), stressing the peculiarity of this month.

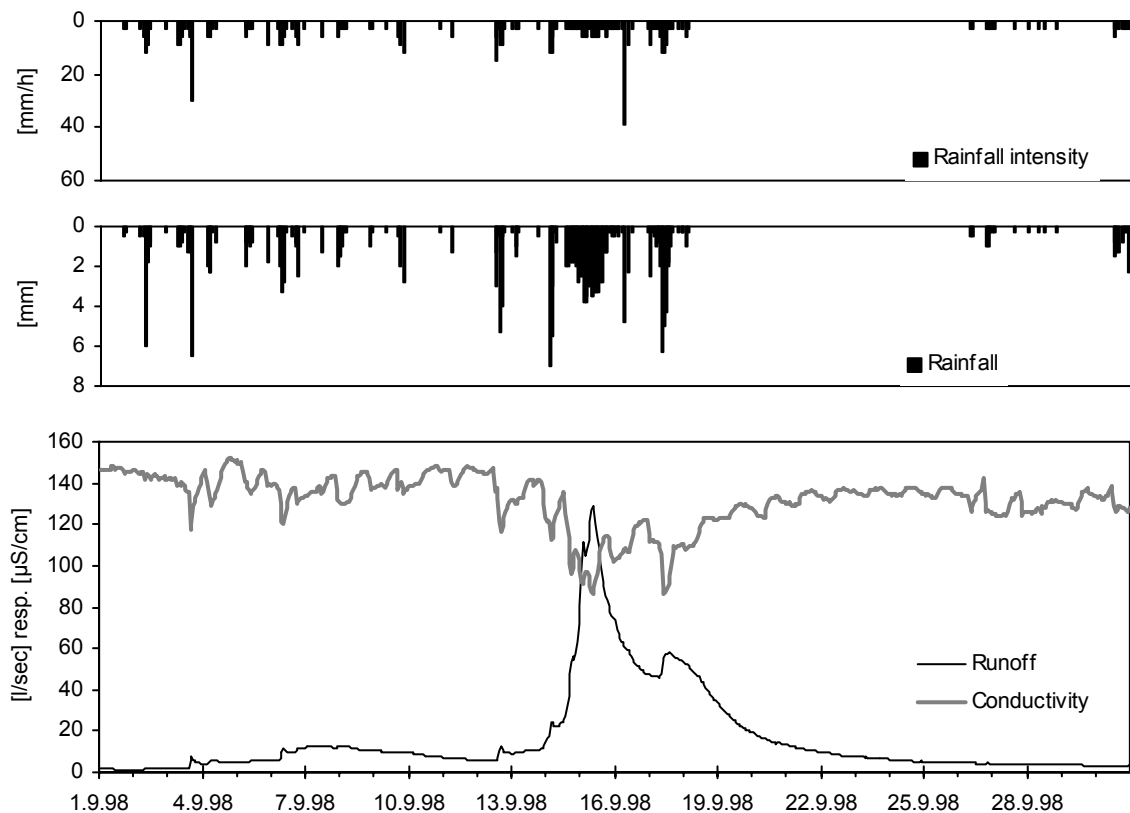


Fig. 22: Runoff, conductivity, rainfall amount and rainfall intensity measured in September 1998.

Despite this high rainfall amount the rainfall intensities were, excluding two exceptions, lower than 10 mm/h (Fig. 22). Consequently, in this case steady rain was predominant, in contrast to the previous described examples. The highest daily rainfall was observed on 15.09.98 with 56.25 mm and with a maximal rainfall intensity of 6 mm/h inducing a runoff peak of 135.7 l/sec and a daily discharge of 30.2 mm.

Unfortunately the gauging station was somewhat undersized to capture this unexpected dimension of discharge rate. For this reason, water was probably flowing around the settling channel of the station; thus the real maximum peak may be even higher. Furthermore, some driftwood had accumulated within the gauging station, probably influencing the measurement. Nevertheless, the course of the discharge reveals very well the runoff response of this extreme event. The rainfall from 13.09.98 until 17.09.98 (135.75 mm in total) can be assumed as input for the high flow response from 14.09.98 until 30.09.98. In the period from 26.08.98 until 01.09.98 only 3.25 mm rainfall were measured and the daily discharge rate decreases to a value of 1.43 l/sec, which can be used to assess a groundwater discharge rate of about 0.02 mm/day at this time. Subtracting the groundwater discharge from the total runoff discharge, a storm runoff of 107.3 mm can be calculated. The resultant coefficient of discharge is about 79 %, which is realistic under these circumstances.

In contrast to the events described above, there is no second rising of the discharge rate after the rainfall has ceased, except the less evident peak at 07.09.98, showing similar characteristics. Thus just taking the course of discharge rate, no separation of the overland flow components, like direct runoff from the roads and the hillslopes from the slower response of the interflow, can be made.

Because of the low rainfall intensity, it can be expected that no Hortonian overland flow occurred. Otherwise, during the preceding two weeks a total amount of 127.5 mm rain had fallen. Hence the relatively thin soils may have been saturated, especially in the valley plain, prior to the 15th/16th of September 1998 rainfall event. Therefore it can be expected that the discharge was comprised of saturated overland flow to a certain extent. However, since the valley plain in the catchment of the Berrensiefen is limited to the direct surrounding area of the western half of the brook, interflow must be the dominant runoff component contributing to the high discharge event.

The course of the conductivity reveals the existence of different runoff processes. Due to the influence of the direct runoff, the runoff water is diluted to values of about $92 \mu\text{S}/\text{cm}$ during the highest peaks. By means of the separation method described above, a direct runoff volume of approx. 1445 m^3 can be calculated for the 14th and 15th of September 2000 (Fig. 23).

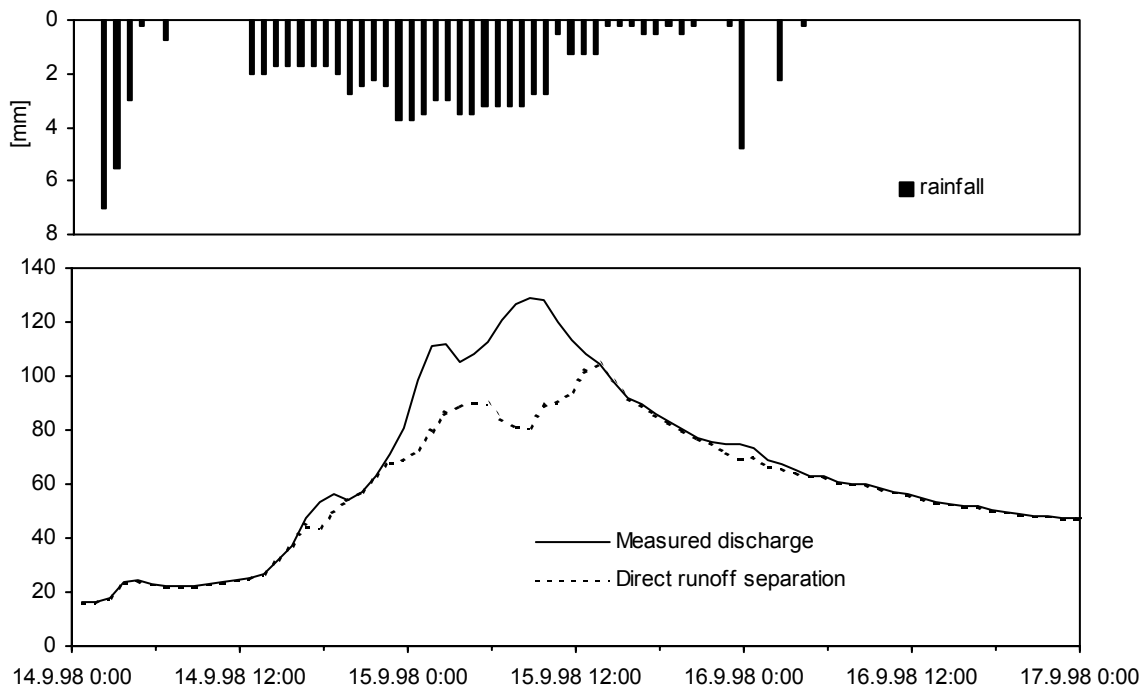


Fig. 23: Separation of the direct runoff from the discharge hydrograph using the measured conductivity.

During the period of overland flow, a rainfall amount of about 63 mm is measured. Considering that the direct runoff is predominantly produced by saturated overland flow, it is possible to roughly calculate the involved area affected by saturated overland flow. In this case, a size of the saturated area of about 2.3 ha results, which is only 8 % of the whole catchment area. This finding indicates that saturated overland flow is restricted only to the valley plain of the Berrensiefen.

Furthermore, Fig. 23 reveals a change in the base flow chemism. On the first five days of the month, runoff and conductivity have mean values of about $3.3 \text{ l}/\text{sec}$ and $142 \mu\text{S}/\text{cm}$, respectively (see Fig. 22). At the end of the month the conductivity fluctuates around approx. $131 \mu\text{S}/\text{cm}$, although runoff has declined to a rate of about $3.3 \text{ l}/\text{sec}$ again.

It can be concluded that due to the rainfall event a considerable displacement of soil water and groundwater took place, and therefore old water of higher concentration was displaced by new water of lower concentration.

4.1.2.3 Comparison with other sub-catchments

In this section, the differences between the sub-catchments Berrensiefen, Hellenkeutelsiefen and Steinersiefen in respect to runoff generation is projected in order to elucidate the influence of geomorphological and landuse characteristics. Additionally, the sub-catchments Schlößchensiefen and Stucksiefen are taken into consideration. They are not instrumented for continuous measurement, but both basins are weekly sampled in order to characterize solute and sediment transport.

In order to characterize the selected sub-catchments some important properties are listed in Tab. 5 (Chapt. 3.1.4), and Figs. 24 and 25 show the slope distribution of each basin. The basin of the Berrensiefen reveals the lowest mean slope value. This finding is also visible in Fig. 24. Generally, the basin can be subdivided into three sections: First of all, there are the hillslopes beside the brook up to its forking into two branches, which show very low slope values in the direct surrounding of the Berrensiefen and maximum slope values of about 10-12 % at the middle hillslopes. The second section stretches to the 280m-isohypse where the channel heads are located. It reveals deep valley cuts in both branches with maximum values of about 22 %. The third section exhibits a relatively less structuring and maximum values of only 6 %.

The other sub-catchments reveal a different morphological shaping, which is indicated through their higher value of mean slope. All basins have in common that they exhibit deep valley cuts along the brook courses. However, the relation between the length of the brook and the catchment area differs considerably, with the basin of Hellenkeutelsiefen having the smallest drainage density (2.6 km^{-1}) and Stucksiefen the greatest value (3.1 km^{-1}). A valley plain in these basins is either restricted to a very low extent or is completely missing. The valley walls are very steep, especially in the basin of the Steinersiefen with slope values over 30 %. The areas of highest slope values are predominantly covered by forest.

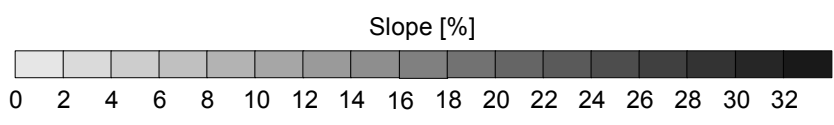
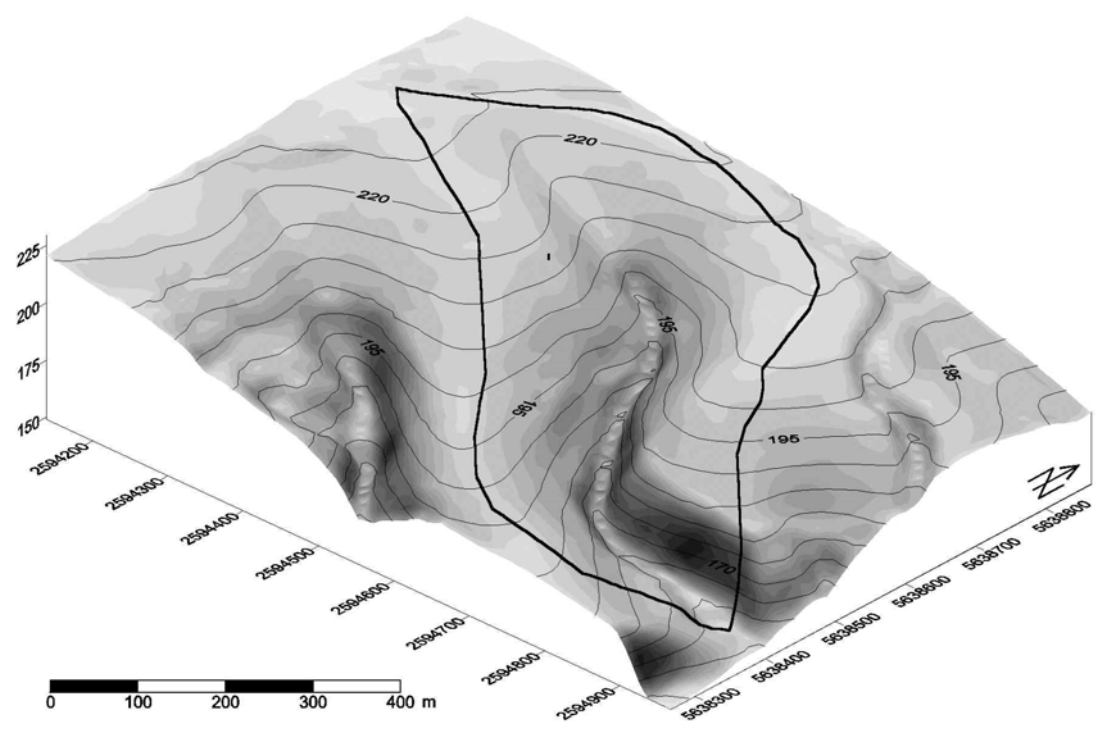
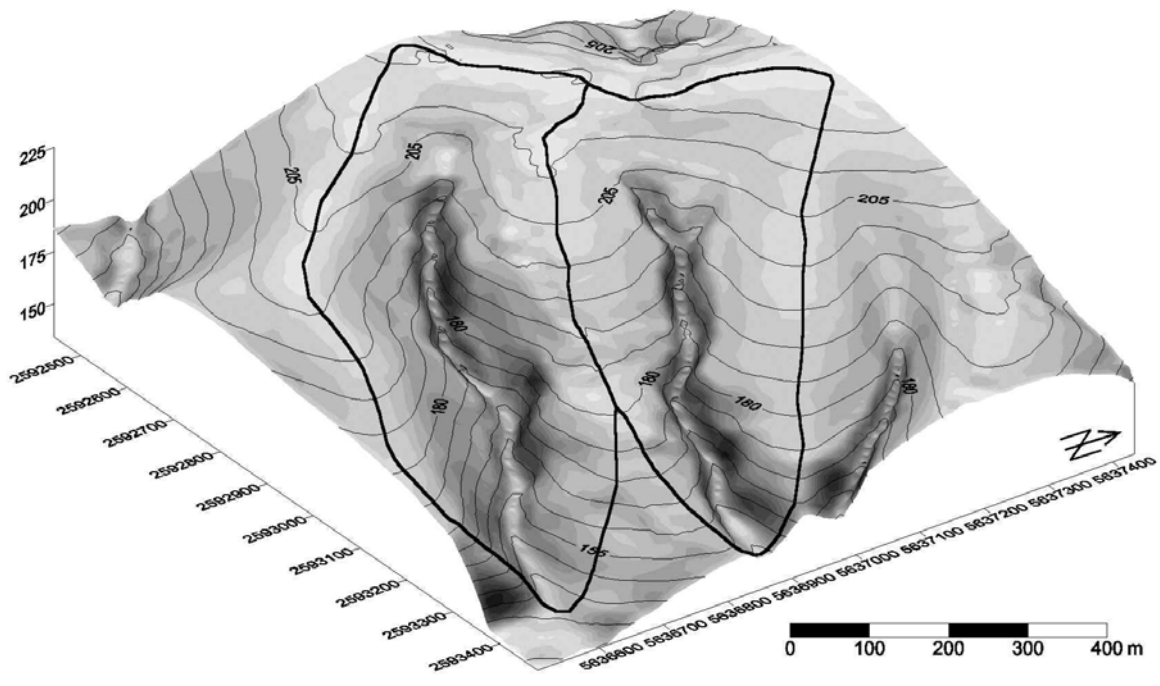


Fig. 24: Block diagrams of the sub-catchments Stucksiefen (above, right), Schlößchensiefen (above, left) and Steinersiefen (below) displaying the slope distribution calculated from a digital elevation model with 5 m resolution; the bold lines mark the basin boundaries.

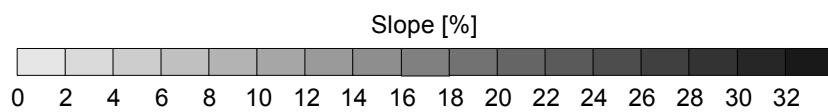
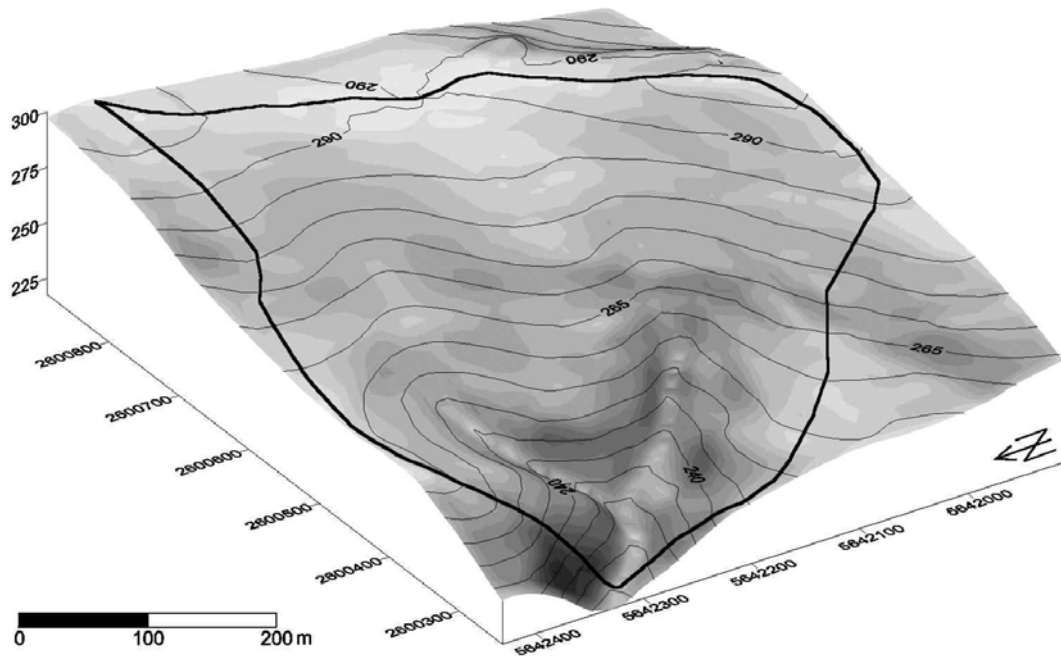
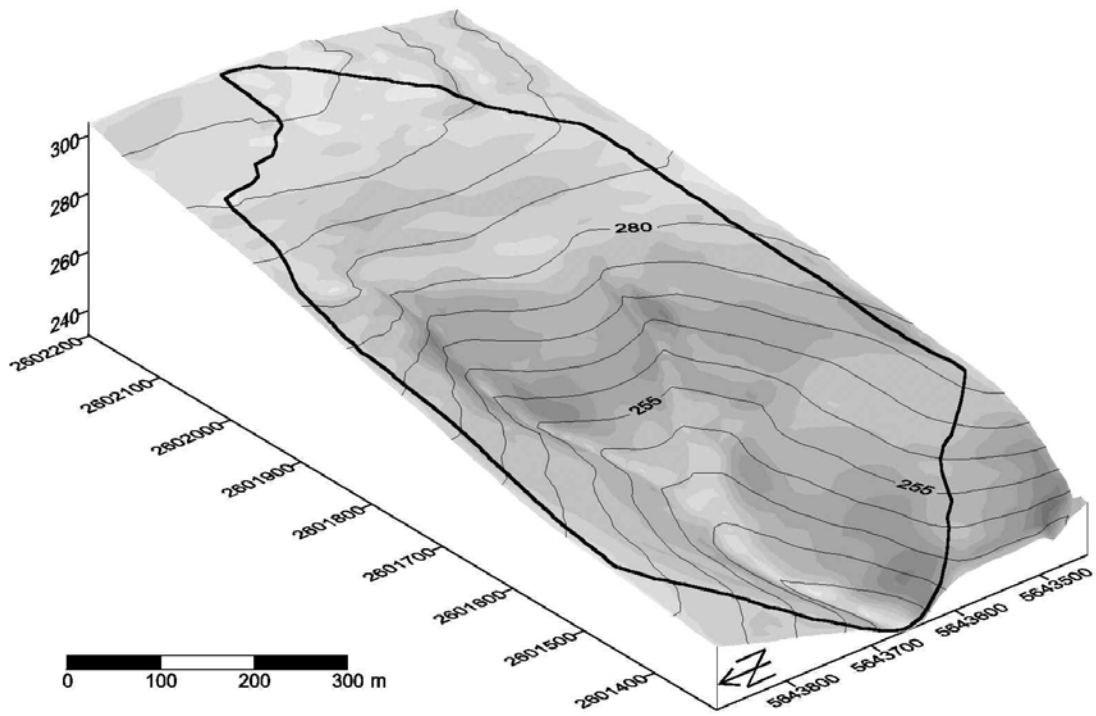


Fig. 25: Block diagrams of the sub-catchments Berrensisiefen (above) and Hellenkeutelsiefen (below) displaying the slope distribution calculated from a digital elevation model with 5 m resolution; the bold lines mark the basin boundaries.

The regional runoff responses during September 1998 of the basins of Berrensiefen (Sub1), Hellenkeutelsiefen (Sub2) and Steinersiefen (Sub3) are presented in Fig. 26 in order to evaluate differences in the runoff generation process.

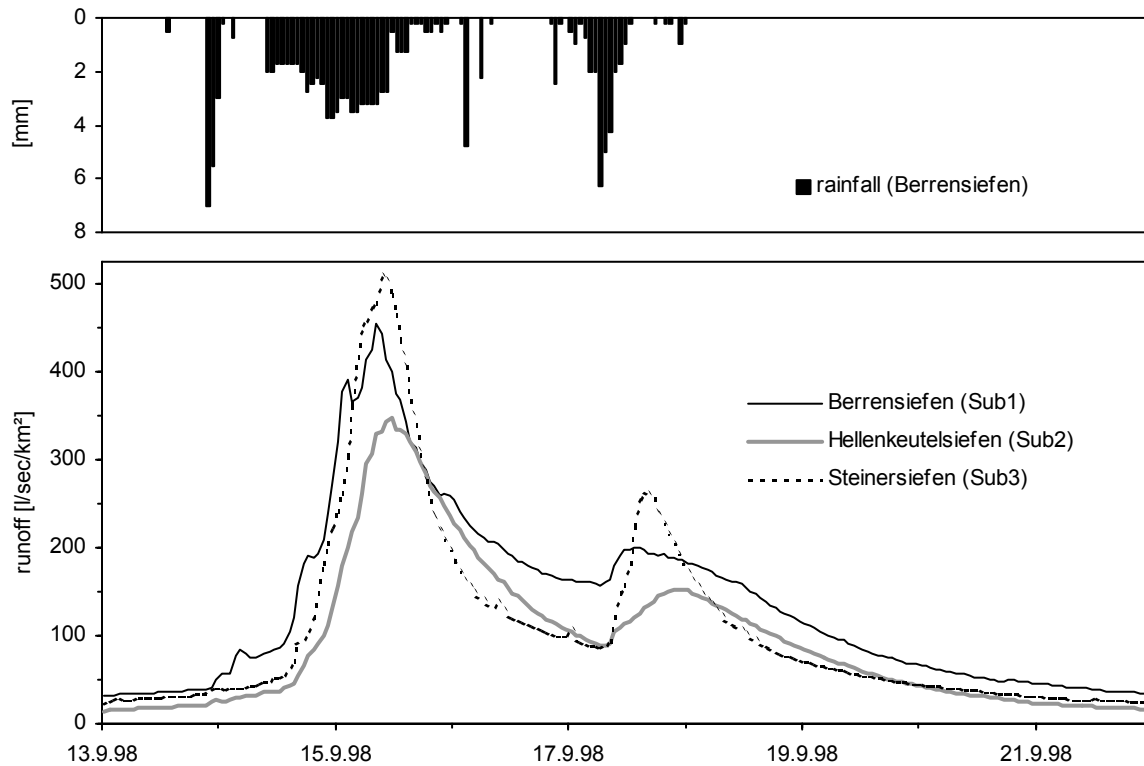


Fig. 26: Regional runoff responses of the sub-catchments Berrensiefen (Sub1), Hellenkeutelsiefen (Sub2) and Steinersiefen (Sub3) from 13.9.98 until 22.9.98.

The rainfall amount from 13.09.98 until 17.09.98 in Sub3 (132.8 mm) was almost the same as in Sub1 (135.75 mm), thus the lower runoff value must be a result of the different catchment characteristics. In contrast to both other basins, Sub3 shows a considerable percentage of arable land as well as of loess coverage. On arable land, by-pass flowpath like macropores are destroyed due to annual tillage operations like ploughing. The up to three-meter thick loess coverage is able to retain more water on the hillslopes than the thin skeletal soils of Sub1.

During the period from 13.9.98 until 22.9.98 a total runoff of 97 mm was measured in Sub1, whereas the other basins reveal significantly lower values (Sub2: 68 mm and Sub3: 79 mm). Thus Sub2 reveals a 30 % lower value as Sub1, although their distance is just two kilometres, and hence a low difference in rainfall amount can be expected. One reason may be the greater amount of initial abstraction of the rainfall due to the high percentage of forest in the basin.

But due to the extreme amount of the rainfall event, the influence of landuse may be of lower importance.

Another reason for the difference in runoff amount may be founded in the geomorphological characteristics of the sub-basins. For example, the drainage density of Sub2 (2.6 km²) is significantly lower than of Sub1 (3.1 km²), indicating longer travel-distances of overland flow components as well as of subsurface flow components. This leads to a higher possibility of both water flowing on the hillslope surface and water infiltrating into the soils being retained on the hillslopes. On the one hand, these circumstances result in a stronger retardation of the runoff. On the other hand, the runoff amount is lower compared to sub-basins with higher drainage densities, because the retained water is decreased by plant uptake.

However, Fig. 26 reveals a higher peak runoff of Sub3 than Sub1. Since significant overland flow rates cannot be expected due to the low rainfall intensities, the difference has to be explained by the geomorphological characteristic of the basin. Due to the intensive incision of the Steinersiefen, no alluvial deposit could have been accumulated in the basin. Thus a considerable groundwater body in the alluvial fillings is not present like in Sub1. The alluvial deposits may lead to a retardation of the water coming quickly from the hillslope via pipes, and thus weakening the peak discharge. On the other hand, the tailing is much more pronounced for Sub1 than for Sub3.

It can be concluded that on the one hand factors like landuse and geology can explain differences in the course of discharge from the basins. But on the other hand, geomorphological features have also to be taken into consideration for a complete explanation of the runoff characteristics.

4.1.3 Solute transport

In the next section, the weekly measurements of the main base anion and cation concentrations of the Berrensiefen during September 1998 are used for further interpretations of runoff mechanisms as well as solute transport processes.

It is a common assumption in studies of spatial controls of base cations in drainage waters from hillslopes and small catchments that the concentrations increase with subsurface residence time (Trudgill et al., 1996). This hypothesis is the basis for the calculation characteristic flow path lengths. Generally, the base cation concentrations increase with the residence-time of the subsurface water flows, whereas soluble anions like chloride and nitrate are rapidly transported through the soil matrix by convective mass-transport (Luxmoore & Ferrand, 1993). Cation concentrations are increased by dissolution of minerals and diffusion from smaller pores with higher concentrations to larger and thus more hydrologically active pores with lower concentrations. Burns et al. (1998) found that base cation transport is affected by preferential flow with cation concentrations in pipe flow being lower than those in matrix flow. Due to these circumstances, they concluded that flow path length calculations might not be valid for drainage areas smaller than 0.01 km².

Fig. 27a shows the course of the sum of base cations (SBC) and base anions (SBA) during September 1998 including the rainfall events discussed in the previous chapter. SBC is calculated from the concentrations of calcium, magnesium, potassium and sodium, whereas SBA is calculated from the concentrations of nitrate, chloride and sulphate. The value of SBA is steadily rising from 15.2 mgeq/l to 15.9 mgeq/l except for a slight decline at the beginning of the rainstorm. The SBC shows the opposite trend with a steady decrease in concentration except for the last sampling date with a distinct rise in concentration. Although the variations in concentration are relatively low, they can be used for an interpretation of the involved processes. However, one should notice that the exactness of measurement is between 5 and 10 %, thus some artificial scattering of the values may be involved.

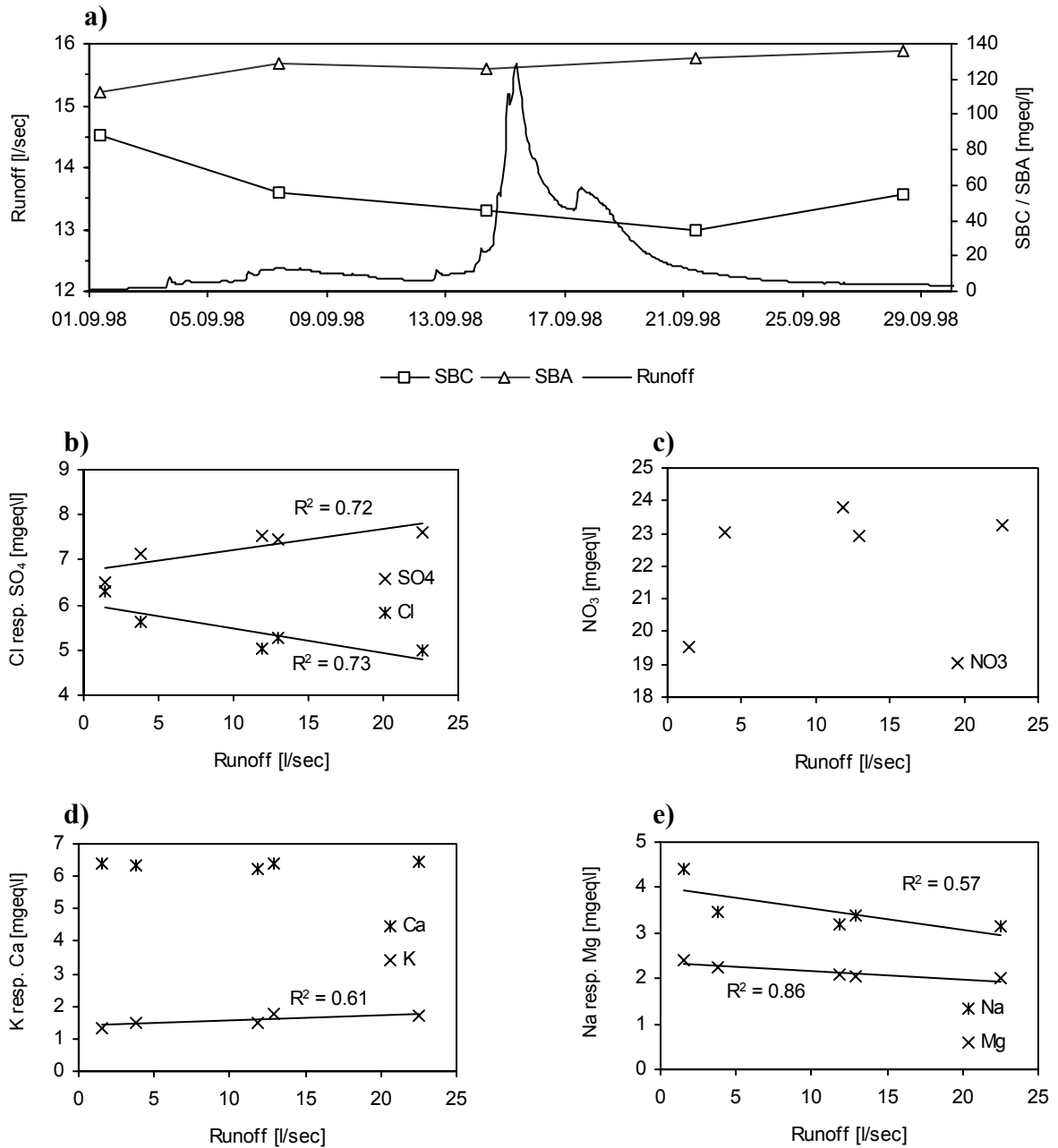


Fig. 27: The course of the sum of base cations and anions during September 1998 (a) and the cation and anion concentrations as a function of discharge: (b) chloride and sulphate, (c) nitrate, (d) Ca²⁺ and K⁺ and (e) Na⁺ and Mg²⁺.

The most pronounced change in SBC and SBA concentration occurs from the first to the second sampling date. Due to the antecedent dry conditions, the runoff of the first sampling date was completely comprised of slow groundwater flow; thus the first value represents the concentrations of SBC and SBA of the deep groundwater. Due to the anaerobic conditions of the deep groundwater, denitrification processes are common. This leads to an effective reduction of nitrate concentration, thus the calculated SBA value is relatively low at this time.

The SBC value is relatively high due to the long residence-time of the groundwater, enabling a significant release of cations by the dissolution of bedrock minerals.

Figs. 27 b to 27e display the cation and anion concentrations as a function of discharge. The chosen elements reveal different reactions on the rainfall input. This is a result of the inherent runoff processes as well as of the agricultural management practices. One has to differentiate between elements that are enriched by fertilization or by natural processes like mineralization. For example, Fig. 27b reveals sulphate and chloride having an opposite trend. Chloride concentration is reduced with increasing discharge, whereas sulphate shows a positive trend indicating washing-out during the rainstorm. In principle, the latter reaction is also observed for nitrate (Fig. 27c), but in this case no linear trend exists. Normally, both sulphur and nitrogen are highly available in soils due to permanent supply by fertilization or precipitation entry. Thus sulphur and nitrogen are subject to excessive eluviation during the occurrence of heavy rainfall. In contrast, the content of chloride is mainly determined by the geological situation and input via fertilizers is less distinct. Consequently, chloride concentration is reduced during high discharge rates by the low concentrated subsurface flows.

The same argumentation is applicable for the cations (Fig. 27d - 27e). Sodium and magnesium are not subject to fertilization and thus a decrease in concentration with increasing discharge occurs. Potassium shows the opposite trend because it is fertilized, and thus the content in the soils is higher than in the groundwater. Additionally, subject to intensively adsorption on clay minerals, the transport into deeper groundwater layers is reduced. However, calcium concentrations do not seem to be influenced by the discharge rate, indicating that calcium concentrations of soils and groundwater are similar.

In conclusion, anions are subject to washout more easily than cations during rainstorm events. Consequently, subsurface flows are comprised of a relatively high amount of anions, thus increasing the SBA value during high flows. Conversely, due to the low cation concentration of cations of the subsurface flow, the SBC value is reduced during high flows.

4.1.4 Sediment transport

In addition to the measurements of solute concentrations, the sediment transport was subject of investigation of the research project B14. To elucidate the sediment transport processes within the sub-catchments, a weekly measurement of the suspended load concentration was carried out. Furthermore, the weekly bed-load discharge was determined using bed-load samplers.

Fig. 28 displays the course of the suspended load concentration and the weekly amount of bed load during September 1998.

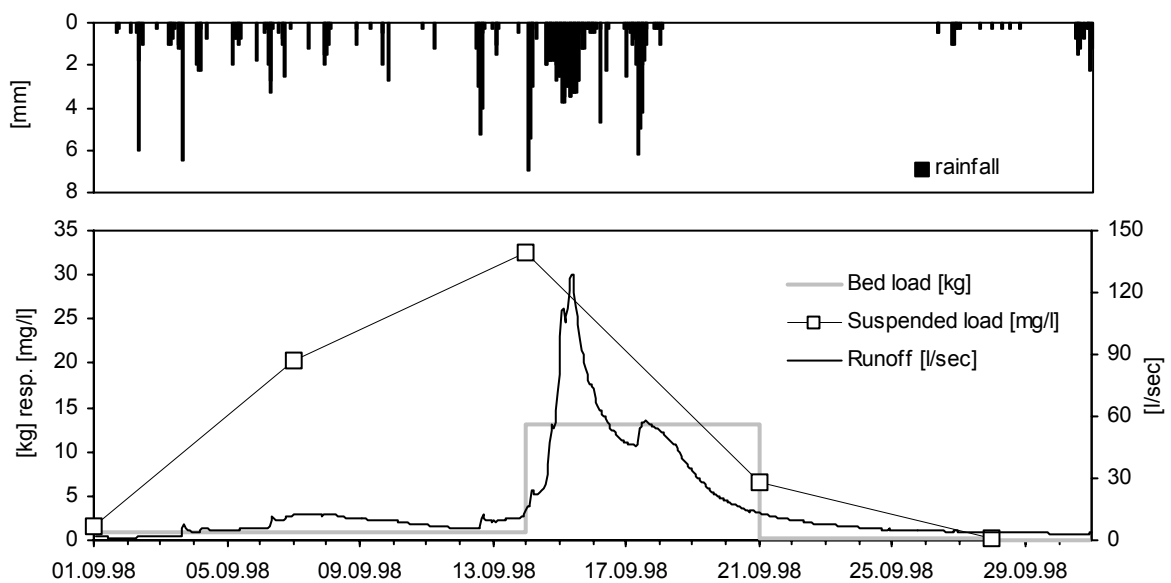


Fig. 28: Suspended load concentration, bed load discharge and runoff of the Berrensiefen during September 1998.

4.1.4.1 Bed Load

In the first two weeks a total bed load amount of about 1.73 kg was collected with the bed-load sampler. During the next week, including the time of the rainstorm event, a sediment amount of 13.04 kg accumulated in the bed-load sampler. The real transported sediment amount might have been even higher, because the bed-load sampler was completely filled up and additional bed load material had accumulated within the settling basin of the gauging station. After the rainstorm the sediment discharge rate decreased significantly to a value of about 10 g per day.

In general, the main origin of bed-load is the channel itself. In the case of the Berrensiefen the channel is, especially in the lower parts, artificially consolidated with coarse stones in order to prevent channel incision. Therefore the sources for bed-load are restricted to the upper parts of the channel and hence relatively low compared to the other sub-catchments. However, during the rainstorm event considerable incision took place in the upper part of the Berrensiefen channel, where the channel bed is unprotected. Sediment transport increased significantly, producing a ten times larger sediment discharge as before the rainstorm event.

4.1.4.2 Suspended Load

In the beginning of September 1998 the suspended load concentration was comparatively low (1.58 mg/l), as indicated in Fig. 28. With higher discharge rates the concentration of suspensoids increased to a maximum value of 32.5 mg/l. After the flood wave the concentrations of suspensoids decreased again to a value of 0.34 mg/l. The discharge of suspensoids was lower than before the rainfall event, indicating that the detachment rate is reduced because the temporal sediment storages in the sub-catchment were degraded.

To explain the origin of the suspensoids the hillslopes and the channel itself can be differentiated as two main sources. As already mentioned in Chapt. 4.1.2.2, the occurrence of considerable overland flow during the rainstorm event, especially within the valley plain, can be presumed. Due to influence of cattle the turf in this area was affected to some extent, thus soil material may be transported by soil erosion from the hillslopes into the channel. Furthermore, the high amount of interflow indicates that subsurface erosion may have played a significant role due to pipe flow. Some pipes have been observed in the deep valley cuts of the Berrensiefen. This process is particularly observed in the southern part of the Wahnbach catchment (Botschek, 1999), where pipes are formed in the loessial coverage exporting considerable amounts of sediments from the hillslopes.

As a result of the antecedent dry period with low discharge rates, sediments may have accumulated in the channel due to low transport capacities. The increased velocity of channel flow leads to an enhanced shear stress at the channel bed-water interface and hence induce an increased detachment rate. Simultaneously, the increased discharge volume enlarges transport capacity, thus sediment material could have been transported downstream effectively.

However, the relatively low resolution of this data does not allow a detailed differentiation of these processes. In order to extend the perceptiveness of the involved processes, the grain-size distribution of the sediment probes was measured with a laser analyzer ('Analysette 20', company FRITTSCH). For the application of this method, the suspensoids had to be concentrated to some degree, because the laser analyzer needs a certain concentration of suspensoids. Unfortunately, some probes could not have been concentrated in a sufficient way and thus the measurement of the grain-size distribution failed.

Fig. 29 shows the grain-size distribution of three different suspended load probes taken before (7th and 14th of September 1998, respectively) and after the storm event (28th of September 1998).

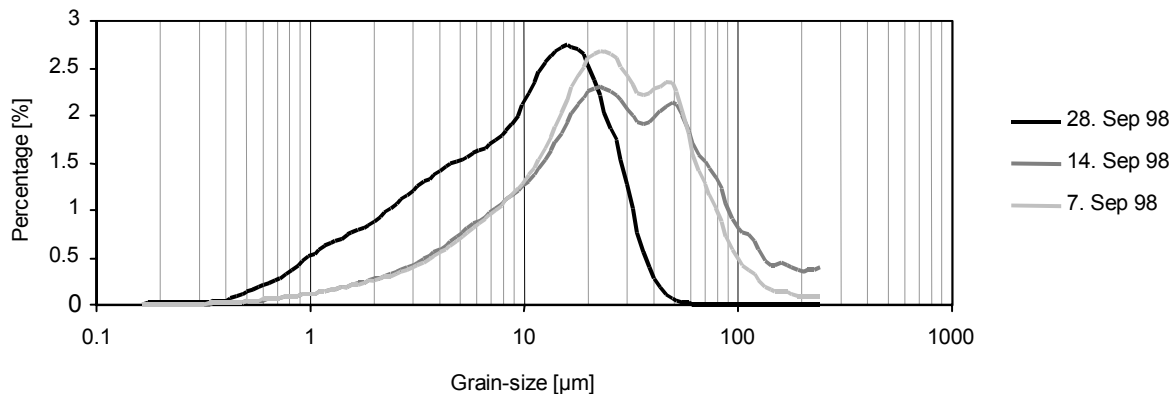


Fig. 29: The grain-size distribution of the suspended load before (07.09.98 and 14.09.98) and after the rainstorm (28.09.98).

The first two samples have similar left-crooked and bimodal-shaped grain-size distributions with a maximum grain size of about 24 µm. The second probe reveals a slight shift towards coarser grain sizes. In contrast, the third sediment probe reveals that the grain-size distribution has significantly shifted towards smaller grain sizes with a maximal frequency at 17 µm and no bimodality is visible. From this data it can be concluded that grain-size distribution of the transported sediments depends on the discharge rate, thus getting coarser with increasing discharge. This finding corresponds with the fact that with increasing grain diameter higher runoff velocities are needed for transportation. (Kresser, 1964). The different shape of grain-size distribution of the sediment sampled after the rainfall event indicates, that some kind of changes in the channel bed structure could have taken place. Hence other sediment sources may have been activated due to impact of the rainstorm event.

It has to be noted that solute and sediment discharge measurements based on a temporal resolution of one week may not be appropriate to reproduce the dynamic of transport of matter in an acceptable way, especially in the case of a rainstorm event. This is stressed by the results of the continuous nitrate measurements, showing short-term variations in concentrations, which cannot be described with a weekly resolution. Additionally, it can be expected that even higher concentrations of suspended load could have been measured during this period because of the great amount of sampled bed load material during the storm event. Thus the data used may underestimate the total sediment discharge.

However, for data of higher resolution a considerable expenditure is necessary, which was not within the scope of this study. Nevertheless, as shown above, it is possible to derive process understanding from these measurements.

4.2 Processes at the seasonal scale

In the following section, the solute and sediment transport on a medium temporal scale will be investigated. In this context medium temporal scale means the duration of the whole measurement period of 2.3 years, thus including seasonal variations. In order to investigate the dependency of the solute transport processes on catchment characteristics, a comparison of the fluxes of matter in the Berrensiefen catchment with the other sub-catchments of the Wahnbach River (Fig. 11, Chapt. 3.1) is carried out.

4.2.1 Runoff

In this section the gauged discharges of all sub-catchments during the period of measurement are used to evaluate the effects of the different catchment characteristics on runoff generation. Fig. 30 displays the monthly rainfall of the rain gauges PEA and Berrensiefen, representing the southern and northern of the Wahnbach catchment, respectively, and the monthly runoff amounts of the sub-catchments.

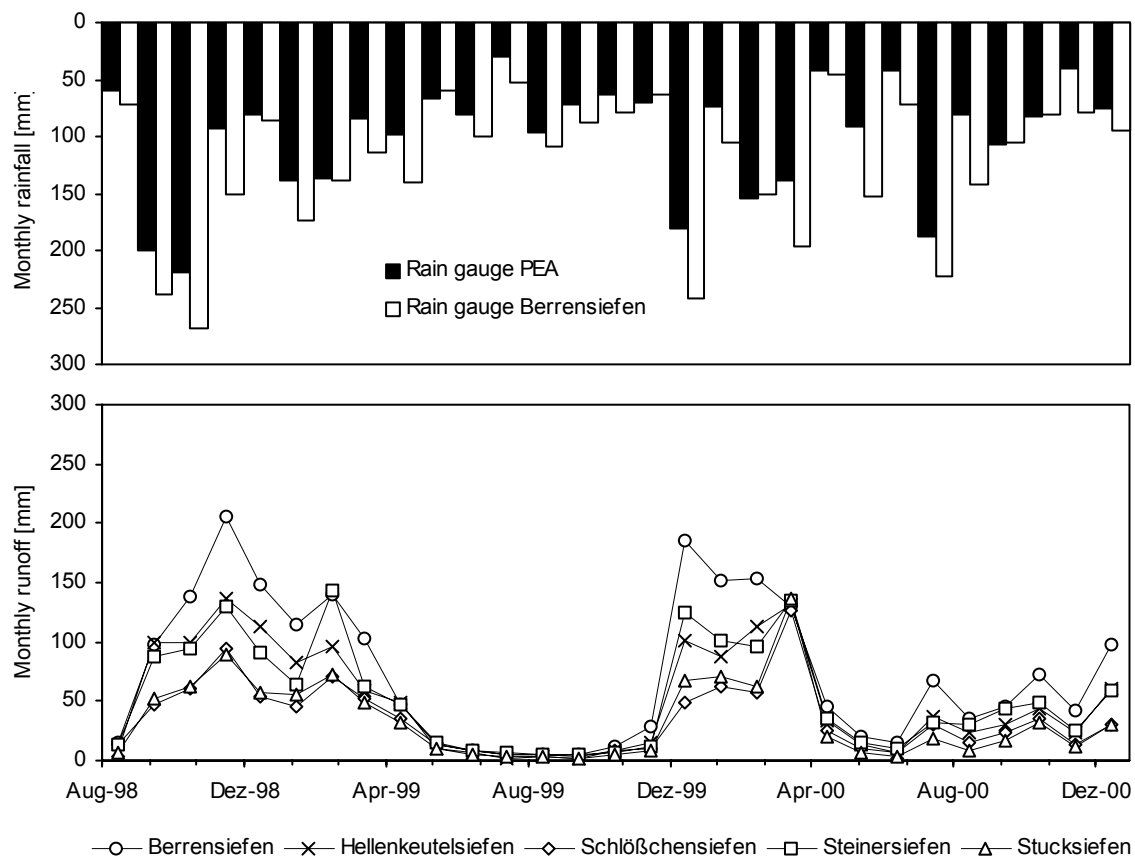


Fig. 30: The monthly precipitation amounts measured of the rain gauges PEA and Berrensiefen, representing the southern and northern part of the Wahnbach catchment, respectively, and the monthly runoff amounts of all investigated sub-catchments.

As it is already mentioned in Chapt. 3.1.2, the Wahnbach catchment exhibits a distinct trend in the precipitation distribution with generally higher rainfall amounts being measured in the northern part. This finding corresponds to the monthly values of gauging stations presented in Fig. 30. Only in five cases the southern station recorded higher amounts than the northern one and the total amounts differ significantly (Berrensiefen: 3622 mm and PEA: 2884 mm). Accordingly the total discharges of the sub-catchments increase from 997 mm (Stucksiefen) to 2151 mm (Berrensiefen).

During the period of measurement high discharge rates are predominately produced during the winter with maximum monthly runoff amounts of over 206 mm (Berrensiefen). Conversely, during the summer periods discharge diminishes to very low values. Especially the summer 1999 was very dry with very low runoff rates below 2 mm/month (Stucksiefen), whereas during the summer 2000 it was relatively wet with mean monthly discharges of up to 38 mm (Berrensiefen). In order to examine the similarity of the discharge behaviour of the sub-catchments, correlation indices are calculated from the monthly runoff amounts, which are listed in Tab. 6.

Tab. 6: Matrix of correlation indices (R^2) calculated from the monthly runoff amounts.

	Hellenkeutelsiefen	Schlößchensiefen	Steinersiefen	Stucksiefen
Berrensiefen	0.915	0.729	0.891	0.762
Hellenkeutelsiefen		0.853	0.917	0.879
Schlößchensiefen			0.852	0.975
Steinersiefen				0.882

The correlation indices are significant in every case, but highest values are obtained when the distance between the sub-catchments is low. For example, the R^2 -value of the adjacent catchments of Stucksiefen and Schlößchensiefen is very high (0.975), whereas the sub-catchments having the highest distance (Berrensiefen and Schlößchensiefen) exhibit the lowest correlation (R^2 : 0.729). One reason for this finding is the different amount and temporal distribution of precipitation in the sub-catchments. On the other hand, it might be possible that the individual attributes of the sub-basins (e.g. landuse, geomorphology) have also an influence on the runoff characteristic at the seasonal time scale, as it has been demonstrated for the event scale in Chapt. 4.1.2.3. This assumption is further discussed in the following sections in the context of solute transport.

4.2.2 Anion concentrations

The mean monthly concentrations of the base anions of all sub-catchments are displayed in Fig. 31 (from August 1998 until December 2000). The aim of this presentation was to exhibit the dissimilar transport behaviours of the anions and simultaneously to put their different seasonal patterns to display. In order to visualize the relation of solute concentration and discharge rate, the average runoff from the sub-catchments is additionally presented in Fig. 31.

4.2.2.1 Chloride

The chloride content in surface waters is predominantly determined by the geological composition of the catchment. Furthermore, chloride is often a component of fertilizers. Because the chloride is only taken up from plants to a very low degree and not subject to adsorption on soil particles, most of the supplied chloride is immediately exposed to washout processes.

The sub-catchments reveal different mean chloride concentrations, from 6.48 mg/l (Berrensiefen) to 15.2 mg/l (Steinersiefen). The low values of Berrensiefen and Hellenkeutelsiefen, both located in the northern part of the Wahnbach catchment with Devonian subsoil prevailing, reflect the low mineralization rates of chloride in this region. The higher values of the remaining sub-catchments may be the result of higher fertilization rates, which is likely because of the relative high percentage of surface being ploughland in the Steinersiefen and Schlößchensiefen sub-catchments (Tab. 4, Chapt. 3.1.4). However, the high concentrations of Stucksiefen, of which catchment has a similar land utilization as the Berrensiefen catchment, indicate that the loessial coverage in the southern part of the Wahnbach catchment increases the chloride concentrations, too.

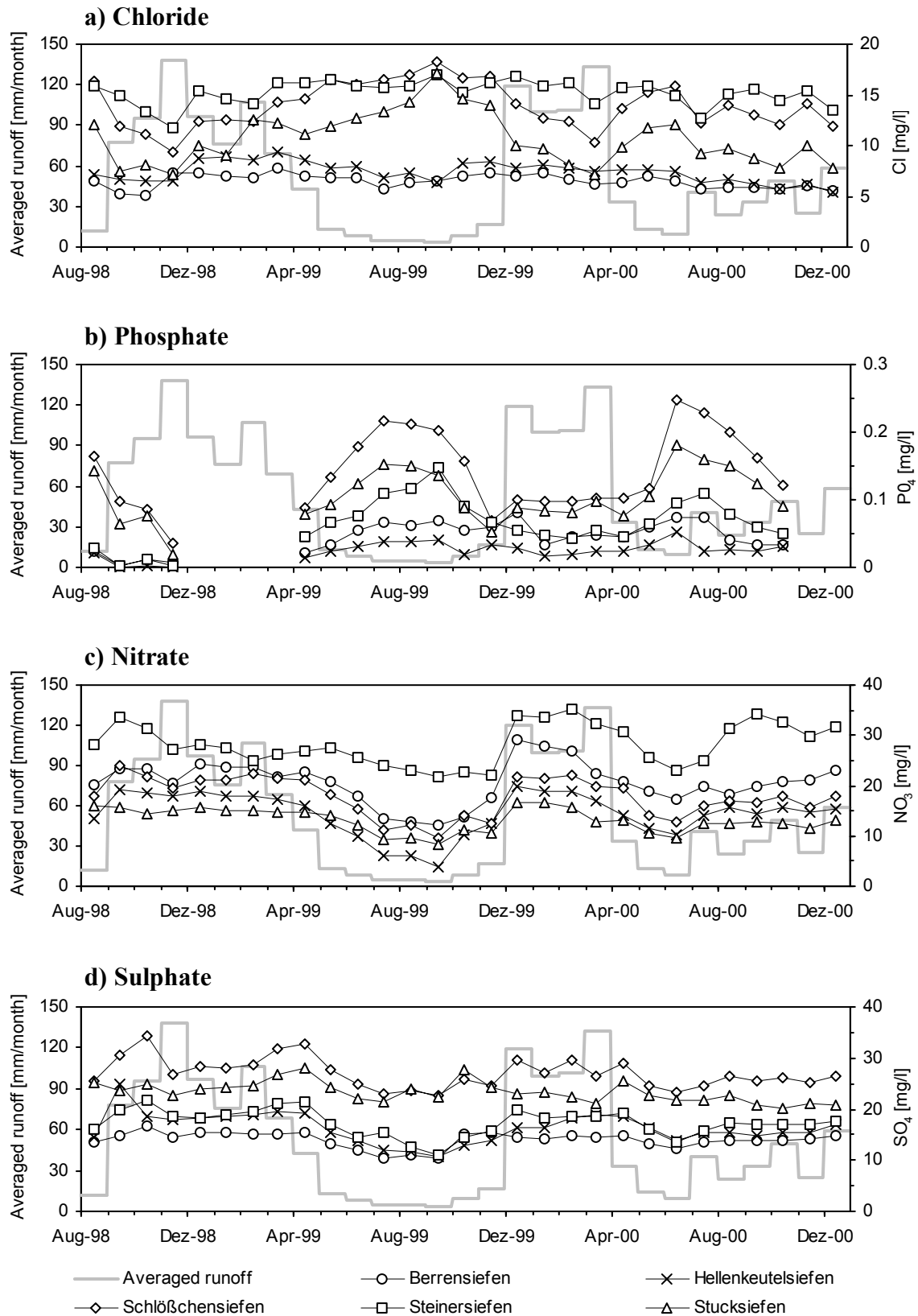


Fig. 31: The mean monthly concentrations of the base anions of all sub-catchments and the mean monthly discharge averaged over all sub-catchments from August 1998 until December 2000: a) chloride b) phosphate, c) nitrate, and d) sulphate.

The courses of chloride concentration of the sub-catchments differ in their seasonal patterns. This is particularly striking in summer half-year 1999. During this period the chloride concentration of Berrensiefen and Hellenkeutelsiefen decrease in correspondence to the decline of the discharge. Conversely, the other sub-catchments are showing an increase of chloride concentration that is negatively correlated with discharge. This finding suggests that the temporal patterns of chloride concentration are to some extent related to the geological situation, too. Hence it might be possible to use the course chloride concentration as an indicator for the geological structure of the Wahnbach catchment.

In the following, this assumption is analyzed in more detail. First, a correlation matrix calculated from the monthly chloride concentrations of each possible pair of sub-catchments is generated (Tab. 7). The obtained R^2 -values differ considerably among the combinations, from 0.05 indicating no relation and 0.82 indicating significant correlation.

Secondly, the mean distances between the sub-catchments are measured. In Fig. 32 these values are plotted against the values of correlation matrix of chloride concentration, indicating a significant correlation. Then the R^2 -value is calculated in order to obtain a measure for the spatial correlation of the specific anion. In the following part this measure is named coefficient of spatial correlation (CSC).

Tab. 7: Matrix of correlation indices (R^2) calculated from the monthly chloride concentrations.

	Hellenkeutelsiefen	Schlößchensiefen	Steinersiefen	Stucksiefen
Berrensiefen	0.64	0.05	0.15	0.13
Hellenkeutelsiefen		0.05	0.17	0.11
Schlößchensiefen			0.74	0.82
Steinersiefen				0.31

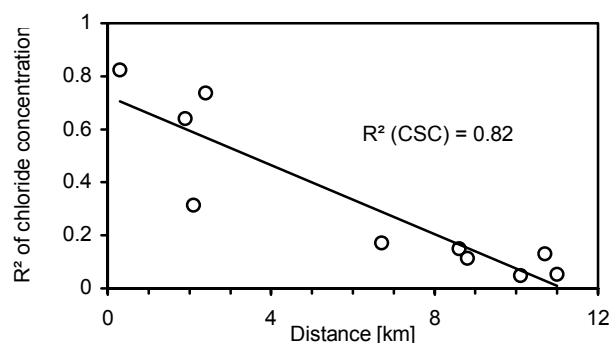


Fig. 32: R^2 values of Tab. 7 plotted against the distance of sub-catchments.

The high value of CSC (0.82) suggests that the dynamic of chloride concentration depends to a large degree on the position within the Wahnbach catchment. Thus it can be concluded that the influence of the landuse on the amount of chloride discharge as well as on the dynamic of chloride concentration seems to be less important than geology.

4.2.2.2 *Phosphate*

Due to the fact that phosphate is subject to a strong adsorption on soil particles, it is relatively immobile and hence in contrast to chloride, only a small part of supplied phosphate enters groundwater or surface water. This characteristic is confirmed by the low concentrations of phosphate in the subcatchments (Fig. 31b) with maximum concentrations of only 0.25 mg/l. From Fig. 31b, one main trend can be recognized appearing simultaneously in all sub-catchments: the phosphate concentrations increase during summer and decrease during winter, indicating that remobilization of adsorbed phosphorus occurs during these periods. Because of the immobility of phosphate, the groundwater has generally very low phosphate concentrations (v. Kamp, 1983). Hence the high PO_4 -values during summer cannot be explained by the influence of groundwater flow. It is more likely that a remobilization of phosphate adsorbed on sediments, which are stored in the channel, takes place during summer (Peter, 1988). In contrast, phosphate concentration is reduced during winter, which can be explained by dilution effects of low concentrated subsurface flows.

Additionally, differentiation between the catchments is recognisable. Lowest values are always found in the Hellenkeutelsiefen and Berrensiefen catchments, whereas highest values are measured in the Stucksiefen and Schlößchensiefen catchments during the whole period of measurement. This finding is in accordance with the distribution of soil erodibility within the Wahnbach catchment. The soils developed within the loessial cover are more susceptible to soil erosion than the soils developed in the Devonian bedrock. Thus in the stream channels located in the southern part of the Wahnbach catchment more erosion products are present and subject to phosphate desorption. The slower the runoff velocity and higher the water temperature is the more likely is the phosphate enrichment of the streamwater, thus causing an increase of phosphate concentration (Peter, 1988).

4.2.2.3 Nitrate

Main input sources for nitrate in soils without agricultural utilizations are precipitation, dry deposits or fixation of nitrogen gas, because nitrogen does not occur to a noteworthy extent in primary minerals. Both organic and inorganic fertilizers are used in order to compensate nitrogen losses due to plant consumption or washout.

Fig. 31c reveals that nitrate shows more or less the opposite course of concentration than phosphate, thus when discharge increases nitrate concentration increases as well. In contrast to the relatively insoluble phosphate, nitrate is very mobile and is subject to mass transport with the percolating soil water (Sparks, 1995).

During winter, percolation increases due to reduced evapotranspiration rates, initiating the rapid transportation of soil nitrogen in the form of nitrate into the channel via interflow. During summer, when the subsurface flow from the hillslopes diminishes, the nitrogen discharge is increasingly supplied from groundwater. Owing to the very dry conditions in August and September 1999 the averaged discharge decreases to very low values (< 5 mm/month), indicating that runoff is completely fed by deep groundwater. During this time the lowest nitrate concentrations are measured in all sub-catchments. These values may reflect the local nitrate concentrations of deep groundwater layers, where denitrification processes reduce nitrate concentration. After this dry period, nitrate concentrations increase very sharply again, indicating the initiation of subsurface flows of high nitrate concentration.

Steinersiefen shows the highest concentrations with values up to 35 mg/l, which is quite serious given the fact that the limit of nitrate concentration of drinking water is 50 mg/l within the EU (Schachtschabel, 1998). This sub-catchment shows the highest percentage of arable land (Tab. 4, Chapt. 3.1.4), which supports high nitrogen losses into groundwater as well as into surface water (Walther, 1999).

The course of nitrate concentrations of the sub-catchment Hellenkeutelsiefen shows distinct amplitudes from relatively high values in winter to very low values in summer. The high values indicate that, although forest is predominant, considerable amounts of nitrate are mobilized during wet conditions from pastureland and transported through interflow. In contrast, the low nitrate concentrations during the summer indicate that the nitrate

concentration of the local groundwater reservoir is relatively low due to the high percentage of forest in the Hellenkeutelsiefen catchment.

4.2.2.4 Sulphate

The courses of sulphate concentrations are similar to the nitrate concentrations, but the peaks are less pronounced. This finding corresponds with the stronger adsorption of sulphate on soil particles compared to nitrate, thus causing improved retention. Peter (1988) observed in a wooded catchment near the study area higher sulphate concentration in the runoff water than in intensively, agriculturally used catchments. Peter (1988) related this finding to the higher filter capability of forests in respect to atmospheric sulphur compounds. This conclusion can be confirmed with reservations, because on the one hand the mean sulphate concentration (16.3 mg/l) is significantly higher than in the runoff of Berrensiefen (14.0 mg/l), but on the other hand the concentrations in Stucksiefen and Schlößchensiefen are on average 35% higher than in the other brooks. This may be a consequence of the reduction of sulphur emissions in the past decades (Walther, 1999).

Although the southern catchments have significantly higher concentrations, indicating that the geological situation may also play an important role in the quantity of sulphate transport, the CSC-value equals zero. This finding suggests that other characteristics of lower spatial scale (e.g. landuse, topography etc.) determine the pattern of sulphate concentration.

4.2.3 Cation concentrations

Fig. 33 displays the mean monthly concentrations of the main cations (potassium, sodium, magnesium and calcium) investigated in research project B14. The diagram has the same structure as Fig. 31.

4.2.3.1 Potassium

Apart from the geological situation and precipitation as input factors, the amount of potassium discharge often expresses the fertilization conditions. Potassium, being a main nutrient, is reduced by plant uptake and is additionally subject to an intensive adsorption on clay minerals (Sparks, 1995).

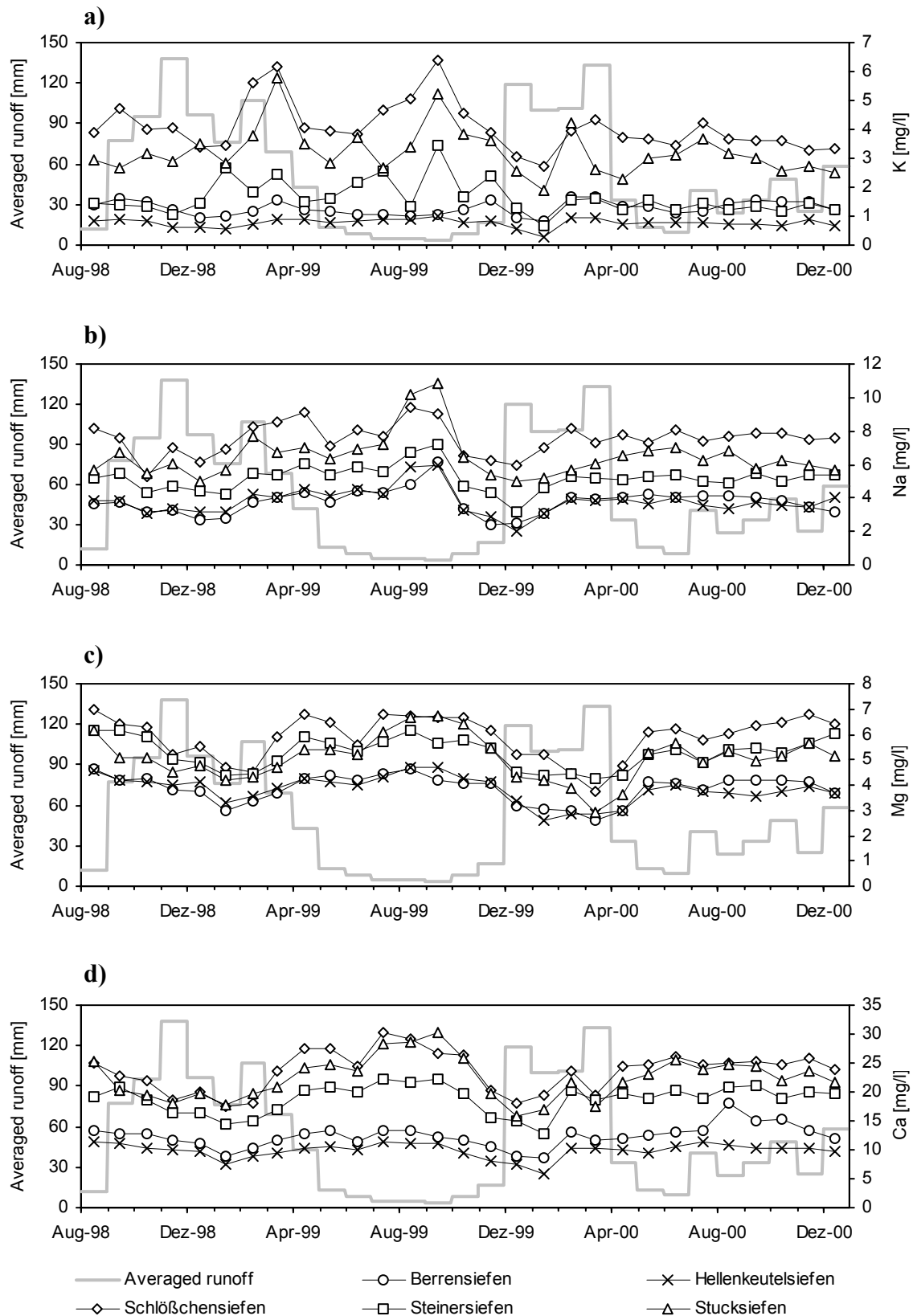


Fig. 33: The mean monthly concentrations of the base cations of all sub-catchments and the mean monthly discharge averaged over all sub-catchments from August 1998 until December 2000: a) phosphate, b) nitrate, c) chloride and d) sulphate.

Compared to the other base cations (Figs. 33b - 33d), potassium shows an insignificant seasonal dynamic. No correlations between discharge and potassium concentration are detectable, thus other processes have to be considered to explain the dynamic.

The weekly measurements of Steinersiefen exhibit a coefficient of variation of 58 % with unique deviations from the mean value of over 300 %. It has to be noted that the sampling interval might have been not adequate and the fluctuations are even more pronounced in reality. This high dynamic of the concentration fluctuations, which is also visible in the courses of potassium of Schlößchensiefen and Stucksiefen, is an indication of event-based processes. Therefore, it is very likely that the potassium discharge in the research area is coupled with processes related to soil erosion. This is also suggested by the strong adsorption of potassium on clay particles (Sparks, 1995), reducing the potassium-transport into deeper soil layers.

The sub-catchment Hellenkeutelsiefen has a relatively low mean potassium concentration (0.77 mg/l) and also the coefficient of variation is relatively low (27 %). This finding can be explained by the low proportion of agricultural land within the catchment, which implies low fertilization and soil erosion rates.

4.2.3.2 *Sodium*

Sodium is the most mobile of the base cations described in this study and is relatively unimportant for plants. The mean concentrations of sodium are on average about twice the amount of potassium. Highest concentrations of sodium are observed in the sub-catchments located within the loess coverage (Steinersiefen, Stucksiefen and Schlößchensiefen). This finding corresponds to the fact that the natural sodium concentration in soils is predominately determined by the content of feldspar (Schachtschabel, 1998), which is a frequently occurring mineral in loess.

In contrast to potassium, the courses of sodium concentration are less distinct (average coefficient of variation 38 % for potassium and 22 % for sodium). Most of the variation is produced in the time from August 1999 until January 2000. During very low discharges in the beginning of this period, sodium concentration increases and with enhanced discharge in autumn sodium concentration decreases sharply again. This pattern is caused by an alternation of the domination of high concentrated groundwater flows in summer and dilution effects, due

to high rates of low concentrated subsurface flows in autumn. During the winter season, sodium concentration increases again. This is an indication for an increasing proportion of groundwater on the discharge, levelling out the dilution effect of the subsurface flows.

It can be concluded that the amount of sodium discharge depends on the geological situation, but the pattern of sodium concentration is similar in all sub-catchments, and therefore depends not on the position within the Wahnbach catchment. This statement is also confirmed by a very small value of CSC (0.01).

4.2.3.3 Magnesium

Magnesium is subject to plant uptake and, therefore has to be fertilized on agricultural-used soils to compensate for magnesium losses through crop harvest and elution. Due to the higher contents of magnesium in the loess coverage compared to the silicate rocks, which are predominantly located in the northern part of the Wahnbach catchment, the geology influences the amount of magnesium discharge, again.

Like sodium, the courses of magnesium concentration are similar among the sub-catchments, but the temporal distributions of minimum and maximum values of the cation types are significantly different. For example, the magnesium concentration decreases from relatively high values in September 1999 to a minimum value in March 2000, while the lowest value of sodium concentration occurred already in December 1999. This temporal discrepancy of the minimal values can be explained by the different distribution of these cations in the compartments soil and groundwater. Sodium is mainly released by mineralization processes within the groundwater body, which is also indicated by the high sodium concentrations during low discharges. Generally, the sodium contents in the soils are low, while the magnesium contents are relatively high due to magnesium fertilization. Owing to the relative high delivery rate from the soils, the magnesium concentration does not decrease with increasing subsurface flow as quickly as the sodium concentration.

During the winter period magnesium is washed out from the soils, and hence the content of mobile magnesium in the upper soil is reduced more and more. Consequently, the concentration of magnesium of the subsurface flow decreases and, thus of the discharge, as well. Again the value of CSC is low (0.15), indicating that this process is not spatially bounded.

4.2.3.4 Calcium

Calcium has similar chemical characteristics as magnesium. As an essential nutrient for plants, it is also fertilized and thus relatively high calcium contents can generally be found in the soils (Schachtschabel et al., 1998).

As a result of the relatively high contents of calcium in loess soils, the concentrations of calcium in the southern sub-catchment are significantly higher. For example, the mean concentration in Schließchensiefen is 23.6 mg/l, whereas Hellenkeutelsiefen reveals only a mean concentration of 9.9 mg/l.

The courses of calcium and magnesium concentrations are quite similar. The similarity in transport behaviour is also confirmed by the significant correlation of both cations for all sub-catchments (Fig. 34).

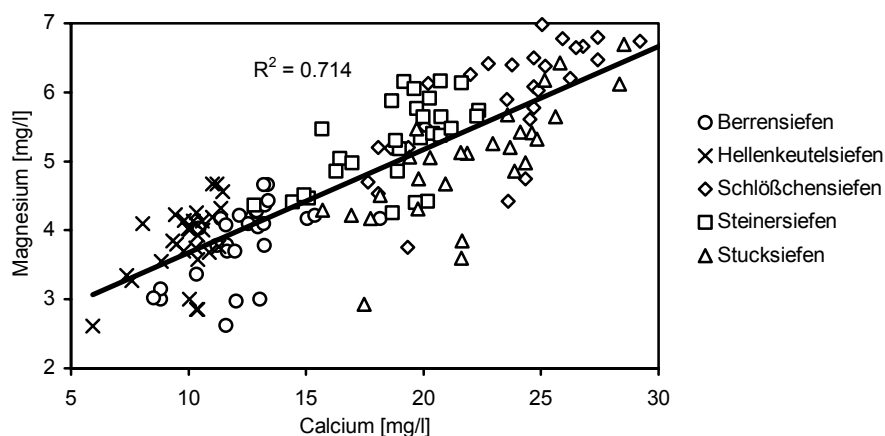


Fig. 34: Correlation of monthly magnesium and calcium concentrations of all sub-catchments.

Beside the similarity of these cations, Fig. 33d reveals that the decline in concentrations of calcium is sharper and the minimal concentration is reached some months earlier. This effect may be due to the higher calcium concentration of the groundwater flow.

A further difference is that the value of SCS is relatively high (Fig. 35), suggesting that the processes determining the dynamic of calcium concentration are spatially bounded to some extent.

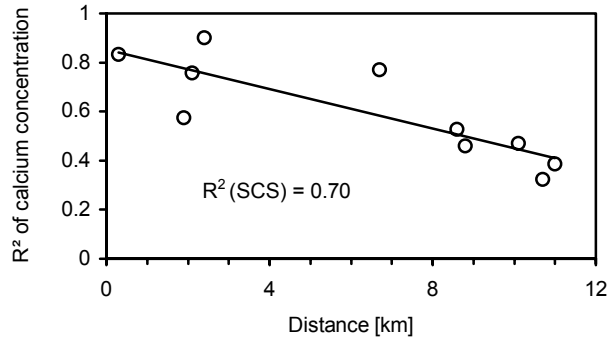


Fig. 35: R^2 of calcium concentration plotted against the distance of sub-catchments.

It can be concluded that calcium reveals similar discharge behaviour as magnesium. However, some differences have been discovered, suggesting that differences in calcium mineralization intensity lead to a more differentiated distribution of calcium in the groundwater and thus to a more significant spatial dependence on the dynamic of calcium concentration.

4.2.4 Suspensoid concentrations

Fig. 36 displays the mean monthly concentrations of suspensoids in the investigated sub-catchments. The suspended load reveals a very high dynamic, which is the reason for choosing a logarithmic scaling in Fig. 36.

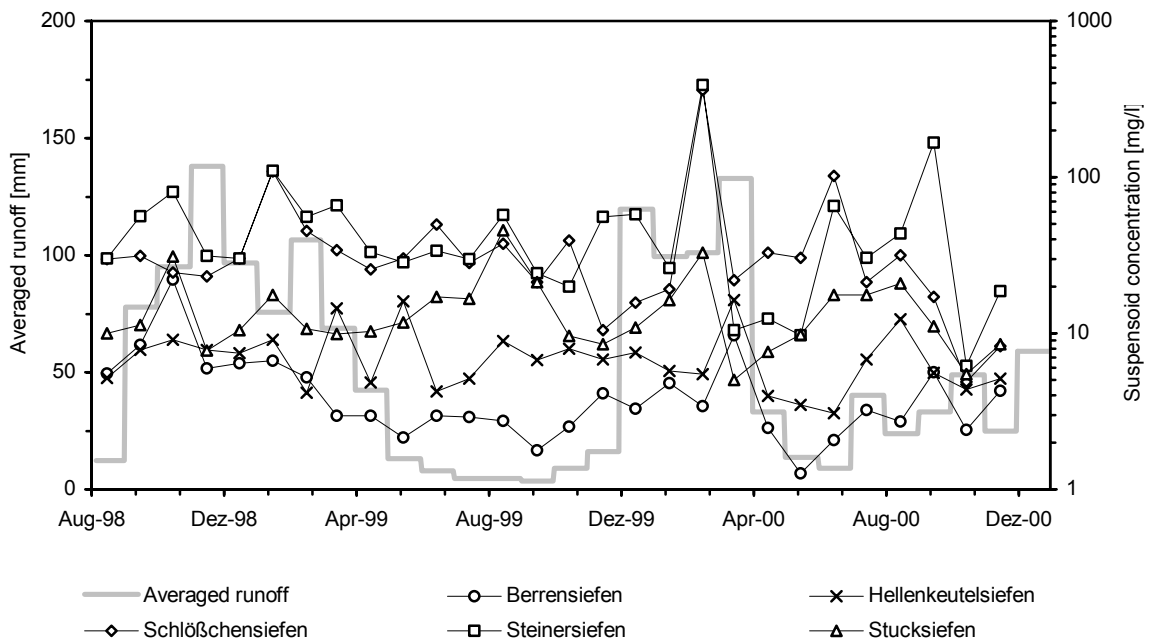


Fig. 36: The mean monthly concentrations of suspensoids of all sub-catchments and the mean monthly discharge averaged over all sub-catchments from August 1998 until November 2000.

The mean values averaged over the whole observation period reveal significant differences in the suspensoid transport behaviour of the sub-catchments. The lowest value of the five sub-catchments was measured in Berrensiefen (4.7 mg/l), whereas in Hellenkeutelsiefen, though forest predominates, nearly twice the amount is observed (7.4 mg/l). The low value of Berrensiefen can be explained by the artificial consolidation of the lower part of the channel reducing the supply of suspensoids from the channel bed. The mean suspensoid concentration of Stucksiefen is also relatively low (14.9 mg/l), but Steinersiefen (56.4 mg/l) and Schlößchensiefen (44.1 mg/l) exhibit a nearly tenfold mean concentration of suspensoids compared to Berrensiefen. Both sub-catchments contain ploughland, and thus it can be expected that soil erosion is an important process transporting suspensoids into the channels. The coefficients of variation of these sub-catchments are also very high (239 and 295 %, respectively), reproducing the discontinuity of the soil erosion process.

However, it has to be taken into account that the channels function as a temporary storage for the incoming eroded sediments. Additionally, sediments produced by soil erosion are likely to be temporally stored on the hillslopes (Reid and Dunne, 1996). Therefore a direct connection from the hillslopes to the catchment outlet is rarely the case. Furthermore, the channel is subject to intensive incision and thus the sediment yield may be to a certain extent comprised of eroded bed material. Finally it has to be noted, that the infrastructure can lead to a selective increase of soil erosion, e.g. due to roads, producing direct runoff (Briese, 1984).

4.3 Processes at the long-term scale

In order to evaluate the effect of precipitation on long-term sediment discharge, the rainfall deviation from long-term average (964 mm) is compared with the calculated sediment discharge (Fig. 37). The sediment export from the Wahnbach catchment is calculated using turbidity measurements in the Wahnbach during 1981 and 1999 and suspensoid concentrations gauged during 1999 and 2000 (Giertz, 2000).

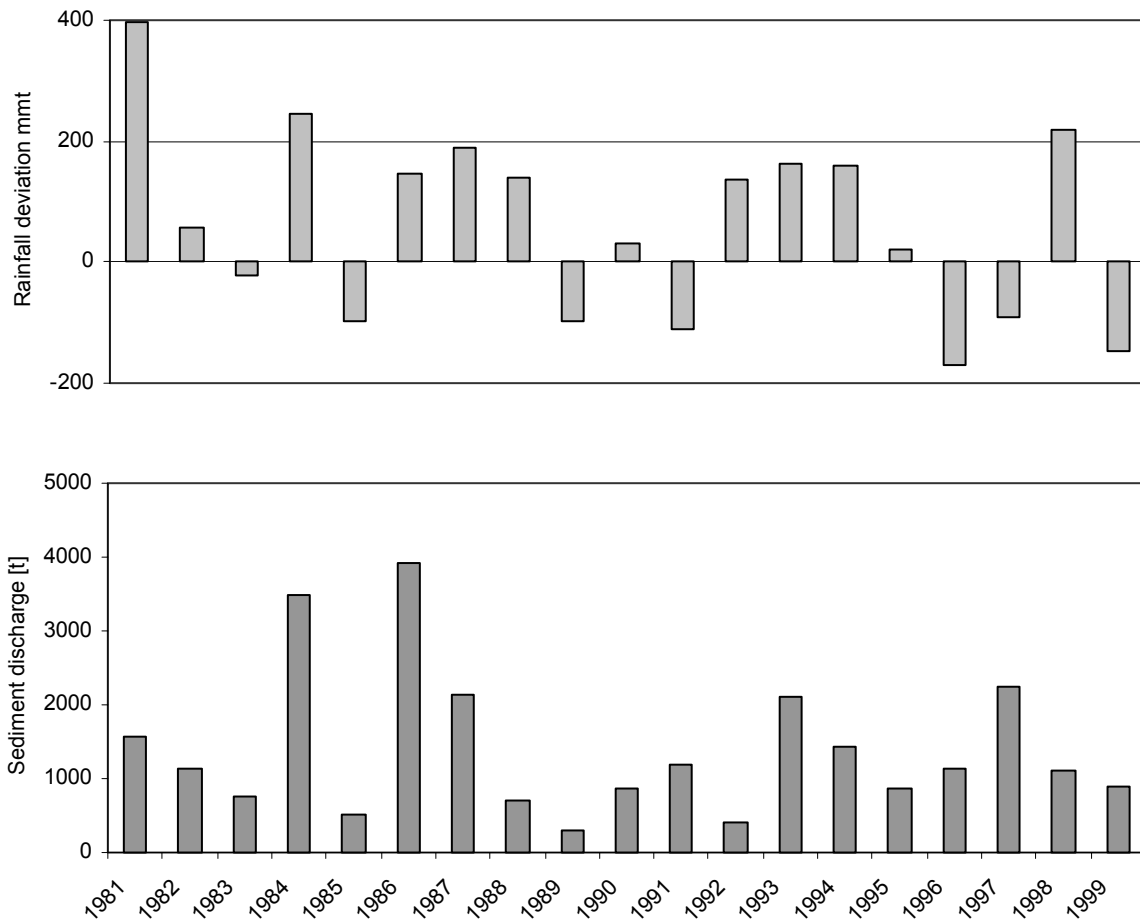


Fig. 37: Rainfall deviation from long-term average (above) and sediment discharge of the Wahnbach River (below).

It is obvious that no significant correlation between the yearly rainfall event and the sediment export exists. For example, the highest rainfall amount was measured in 1981 with 1360 mm, but the sediment discharge in that year was only 10 % higher than the average of the whole period (1408 t). Furthermore, the sediment discharges of the years 1986 and 1988 differ considerably (3926 t and 698 t) although the rainfall amounts were almost equal (145 mm and 140 mm).

This finding indicates that the processes at the lower scale have to be considered in order to describe the long-term export of sediments. For example, the effects of rainfall intensity on the amount of soil erosion have to be taken into consideration.

4.4 Development of a perceptual model

In this section the most important statements of the previous chapters are summarized in order to develop a perceptual model, which contains the main processes determining the fluxes of matter in the study area. The result of this synthesis will be used for advancing the OPUS model in order to adjust the model system to the natural situation. Generally speaking, in this part of the study it is attempted to enhance the transfer of the ‘real world’ into the ‘model world’.

4.4.1 Runoff

Through the analysis of the measured hydrograph and continuous gauging of conductivity and nitrate concentration, the following conclusions can be drawn.

During the frequent convective rainfall events in the summer half-years (see Chapt. 4.1.2.1), Hortonian overland flow is likely to be produced on the hillslopes. This statement is verified by analyzing the rainstorm event on 21.06.2000 of 13.25 mm that happened after a very dry period. Through the calculation of the area which is affected by direct runoff, it is assumed that an area of approx. 1700 m² was affected by Hortonian overland flow. This is only 0.008 % of the area covered by pastureland, thus indicating that most of the rainfall is infiltrated into the soils because of the dry antecedent condition. Nevertheless, the increase in nitrate concentration proves that overland flow from the hillslope had occurred.

The next example shows that a convective rainfall event of 28.25 mm on 25.07.00 produced a direct runoff area of about 1.8 ha, which is more than the tenfold amount of the previous event. This comparison shows the non-linearity of the runoff generation process in respect to the proportion of the direct-runoff contributing area. Furthermore, this example introduces the interflow component that has a slower response time than the Hortonian overland flow, but contributes normally a larger quantity to the discharge. Generally in the winter season, interflow dominates the runoff during heavy rainfall occurrences in the catchment of the

Wahnbach (Erpenbeck, 1987). Interflow is produced in the study area because of the hydraulic characteristics of the topsoils as well as of the bedrock.

Measurements of the soil hydraulic conductivity reveals that one has to distinguish the properties K^* and K_{sat} . The reason for this is the high number of macropores in the topsoils leading to very high K_{sat} -values. On hillslopes covered by pastureland the difference between K^* and K_{sat} is additionally pronounced, due to the reduced K^* -values of the strongly compacted soil surface caused by cattle. Rainfall events having greater intensities than the K^* -value will consequently cause a part of the water quantity not being able to infiltrate into the matrix of the topsoils. This will lead to significant Hortonian overland flow on hillslopes without macropores.

However, in the research area, with hillslopes having a distinct secondary pore system, macropores are able to drain surface water. Due to that a large part of the infiltration excess is drained by the macropore system and not by overland flow. Many authors, e.g. Germann (1990) and Bronstert (1994), have described the importance of this process, which is also called by-pass flow. Before the water flows into macropores, it might have been transported on the soil surface for a while. This implies that the probability of infiltration-excess water reaching the channel via overland flow is highest in the direct surrounding of the channel and is lowest in the area of the catchment divide.

Due to the very low permeability of the weathered Devonian bedrock (Flügel and Smith, 1999), the downwards-transported water forms a perched groundwater sheet at the soil-bedrock interface. Once free water exists in this area, pipes in the lower soil zones rapidly transport the water downslope. In addition, a large number of field voles have formed a dense network of pipes on the slopes that are capable of draining directly large amounts of the infiltration excess. However, openings of field voles are only found on hillslopes where no seasonal tillage operations like ploughing take place.

The reason for the absence of an interflow peak during the earlier event (Fig. 20, Chapt. 4.1.2.1) in contrast to the subsequent one (Fig. 21, Chapt. 4.1.2.1) is explicable by the adsorbing soil matrix under antecedent dry conditions. Therefore, infiltration-excess water that is draining through macropores will infiltrate into the soil matrix. Furthermore, it is conceivable that a certain capacity of water uptake exists, which is determined by the

properties of the matrix that surrounds the macropores (e.g. porosity). Therefore it can be concluded that the drier the soils are, the more efficient will be the interception of the by-pass flow, thus preventing significant interflow rates. An analysis of the discharge of all sub-catchments during a period of 28 months revealed the processes of runoff generation at the seasonal scale (Chapt. 4.2.1). Beside the factors landuse and geology, which influence the amount of runoff to a large extent, it is indicated that the geomorphological characteristic has a significant effect on the course of discharge.

Fig. 38 shows perceptual models of the runoff generation processes in the research area, in which a differentiation between V-shaped valleys and trough valleys is introduced. Both valley types can be found in the catchment of the Wahnbach River. The V-shaped valleys in this region are called ‘Siefen’ (Chapt. 3.1.1). Nicke (1989) described observations, where a forested Siefen-type valley was cleared and which developed in the following period to a trough valley-type, indicating that these geomorphological forms are often bound to the type of vegetation on the valley walls. In fact, most of the Siefens are forested in the catchment of the Wahnbach River. A sub-catchment can either show only one of these valley types (e.g. Steinersiefen) or can exhibit a combination of both types (e.g. Berrensiefen).

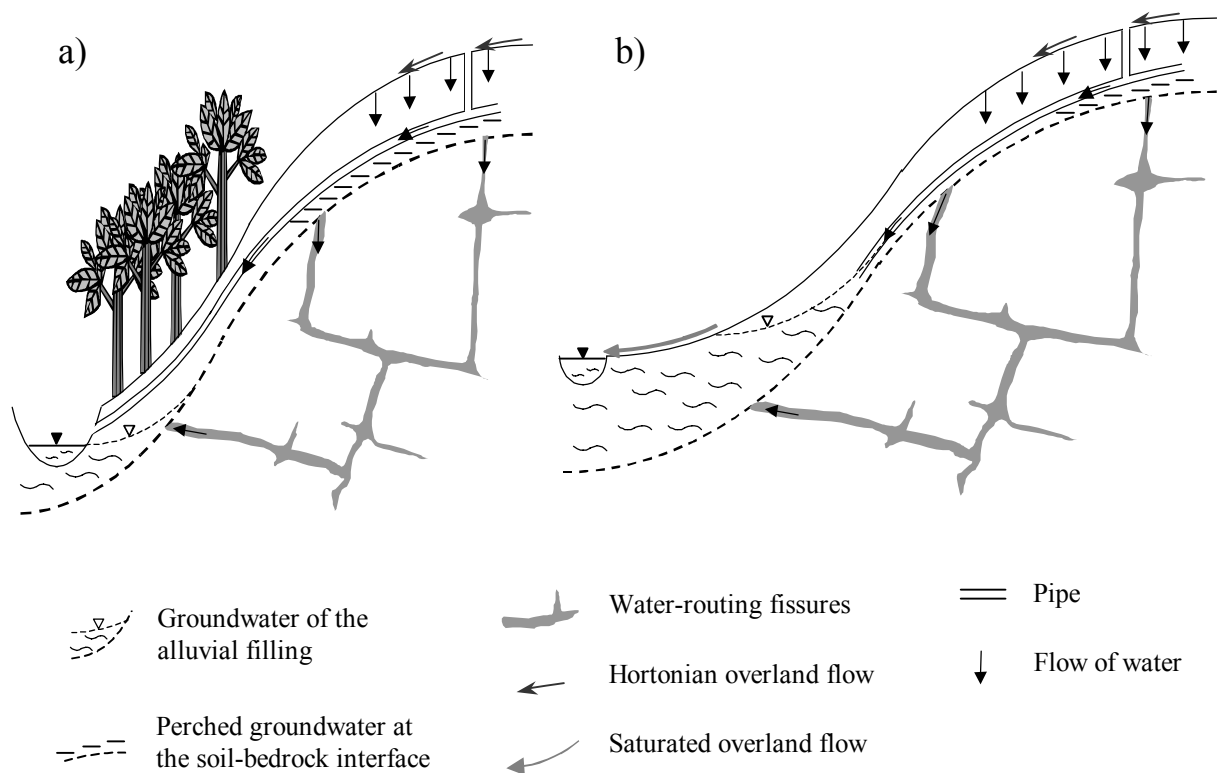


Fig. 38: Runoff generation in the research area with special consideration of the interflow process; a) cross-section of V-shaped valley, b) cross-section of a trough valley including an alluvial filling.

The main difference between both valley types is the presence of a valley plain and accompanying alluvial fills, which has certain consequences on the runoff generation process. The pipes end either directly in the sidewalls of the channel, as it can be observed in the parts where the Berrensiefen brook has the form of a deep valley cut, or beneath the surface in the area of the valley plain. This difference leads to a dissimilar interflow response (Fig 38). The runoff of a V-shaped valley is more pronounced, while a trough valley leads to a more distinct tailing of the discharge after the rainfall has ceased. Furthermore, during wet seasons saturated overland flow plays a role in basins with valley plains, whereas in V-shaped valleys surface flows from the hillslopes are mainly comprised of Hortonian overland flow.

In addition, water-routing fissures are shown in Fig. 38. These features are always present in the Devonian bedrock of the Wahnbach catchment. Due to the low permeability of the fissures (von Kamp, 1983), only an insignificant contribution of these flowpaths can be expected. However, they are possibly the sole contributor to water and solute transport during dry seasons and therefore have to be considered as well. Furthermore, it is possible that connected fracture systems that are full of water can act as pipe systems transmitting fresh groundwater rapidly to the channel system (Beven, 2001).

In the following section, the analyzing of the solute concentration is used to provide a clearer differentiation of these processes.

4.4.2 Solute and sediment transport

The analysis of the SBC and SBA concentrations of Berrensiefen during September 1998 showed that the chemical composition of the discharge water changed significantly during the flood discharge. The concentrations of some anions (mainly sulphate and nitrate) are significantly increased, indicating considerable washout from the soils; while most cations display a decrease in concentration, demonstrating dilution effects of the surface and subsurface flows. The increase of potassium concentration during high water flows is an indication of surface flows (Mollenhauer and Wohlrab, 1990).

By comparing the solute concentrations of all investigated sub-catchments for the period from August 1998 until December 2000, the seasonal pattern of the solute transport is revealed. The findings of the previous analysis are also present on this temporal scale, thus interflow is

indicated in the case of high concentrations of nitrate and sulphate; whereas high concentrations of most cations indicate the dominance of groundwater flow.

The high concentration of potassium and phosphate during the dry period 1999 may either be interpreted as indication of overland flow or desorption processes in the channel. However, the generally higher concentrations of these substances in the southern sub-catchments strongly indicate a pronounced susceptibility for soil erosion of basins having a considerable proportion of loess coverage in the Wahnbach catchment.

During high flows the concentration of suspensoids and bed-load discharge increases significantly, indicating soil erosion on the hillslopes due to overland flow and pipe flow as well as channel incision. The grain-size distribution of the suspensoids is effected by the discharge rate, getting coarser with increasing discharge. However, due to the impact of the 15th/16th of September 1998 rainfall event, the channel bed structure may be changed, leading to a different shape of the grain-size distribution. The concentration of suspensoids is also influenced by the landuse of the catchment. The sub-catchments with significant agricultural farming exhibit significantly higher sediment concentrations. At the catchment scale, annual precipitation amounts are showing no correlation with annual sediment export, indicating that small-scaled processes are of significant importance for the sediment transport.

However, it has to be noted that the differences in geology, topography and human impacts (channel bed consolidations, roads etc.) of the sub-catchments make it difficult to examine the influence of single factors.

5 Application scheme of the model system

The model system OPUS is applied at different spatial and temporal scales, beginning at the slope scale and a temporal scale of single events up to three years. In the next step, the results of the local scale are transferred to the catchment scale, which involves generalisations in the parameterization scheme. Furthermore, a simulation of the channel processes with the HEC 6 model is carried out at this scale. The last step is the long-term application of the OPUS model, introducing further simplifications of the process description and generation of input data.

5.1 The sub-catchment scale

At the sub-catchment scale single processes and state variables can be measured and input data are available to a sufficient extent. Therefore, at this scale model improvement, sensitivity analysis and parameter calibrations are carried out.

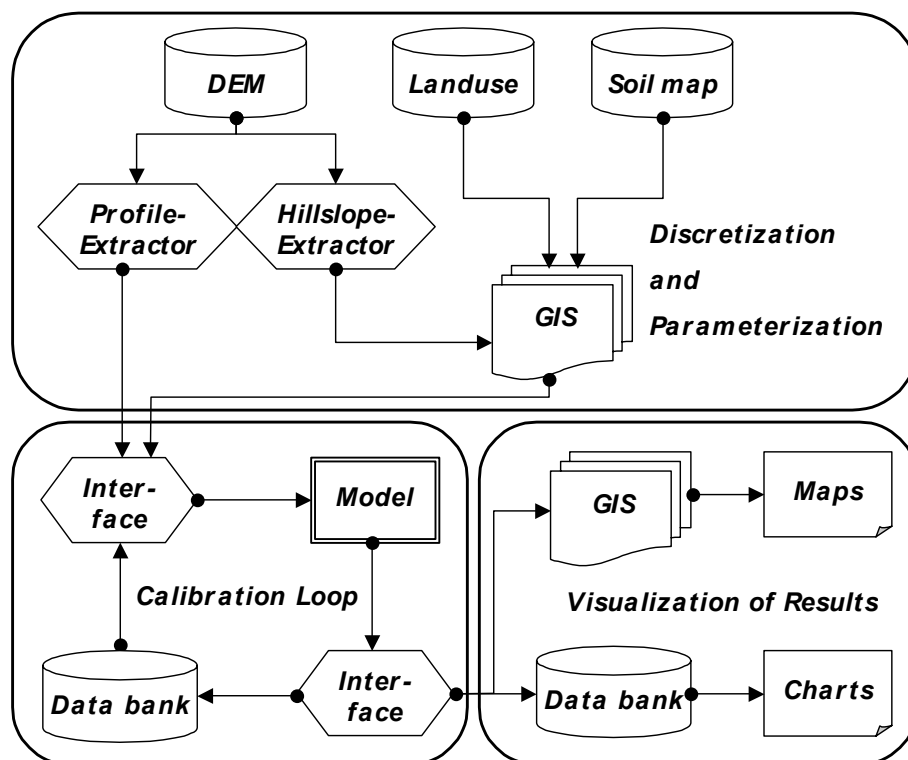


Fig. 39: Application scheme for the simulations with the model system OPUS, including discretization, parameterization, calibration and presentation of results.

Fig. 39 displays the three parts of the application scheme, which are the ‘discretization and parameterization element’, the ‘calibration loop element’ and the ‘visualization-of-results element’. The first part is connected with the second one via an interface, which is able to automatically generate control files to run OPUS. The model output is either analyzed manually or automatically via another interface. Generally, the manual procedure is used to calibrate the modified OPUS model. A calibration is necessary because the modified version contains parameters that are not measurable in the field. In the following sections the elements of the application scheme are presented in detail.

5.1.1 Parameterization of the OPUS model

In this chapter a description of the parameterization scheme for the sub-catchments is given, which has been developed in order to put the ‘catchment space’ – determined by land utilization, topographic features and soil variability - as best as possible into the ‘model space’.

5.1.1.1 Parameterization of topography

In this section it is described how topographic features of the sub-catchments are interpreted in terms of a hydrologically representative set of rectangular fields and receiving flow-paths. Fig. 40 schematically displays the general approach for the discretization of an arbitrary catchment using geographical information systems (GIS), including catchment delineation, delineation of stream network and hillslopes, allocation of input data and simplification of topographic and watercourses.

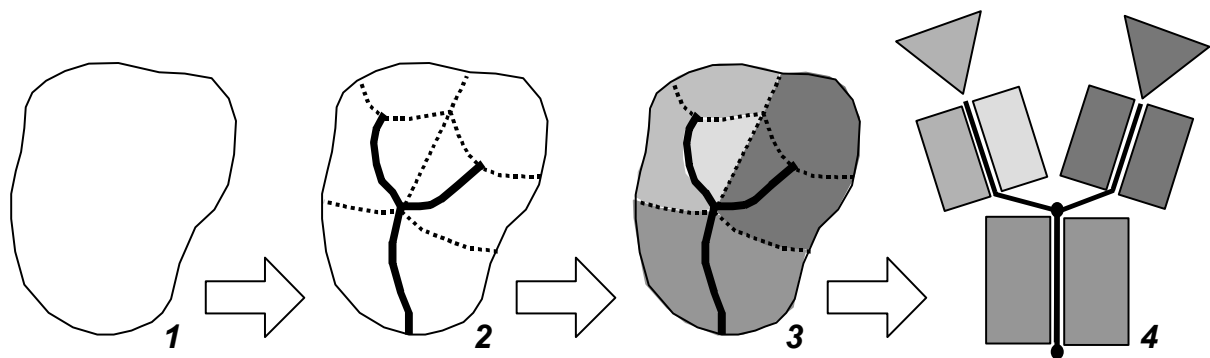


Fig. 40: Generalised discretization scheme for the division of catchments into single planes for OPUS applications: 1) catchment delineation, 2) delineation of stream network and hillslopes, 3) allocation of input data and 4) connecting the hillslopes with a channel model.

Due to the model concept, topography has to be simplified for its implementation into the model scheme. The transformation of the actual topographic features into the geometrical hydrologic equivalents is partly subjective, but the resulting abstraction should preserve the following features: area, mean surface flow-path length, net slope of mean flow-path and concentrated flow-path length (Ferreira & Smith, 1992).

On the basis of a digital elevation model with a resolution of 5 m, the water divide of the basin is generated. Afterwards, hillslopes are separated and overlaid with the digitized landuse map. Through this operation additional planes are obtained in order to achieve an appropriate representation of the landuse distribution. This operation is only carried out at the sub-catchment scale, where relative small deviations from the real landuse situation may lead to erroneous calculations of the water balance. Fig. 41 displays an application of this methodology to the sub-catchment Hellenkeutelsiefen.

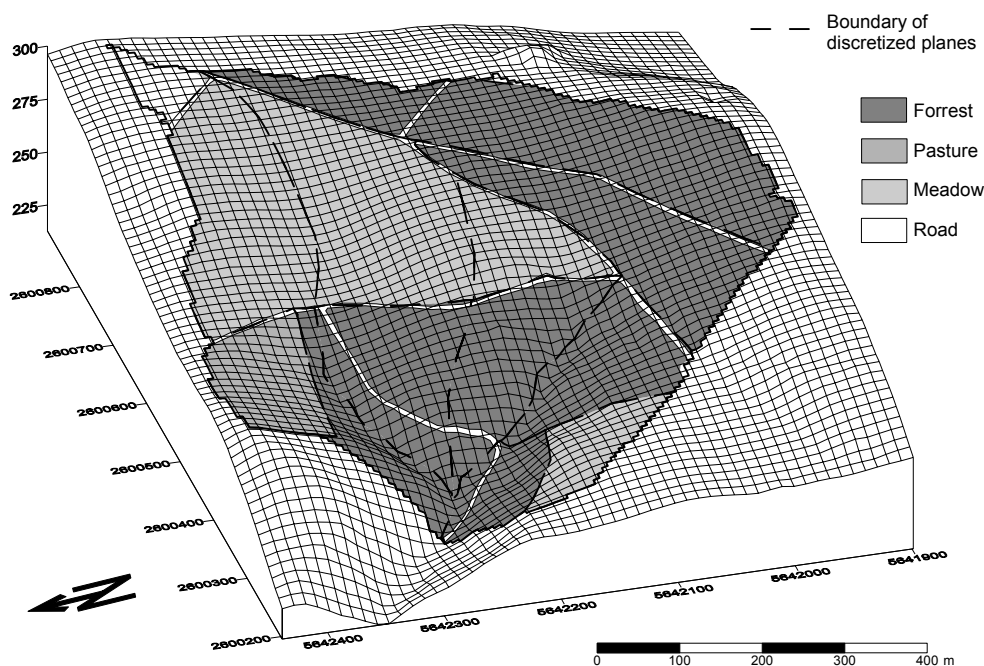


Fig. 41: Discretization of the sub-catchment Hellenkeutelsiefen into several planes; trenches along the roads are considered to have the same effect as the natural channel in respect of gathering overland flow.

The next step is to define characteristic slope profiles for each elementary catchment unit. Obtaining an optimal representation of the hillslopes profile is not trivial, since the selection is always subjective (Goodrich et al., 1991). In order to make this step more objective, the following scheme is applied:

1. Selecting of a point at which the profile starts (typically near the water divide of the catchment unit);
2. Tracing the theoretical flowpath of a raindrop from the defined point to the channel;
3. Selecting the elevation data and distances from starting point along the flowpath;
4. Converting the data into OPUS-readable format.

The theoretical flowpath is generated using the *flowdirection*- and *accumulation*-function of ARC/INFO[®] Grid[™] on the basis of a digital elevation model (DEM), having a resolution of 5 m. Fig. 42 displays the selected profiles for the sub-catchment Hellenkeutelsiefen.

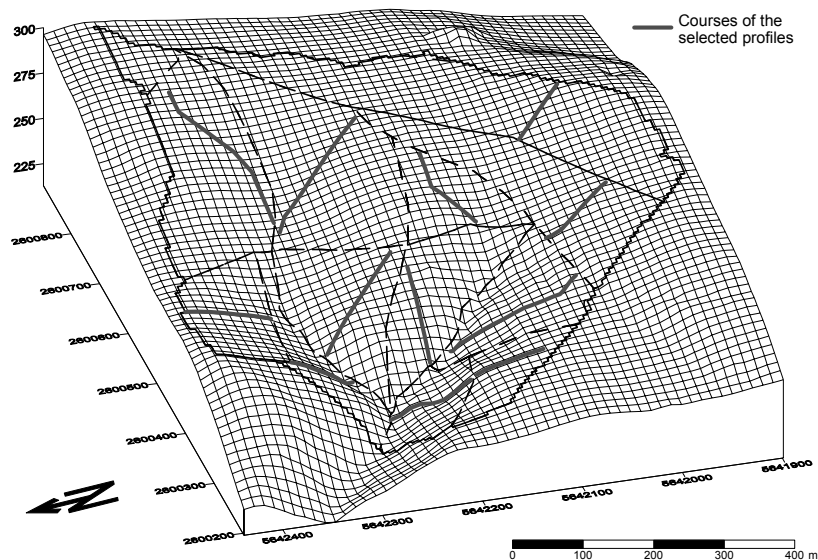


Fig. 42: Representative profiles for the sub-catchment Hellenkeutelsiefen.

Using this procedure, a compromise between the recommendation of the OPUS User Manual (Smith and Ferreira, 1992) and the exploitation of the functionality of a GIS is obtained. The curvatures of the selected profiles are presented in Fig. 43, proving that the great variety of profile forms, from elongated to convex and concave hillslopes, can be well reproduced. The same scheme is used to parameterize perennial channels and concentrated flow-paths within the basin. The roads within the Wahnbach catchment are often accompanied by trenches, which have the same effect as natural channels in respect of gathering surface water coming from the bordering hillslopes. Therefore, at the sub-catchment scale, these trenches are considered as flowpaths in the OPUS simulation as well.

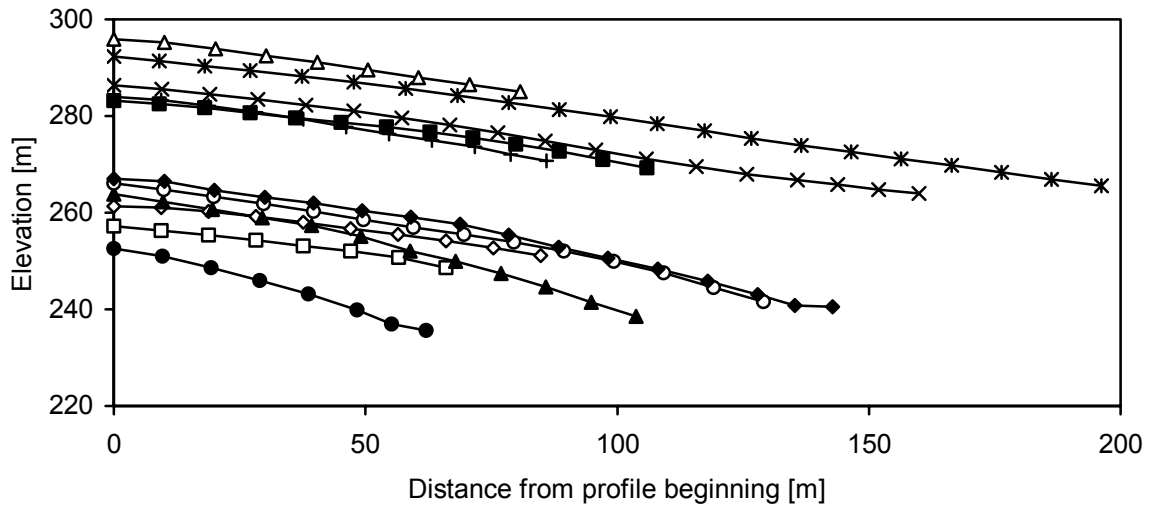


Fig. 43: The curvatures of the selected profiles for the sub-catchment Hellenkeutelsiefen.

5.1.1.2 Parameterization of soil horizons

The properties of the simulated soil column in OPUS can either be done by an overlay operation of the available digital soil map (scale 1:5,000) with the discretization coverage or by allocating measured field data. The former case is applied to the sub-catchments Hellenkeutelsiefen and Steinersiefen, while the latter case is utilized for the Berrensiefen basin. In the following section the parameterization of the sub-catchment Berrensiefen is described.

To provide the chemical and physical properties of the soils and their variability, a detailed soil survey was undertaken in the basin of Berrensiefen. About 180 soil samples were taken from two horizons (A_h - and B_v -horizon) covering the whole sub-catchment. Among other properties texture, soil organic matter and nitrate-content have been measured. Besides the creation of a reliable database for model parameterization, a further aim of this costly soil survey was to capture the spatial variability of the soil properties by means of geostatistical techniques.

Geostatistic is founded on the theory of regionalized variables (Matheron, 1963). The measured soil property at one point is taken as a variable of chance and therefore can be described by a probability density function. It is assumed that the value of expectation is independent of the location and that for all distances a finite semivariance exists. The

geostatistical method to interpolate variables is called kriging, which is the generic term for several variants, e.g. ordinary kriging.

The quantification of the spatial autocorrelation by analyzing the semivariances of all variables is a prerequisite for kriging. Therefore an experimental semivariogram has to be created. This is done by assembling the point pairs into distance classes and subsequently plotting these classes against the mean semivariance of each class. Subsequently, a variogram model, e.g. linear or spherical model, interpolates the gained scatter plot. Finally, the fitted variogram model is used as the weighting function of the kriging interpolation.

In this study the variogram analysis is carried out using the tool VESPER (McBratney et al., 1999) and the software package SURFER[®] is used for the kriging interpolation. Fig. 44 shows exemplarily the semivariograms of the measured sand and clay content of the topsoil and the subsoil. Each experimental variogram is fitted with a spherical model, which is in the next step used for the interpolation of the soil properties using ordinary kriging (Fig. 45).

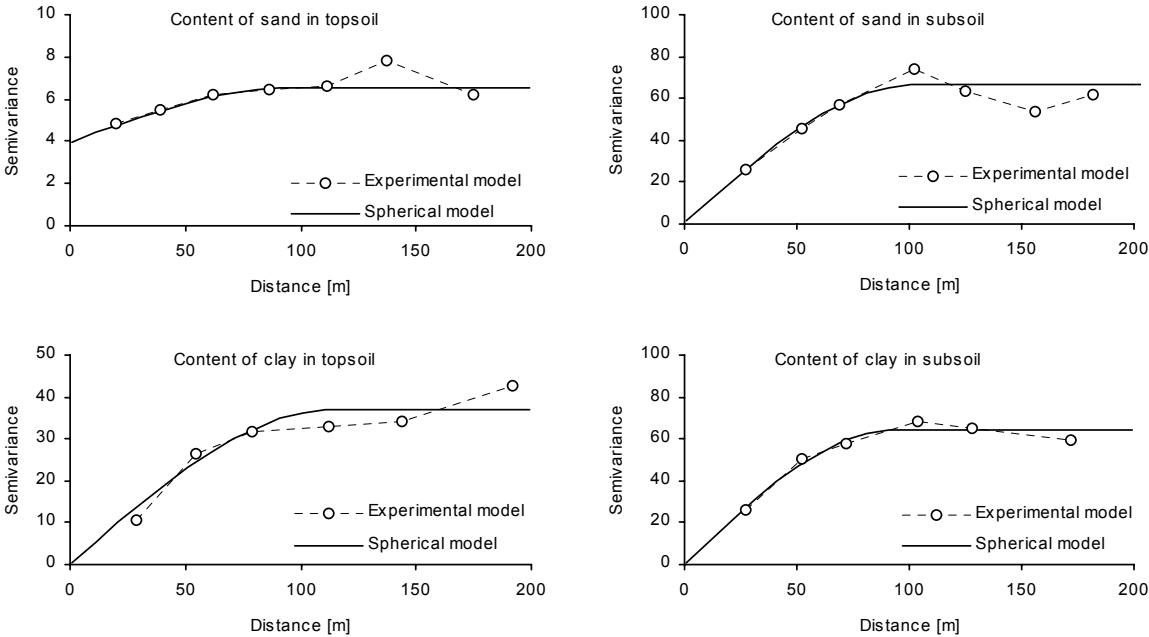


Fig. 44: The experimental variograms of sand and clay contents of the topsoil and subsoil, as well as the fitted variogram models for each scatter plot.

For the OPUS simulation the Berrensiefen basin is subdivided into eight planes and the interpolated soil properties are averaged for every plane in order to parameterize the model.

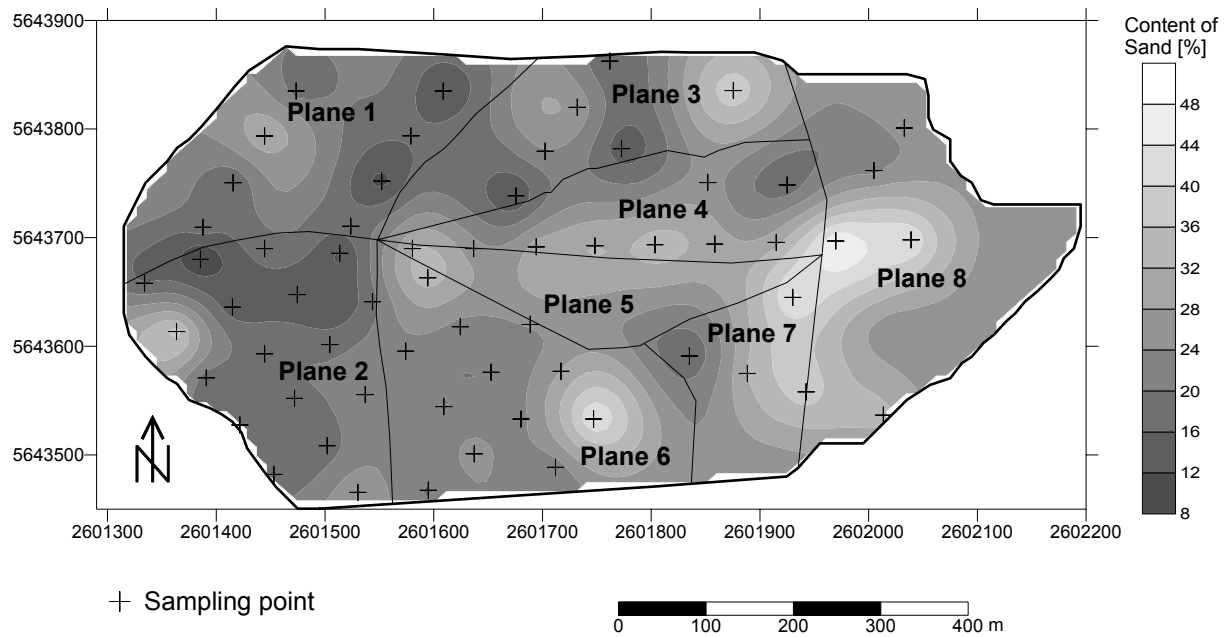


Fig. 45: Discretization of the Berrensiefen sub-catchment into eight planes and interpolated sand content of the topsoil using ordinary kriging.

Tab. 8: The average percentages of sand, clay, soil organic matter and nitrate-content of each plane.

	Plane 1	Plane 2	Plane 3	Plane 4	Plane 5	Plane 6	Plane 7	Plane 8
Topsoil								
Sand [%]	11.2	16.1	21.3	22.9	22.4	22.6	31.7	24.8
Clay [%]	20.1	19.0	21.5	20.6	20.2	19.3	19.5	25.21
C _{org} [%]	2.99	3.01	2.97	3.05	3.01	2.88	2.85	3.22
Nitrate [mg/kg]	32.8	45.2	40.1	46.4	49.9	47.6	45.1	33.7
Subsoil								
Sand [%]	17.8	17.3	21.6	26.0	28.3	26.2	33.5	30.3
Clay [%]	16.8	17.9	21.1	18.2	17.7	20.4	22.4	23.6
Nitrate [mg/kg]	24.4	26.2	15.6	29.7	30.0	19.7	12.8	17.5

Tab. 8 lists the average percentages of sand, clay soil organic matter and nitrate content of each plane. On the basis of the investigated soil data, soil-hydrological parameters (hydraulic conductivity, residual water content, bubbling pressure, pore size distribution index and saturated water content) were calculated using the Rawls & Brakensiek-pedotransfer functions (PTF) (Rawls and Brakensiek, 1985). These parameters are used to describe the relations between water content, capillary suction, and hydraulic conductivity in order to solve numerically the non-linear Richard's equation (2). Very recently, the problem whether it is better to interpolate at first and use PTF-functions in a second step or the other way around was examined (Herbst, 2001).

5.1.1.3 Crop and management data

Five different land utilizations are implemented in the OPUS model: annual crops, meadow, pasture, fallow and forest. These landuse types can be exchanged within a rotation cycle that is repeated after five years.

In order to simulate the vegetation dynamic, a mechanistic plant-growth module is implemented in OPUS. This module requires several plant parameters describing optimal size at mature stage and yield, optimum growth-determining temperature, aging rates and nutrient contents. Due to the mechanistic character of the module, these parameters are mainly obtained by fitting. However, input data are already available to a large extent (e.g. Ferreira & Smith, 1992). Nevertheless, these parameters have to be adjusted to the special peculiarities of the research area. Fig. 46 shows the course of the LAI-values of corn, winter wheat and pasture.

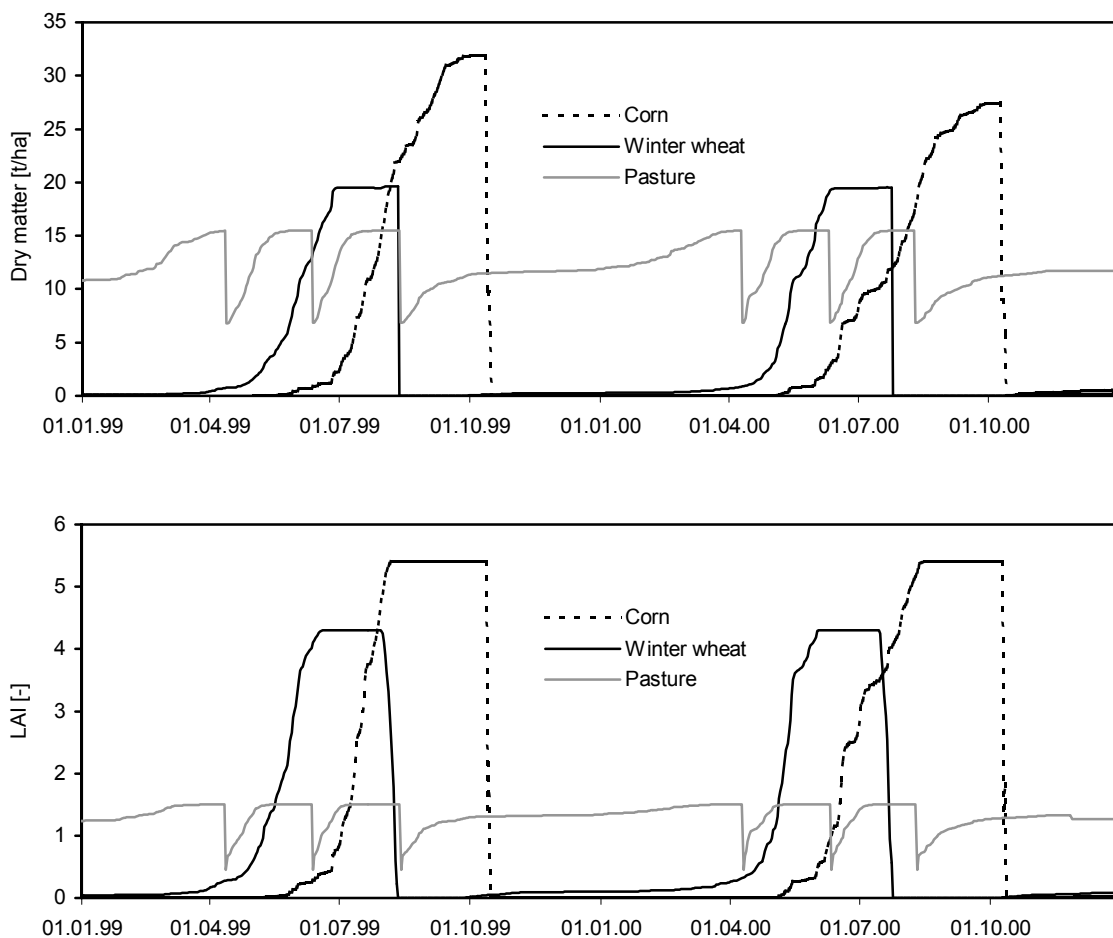


Fig. 46: Simulated dry matter and LAI of corn, winter wheat and pasture by the OPUS model.

Furthermore, tillage operations that are carried out in the catchment have to be described. Five different operations are implemented in OPUS: seed planting, cultivation, harvest or grazing, harrowing and ploughing. Each operation involves specific characteristics, e.g. depth of mechanical mixing, depth of furrows. The appropriate values are taken from the OPUS User Manual (Ferreira & Smith, 1992). The courses of dry matter and LAI reflect the influence of the management operations, e.g. the mowing operations on pastureland, which are common in this region, lead to sharp drops of dry matter as well as LAI. Subsequently, plant growth is enforced until the potential maximum values of dry matter and LAI are reached again.

In order to run a correct simulation of nitrate discharge, the accurate balancing of nitrogen inputs and outputs is a prerequisite. In this respect, the landuse-type pasture is especially significant because of its high percentage of surface area in the Wahnbach catchment, and is therefore described in more detail.

There were about 5200 head of cattle on an area of pastureland of 27.7 km² in the Wahnbach catchment in 1997, which corresponds to a cattle density of approx. 1.9 cattle per hectare pastureland. Assuming a grazing duration of 180 days, which is typical under the given climate conditions, a total sum of approx. 7.2 tonnes of faeces per hectare and year can be calculated (Fürchtenich et al. 1993). This leads to a nitrogen input of about 129 kg N/ha. Additionally, artificial and organic fertilizations have to be considered. According to Fürchtenich et al. (1993), the following fertilization doses are recommended:

Tab. 9: Recommended fertilization amounts of nitrogen for several landuse types.

	N [kg/ha]	Kind of fertilization
Pasture	100-240	Application of slurry one time in spring, artificial fertilizer in front of each plant growth phase
Wheat	180	Slurry and artificial fertilizer, four applications per year
Corn	300	Slurry in spring and artificial fertilizer during late summer
Sugar beet	200	Artificial fertilizer, two times per year

These general values are, as far as possible, adjusted to the specific situations in the sub-catchments by local observations and questioning of farmers.

A certain part of the soil nitrogen-pool is lost due to plant uptake and the subsequently removal of grass by grazing of cattle and mechanical mowing. According to Borstel (1993), the daily grazing amount of cows is about 17 kg dry mass, resulting in a average annual loss of grass of approx. 4 tonnes per hectare. Due to the fact that mowing of pastureland is a common practise, about 8 tonnes of grass are lost in total. This results in a yearly loss of nitrogen of 40 kg/ha.

5.1.1.4 Sediment and erosion data

OPUS considers up to five particle classes into which the sediment particle distribution has to be subdivided for the simulation of soil erosion. For each particle class the effective surface area can either be specified or be calculated internally by OPUS.

Furthermore, the mean USLE soil K erodibility factor has to be specified. Appropriate K-values for Central Europe are calculated using the recommendations of Schwertmann et al. (1987), who adapted the USLE-concept to German conditions. Another possibility is used in the case of the sub-catchment Steinersiefen. Here, for the calculation of the K-value, a relation developed by Martin (1988) was applied:

$$K = \left[6 \cdot 10^{-4} \cdot S \cdot (1 + 0.0015 \cdot A \cdot C) \cdot (12 - C_{org}) + 0.021 \cdot (K + Na) \cdot e^{-0.05 \cdot ST} \right] \quad (34)$$

where C, S and A are the contents of clay, silt and sand respectively in percentage, C_{org} is the percentage of soil organic carbon, K and Na are the percentages of potassium and sodium on the base exchange capacity and ST denotes the content of skeleton [%].

By including the percentages of potassium and sodium into the base-exchange capacity in equation (34), it is possible to consider the influence of fertilization on the soil erosion process.

5.1.2 Modifications of the OPUS model

Whelan et al. (1995) argue that modelling of solutes in catchment drainage has to be empirical to some extent, because the internal mechanisms in most catchments are unknown.

Nevertheless, the main processes taking place in the catchment have to be investigated and, if possible, they should be implemented in the model - to a reasonably extent - in a physically-based way. In order to meet this goal, process studies at the sub-catchment scale have been carried out and the knowledge acquired was integrated into OPUS.

The analysis of the processes determining runoff and transport of dissolve and solid matter discovered that runoff during heavy rainfall events in the winter season are dominated by interflow (see Chapt. 4). Originally, OPUS was not able to simulate the processes determining interflow discharge. In order to get realistic simulation results, an appropriate modification of the model was introduced.

In Chapt. 4 it is explained that the interflow is mainly produced because of a combination of preferential flow-paths in the soils producing by-pass flow and a low hydraulic conductivity of the underlying bedrock. Thus, in order to consider the influence of preferential flow-paths like macropores on hillslope hydrology, the process of by-pass flow has to be implemented into the model scheme.

A second reason for the consideration of preferential flow in the model scheme is related to the solute transport. In most cases of erosion simulations on soils containing a considerable amount of macropores, a calibration of the K_s -value of the topsoil is carried out in order to simulate the correct amount of overland flow on the hillslopes. This calibration causes an increased nitrate-washout because then the main water flux takes place through the soil matrix.

For modelling the water and solute transport successfully, the model system OPUS is extended by a module that facilitates the simulation of the interflow induced by macropores (Bogena and Diekkrüger, 2000). Fig. 47 schematically displays this implementation into the model scheme. The infiltration excess simulated by OPUS is divided into overland flow (1) and macropore flow (2), in which the latter corresponds to interflow. The division of overland flow and macropore flow is carried out by using a factor (Ma) that specifies the percentage of the infiltration excess, which flows into the macropores.

Furthermore, it is taken into account that a small groundwater reservoir is situated in the valley plain, which has direct contact to the channel and causes a retardation of the downslope-transported water (3) from the hillslope. The two components interflow and quick groundwater flow are simulated using linear single storage models. To reproduce the base flow (4), a slow groundwater storage model is introduced. For the simulation of the solute transport in the catchment, each storage model is coupled with a simple complete solute-mixing model.

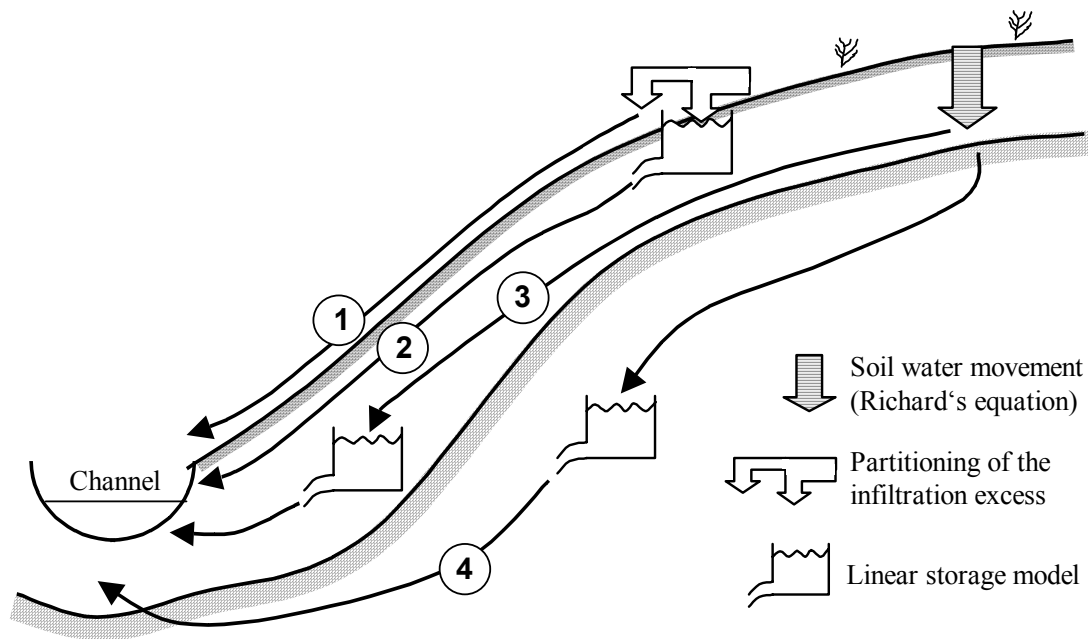


Fig. 47: The modified model system OPUS with four different flow components: overland flow (1), interflow (2), quick groundwater flow (3) and slow groundwater flow (4).

In order to implement the impermeable bedrock, the lower boundary is simulated with the draitile option of OPUS, which is based on an analytical expression developed by Bouwer and van Schilfegaard (1963):

$$q_d(h_{\max}) = y \cdot q(z, t) - \phi \cdot y \frac{d\bar{h}}{dt} \quad (35)$$

with q_d is the drain discharge [$\text{mm}^3/\text{mm}^2/\text{min}$], h_{\max} and \bar{h} are the maximum and mean groundwater levels [mm], y is the draitile spacing [mm], q_p is the percolation rate [mm^3/min] and ϕ is the effective soil porosity.

Fig. 48 illustrates this approach to link the unsaturated and saturated flow regions.

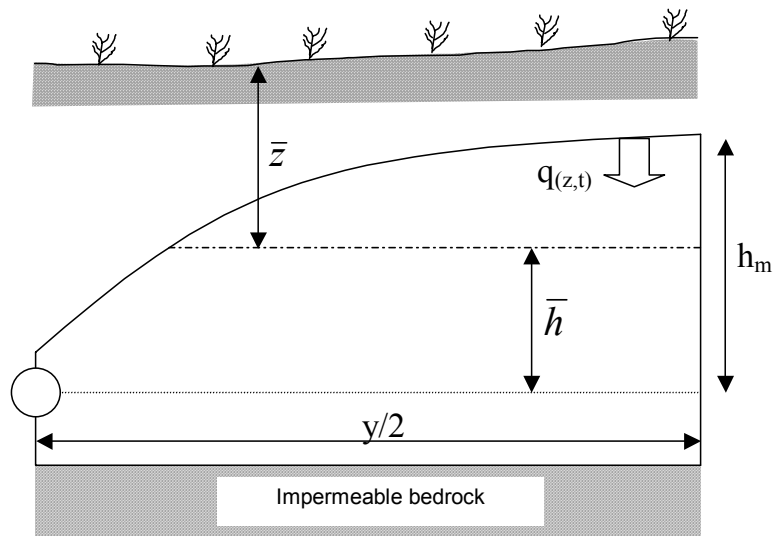


Fig. 48: Illustration of the equation used for the linking of unsaturated and saturated flow regions (redrawn from Smith, 1992).

The use of equation (35) is restricted to regions where the following assumptions are fulfilled:

- An impermeable layer is located beneath the soil;
- Horizontal water flow dominates;
- Flow velocities are proportional to the slope of the impermeable layer;
- An elliptical shape can describe the surface of the groundwater.

Although the saturated zone in the study area is restricted to a relatively small layer between the soil and the impermeable bedrock, these assumptions are satisfied, because channels are acting similar like drain tiles and the soil-bedrock interface shows an elliptical-like shape.

Thus the drain tile option of OPUS can be applied.

The use of equation (35) for the computation of the lower boundary implies an always-present groundwater table and therefore groundwater is permitted to rise into the soil layer during dry periods. However, this is only the case in the direct surroundings of the channel and is therefore restricted to a very small part of the sub-catchment. For a better reproduction of the hydrologic conditions, OPUS was modified again now to prevent the rise of both water and solutes into the bottom soil layer.

5.1.3 Sensitivity analysis

In order to examine the effects of input parameter variations upon the model output, a sensitivity analysis of the OPUS model was undertaken. The procedure used for the sensitivity analysis is to run a set of simulations in which the value of a system parameter is changed by a fixed amount in each model run. The aim for such an analysis is to test whether a model is sensitive to a particular parameter in such a way that reliable results cannot be obtained (De Roo, 1993).

In this study a simple index that describes the sensitivity of a variable is used:

$$S = \frac{|R_i - R_d|}{R_b}$$

where S is the sensitivity within a ten percent range, R_i and R_d are the model results with a variable being increased and decreased by 10 %, and R_b is the baseline simulation.

This method is not capable of reproducing the non-linear relationships of the different variables and process descriptions in a physically-based model, but gives an idea of their importance on the model result (De Roo, 1993).

Two aspects are scrutinized in the following section. It is tested whether the averaging of parameters measured in the lab influence the model results and, on the other hand, the importance of certain parameters for the simulation is analyzed.

The sensitivity analysis was undertaken with the OPUS model parameterized for the simulation of one hydrological unit of the Berrensiefen sub-catchment. The variables 'median of particle-size distribution', 'content of organic carbon (C_{org})', 'porosity', 'roughness coefficient' and 'saturated hydraulic conductivity (K_s)' are tested for their influence on overland runoff, nitrate-washout and nitrate-content in surface runoff. Furthermore, the effects of the content of organic carbon, the pH-value, the fertilization amount and the nitrate content in the soil on the simulation of nitrate-washout are investigated. The results of this analysis are listed in Tab. 10.

Tab. 10: Sensitivity indices of variables effecting the simulation of overland flow, nitrate washout and nitrate content in surface runoff simulated by OPUS due to 10 % input changes.

	Overland flow	Nitrate washout	Nitrate content of overland flow
Median of grain-size distribution	0.11	0.002	0.2
C _{org}	0	0.027	0.001
Porosity	0.078	0.149	0.126
K _s -value	0.295	0.019	0.29
Roughness coefficient	0	0	0
pH-value	-	0	0.03
Fertilization of nitrogen	-	0	0.006
Content of nitrate in the soil	-	0.186	0

The determined indices in Tab. 10 suggest that the amount of overland flow and nitrate content of overland flow are mainly influenced by the K_s-value, the grain-size distribution and the porosity. The nitrate content and the porosity of the soil, and the content of organic carbon mainly influence the extent of nitrate washout. The main reason for the fact that fertilization has no effect on the nitrate washout in this analysis is the increased nitrate uptake of the vegetation, buffering up the additional nitrate to a certain extent. The low sensitivity of the K_s-value on nitrate washout may also be caused by the influence of the implemented macropore flow component.

The following sensitivity analysis is undertaken in order to scrutinize the effects of some variables on the soil erosion simulation. This investigation is carried out on the basis of the parameterization of the modified OPUS model on a hillslope of the Steinersiefen sub-catchment. This hillslope is used for cultivation of corn and winter wheat and was subject to an intensive investigation of soil properties and overland flow (Steffen, 2001). The results of the sensitivity analysis are presented in Tab. 11.

Tab. 11: Sensitivity indices of variables effecting the simulation of overland flow and soil erosion of Steinersiefen by the OPUS model due to 10 % input changes.

	Overland flow	Soil erosion
Slope of the plane (S)	0.42	2.55
Length of the concentrated flow-path (L)	0.46	2.44
Percentage of infiltration excess water draining into the macropores (Ma)	0.89	2.87
Content of clay in the topsoil (C)	0.08	0.06
Soil erodibility (K)	0.43	2.82
Manning's roughness coefficient (M)	0	0.04
Saturated hydraulic conductivity (K_s)	0.75	2.69
Mean sensitivity	0.43	1.94

In almost all cases in Tab. 11 soil erosion is stronger effected by the variation of the input parameter than the overland flow. Thus the mean sensitivity for soil erosion is 72 % higher than for overland flow, showing the great importance of a cautious parameterization of OPUS in respect to simulation of the transport of sediment. This analysis exhibits that the Ma-value is the most sensitive value for both overland flow and soil erosion, whereas the C- and M-values show almost no effect.

Furthermore, the sensitivity of the K_s -value is higher than for the Berrensiefen basin. This difference suggests that the simulated overland flow on ploughland is stronger effected by the K_s -value than on meadow.

5.1.4 Calibration of the OPUS model

The aim of a calibration procedure is the estimation of values for those parameters which cannot be assessed directly from field data. According to Refsgaard and Storm (1996), three types of calibration procedures can be differentiated:

1. Trial-and-error, manual parameter adjustment;
2. Automatic, numerical parameter optimisation;
3. A combination of (1) and (2).

Refsgaard and Storm (1996) argued that the first method is the most common, and especially recommended for the application of more complicated models in which a good graphical representation is a prerequisite. Alternatively, an automatic calibration involves the use of a numerical algorithm which finds the optimum of a given numerical objective function. This is carried out by applying the model to numerous combinations and permutations of parameter levels, in order to find the best parameter set in terms of satisfying the criterion of accuracy. The combination means that the manual method is placed at the beginning of the procedure in order to delineate rough orders of magnitude, which is followed by the automatic calibration for fine adjustment. The reverse procedure is also possible, whereby the automatic method is used as a kind of sensitivity analysis to find the most important parameters, which are afterwards manually calibrated.

In the following section the calibration of the K_s -value of the topsoil and the percentage of infiltration excess water draining into the macropores (Ma) are presented in more detail. Both variables reveal a distinct sensitivity by the simulation of the runoff generation process as well as for the transport of solute and sediment transport with OPUS (see Chapt. 5.1.3). Furthermore, both parameters are strongly correlated, because the K_s -value determines the amount of water remaining on the soil surface and thus the amount that is potentially drained into the macropores. For this reason, a two-dimensional calibration procedure is applied in which both variables are varied alternately.

The Berrensiefen basin has been selected for the application of this method. Owing to the extensive data basis of the sub-catchment Berrensiefen, it can be expected that the degree of uncertainty of the parameterization of the remaining variables is relatively low.

The K_s -measurements of the soil revealed a maximum in the class of 1 to 2 mm/h in the frequency distribution (Fig. 18, Chapt. 4.1.1). According to this result, a K_s -value of 1.2 mm/h is used as starting point for the automatic calibration procedure for the saturated hydraulic conductivity. In 10 % steps the K_s -value is varied upwards and downwards. The factor Ma (see Chapt. 5.1.2), as being an exclusively conceptionally parameter, cannot be measured in the field. Based upon the observation of frequent macropores in the soils, the base value of Ma is chosen to be relatively high. First trial-and-error simulations also revealed that the optimal Ma-value has to be found between 0.8 and 0.99. Within this range the value of Ma is also varied in 10 % steps.

The index of agreement (IA), which is described in Chapt. 3.5, is selected as the numerical objective function in the calibration procedure. The calibration and validation of a model should always be a multi-criteria analysis, which means that not only one model output should be a criterion for judging the quality of a model result. Therefore, besides the quality of runoff reproduction, the simulated course of nitrate concentration is also taken into consideration in judging the model performance. The daily average runoff and the weekly nitrate concentrations measured in the period from September 1998 until December 2000 served as a basis for the calculation of the IA-values.

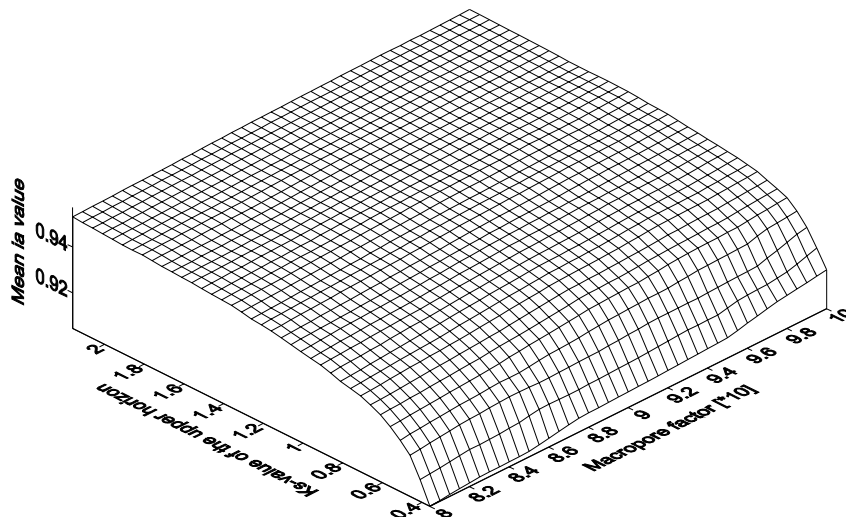


Fig. 49: The calculated IA-values displaying the quality of the runoff simulation results of the automatic calibration procedure; K_s -values in mmh^{-1} .

Fig. 49 reveals that the IA-values of the runoff simulation are stronger effected by the alternation of the K_s - value than the Ma-value, especially in the lower ranges. However, no significant peak is visible in Fig. 49. The best simulation result (IA: 0.957) is obtained with a

K_s -value of 2.16 mmh^{-1} and Ma -values of 1.0, which are the maximum values used in the calibration procedure. Therefore it can be assumed that even better IA -values could be obtained with higher K_s -values. However, a Ma -value of 1.0 means that no overland flow can occur at all. However, the investigation of runoff generation revealed that overland flow is a common feature in the Berrensiefen catchment (Chapt. 4). This finding exhibits the problem of automatic calibration procedures in the case of physically-based models. The most appropriate calibration is not always the most realistic simulation result (Seibert & McDonnell, 2001).

In order to by-pass this problem, further objective criteria are used in this study. IA -values are calculated again, but this time they reflect the ability of the model to match the weekly nitrate concentration. Fig. 50 reveals calculated IA -values of the nitrate concentration simulations. In this case the best simulation result (IA : 0.744) is obtained with a K_s -value of 0.9 mmh^{-1} and Ma -values of 0.95. The mean value of IA (0.69) is significantly lower than for the runoff simulations (0.95), indicating that more uncertainty is involved in the simulation of nitrate discharge.

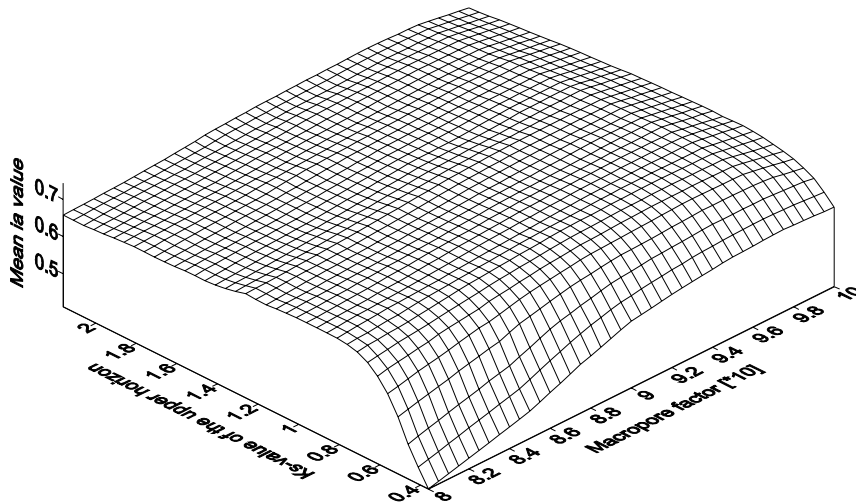


Fig. 50: The calculated IA -values displaying the goodness of the nitrate concentration-simulation results of the automatic calibration procedure; K_s -values in mmh^{-1} .

To facilitate a combination of both IA -distributions as a criterion for the finding of optimum values of K_s and Ma , an average spreading is calculated. The result is shown in Fig. 50, indicating that the most appropriate value for K_s is 0.99 mmh^{-1} and for Ma is 0.95 with an IA -value of 0.848.

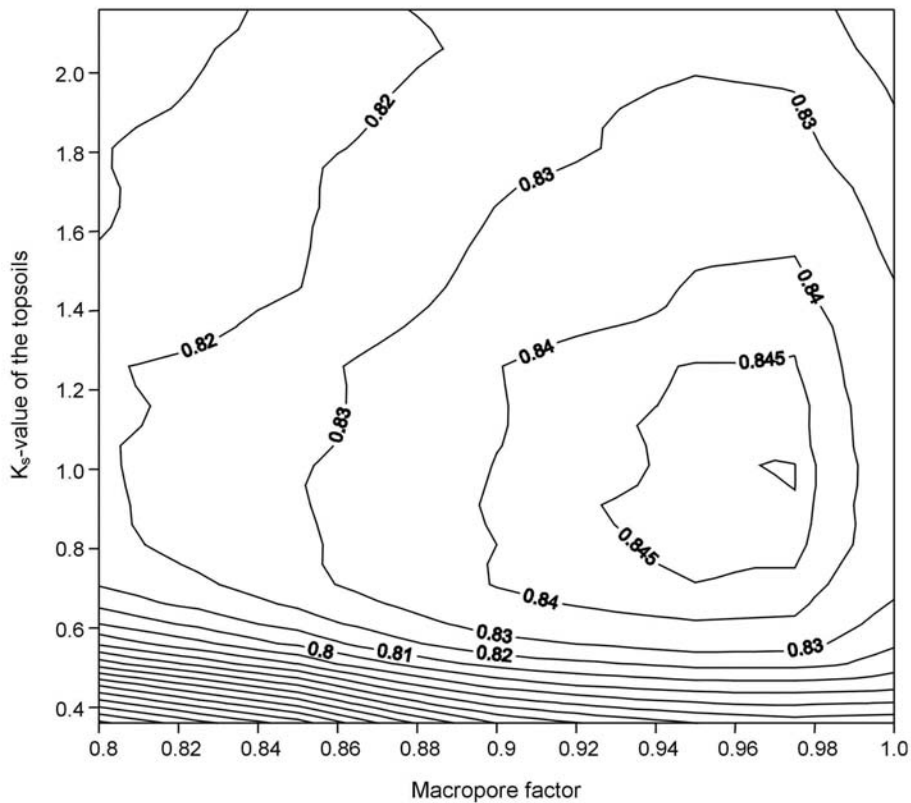


Fig. 51: Average IA-values of the automatic calibration procedure; the best fitting is obtained with a K_s -value of 1.0 mmh^{-1} and a Ma-value of 0.97.

In conclusion, the multi-criteria calibration procedure leads to more reliable simulation results, whereas automatic calibration-procedures with only one criterion may lead to unrealistic adjustments of the parameter set. However, due to the inclusion of nitrate-discharge as a criterion of accuracy, the final IA-value is lower. According to Seibert & McDonnell (2001), the lower value of a model accuracy measure is sometimes ‘the price we have to pay’ in order to obtain a better overall model performance.

Finally, it has to be noted that this analysis depends on the parameterization of the remaining variables. Most of the variables have not directly been measured in the field and thus they had to be assessed with the support of data from other investigations. It is possible that another parameter set will lead to a different calibration result. Therefore the result obtained in this analysis cannot be considered as a final result. In this context the term ‘*equifinality*’ (Schultz et al., 1999; Beven, 2001a) has to be mentioned, which means that an equally good description of a certain process can be achieved by a great number of different parameter sets.

However, due to the abundance of variables in OPUS, a consideration of all possible combinations is impossible and therefore has to be limited to the most sensible parameters.

5.2 The catchment scale

This section introduces the methodology of transferring the OPUS model to the catchment scale under consideration of the experience made at the local scale.

5.2.1 Regionalization of the OPUS model

For a distributed application of the model system OPUS, a regionalization scheme for the sub-catchment scale has already been described (Chapt. 5.2.1). In the following sections, the enhancements for the application of the regionalization procedure at the catchment scale are described.

5.2.1.1 Spatial discretization of the Wahnbach catchment

Fig. 40 (Chapt. 5.1.1.1) schematically displays the general approach for the discretization. For the discretization of the Wahnbach catchment, the software package TOPAZ (TOPographic PArameteriZation) (Garbrecht et al., 1996) is applied. TOPAZ is able to subdivide basins into several single hillslopes using an automatically-generated channel network. The channel delineation is carried out using the 'deterministic-eight-neighbours-method' on the basis of a DEM, in which the flow direction of a grid cell is calculated within a 3*3 surrounding. The flow direction corresponds to the greatest difference in height of the central cell compared to the eight surrounding cells (Grunwald 1997).

In order to generate the channel network, a threshold value, which is called critical source area (CSA), is introduced. The CSA value defines the position of the channel heads in the catchment and has to be tuned by using a manually digitized stream network. Furthermore, a minimal source-channel length (MSCL) is introduced, in order to prevent the generation of too small channel segments. In this study optimal values for CSA and MSCL of four hectares and 200 m, respectively, were found by comparing generated and observed channel networks. Subsequently, for each junction in the stream network a sub-catchment is delineated. In order to obtain elementary hydrologic elements, these sub-basins are subdivided into one hillslope draining into the channel head and two hillslopes draining laterally along the channel

segments. Fig. 52 displays the resulting coverage of the catchment discretization procedure with the catchment subdivided into 890 elementary hydrologic elements.

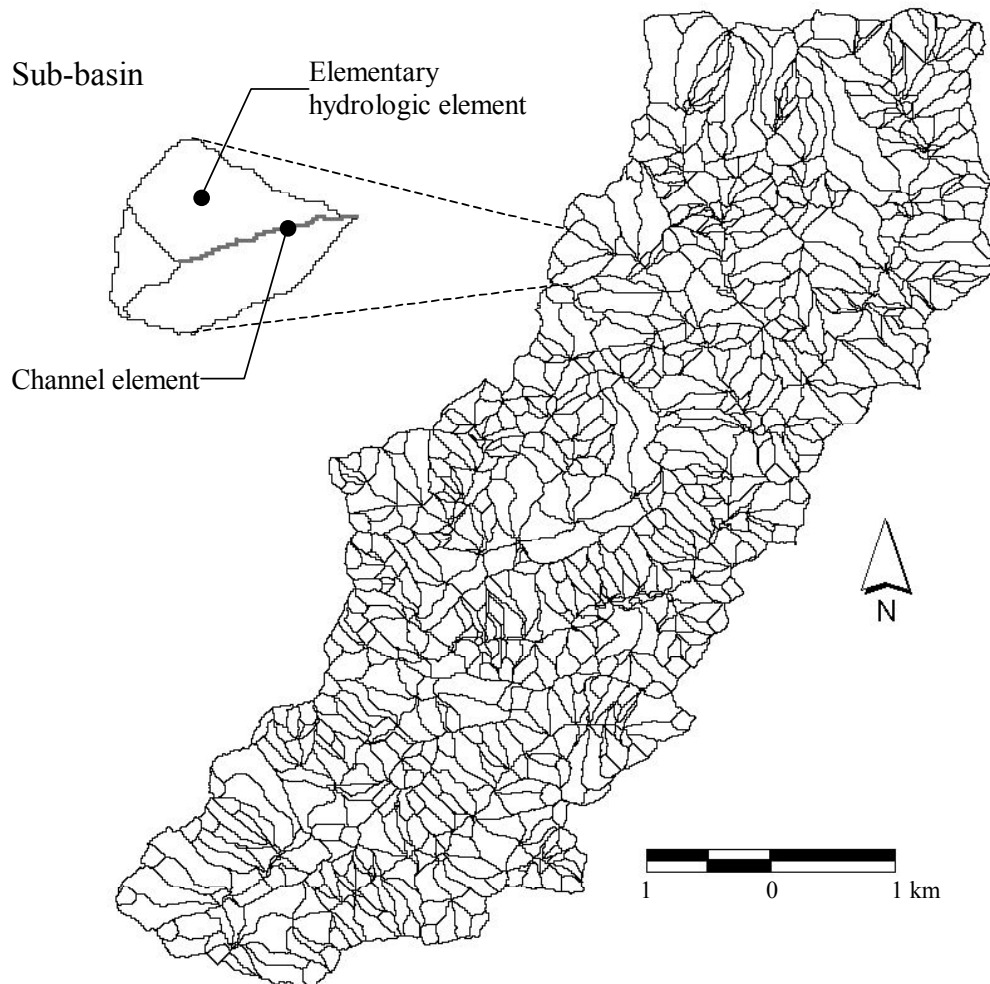


Fig. 52: Discretization of the Wahnbach catchment into sub-catchments; the enlarged sub-basin explains the subdivision into three single hillslopes.

5.2.1.2 Parameterization of the hillslopes

The allocation of the model input data, e.g. soil attributes or landuse types, is carried out using the raster based module ARC/INFO[®] Grid[™]. The respective spatial information is transferred into grid format and then overlaid with the map of discretized hillslopes. By using the *zonal*-functions of ARC/INFO[®] Grid[™], the information covering the maximum area of each polygon of the discretized catchment is allocated to the corresponding hydrologic element unit.

5.2.1.3 *Generation of hillslopes and channel profiles*

For each elementary hydrologic element a characteristic hillslope profile is generated. Therefore a grid is used, with each cell having the local slope information calculated within a 3*3 surrounding on the basis of a DEM. In order to get discrete areas of equal slope values, the continuous values are divided into six slope classes. Subsequently, the corresponding classified slope coverage is overlaid with the discretization coverage. The resulting coverage, which contains the hillslope segments, is used to calculate the mean slope values of each segment. Finally, the mean slope length of each segment is calculated with the *flowlength*-function of ARC/INFO[®] Grid[™].

The same procedure is applied for the generation of characteristic channel profiles. Due to the automatic procedure it is nearly inevitable that, to some extent, unrealistic slope values are produced. Furthermore, OPUS is not able to process very low slope values. For these reasons, only values between 4 and 30 % and between 1 and 10 % are used for the generation of characteristic hillslope and channel profiles.

5.2.2 **Parameterization of the HEC-6 model**

The model HEC-6 requires extensive input data, which can be classified into three groups: morphological, hydrological and sedimentological parameters. Due to the large expenditure involved in the parameterization, the application of the HEC-6 model in this study is restricted to the catchment of the Wendbach River, which is the greatest tributary of the Wahnbach River (Fig. 10, Chapt. 3.1). The Wendbach River has a stream length of 6.62 km and a mean river gradient of 16,1 ‰.

5.2.2.1 *Morphological parameter*

The Wendbach River is subdivided into 18 segments (Fig. 53). Each segment is marked by a characteristic cross-section. In order to obtain reliable cross sections, a manual field measurement was carried out. The profiles of the potentially flooded valley-bottom are generated using the *profile extractor*-extension of ARCVIEW[®] Spatial Analyst[™] on the basis of a DEM with a resolution of 5 m.

5.2.2.2 Hydrological parameter

Local inflows of water and sediments are simulated with the OPUS model. Due to the limitation that the HEC-6 processes only a restricted amount of inflows, the simulated hillslopes are assembled into nine clusters (Fig. 53). In order to reduce the computation expenditure, the daily-resolution of the OPUS-simulation was reduced into a 10 day-resolution. Furthermore, the length and mean slope of the segments are derived from the DEM (Tab. 12).

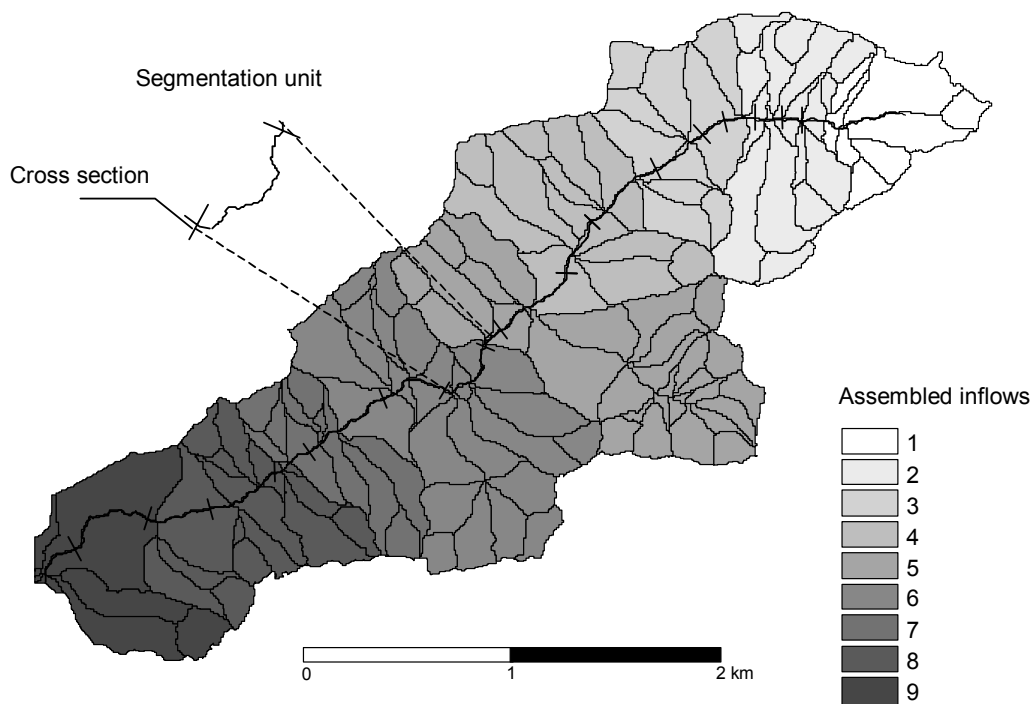


Fig. 53: Segmentation of the Wendbach River for the HEC-6 simulation and the assembled inflows of the OPUS simulation.

5.2.2.3 Sedimentological parameter

The model HEC-6 requires a typical grain-size distribution of the riverbed and the embankment of each channel segment. Therefore, for all segments being unconsolidated, a grain-size analysis has been carried out. The grain-size distribution is described by the median particle diameter (D_{50} -value). The calculated D_{50} -values of the unconsolidated segments are listed in Tab. 12.

Furthermore, the surface roughness of the riverbed and the flood plains has to be defined for every segmentation unit and are expressed as the Manning's n coefficients (Tab. 12).

Tab. 12: Characteristics of the segment units; missing D_{50} -value indicates that the riverbed is mainly consolidated in the corresponding segment.

Segment	Length [m]	Mean slope [%]	D_{50} -value [mm]	Manning's n coefficient [$s/m^{1/3}$]		
				Left flood plain	River bed	Right flood plain
1	264.8	1.17	-	0.083	0.04	0.083
2	667.8	1.16	-	0.068	0.022	0.068
3	487.5	0.78	5.5	0.083	0.022	0.083
4	731.4	1.36	7.0	0.066	0.022	0.083
5	171.7	0.68	4.4	0.066	0.022	0.083
6	269.2	0.92	4.3	0.068	0.022	0.068
7	655.2	1.08	6.3	0.066	0.022	0.083
8	428.6	1.105	4.1	0.066	0.022	0.083
9	449.2	0.98	4.2	0.06	0.02	0.06
10	64.3	3.40	-	0.04	0.04	0.04
11	628.3	1.36	3.5	0.068	0.04	0.068
12	128.9	0.25	1.5	0.06	0.022	0.06
13	583.6	0.77	3.5	0.034	0.022	0.034
14	455.7	0.84	1.02	0.083	0.022	0.066
15	190.6	1.17	2.1	0.083	0.022	0.083
16	198.2	1.43	-	0.034	0.04	0.034
17	132.2	0.88	-	0.034	0.04	0.034
18	227.3	1.83	-	0.066	0.04	0.066

Finally, a sediment-discharge ratio curve has to be defined by correlating discharge with suspended sediment concentration. Due to the fact that measurements of discharge and sediment concentration within the Wendbach catchment are missing, the data of the sub-catchment Steinersiefen, which is located in direct surroundings of the Wendbach catchment, were used. By analyzing the data, a ratio of bed load to suspension load of 15:85 can be assumed. The D_{50} -value of the inflowing sediment is 0.021 mm. This is the basis of the sedimentological calculations of HEC-6.

5.2.3 The long-term scale

A complete data set is a prerequisite for using the OPUS model for long-term simulations. In this chapter the methodologies are presented, used for filling the gaps of climate and landuse data.

5.2.3.1 Generation of long-term climate data

The necessary statistical parameters for WGEN are calculated on the basis of the measured and regionalized rainfall data (described in Chapt. 3.3). The available temperature and radiation data set, which covers a 20-year period (1980 –2000), is sufficient to obtain reliable statistical parameters (Richardson and Wright, 1984), so that the climate data of the period from 1950 until 1980 could be generated with the WGEN model. Fig. 54 shows that the measured radiation in 1999 and the equivalent generated by WGEN are quite similar. The daily rainfall amounts from 1950 until 1959 were generated with WGEN.

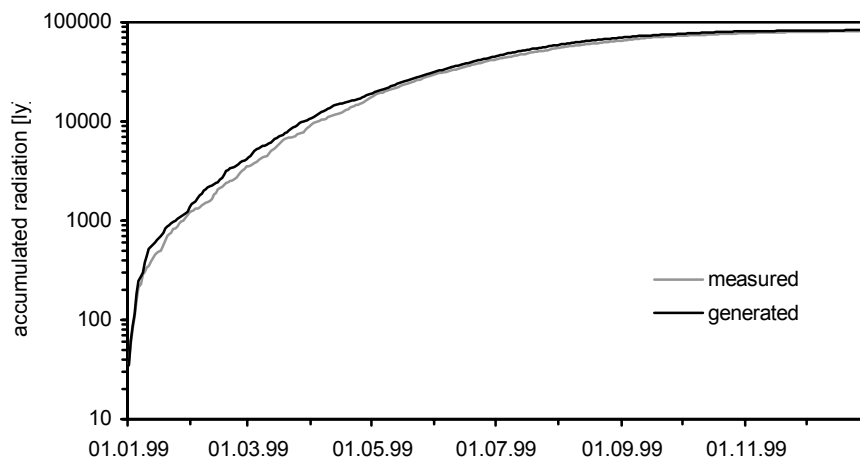


Fig. 54: Measured and generated radiation of the year 1999.

5.2.3.2 Parameterization of the historical landuse development

The spatial distribution of landuse is an important factor in hydrological modelling and therefore has to be considered as accurately as possible. Several methods are used to reconstruct the historical development of the landuse distribution within the catchment. By digitizing annual mappings, a very precise spatial distribution of landuse at the field scale for the past 11 years is obtained. Furthermore, three sets of aerial photos from 1971, 1980 and 1989 are available which are also used for determining landuse distribution.

Additionally, through analyzing agrarian statistics the landuse distribution of the period between 1950 and 1970 could be explored. Putting this data together, a consistent picture of the landuse development results in respect to the proportion of pasture to arable land (Fig. 55).

From this work it can be concluded that the temporal development of the landuse is characterized by a significant decrease in arable land due to WTV policy. The cultivated area decreases from over 30 % in 1950 to less than 10 % in the seventies and to relatively stable values between 6 and 7 % in the eighties and nineties. The whole period is arbitrarily divided into three sub-periods to represent this development in long-term simulations. Through polynomial interpolation, annual percentages of area of pasture and arable land are obtained. Afterwards, these values are averaged in order to get representative percentages for each period (Tab. 13).

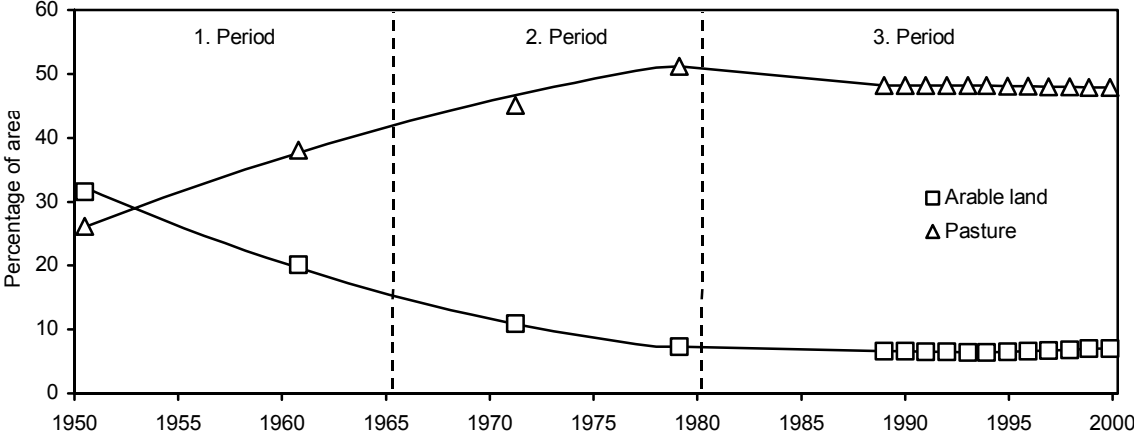


Fig. 55: Development of landuse in the catchment of the Wahnbach River since 1950 (percentage of area of pasture and arable land from the whole catchment area) and the division of the whole period of time into three sub-periods (triangle and squares denote measured values, whereas the lines are denoting polynomial interpolations).

Tab. 13: Average percentage of area of pastureland and arable land of each period.

	1. Period	2. Period	3. Period
Arable land	23.15	9.97	6.76
Pastureland	34.25	47.55	48.74

As mentioned above, the landuse before 1970 was stochastically distributed in the catchment using agrarian statistics and the parcels of land boundaries digitized from aerial photos taken in 1970. The main assumption is that all additional arable land of the past was located where currently is pastureland. This hypothesis is strongly indicated through the development of the land utilization (Fig. 55). As spatially-distributed information is only available for the past thirty years, the landuse before 1970 was stochastically distributed in the catchment using agrarian statistics and the parcels of land boundaries digitized from aerial photos taken in 1970. As already mentioned, for considering the landuse development the whole study period was divided into three sub-periods (Fig. 55). These sub-periods are used for the three independent simulations representing the whole period.

Fig. 56 summarizes the landuse and climate data used for the long-term simulation covering a period from 1950 until 2000.

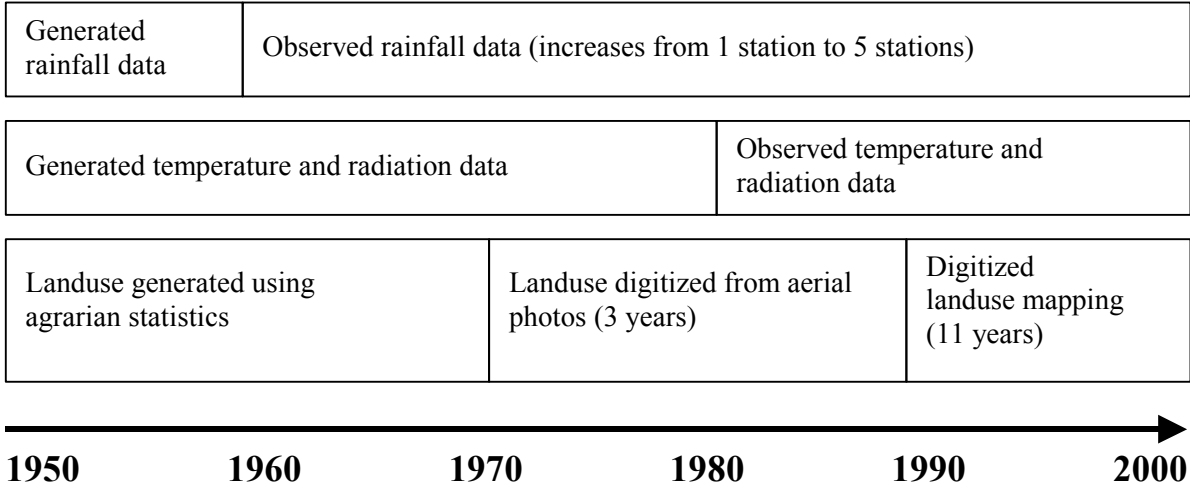


Fig. 56: Landuse and climate data used for the long-term simulation with OPUS; note that the different data quality from completely generated data in the fifties to data of high reliability in the nineties.

5.2.3.3 The daily option of the OPUS model

Owing to the fact that high-resolution rainfall data are not available, the daily option of the OPUS model was chosen for the long-term simulation. OPUS provides a spatially-lumped conceptual model to estimate daily runoff and peak runoff rates from daily rainfall data. This method is accompanied by a calculation of the sediment loss using a modified MUSLE approach.

In order to run the OPUS model with the daily option, appropriate CN-values for solving the SCS-Curve number equation had to be found (Tab. 14). Furthermore, the Ma-values were adjusted in correspondence to the results obtained using the breakpoint data option.

Tab. 14: The runoff curve numbers and Ma-values used for the daily option of OPUS.

Hydrologic soil group	Runoff curve numbers		Ma-values
	B	C	
Forest	80	82	0.99
Meadow	80	85	0.95
Pasture	80	85	0.95
Settlements (sealing < 25 %)	80	85	0.95
Settlements (sealing 25-50 %)	85	90	0.97
Settlements (sealing > 50 %)	90	95	0.99
Bushes	80	83	0.95
Cereals	75	80	0.75
Corn	75	80	0.75
Sugar beet	75	80	0.75
Golf court	80	80	0.95

6 Modelling the fluxes of matter

*Modelling is a game, but it is a serious game.
(Beven, at the 2001 EGS conference in Nice)*

The aim of this chapter is to present the results of the simulation of the fluxes of matter in the Wahnbach catchment. Nitrate was chosen as representative for the wide range of solutes which have been analyzed and presented in Chapt. 4.2.2.3. OPUS is able to simulate several processes, for example plant growth, denitrification rates, turnover rates of organic carbon, to name just a few. Due to the lack of appropriate validation data in this study, it is not attempted to provide a full description of all details involved in the simulation. However, it was attention paid that all these factors are simulated in a realistic way during the model calibration.

6.1 The sub-catchment scale

In this chapter the results of the model application at the sub-catchment scale are presented. At this stage, the modified OPUS model is calibrated and effective parameters are obtained, which are in a next step utilized for the simulations at the catchment scale.

6.1.1 Transport of water

6.1.1.1 Simulation of overland flow

The correct simulation of surface water is a prerequisite for the simulation of soil erosion. Therefore hydrograph-separation methods are used in order to validate the ability of OPUS to simulate overland flow.

Fig. 57 displays the direct runoff of the 25th of July 2000 event, calculated from the total discharge using measured conductivity (see Chapt. 4.1.2). At first, the calculated direct runoff is further split up using the linear separation method in order to separate overland flow from fast subsurface flows.

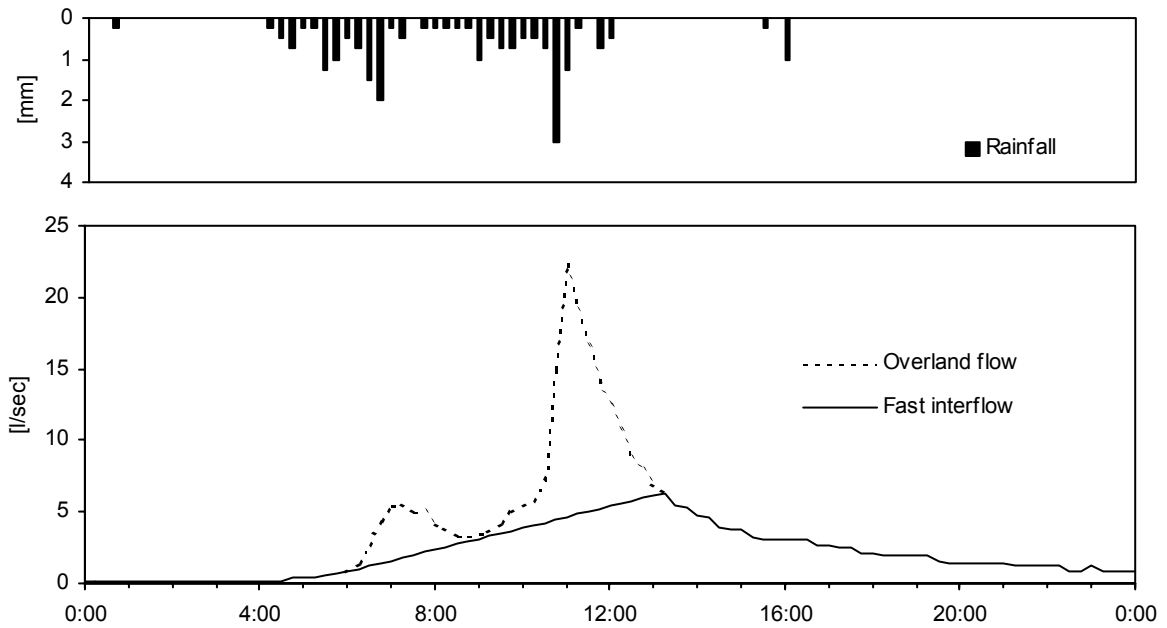


Fig. 57: Linear separation of the direct runoff of the rainfall event on the 25th July 2000.

Fig. 58 exhibits the comparison of the separated and the simulated overland flow discharges. The simulated 25th of July 2000 event is taken from the continuous OPUS simulation of a three years-period (1998 – 2000). By using the separation method a total volume of overland flow of 1520 m³ is obtained, whereas the simulation leads to a value of 1202 m³.

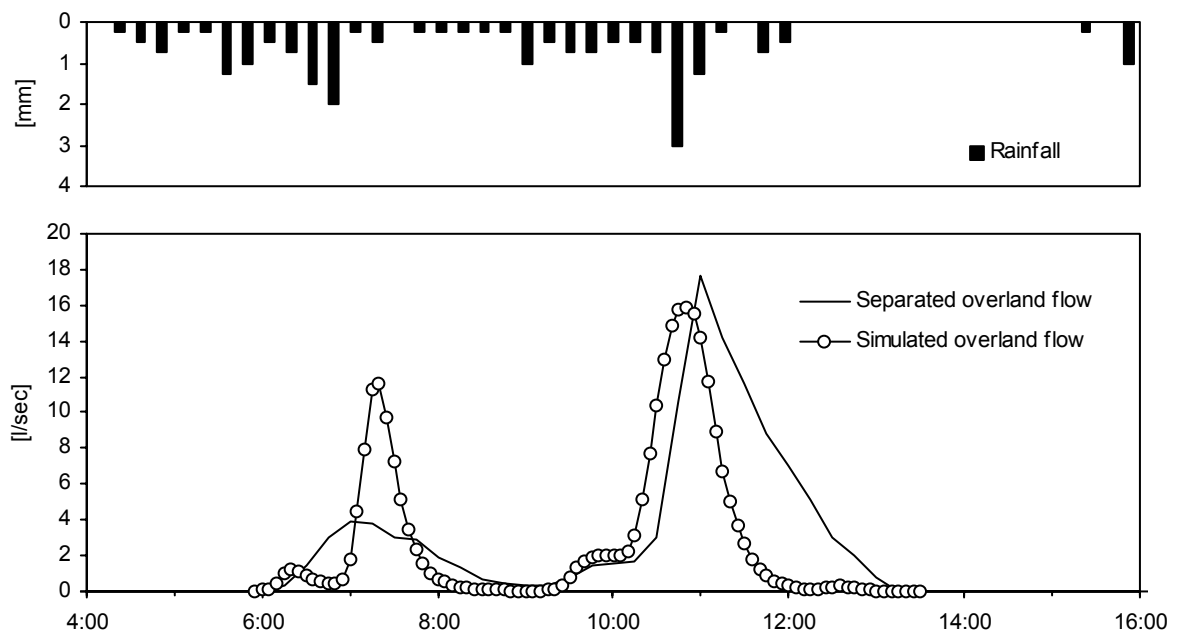


Fig. 58: Simulated and separated overland flow of the rainfall event on the 25th of July 2000; the simulated overland flow was taken from a continuous OPUS simulation (1998 – 2000).

The temporal distances from peak rainfall and simulated peak runoff are getting shorter in the course of time, because of the increasing saturation of the topsoil. This effect is to some extent also visible for the measured runoff, but it is less distinct. Consequently, the first distinct peak of the simulation at 7:20 is somewhat later than the observed, whereas the second peak at 11:00 is slightly earlier. The first simulated peak is significantly higher than the observed one and the small peak in front is completely missing in the measured hydrograph. Therefore it can be expected that the model underestimates the initial abstraction of precipitation in this simulation. However, one must take into consideration that significant uncertainty is involved in the separation method and that the initial conditions (e.g. soil water content) are not calibrated.

6.1.1.2 Influence of rainfall data quality on overland flow simulation

In this section the influence of the quality of rainfall data on the simulation of runoff is analyzed. In the late sixties a rainfall radar was installed at the Meteorological Institute at the University of Bonn. Fig. 59 shows the totalized precipitation of the 3rd of May 2001 event measured with the radar of the Meteorological Institute at the University of Bonn.

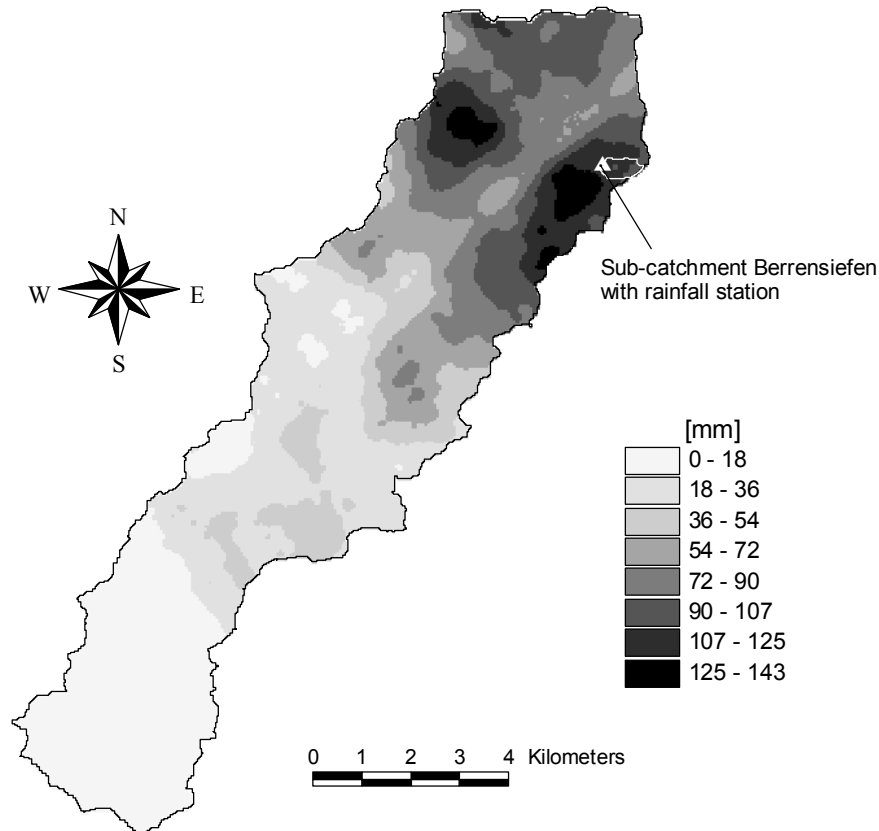


Fig. 59: The totalized precipitation of the 3rd of May 2001 event measured with the radar of the Meteorological Institute at the University of Bonn.

Since March 2001, operational measurements have been performed every five minutes and are therefore applicable for the high-resolution simulation of overland flow by the OPUS model. The radar (Selina METEOR-200) works with a 50 km and a 100 km radius, the former being used in this study.

In order to scrutinize the usefulness of the radar data as input for the simulation of overland flow the extreme event of the 3rd of May 2001 was chosen for a comparison of radar data with standard measurements (tipped bucket). Fig. 60 shows the precipitation distribution using the Thiessen-method. The values of the Thiessen polygons are extracted from the radar measurement.

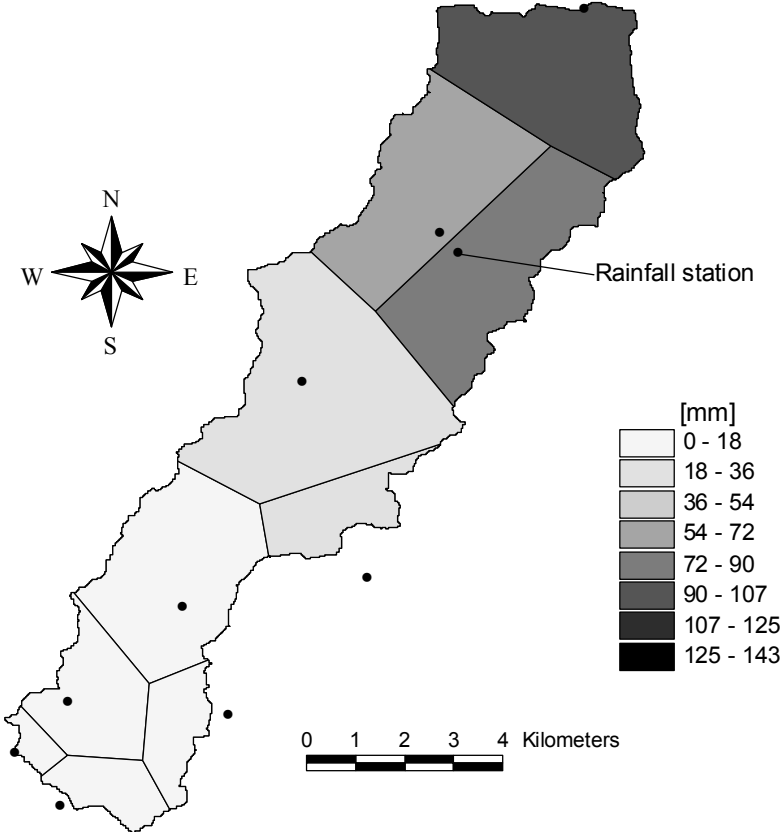


Fig. 60: The totalized precipitation of the 3rd of May 2001 event; the values of the Thiessen polygons are extracted from the radar measurement.

Through the generalization of the Thiessen method the measured values of the radar (maximum: 143 mm) are intensively reduced, however, the regionalized precipitation amount of that event is very similar (radar: 44.5 mm, Thiessen: 43.3 mm). Thus it can be assumed that

the Thiessen method is applicable at the regional scale, but for the treatment of small-scaled rainfall phenomena it may be less practical, especially concerning extreme rainfall events. In order to verify whether the quality of the radar data is comparable with the data of the rain gauge installed within the Berrensiefen catchment, a runoff simulation was undertaken. Fig. 61 shows the simulated runoff and the accumulated precipitation of both methods, whereby the time-resolution for both approaches has been five minutes.

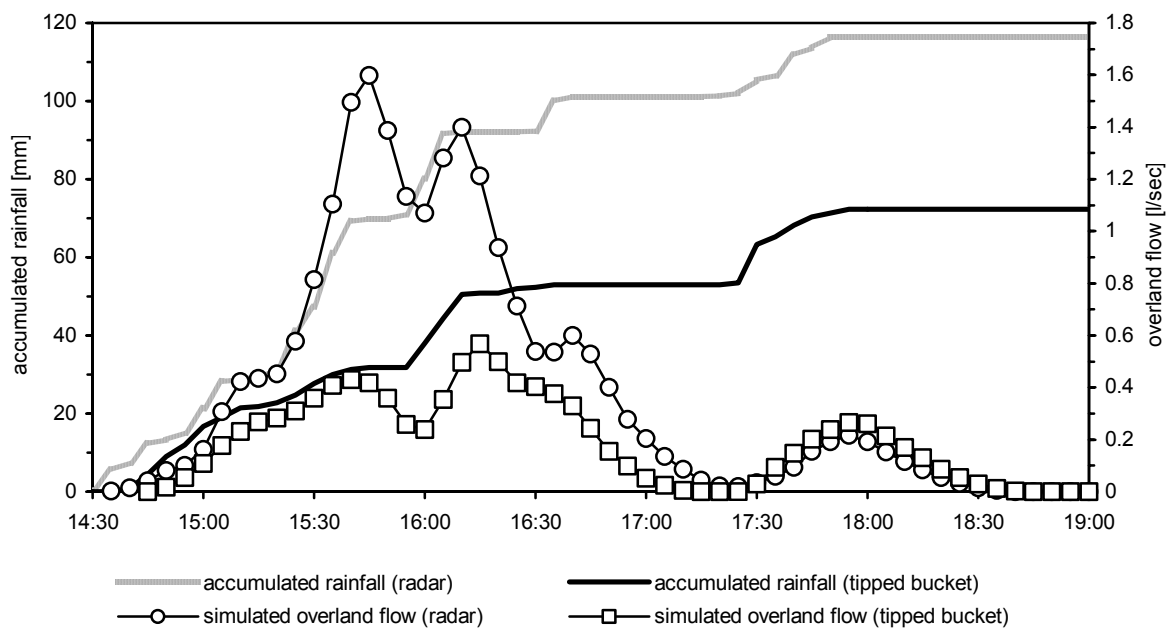


Fig. 61: Comparison of overland flow simulations using radar and tipped bucket data of the 3rd of May 2001 event.

The comparison of the data sets revealed a very well temporal correspondence of the rainfall peaks. Consequently, the peaks of the overland flow simulation also occurred simultaneously. However, during the period from 15:15 until 15:45 the radar data show very high rainfall intensities with maximum values of 166 mm/h, whereas the tipped bucket exhibits only maximum values of 36 mm/h. This discrepancy is presumably caused by ice crystals increasing the reflectivity of the precipitation. Due to this the quantity of simulated overland flow is highly increased compared to the simulation with the tipped bucket data (radar: 6.46 m³, tipped bucket: 2.97 m³).

The result of this analysis can be summarized as follows: the radar data deliver rainfall data of very high spatial and temporal resolution. However, in the case of thunderstorm events as described above, the radar may involve significant errors leading to exaggerated simulations of overland flow.

6.1.1.3 Simulation of daily runoff

The aim of this study was not to simulate runoff and solute transport at a resolution below one day, because the water movement within the soil is simulated in OPUS on the daily-time step. Consequently, the additional modules of the modified OPUS version are also working with a daily resolution (see Chapt. 5.1.2). Therefore the simulation results are obtained by averaging the overland flow discharges and adding all runoff components in order to obtain the total runoff volume.

The whole simulated period spans from January 1998 until December 2000. However, for the calibration and validation only a period from August 1998 until December 2000 is available, except for Hellenkeutelsiefen, which has been sampled since 1997. Since no initial conditions of the water content of the soils were available, it is assumed that through this leading time of about eight months the soil water contents have reached realistic values.

Fig. 62 shows the simulated soil water content of the Steinersiefen sub-catchment from January 1998 until December 2000. The daily values of all simulated planes are averaged. In order to display the vertical distribution, the soil water content of three different depths (0-30 cm, 30-60 cm, 60-90 cm) is presented in Fig. 62.

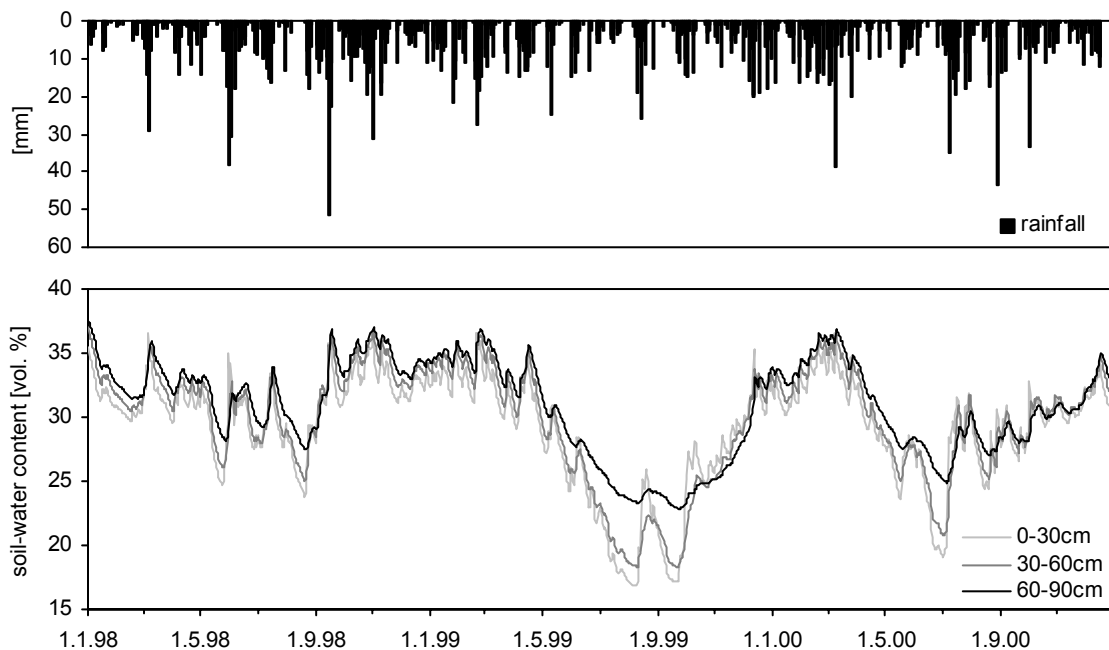


Fig. 62: Observed rainfall and simulated mean soil water content in three different depths of the Steinersiefen sub-catchment.

During the winter time the upper 90 cm of the soils are nearly completely saturated for short times (37,6 vol.%) and no significant differences between the layers are visible. Conversely, during dry periods a clear differentiation of the layers can be observed, with lowest values in 0-30 cm and highest values in 60-90 cm. During the very dry conditions in summer 1999 lowest soil water content values are simulated (16,8 vol.% in 0-30 cm, 18,3 vol.% in 30-60 cm and 22,9 vol.% in 60-90 cm depths).

In order to adjust the linear storage models of the modified OPUS version (see Chapt. 5.1.2), OPUS was adjusted to permit most of the infiltration-excess water to drain through the macropore system (see Tab. 14 in Chapt. 5.2.3.3). For example, the simulation of the hydrograph of Berrensiefen (Fig. 63) indicates that about 95 % of the infiltration excess is drained through the macropore system. After calibration of the linear storage modules, the simulated and the observed hydrographs of the sub-catchments are quite similar for the calibration period and even for the validation period (Fig. 63 and Tab. 15).

Tab. 15: Performance indices reflecting the quality of the runoff simulation of the sub-catchments.

	Calibration period		Validation period	
	IA	CME	IA	CME
Hellenkeutelsiefen	0.94	0.73	0.88	0.57
Steinersiefen	0.90	0.71	0.90	0.70
Berrensiefen	0.96	0.83	0.95	0.81

IA: Index of Agreement (Willmott, 1981), CME: Coefficient of Model Efficiency (Nash & Sutcliffe, 1970)

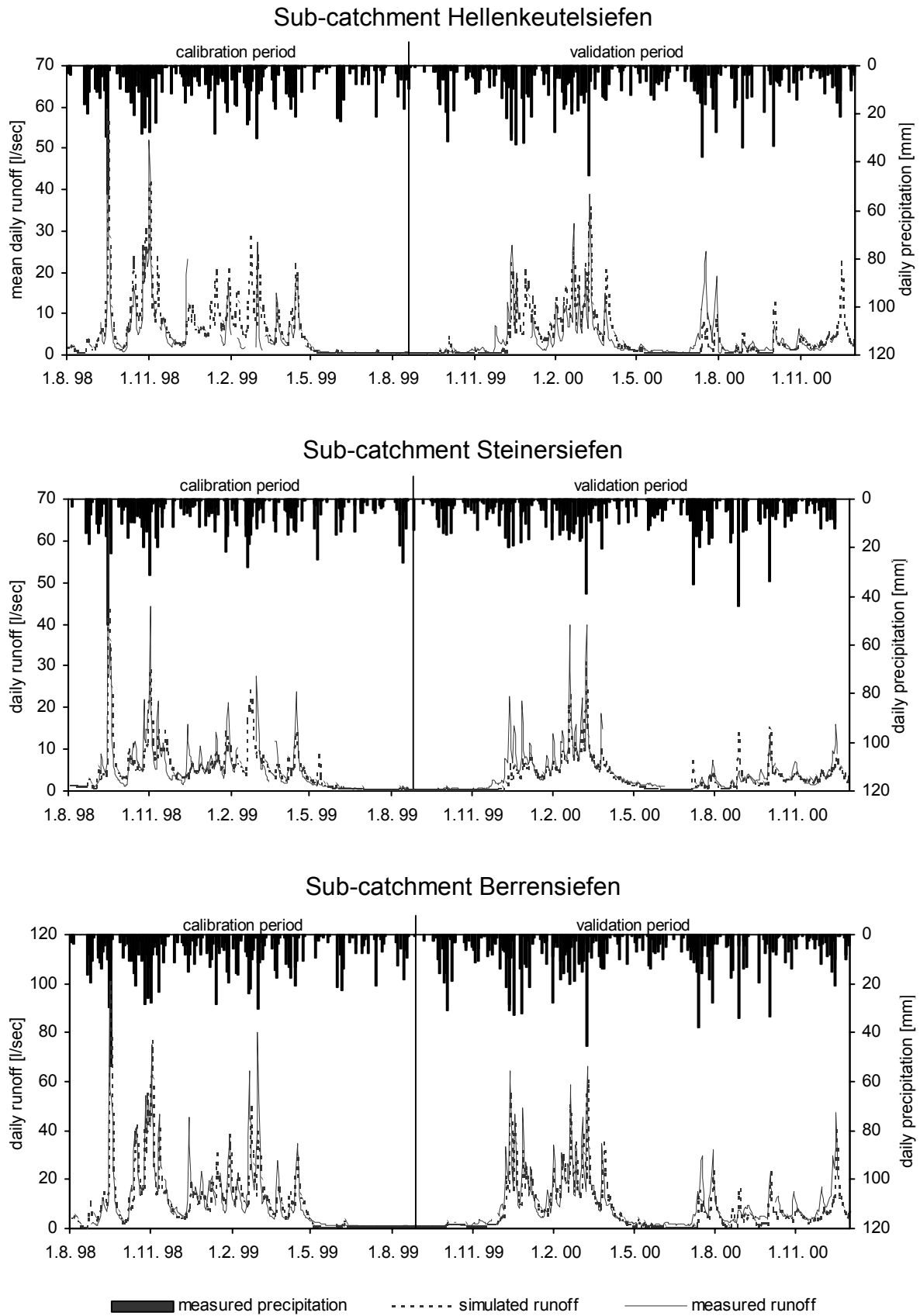


Fig. 63: Measured (dotted line) and simulated (solid line) mean daily runoff of Hellenkeutelsiefen, Steinersiefen and Berrensiefen and the measured daily precipitation amounts; note that the measured runoff data are not complete due to technical problems.

However, Tab. 15 reveals that the values of the model performance measures – especially the CME-value - for the validation period of the Hellenkeutelsiefen turned out to be quite low. This may be a result of the relatively poor representation of forest in OPUS, owing to the fact that OPUS was originally created for agricultural fields.

Tab. 16 lists the measured and simulated water discharges of the whole simulation period.

Tab. 16: Measured and simulated water discharges between September 1998 and December 2000.

	Precipitation	Measured water discharge		Simulated water discharge	
	[mm/year]	[l]	[mm/year]	[l]	[mm/year]
Berrensiefen	1408	7.50*10 ⁸	953	6,93*10 ⁸	880
Hellenkeutelsiefen	1408	3,37 *10 ⁸	697	3,77*10 ⁸	779
Steinersiefen	1224	3,43*10 ⁸	709	3,06*10 ⁸	633

The total simulated discharge quantity differs in all cases to some extent. On the one hand, the discharge of Berrensiefen and Steinersiefen is overrated (8,6 % and 10,8 %) and on the other hand the discharge of Hellenkeutelsiefen is underrated (10,6 %). This finding suggests that the transpiration of forest is overestimated by the model, whereas an underestimation of the remaining landuse types may occur. However, it has to be noted that in the groundwater flow simulation is rather simple.

Nonetheless, the calculations of water discharge by the modified OPUS model are altogether encouraging, so that it can be assumed that the model is able to simulate the runoff in the Wahnbach catchment in a satisfactory way.

6.1.1.4 Influence of rainfall data resolution on the runoff simulation

In this section, the daily option of OPUS is tested for its applicability of simulating the daily discharge of the Berrensiefen sub-catchment. In this modus, runoff is calculated with the SCS-CN method (USDA-SCS 1972) and peak runoff is estimated from runoff volume.

Fig. 64 shows a comparison of the simulated runoff from August 1998 until December 2000 with both methods. The diagram reveals that some runoff peaks are underestimated by the daily option (up to 53.1/sec) as well as by the breakpoint option (up to 31.9 l/sec).

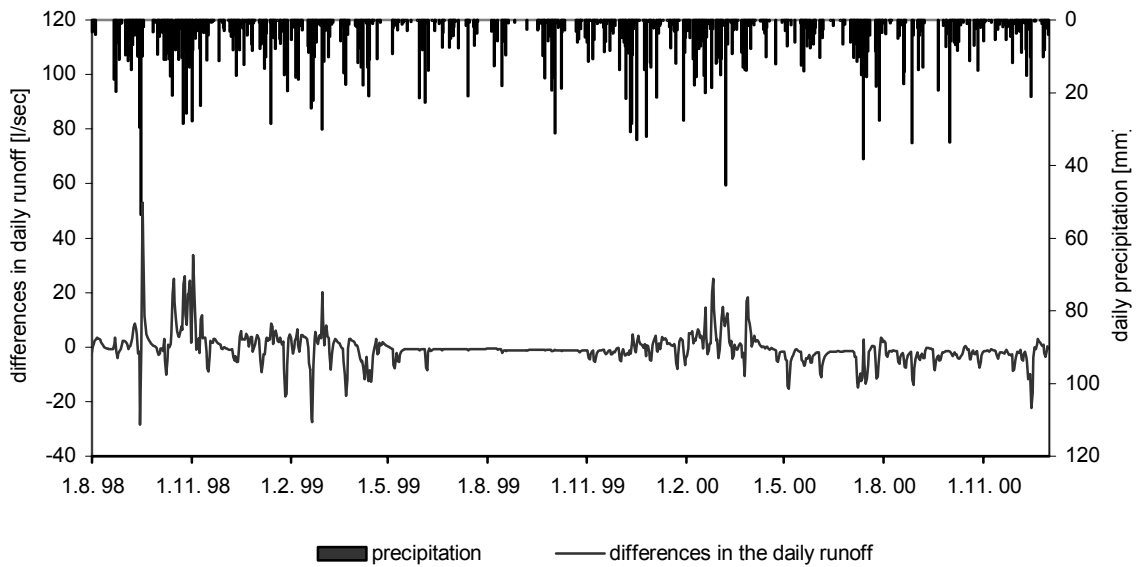


Fig. 64: The differences of the daily runoff simulations of Berrensiefen using the breakpoint and the daily option of OPUS; the positive values indicate that the breakpoint option produces more runoff than the daily option.

Tab. 17 exhibits that the total amount of simulated water discharge is lower compared to the breakpoint option and that the values of the performance measures drop to some extent. However, it can be concluded that the daily option of OPUS still yields reasonable results.

Tab. 17: Simulated water discharges and the performance indices of both simulation methods.

	Simulated water discharge		Performance measures	
	[l]	[mm/year]	IA	CME
Breakpoint option	$6,81 \cdot 10^8$	865	0.95	0.82
Daily option	$7,25 \cdot 10^8$	920	0.91	0.73

IA: Index of Agreement (Willmott, 1981), CME: Coefficient of Model Efficiency (Nash & Sutcliffe, 1970)

6.1.2 Simulation of nitrate discharge

A further criterion for the ability of the modified OPUS model to simulate the fluxes of matter of the Wahnbach catchment is the nitrate concentration of the stream water. Tab. 18 and Fig. 65 display the results of the simulation of nitrate concentrations in the same period as for the runoff simulation.

Tab. 18: Indices reflecting the quality of the nitrate concentration simulation at the sub-catchment scale.

	Calibration period		Validation period	
	IA	CME	IA	CME
Hellenkeutelsiefen	0.76	0.05	0.71	-0.11
Steinersiefen	0.68	-0.38	0.72	-0.03
Berrensiefen	0.83	0.12	0.82	-0.02

IA: Index of Agreement (Willmott, 1981), CME: Coefficient of Model Efficiency (Nash & Sutcliffe, 1970)

In Tab. 18 the weekly measured nitrate concentrations are compared with the simulation outcome. The IA-values remain still relatively high during the calibration period (between 0.68 and 0.83), but the CME-values decrease to low values. However, the simulation of nitrate concentration in the catchment of the Berrensiefen for the period between October 1998 and October 2000 reveals a quite good CME-value of 0.41.

The relatively low values of the performance measures of the nitrate concentration simulation can be explained with the too slow simulation of nitrate washout at the beginning of each winter season too. This behaviour of the OPUS model is especially pronounced for Hellenkeutelsiefen during autumn (Fig. 65).

The deviation is probably caused by a natural process involved in the solute transport, which can be explained as follows. During dry periods, water percolation through macropores after heavy rainfall events will be adsorbed by the unsaturated soil. Therefore the surroundings of the macropores get more or less saturated inducing accelerated water and nitrate percolation through the matrix into lower parts of the soil. Consequently, nitrate is transported into the region of the soil-bedrock interface, where typically the fast interflow through seepage pipes takes places. However, owing to the dry situation in this zone during this period, interflow is

low or even absent, because the link between the macropores and the pipes is disconnected. These circumstances lead to an enrichment of nitrate and other soluble matters in the soil-bedrock interface during dry periods.

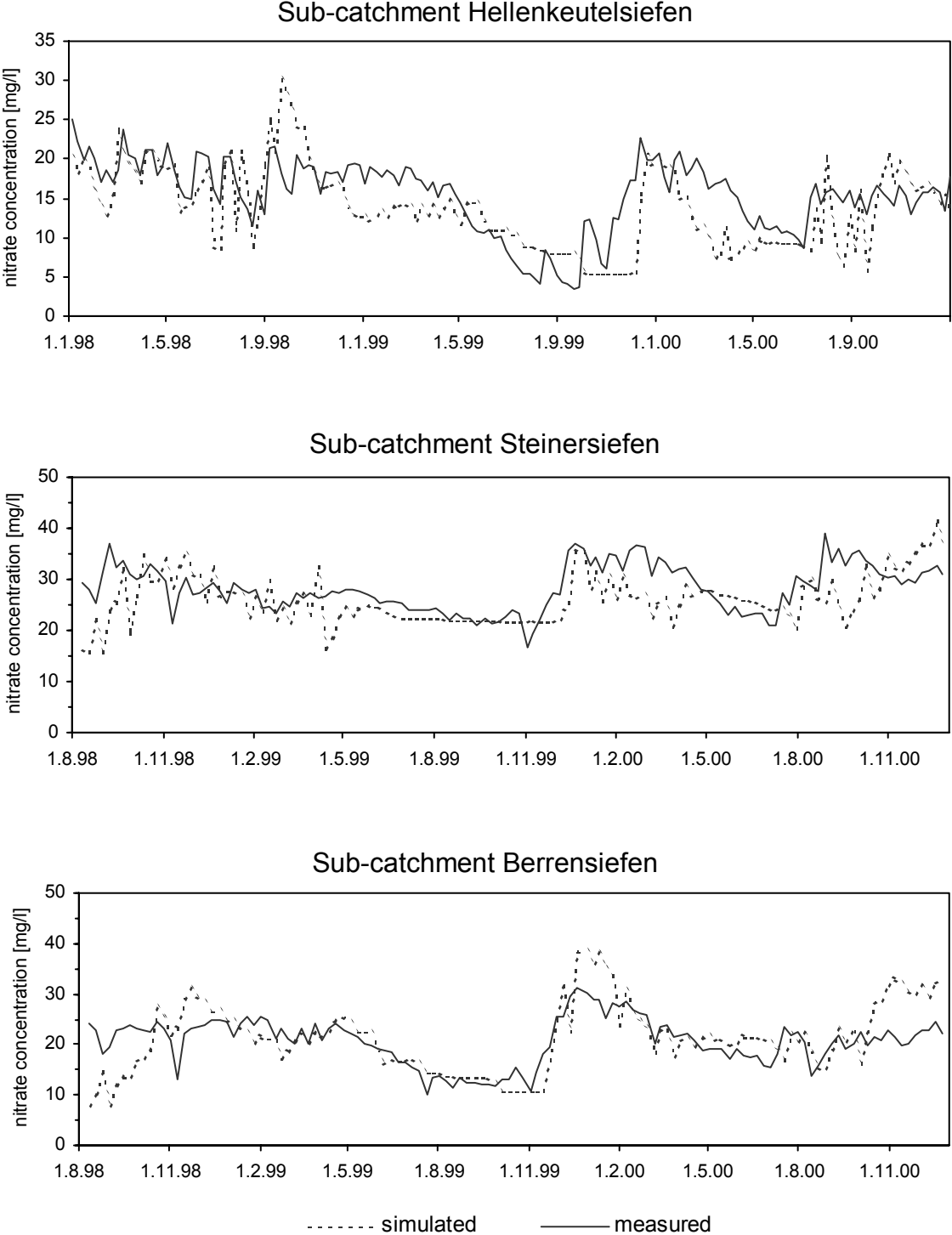


Fig. 65: Weekly measurements of the nitrate concentration at the outlet of the sub-catchments (solid line) and simulated nitrate concentration (dotted line).

At the beginning of the winter season with low evapotranspiration and high rainfall amounts, the thin soils are getting rapidly wet and the soil-bedrock interface is becoming saturated. Hence, the macropores of the soil and the pipes are connected again causing considerable interflow rates. In the first part of this wet period the discharge shows relatively high solute concentrations. The reason for this is possibly a high percentage of old water. Old water may be displaced from isolated ‘dead zones’ by the increased subsurface flow (see Fig. 5, Chapt. 2.1.1.2). This leads to a nitrate-flash during the first considerable rainfall events in the wet period.

Owing to the simplification in the modified OPUS model – water is flowing through the macropores without any interaction with the soil matrix - the observed nitrate-flash cannot be reproduced properly in the simulation. For a better simulation of nitrate discharge, the model should be further improved in order to be able to consider macropore-matrix interaction.

Tab. 19 lists the measured and simulated quantities of nitrate discharge of the whole simulation period (between September 1998 and December 2000).

Tab. 19: Measured and simulated nitrate discharges between September 1998 and December 2000.

	Measured nitrate discharge		Simulated nitrate discharge	
	[t]	[kg/ha/year]	[t]	[kg/ha/year]
Berrensiefen	17,3	220	16,0	203
Hellenkeutelsiefen	5,96	123	5,9	122
Steinersiefen	10,4	215	8,34	172

The total quantity of nitrate discharges of Berrensiefen and Hellenkeutelsiefen is in both cases only to a minor amount underrated (7,7 % and 0,8 %). However, the nitrate discharge of Steinersiefen is significantly underestimated by the model. There are several possible explanations for this difference (e.g. an overestimation of nitrate uptake of the plants). The most likely explanation may be that the fertilization amounts as reported by the farmers are too low. This finding emphasizes the importance of input data for the correct simulation of solute transport.

6.1.3 Simulation of sediment transport

In this section the results of the sediment transport simulations at the sub-catchment scale are discussed. Tab. 20 lists the measured and simulated sediment discharges between September 1998 and December 2000.

Tab. 20: Measured and simulated sediment discharges between September 1998 and December 2000.

	Measured sediment discharge		Simulated sediment discharge	
	[t]	[t/ha/year]	[t]	[t/ha/year]
Berrensiefen	5.17	0.24	3.64	0.17
Hellenkeutelsiefen	2.77	0.17	3.66	0.23
Steinersiefen	25.1	1.56	13.4	0.83

6.1.3.1 *Berrensiefen*

The shape of the simulated sediment discharge equals the calculated one from March 1999 until December 2000 in an acceptable way, which is also indicated through a relatively high IA-value of 0.75 (Fig. 66). However, the first seven months differ rather distinctively. The time shift of the first peak may be caused by sediment storage processes in the catchment, which retard and modify the temporal distribution of sediment discharge from the hillslopes. This processes are unconsidered in the model at present.

The calculated erosion amount differs from the observed sediment discharge at the catchment (measured: 5.17 t, simulated: 3.64 t), indicating that additional sediment sources (e.g. channel scour) may be involved. It should also be noted that calculation of sediment export in this study is based on weekly measurements, which can lead to significant under- or overestimations of the actual sediment discharge amounts (Robertson and Roerish, 1999).

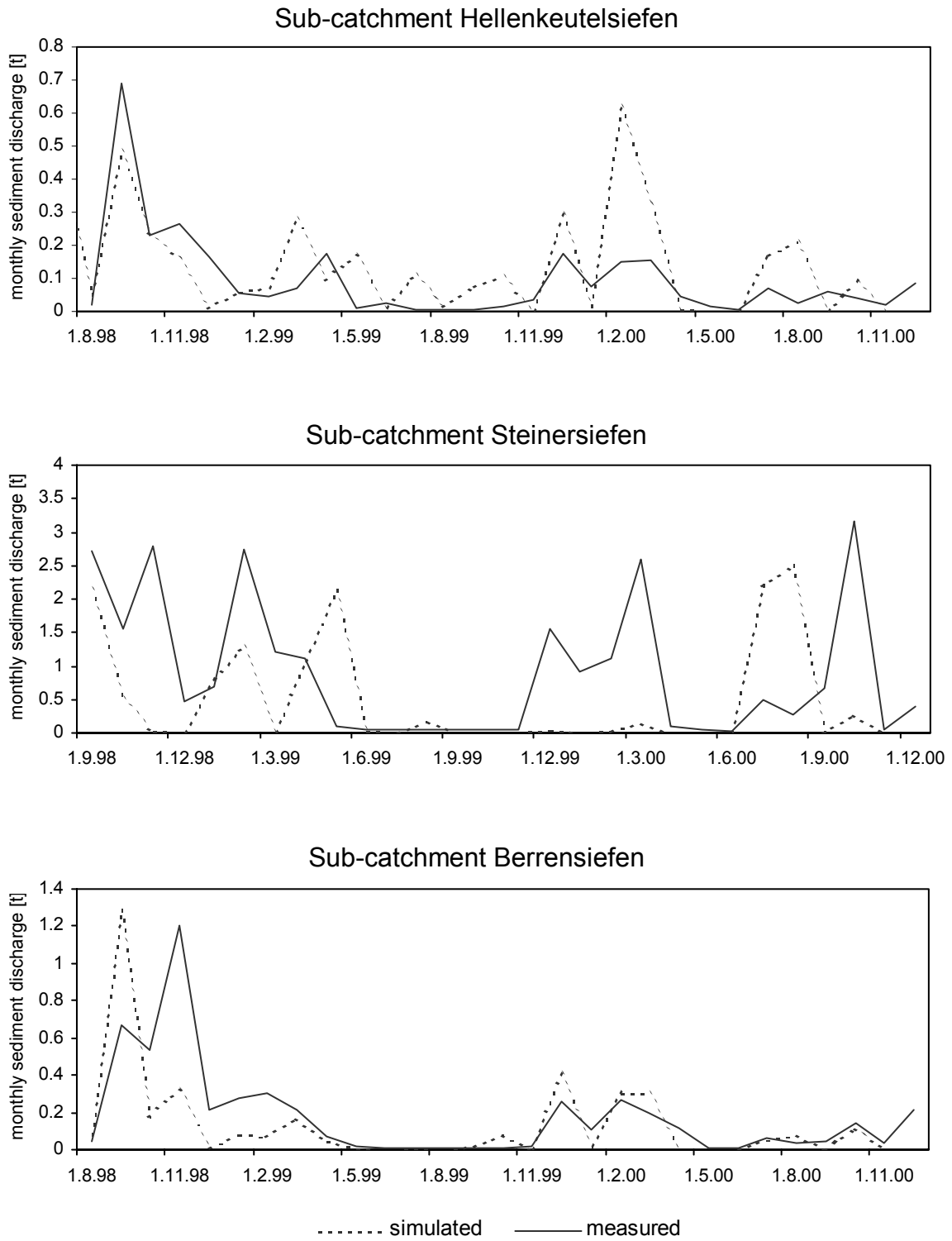


Fig. 66: Monthly sediment discharge (solid line, calculated from measured runoff and sediment concentration) and the simulated monthly soil erosion (dotted line).

6.1.3.2 *Hellenkeutelsiefen*

The simulated soil erosion in the Hellenkeutelsiefen catchment corresponds also quite well to the measured discharge (IA: 0.75). In this case, no significant discrepancy of single peaks are visible. However, during winter and summer 2000 the sediment discharge volume is considerably overestimated. Altogether 3.66 t of sediment export are simulated, whereas only an amount of 2.77 t are measured (Tab. 20). Thus, in contrast to the results of the Berrensiefen simulation, the sediment discharge is overrated. This might be the result of the different topographic features of these sub-basins. The pasturelands, which are more susceptible to soil erosion than the forested hillslopes, are not located next to the brook like in the basin of Berrensiefen. Thus eroded sediment may be trapped on its way to the channel reducing the sediment discharge.

6.1.3.3 *Steinersiefen*

Owing to the greater diversity of the land utilization in the sub-catchment Steinersiefen, the effect of landuse on soil erosion is described in more detail in this section. Fig. 67 and 68 show the distribution of landuse and of the simulated soil erosion amounts within the basin of Steinersiefen.

During the simulation period no significant changes in landuse have been recognized and thus the land utilization was not varied during the simulation. The deep valley cut of the Steinersiefen is covered by forest so that, despite of the very steep hillslopes - values of up to 32 % are detected (see Fig. 24, Chapt. 4.1.2.3) - the simulated soil erosion can be neglected (lower than 0.1 t/ha/year). However, denudation due to soil creep may take place to some extent, but cannot be reproduced by the OPUS model. Most of the erosion is simulated on the planes covered by wheat and corn. Despite of the relatively low slope values of these planes with values up to 10 %, considerable soil erosion amounts are simulated by OPUS with total values up to 14.92 t/ha/year during the simulation period.

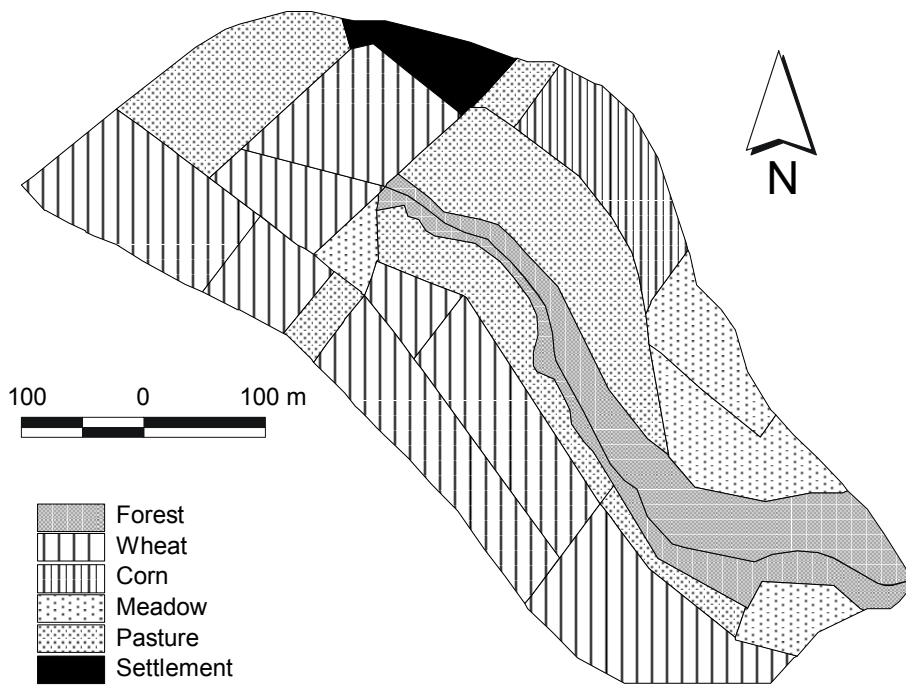


Fig. 67: Landuse distribution within the sub-catchment Steinersiefen as used during the whole simulation period.

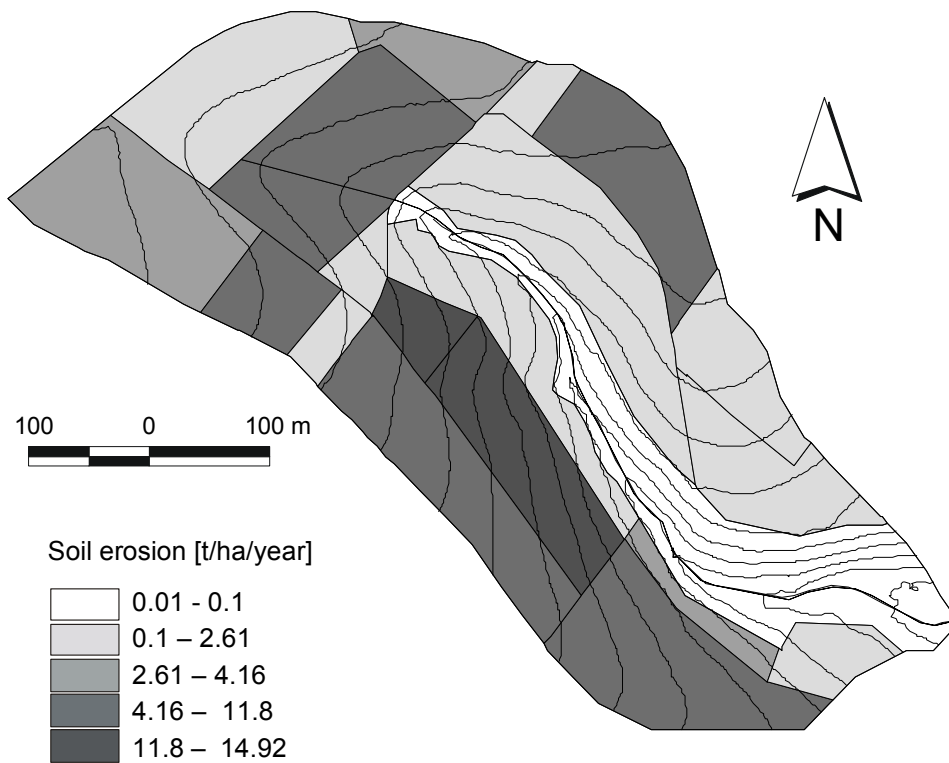


Fig. 68: Mean soil erosion rates of the years 1999 and 2000 from the distributed OPUS simulation of the sub-catchment Steinersiefen.

The total amount of simulated soil erosion during the time from September 1998 until December 2000 (13.4 t) is only about half of the totally measured sediment discharge in that period (25.1 t). Furthermore, by comparing the courses of the measured and simulated sediment discharges of the Steinersiefen, a significant temporal discrepancy of the occurrence of peaks is visible. This finding suggests that both additional sediment sources in the channel and temporal storages are involved in the sediment transport in the Steinersiefen basin.

Field observations of the channel processes indicated that a considerable amount of sediment is released from a former pond. This pond was filled up with sediment coming upstream, and currently the brook incises into these accumulations and thus increases sediment discharge. Furthermore, erosion products may be trapped in the forests surrounding the hillslopes. Therefore sediment discharge is highly correlated with processes in the channel and is not directly coupled with soil erosion on the hillslopes. Consequently, the course of sediment discharge can hardly be used as a basis for validation purposes of soil erosion models.

However, the simulated soil erosion amounts are within a realistic range, which is also confirmed by field observations. Therefore it can be concluded that the modified OPUS model is also suitable for the simulation of soil erosion on arable land in the Wahnbach catchment.

6.2 The catchment scale

As OPUS is designed for single slopes several enhancements were necessary, especially concerning the regionalization of the input data. The catchment is discretized into 890 single hillslopes which are considered to be spatially uniform as far as soil properties, landuse and rainfall are concerned (see Chap. 5.2.1.1.). A tool was developed to link the landuse and soil database with the model, which is also able to calculate automatically lumped parameters like, for example, the erodibility factor.

Two aims are pursued in this chapter. At first it is examined if the modified OPUS model calibrated at the sub-catchment scale is able to reproduce the transport of matter at the catchment scale. Secondly, it is scrutinized whether the SCS-CN method can be used to extend the simulation period.

6.2.1 Simulation of daily runoff

Fig. 69 displays the runoff simulation performed for the catchment of the Wahnbach River for a period of two years (1998 and 1999), utilizing the breakpoint option of OPUS.

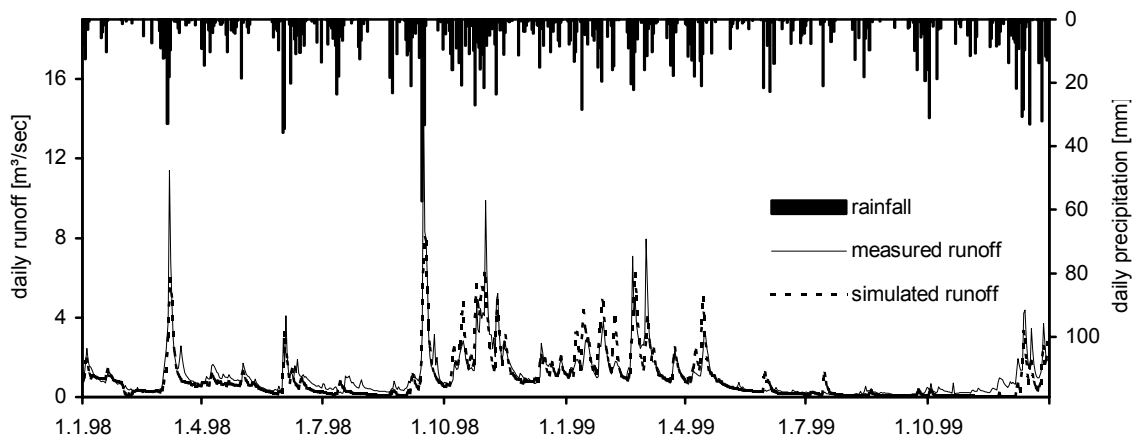


Fig. 69: Measured daily runoff amount at the outlet of the upper Wahnbach catchment (54 km²) (dotted line) and the mean daily runoff amounts (solid line) using the breakpoint option.

The high values of CME and IA (0.72 and 0.92) indicate that the model is applicable at the catchment scale. The CME-value is relatively low because the measured mean value (1.10 m³/sec) differs significantly from the simulated ones (0.97 m³/sec), for which CME is very sensitive. This is not surprising as only one station with breakpoint data was available, which was not enough to match the runoff amount correctly. Furthermore, it has to be noted that no

calibration of the hydrological parameters and no routing of the surface water had been carried out.

6.2.2 Simulation of soil erosion

Fig. 70 shows the result of the soil erosion simulation using the breakpoint option. As expected from the results of the simulations at the sub-catchment scale, only the agriculturally used hillslopes (40 planes) provided a noteworthy amount of soil erosion in both simulations. All other hillslopes revealed soil erosion rates lower than 1 t/ha.

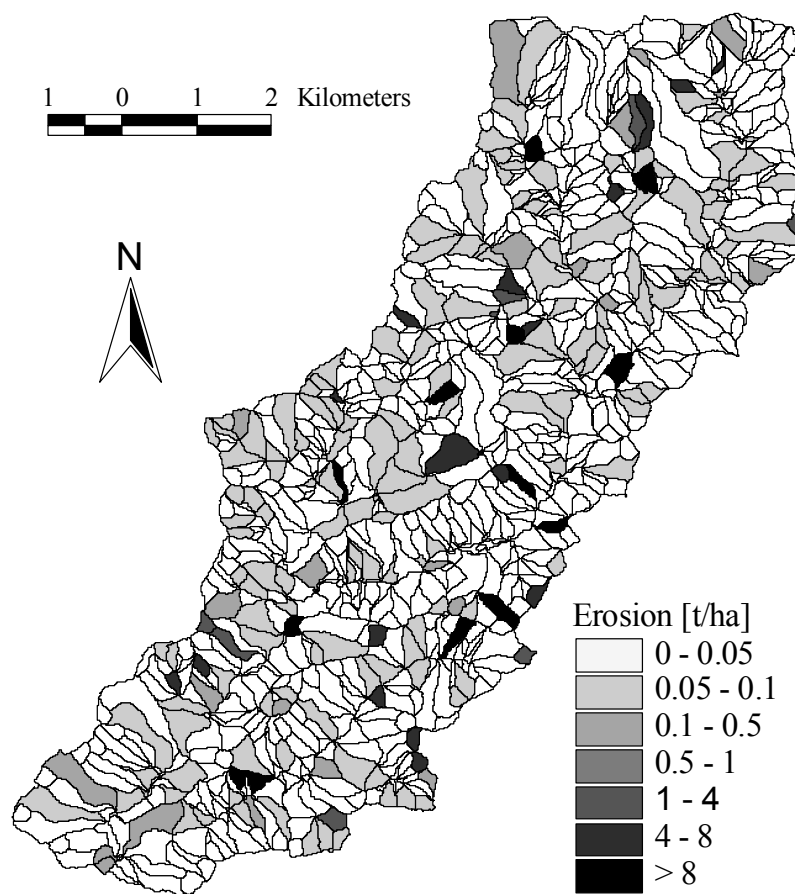


Fig. 70: Continuous simulation of soil erosion in the year 1998 using the modified OPUS model.

With regard to the evaluation of the simulated sediment transport, the best validation would be a detailed measurement of the soil erosion directly on the hillslopes, which is, however, in most cases too expensive at the catchment scale. Another possibility to validate a model is a comparison with an independent simulation. The alternative simulation was carried out with the model AnnAgNPS to evaluate the OPUS model results (Giertz, 2000). A comparison was

possible, because both models work continuously and on a similar spatial discretization of the catchment and because the simulation with AnnAgNPS was realized using the same data base (soil, landuse, rainfall, slope profiles etc.). The result of the AnnAgNPS-simulation is presented in Fig. 71.

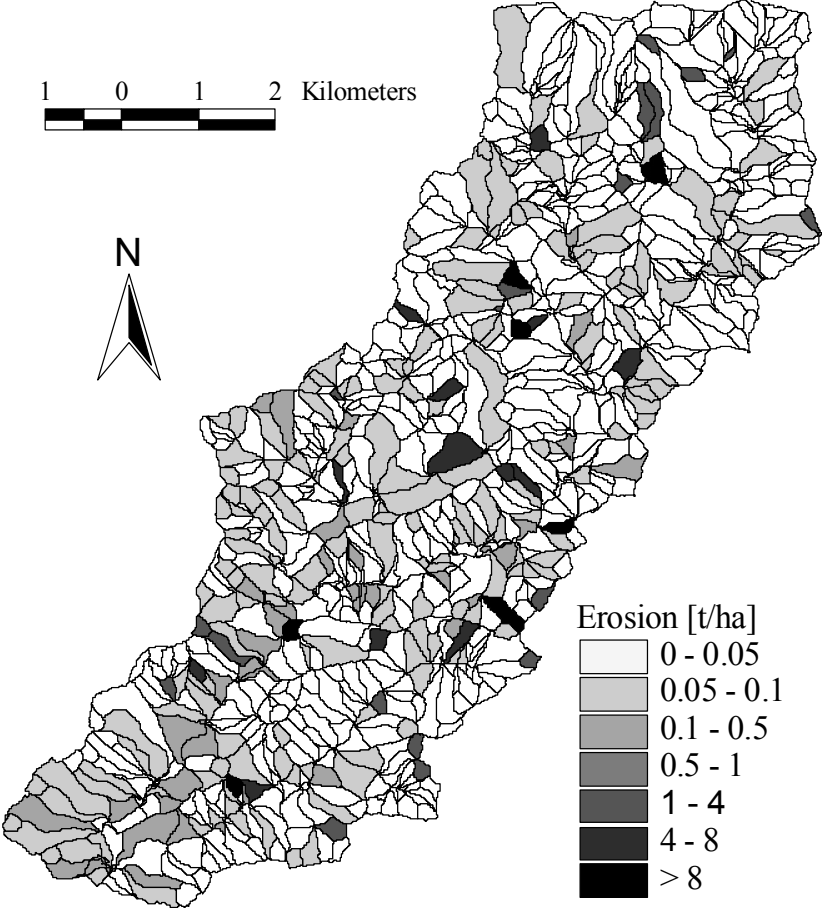


Fig. 71: Continuous simulation of soil erosion in the year 1998 with the AnnAgNPS model.

Fig. 72 shows the comparison of the model results diagrammed by plotting the simulated soil erosion for each slope by AnnAgNPS against the simulations of OPUS. The Pearson-coefficient of 0.89 and the similarity of the whole erosion quantity (OPUS: 1791 t and AnnAgNPS: 1547 t) indicates that OPUS produces reasonable soil erosion results at the catchment scale.

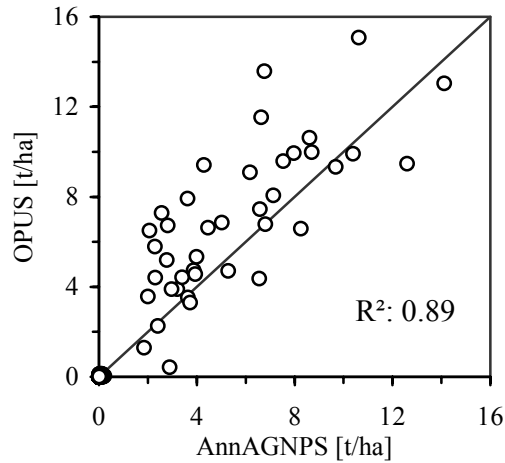


Fig. 72: Comparison of the model results of OPUS and AnnAgNPS; the correlation of the simulated soil erosion for the 890 planes; note that about 850 planes show erosion values near zero.

6.2.3 Simulation of the fluvial sediment transport

In order to evaluate the influence of the channel on the sediment transport, a simulation of the sediment discharge of the Wendbach River, which is the main tributary of the Wahnbach River, was undertaken. In this section the main results of the application of the HEC-6 model are presented (Lamers, 2001). The simulation period spans from January 1999 until December 2000 and the temporal resolution was 10 days.

Fig. 73 shows the simulated runoff of the Wendbach by OPUS in comparison to the measured daily discharge. The daily runoff simulation was downscaled to a ten-day resolution in order to use it for the HEC-6 simulation.

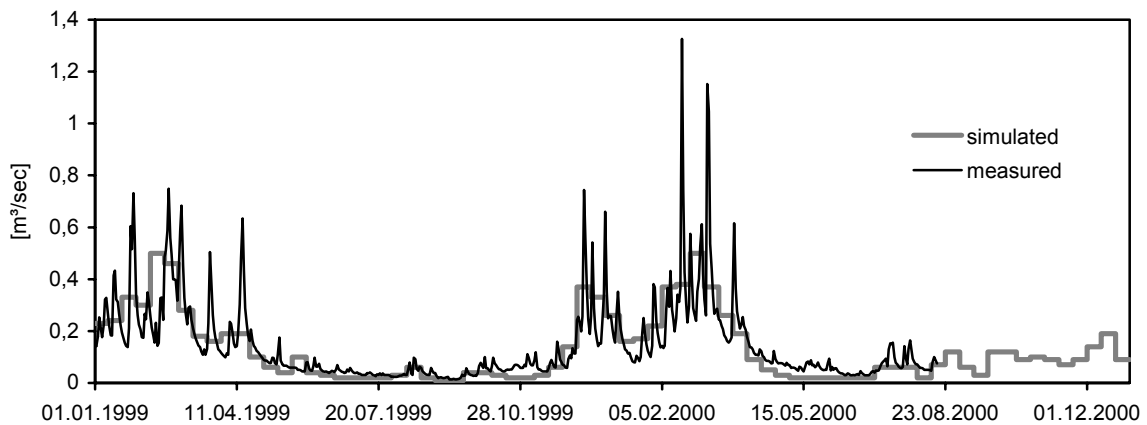


Fig. 73: Simulated runoff with OPUS and measured discharge of the Wendbach River.

To facilitate the validation of the sediment transport calculations of HEC-6, the simulated concentration of suspended solids was compared with measurements at the catchment outlet of the Wendbach River. Fig. 74 displays a comparison of the simulated and measured concentrations of suspended solids at the outlet of the Wendbach River.

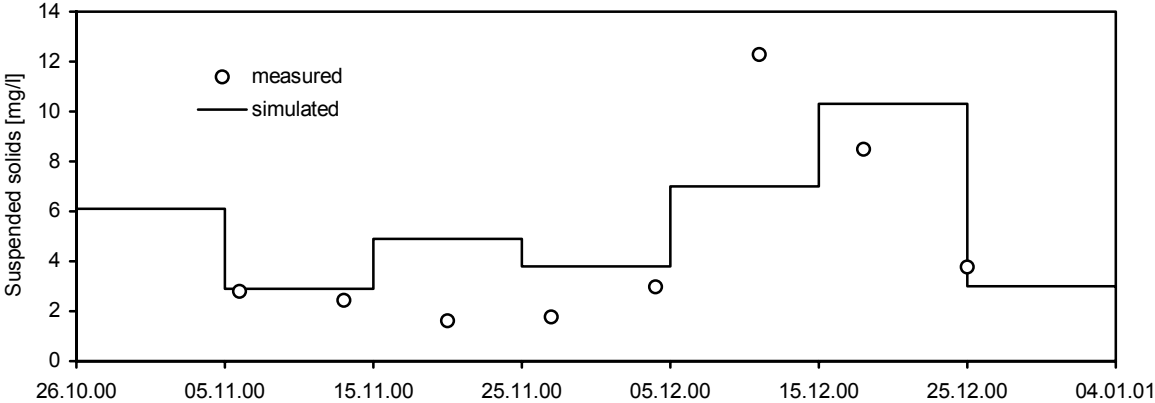


Fig. 74: Measured and simulated concentrations of suspensoids of the Wendbach River.

Although the model failed at some point measurements, the general trend is reflected by the simulation quite well. One should keep in mind that in Fig. 74 one sample of suspended solids is compared with the simulated value of a 10-days time step, which involves considerable uncertainties in the face of the high dynamic of sediment transport.

The main aim was to evaluate whether the HEC-6 model is able to represent seasonal dynamics of sediment transport. In Fig. 75 the sediment balances of each segment in which the Wendbach River was discretized (see Fig. 53, Chapt. 5.2.2) are presented.

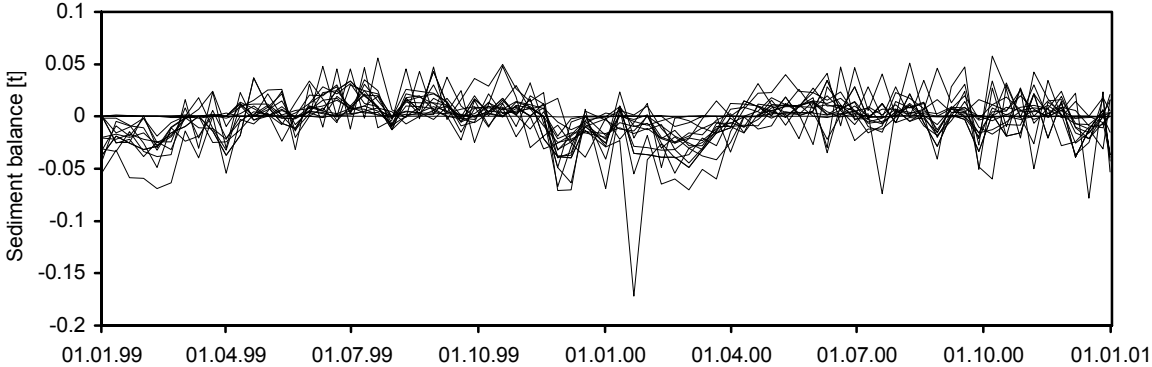


Fig. 75: Temporal sediment storages and releases during the HEC-6 simulation of each channel segment; positive values indicate sediment accumulation and negative values indicate channel scour. Note that some segments show no dynamic at all, because the channel bed is artificially consolidated.

The great difference in the temporal storages and releases within the channel reflects the variation in channel properties, e.g. the degree of consolidation of the channel bed.

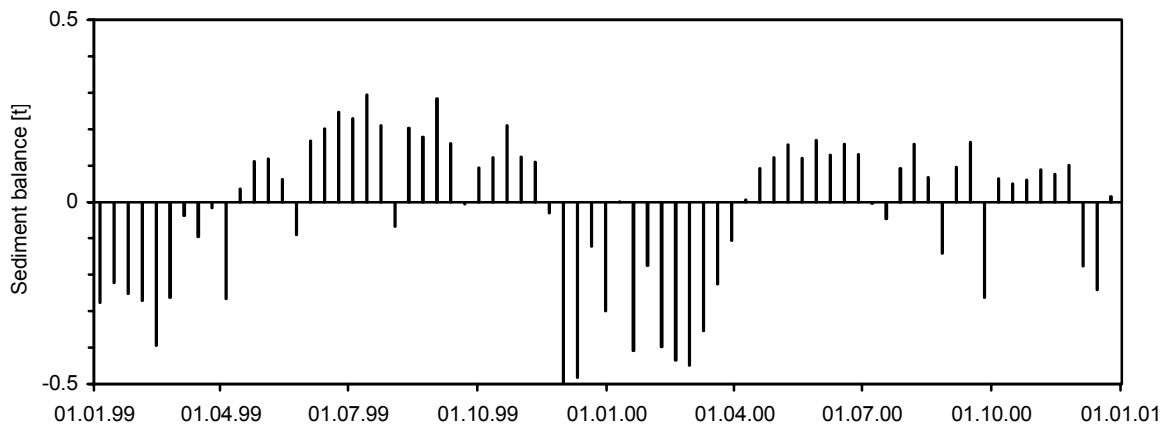


Fig. 76: Total amount of temporal sediment storages and releases during the HEC-6 simulation.

Fig. 76 displays the temporal sediment storages and releases during the HEC-6 simulation. The absolute balance at the end of the simulation period of -0.027 t indicates that channel scour predominates sediment accumulation. However, Lamers (2001) showed that the absolute balance depends strongly on the transport equations used for the HEC-6 simulation.

It is clearly visible that periods of dominant sediment storage in the channel are simulated during summer (positive sediment balances), whereas during the high flows in winter considerable sediment is flushed out (negative sediment balances). Thus the HEC-6 model is appropriate to simulate the temporal discontinuities involved in the sediment transport process at the catchment scale.

Assuming that the characteristic of the Wendbach River resembles to a great extent the Wahnbach catchment, it is possible to calculate the sediment discharge. Taking the percentage of surface area of the Wendbach (16.4 %), the ratio of the total sediment discharge can be calculated. For the year 1999 a total measured sediment discharge of approx. 899.7 t is calculated (Chapt. 4.4.2), which corresponds to a sediment export of the Wendbach catchment of 147.6 t. The sediment discharge of 1999 simulated by the HEC-6 model is 77.7 t. This discrepancy can either be an underestimation of sediment inflow into the channel or an incorrect proportion of scour and accumulation.

6.2.4 OPUS simulations with daily rainfall data

Since rainfall data of high resolution are only available since 05.01.92 (Tab. 1, Chapt. 3.1.2), long-term simulations with the breakpoint data option of OPUS cannot be carried out. Therefore the daily option of OPUS, which has proven its applicability of simulating the runoff of the sub-catchment Berrensiefen (Chapt. 6.1.1.4), is used for long-term simulations.

6.2.4.1 Simulation of monthly runoff

A period of 20 years was chosen for model calibration and validation, whereby the amount of macropore flow was adjusted in correspondence to the simulation using the breakpoint data option. Five rainfall stations spread over the catchment area were used for this simulation. Fig. 77 shows the simulated and measured monthly runoff of the Wahnbach catchment of the past twenty years.

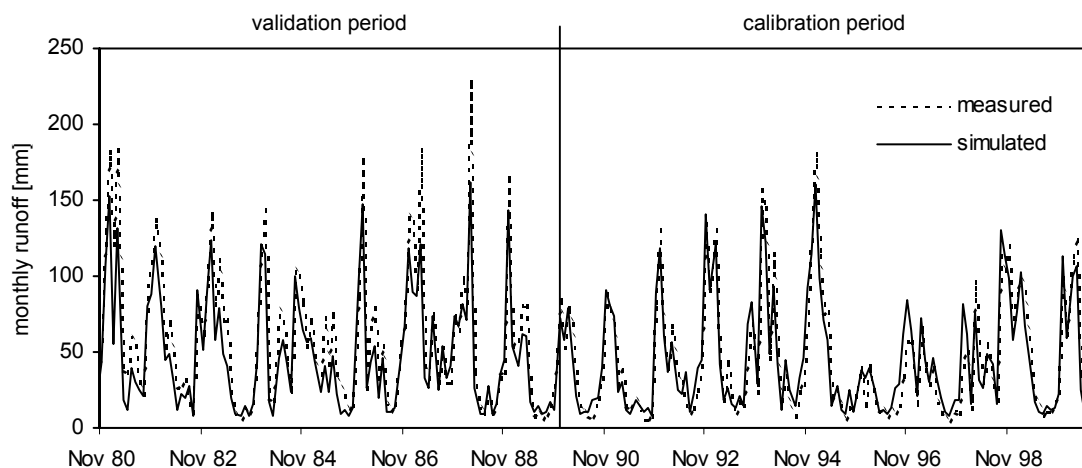


Fig. 77: Simulated and measured monthly runoff of the Wahnbach catchment (54km²).

The period from 1990 until 2000, which was used for model calibration, shows a good agreement of simulated and measured runoff (CME: 0.92 and IA: 0.98). In the case of the validation period, the values decrease to some extent (CME: 0.84 and IA: 0.95), but are still very satisfying.

6.2.4.2 Simulation of monthly nitrate discharge

The simulated nitrate discharge is displayed in Fig. 78. While during the calibration period a very good correspondence to the observed data (CME: 0.74 and IA: 0.92) has been obtained, values for the validation period are less convincing (CME: 0.49 and IA: 0.81).

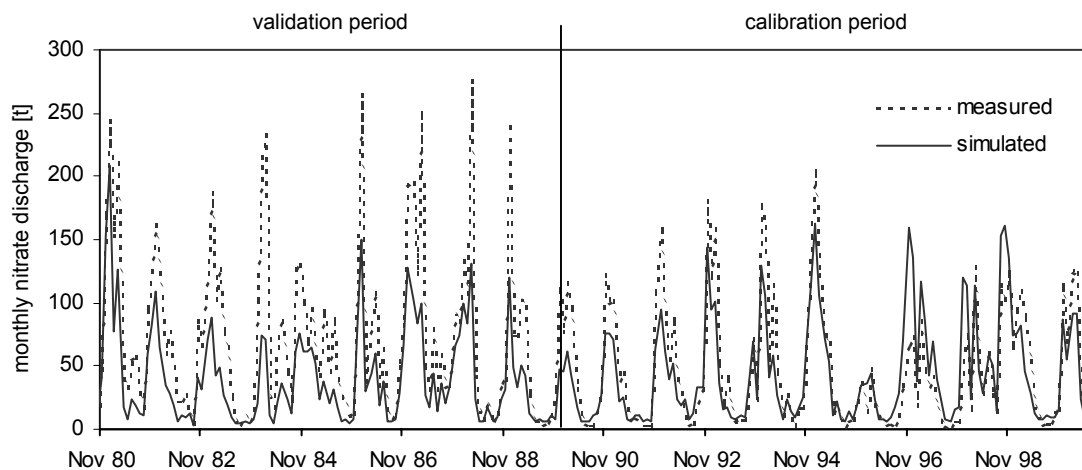


Fig. 78: Monthly nitrate discharge at the outlet of the Wahnbach catchment (dotted line, calculated from measured runoff and nitrate concentration) and mean monthly nitrate discharge of the simulated hillslopes (solid line).

The measured and simulated nitrate discharge amounts of the calibration period fit very well (Tab.21). However, during the validation period the simulated nitrate discharge is significantly underestimated.

Tab. 21: Measured and simulated nitrate discharges between September 1998 and December 2000.

	Measured nitrate discharge		Simulated nitrate discharge	
	[t]	[kg/ha/year]	[t]	[kg/ha/year]
Calibration period	5995	122	5577	113
Validation period	8105	138	4502	77

The deterioration in simulation quality is the result of several uncertainties being involved in the simulation of the long-term solute transport. The main problem hereby may be the inadequate information about the agricultural practice of the past and the influence of sewage discharges into the main rivers. Furthermore, the self-modifying character of ecosystems along larger time scales has to be considered (Lange, 1998). For example, the seasonal sustainability of riparian zones in buffering the fate of nitrate may be maintained by

vegetation uptake in summer and by denitrification during the dormant season, whereas the long-term sustainability may be affected by declining availability of organic carbon for denitrification (Haag and Kaupenjohann, 2001). Finally, it has to be noted that the interval of nitrate measurement during the calibration period was five times per week and during the validation period only one time per week. Thus it has to be taken into account that the values of nitrate discharge during the validation period are less reliable.

6.2.4.3 Simulation of monthly soil erosion

Fig. 79 shows the simulated monthly soil erosion and the monthly sediment export from the Wahnbach catchment, which is calculated using measured runoff and turbidity data from the WTV (Giertz, 2000). The simulation spans a period from 1980 until 2000. Since the measurement of turbidity before 1990 was on a weekly basis, it was only possible to calculate reliable sediment discharges for the second half of the simulation period.

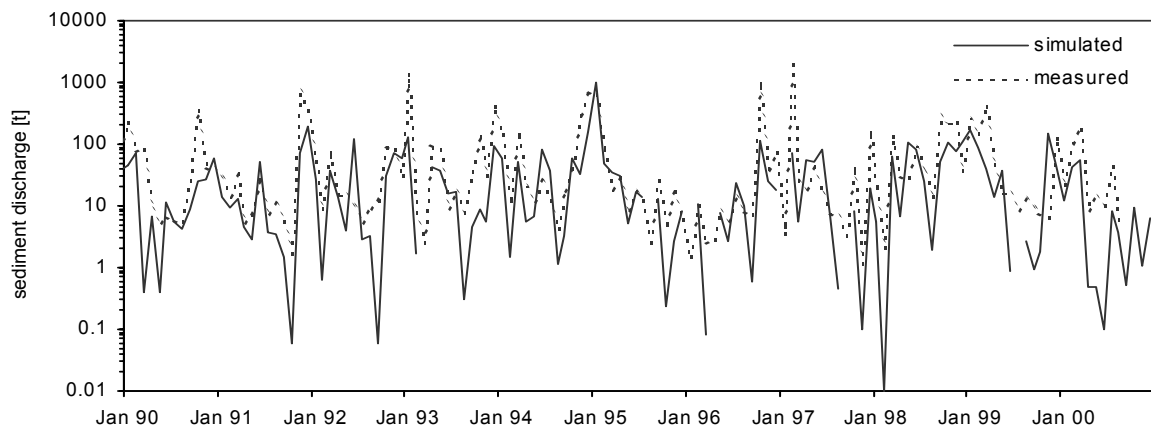


Fig. 79: Monthly sediment discharge at the outlet of the Wahnbach catchment (dotted line, calculated from measured runoff and turbidity) and mean monthly soil erosion on the simulated hillslopes (solid line).

The performance of this simulation is less satisfying than the water and nitrate discharge simulations (IA: 0.39). Furthermore, the measured mean annually sediment export (1226 t/year) is significantly higher than the simulated soil erosion (478 t/year). One reason for this difference is the fact that the fluvial sediment transport is not considered in the simulation. As described in Chapt. 4.1.4 and Chapt. 6.1.3, there are several sediment sources and temporal storages involved in the process of sediment export at the sub-catchment scale. Furthermore, the investigations in Chapt. 6.2.3 have shown the importance of the channel

processes at the catchment scale. This results emphasize the problem of validating simulated soil erosion rates by using suspended load measurements in the fluvial systems.

Consequently, for a better simulation of the sediment discharge, channel processes have to be integrated into the model scheme. However, the results of the simulations of water and solute fluxes suggest that the daily option is also adequate for the catchment scale and can be used for a long-term simulation.

6.3 The long-term scale

In this section the application of the modified OPUS model for the simulation of soil erosion spanning a period from 1950 to 2000 is presented.

The generated landuse distribution, reflecting the historical landuse development, was used for the long-term simulation with OPUS (Chapt. 5.2.3.2). To overcome the lack of climate data, a part of the data set was completed using the weather generator WGEN (Chapt. 5.2.3.1). Following this development of arable land, the whole period was subdivided into three sub-periods, obtaining mean values of landuse distribution. These sub-periods are used for the three independent simulations representing the whole period.

Fig. 80 displays the result of the three simulations and, for comparison, the measured sediment discharge of the past 20 years as well as the mean sediment yield of the Wahnbach catchment (about 1330 t/year), calculated from the reservoir deposits (Chapt. 3.1.6). The simulation of the 1st period based on a landuse distribution with about 20 % arable land shows a high variation of the yearly sediment discharge (from 590 t up to 12817 t).

Furthermore, the simulation indicates that a total sediment yield of about 39000 t occurred from 1958 until 1964. Based on the analysis of the accumulated sediment in the reservoir of the Wahnbach catchment, it can be assumed that about 48.000 t of sediment have been accumulated in the reservoir in total (Chapt. 3.1.6). That would mean that almost all of the sediments in the reservoir have accumulated in this period. This is obviously not true because the measured annual sediment yield from 1981 until 1999 indicates a total sediment yield of 26750 t (Chapt. 4.4.2).

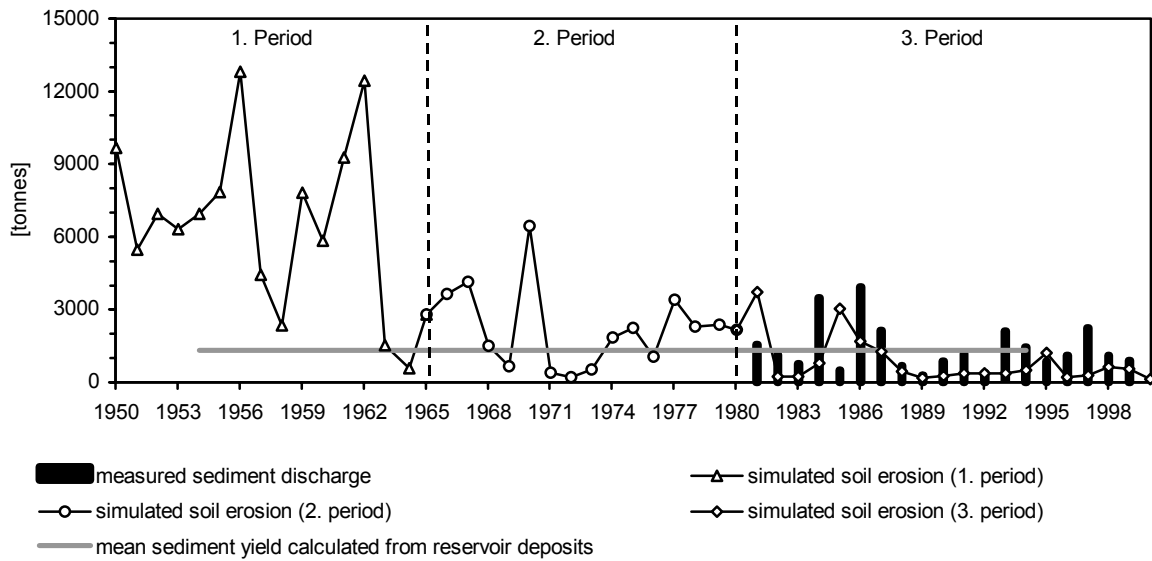


Fig. 80: Simulated soil erosion in the catchment of the Wahnbach River of the past 50 years with three landuse distributions, measured sediment discharge at the catchment outlet and the mean sediment yield calculated from the reservoir deposits.

The mean sediment yield of the three simulations differ significantly (1st period: 6682 t/y, 2nd period: 2235 t/y and 3rd period: 890 t/y). One reason for this might be that the erosion rate on arable land is simulated by OPUS too high while the erosion rate of other landuse is too low. Furthermore, this discrepancy might be increased due to the random allocation of arable land on the surface area, which is actually covered by pastureland (see Chapt. 5.2.3.2). Through this operation ploughland planes with unrealistically high slope values may have been created. This results in higher erosion values due to the high sensitivity of the OPUS model to changes in slope values (Chapt. 5.1.3, Tab. 11). However, since landuse maps of that time do not exist, it is impossible to scrutinize up to which slopes agricultural farming was carried out.

A simulation of the 3rd period with the landuse distribution of the 1st period yields a mean sediment discharge of 3013 t/year, which is 55 % less than the simulation of the 1st period. This indicates that the high erosion rate of the 1st period is also caused by the meteorological conditions during that time. The total simulated sediment yield in the period from 1958 until 1994 is about 89000 t, and therefore almost twice the amount calculated from the deposits. As already emphasized in the previous chapter, this indicates that sediment storages may play an important role in the Wahnbach catchment.

7 Uncertainties in the modelling process

In this chapter the uncertainties that are involved in the process of modelling are investigated. Hereby three main sources can be distinguished (Grunwald, 1997):

- Input data (temporal and spatial variability);
- Model assumptions and algorithms for describing the processes;
- Measurements for model validation.

7.1 Input data

7.1.1 Soil data

Uncertainties are involved in the digital soil map used for calculating the soil parameters of OPUS. On the one hand, inaccuracy in the location of the soil types is inherent in the spatial resolution of the digital soil map (1:50,000). On the other hand, there is uncertainty involved using classes of soil texture. The method of selection of representative values from the corresponding textural class in order to derive soil physical parameters has a significant influence on the simulation results (Bormann, 2001). Bormann (2001) showed that the relation of simulated fast and slow runoff depends significantly on the chosen grain size distribution and that the centre of a textural class may not be the representative selection in order to simulate the correct relation of fast and slow runoff components.

7.1.2 Landuse data

Furthermore, uncertainties are involved in the landuse data. Although the spatial and temporal resolution of the landuse data is quite good, the associated attributes are mainly derived from other investigations. For example, the parameter values used for the crop model are taken from the OPUS User Manual (Ferreira and Smith, 1992), modified during the calibrations at the sub-catchment scale and subsequently applied without further adjustment at the catchment scale. Furthermore, the times of harvest, tillage and fertilization are generalized from the observations in the sub-catchments. For example, a tillage operation can significantly change

the susceptibility of the soils for soil erosion and the fertilization time, and the application amounts effecting plant growth and nitrate washout.

7.1.3 Spatial discretization

The allocation of the data sets onto single hillslopes leads to uncertainties in respect of the spatial reproduction of the natural peculiarities (topography, landuse, soil type). For example, Thieken et al. (1997) observed that through the discretization the distribution of soil types of the hillslopes in the study area are changed. This is also the case for the landuse types. Due to the discretization of the catchment, a change of the landuse distribution is caused (Giertz, 2000). Through the discretization the percentage of pasture is increased, whereas all other landuse types are decreased (Tab. 21). Some landuse types (leguminous plants, potatoes) are completely omitted and the entire plough land area is reduced by 35 %.

Tab. 22: The percentages of the main landuse types in the Wahnbach catchment (54km²) of the year 1998 before and after discretization.

	Landuse [%]	Landuse after discretization [%]
Forest	19,4	16,0
Fields with individual trees and bushes	5,7	2,25
Golf court	14,8	8,24
Settlement and roads	1,22	1,44
Pasture	51,6	67,7
Cereals	2,51	1,75
Corn	3,54	2,29
Sugar beets	0,37	0,24
Leguminous plants	0,01	0
Potatoes	0,03	0
Surface water	0,77	0,07

The slope values are changed through the discretization as well. In Tab. 22 the mean slope values of the parcels of the digitized landuse map are compared with the mean slope values of the discretization map.

The mean slopes of the hillslopes covered by cereals and corn are significantly higher (15%) after the discretization. Since OPUS is very sensitive to changes in slope value (Tab. 11, Chapt. 5.1.3), the spatial discretization may lead to a significant overestimation of soil erosion.

Tab. 23: The percentages of the main landuse types in the upper Wahnbach catchment (54 km²) of the year 1998 before and after discretization; redrawn from Giertz (2000).

	Mean slope on the basis of the landuse map [%]	Mean slope on the basis of the discretization map [%]
Forest	16,5	15,8
Fields with individual trees and bushes	13,7	10,9
Golf court	10,5	109
Settlement and roads	11,4	11,7
Pasture	11,5	12,1
Cereals	9,72	11,5
Corn	8,96	11,1
Sugar beets	10,1	9,73
Surface water	6,50	2,57

7.2 Model assumptions

OPUS is a process-based model capable of simulating simultaneously several processes at the hillslope scale. Due to high complexity of the model structure it is possible that the model produces errors because of false process descriptions. For example, OPUS considers the effect of frozen soils. However, due to this implementation, the water and solute discharges in winter were significantly underestimated. After this implementation has been turned off, the simulation results were better. This experience underlines the thesis of De Roo (1993) that simpler models may in part obtain better results than complex models.

On the other hand, the comparison of the daily and breakpoint data option of OPUS (Chapt. 6.1.1.4) shows that the physically-based calculation of runoff is superior to that of the conceptual SCS-CN method. The main reason for the better simulation results is the better quality of the high-resolution rainfall data. The rainfall data averaged to daily values has lost the information on rainfall intensity. Thus, for example, an amount of 30 mm rainfall can fall during only a few minutes leading to significant runoff or can fall over the whole day without any noteworthy increase in runoff. Consequently, in this case a lower complexity of the model leads to more uncertainty.

7.3 Measurements for model validation

The model validation with data from field measurements is always problematical because the data themselves are a model of the reality (Schmidt, 1993). The selection of data is often subjective in respect to the sampling location and frequency (Grunwald, 1997). A further limitation is that not all model outputs can be validated, because the expenditure of the measurements would be too high. Therefore the modeller is often restricted to the main model outputs like water discharge.

Significant uncertainty is involved in the calculation of the discharges of matter on the basis of a daily or weekly sampling rate, because the concentrations of solutes and suspensoids during high flows are strongly variable (Göttlicher-Göbel, 1987). The method of indirect determination of the suspended load by using turbidity involves further uncertainties. According to Hasenpusch (1995), turbidity measuring instruments generally underestimate high concentrations of suspensoids. A further problem is involved in the uncertainty of the correlation between turbidity and suspensoid concentration.

Finally, the results of this study emphasize the problem of validating simulated soil erosion rates by using suspended load measurements in the fluvial systems, because several sediment sources and temporal storages are involved in the process of sediment export. Therefore, without considering the fluvial processes, simulated soil erosion amounts at the hillslope scale cannot be validated by using measurement of suspended loads in the fluvial systems.

8 Discussion

The aim of this study was to develop and apply an analyzing and modelling concept which is able to cover the main processes determining the fluxes of matter from small scales (point, hillslope and sub-catchment scale) up to a meso-scaled catchment (54 km²). In this chapter this approach is critically examined and problems are discussed.

8.1 The analyzing concept

A method to analyze transport processes in catchments at different time and spatial scales has been described. The observed scales span from daily up to several decades and from micro scale (sub-catchment) up to meso scale (catchment) (Fig. 3, Chapt. 1.2.2). The main assumption of the analyzing and modelling concept is that the export of matter from a catchment is the result of the processes at the hillslope scale.

8.1.1 Processes determining the fluxes of matter

The analysis of the measured hydrographs and continuous gauging of conductivity and nitrate concentration showed that different processes are involved in the transport of water:

Hortonian overland flow, saturated overland flow, interflow and groundwater flow. The extent of their contribution strongly depends on the rainfall characteristic and the antecedent soil water content. Measurements of the hydraulic characteristic of the soils revealed the presence of a secondary porous system. By considering the low permeability of the bedrock and the presence of pipes capable of draining water at a fast rate, it was possible to develop a perceptual model of the processes of water transport (Fig. 38, Chapt. 4.4.1). Furthermore, a differentiation of a V-valley type and trough valley type is suggested, wherein the main difference is the extension of alluvial fillings accompanied by surface-near groundwater.

8.1.2 Influence of landuse on the fluxes of matter

In order to analyze these processes, sub-catchments were selected which were dominated by different land utilizations. The main intention herein was to analyze the influence of landuse on the fluxes of matter.

However, due to the special situation of the research area, this approach is not problem-free, because no sub-basin of the Wahnbach catchment is completely covered by one landuse type (Tab. 4, Chapt. 3.1.4). This is especially the case for arable land, with only a max. 40 % of surface area being ploughland. Furthermore, the fluxes of matter are influenced by geomorphological (e.g. extent of alluvial fillings) and artificial (e.g. roads, drainages etc.) features of the sub-catchments. Every sub-basin is unique in its characteristics, and thus produces individual rainfall-runoff responses and exhibits individual temporal patterns of solute and sediment discharges. Additionally, the transport of solid matter within the sub-catchments shows temporal storages and releases of sediments within the channel, decoupling the fluxes of matter from the hillslopes.

Nevertheless, it was possible to find general tendencies reflecting the landuse distribution within each sub-catchment very well. For example, the interrelation of solute concentrations and land utilization can be explained with the amount of fertilizer applied on the hillslopes. Furthermore, it was possible to use the courses of solute concentrations in order to analyze the dominant runoff processes.

8.1.3 The perceptual model

On the basis of the analysis of the fluxes of water and solutes, a perceptual model of the runoff generation in the catchment of the Wahnbach River has been worked out. Additionally, investigations of runoff mechanisms on the basis of natural tracers (Hangen et al., 2001) can be carried out in order to ensure the validity of the perceptual model. Despite the possibility of inaccuracies, the developed perceptual model could be successfully applied as basis of the modification of the OPUS model.

The instrumentation of additional sub-catchments would eventually improve the possibility of process analyzing. For example, the effect of combinations of different landuse distributions with geology could have been better investigated. Furthermore, the sub-catchments could be instrumented with continuously measuring probes of several solutes and sediments, and

tracers could be applied to facilitate a better characterization of the water flowpaths. However, the expenditure for the installation and maintenance of additional gauging stations and probes may not be justified by the additional gain in information with the aim of analyzing long-term transport behaviour.

8.2 The modelling concept

The second aim of this study was to analyze if a process-based model system is able to simulate scales spanning from daily up to several decades and from the sub-catchment scale up to the catchment scale.

8.2.1 Sub-catchment scale

The results of the simulations of the sub-catchment scale indicated that it is possible to reproduce the courses of runoff and solute concentration with the modified version of the OPUS model. However, because of modifications that were necessary for an accurate simulation of the runoff processes in the sub-catchments, the model has lost its pure physically-based character. The additional parameters have to be calibrated at the catchment scale by comparing the observed runoff with the simulated. This may be regarded as a disadvantage, because the application of the model is limited to gauged catchments. However, the analysis showed that the sub-catchments revealed to a large extent similar runoff behaviour. Therefore it was possible to apply the model on the whole catchment by parameterizing each hillslope with the calibrated parameters of the sub-catchment scale.

The model system is also appropriate for using radar data in order to represent the spatial distribution of precipitation as good as possible. However, a great risk that unrealistic rainfall intensities are obtained is involved in radar data. It could be shown that relatively small deviations from the real rainfall intensities produce great deviations in the simulation of overland flow.

8.2.2 Catchment scale

The main assumption of the modelling concept is that a process-based model developed for small-scaled processes is suitable for the simulations at the catchment scale by using appropriate aggregation approaches. Bormann (2001) has already successfully applied a regionalization method in order to use the process-based SIMULAT model (Diekkrüger, 1996). Although the model works at the local scale, the water balances at the regional scale (990 km²) could be assessed. Bormann (2001) concluded that the results are encouraging and that the model could therefore even be used as a predictive tool for analyzing scenarios. He argued that application is limited only by the availability of data and not by the model- and regionalization concept.

Though the modelling concept of this study is based on the same assumptions there is a clear difference between both studies. Bormann (2001) restricted his analysis to the simulation of water transport, whereas in this study the fluxes of nitrate and sediment are also taken into consideration. The simulation of the transport of solutes and sediments involves more processes to be considered and thus the simulation effort is increased significantly. Therefore, this study was restricted to a smaller area (54 km²) in order to limit the computing duration and to confine the uncertainties involved in the input data.

Lane et al. (1997a) argued that a physically-based simulation of sediment delivery is currently impossible at the catchment scale due to the inability to accurately simulate the catchment runoff. However, this study shows that an erosion model can be successfully applied at the catchment scale in respect to the simulation of runoff and solute transport. Sediment discharge was simulated acceptably at the sub-catchment scale, but significant differences between observed and predicted sediment transport occurred at the catchment scale.

The main problem is that we, in most cases, do not really know the fate of soil particles detached on the hillslope until they are passing the catchment outlet. It is widely agreed that processes determining sediment transport are scale-independent and therefore processes observed at the hillslope scale are also effective at the catchment scale. However, processes of a higher scale, e.g. sediment storage in channels, ponds or floodplains, can overlie small-scaled processes. The release of accumulated sediments may significantly increase the sediment discharge depending on the residence times of the storage pools (Reid and Dunne, 1996).

For example, in the catchment of the Wahnbach River more than 200 ponds exist covering an area of about 13.7 ha. It has been observed that some of these ponds are completely filled up with sediments which accumulated over several decades and they currently release sediment due to channel incision into the deposits. The opposite case is happening to the largest pond of the catchment (3.7 ha, sub-catchment size: 25 km²), which has accumulated sediments since hundreds of years. Due to the decreasing water volume of the pond, the Wahnbach River was artificially diverted around the pond in the seventies, and hence sediment accumulation is significantly reduced.

These examples stress that for a successful physically-based modelling of sediment delivery it is indispensable to analyze the existence and the behaviour of storages and to implement them into the model scheme in a more or less conceptionally way. Therefore analyzing techniques have to be developed and applied to solve this problem. For example, in the case of a long-term examination, the fingerprint technique (Collins et al., 1997) in combination with radiometric dating of sediment deposits (Bogena et al. 2001) may be an adequate way to find out the internal processes of sediment transport in catchments.

9 Conclusions

In this chapter the results of this study are evaluated in respect to its usefulness for process investigations as well as for supporting decision-making at the catchment scale. In this context three questions can be formulated:

- Did the model bridge the gap between several spatial and temporal scales?
- Is it possible to apply the model system on other areas?
- Is the model system suitable for supporting natural resource management?

In general, the obtained simulation results at different scales (from the sub-catchment scale to the catchment scale and from single events to long-term scales) are encouraging. It could be shown that process-based models can be applied at several scales in order to calculate the fluxes of matter. Furthermore, the results show that the considered flux types (water, solutes, sediment) are simulated with different success. The best results are obtained by simulating daily runoff at the sub-catchment scale and at the catchment scale. The solute concentration at the sub-catchment scale and the monthly nitrate discharge at the catchment scale is reproduced satisfactory, but the measures of model accuracy are less high. The sediment transport is simulated with the lowest accuracy.

Two main reasons are responsible for this finding. On the one hand, due to the complicated interaction of the processes determining the fluxes of sediment, the uncertainty in model description as well as in parameters is very high, especially in the case of physically-based models. On the other hand, the measurement of solute and sediment discharge is a complicated task and involves more uncertainty than the measurement of water discharge. Thus, the quality of model calibration and the validation of the simulation results are less reliable. The observations in the sub-catchments and the simulation of fluvial sediment transport revealed that the soil erosion on the hillslopes couldn't be equated with the sediment discharge. The results of this study indicate that the validation of erosion models by using measurements of sediment discharge is not appropriate, especially for short periods.

It can be concluded that process-based models that are originally developed for the local scale can be utilized to simulate several fluxes of matter at the meso-scale, but it can be expected that the quality of simulation results is highest for the water transport and lowest for the sediment transport.

In principle, the model concept is applicable for every other meso-scale catchment. However, due to the high demand on input and calibration data of the model system, the application is limited to catchments with a similar equipment of gauging stations and distributed data (digital elevation model, soil map, landuse map) of high spatial resolution. Furthermore, the success of a model application depends on the quality of the perceptual model of the processes determining the fluxes of matter. Therefore, process observations at the sub-catchment scale should precede the modelling procedure in order to test, whether the model is able to adequately simulate the main processes.

A model system, which is able to simulate the fluxes of matter at different time and spatial scales, enables a number of application possibilities for several types of groups or users in order to support natural resource management. In this connection, Renschler (2000) differentiated three types of groups with different aims and scientific background, who may be interested in such a model system:

- educators for public awareness;
- managers for practical decision support;
- scientists and engineers for detailed research.

It can be expected that the first group is less experienced in the application of physically-based models. Therefore, the expenditure for this type of users would be by far too high and the danger of model misuse is highly accelerated. The second type of group is not interested in this kind of model approach as long as its application fulfils the requirement of supporting decision making. For that reason, it can be expected that the model concept developed in this study is too labour-intensive for many users of this group. Nevertheless, in some special cases the abundance of application possibilities of the model system may be attractive for this type of users. In general, the third group is highly experienced in the processes of solute and sediment transport as well as in modelling purposes. Therefore, it can be assumed that the model approach is most appropriate for that kind of users.

Several application possibilities of the model concept are conceivable:

- the management of drinking water catchments in terms of water quantity as well as water quality;
- the assessment of flood risks on a daily basis at the sub-catchment and catchment scale, including the evaluation of water-levels in the main channels by the HEC6-model;
- the simulated vegetation coverage and evapotranspiration rates can be used as the lower boundary for a process-based modelling of meso-scaled meteorological phenomena;
- to evaluate the effectiveness of protection strategies against soil erosion at the hillslope and catchment scale;
- as an advice basis for farmers in order to achieve optimal harvest yields (e.g. fertilization amounts, irrigation etc);
- evaluating long-term effects (e.g. water and solute discharge, soil erosion and sediment discharge, crop yield etc.) on landuse and climate changes.

Finally, it has to be noted that the aim of this study was not to develop a user-friendly tool for the described application examples, but to evaluate the possibility of process-based models to simulate the fluxes of matter at different temporal and spatial scales. With regard to a practical application, the next step would be to transfer this concept into a working tool for decision-making. This may involve further modifications and simplifications of the model structure as well as the addition of further model components depending on the purpose of the application.

10 Appendix

Abbreviations:

B: Berrensiefen

H: Hellenkeutelsiefen

Ste: Steinersiefen

Stu: Stucksiefen

Sch: Schlößchensiefen

l.a.m.: Concentration is lower than the accuracy of measurement

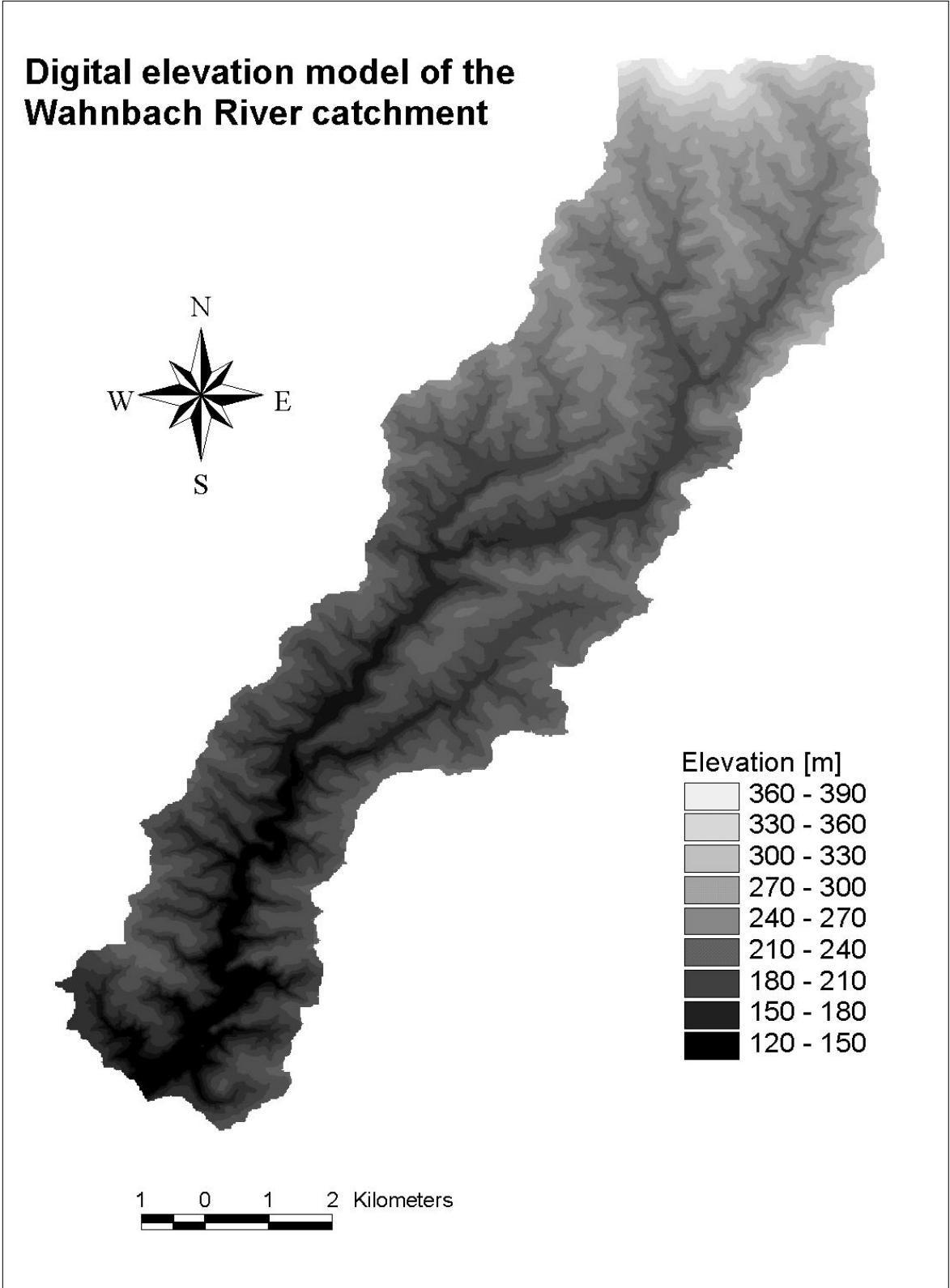


Fig. 81: The digital elevation model of the Wahnbach catchment obtained by laser scanning.

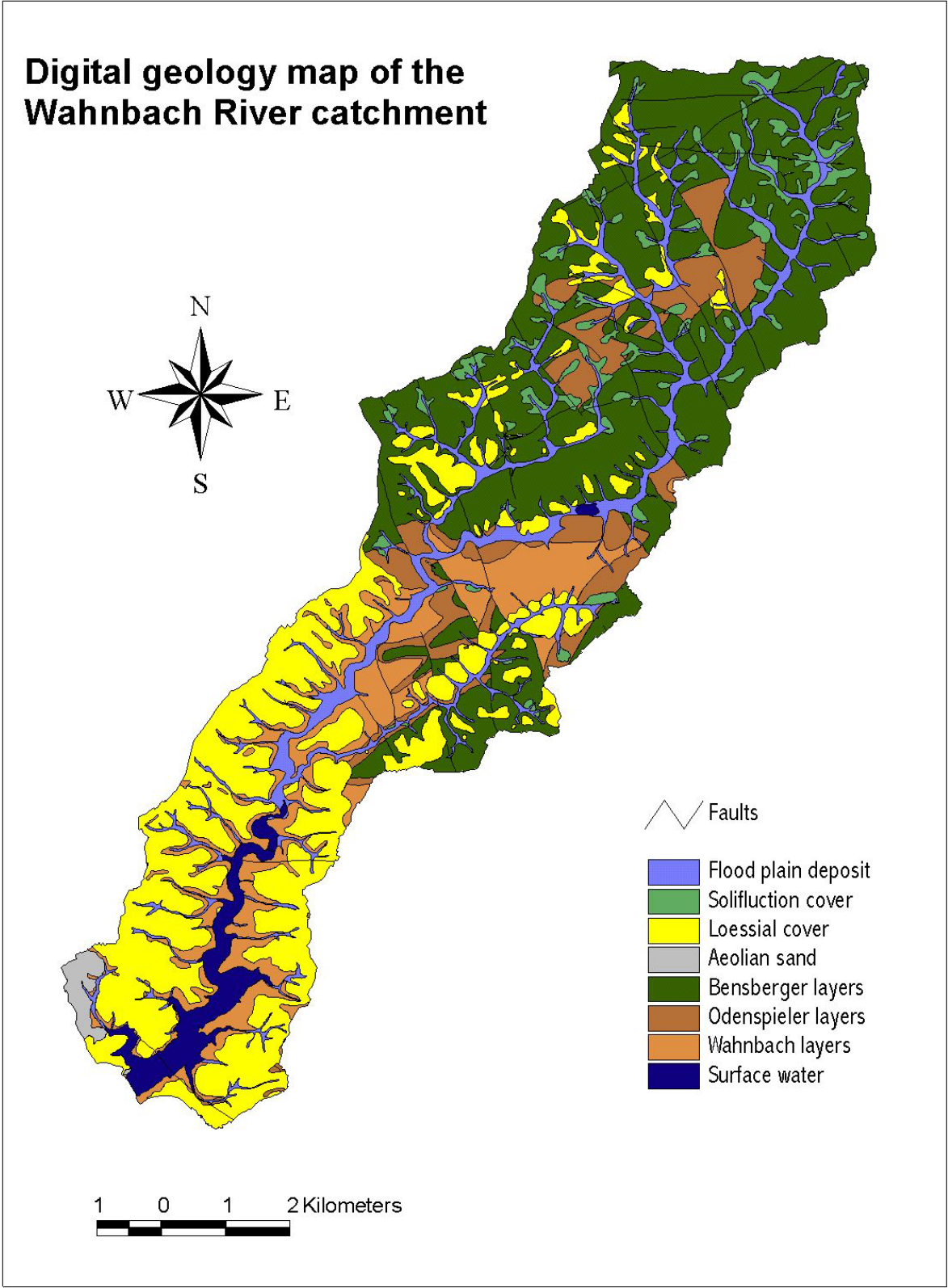


Fig. 82: The digital geology map digitized on the basis of the following analog maps (1:25,000) from the regional geologic department of North Rhine Westphalia (5110 Ruppichteroth, 5109 Lohmar, 5010 Engelskirchen).

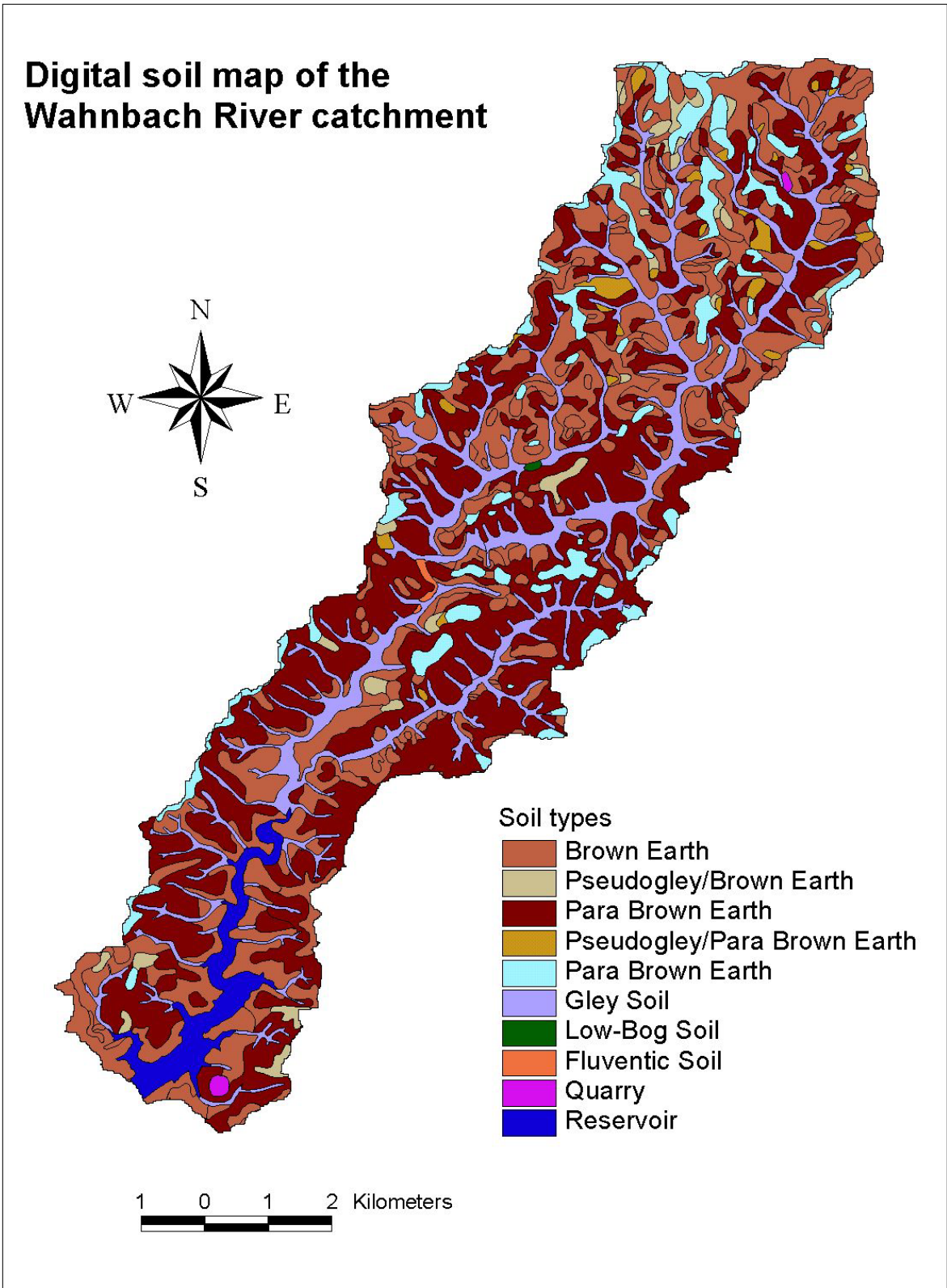


Fig. 83: The digital soil map of the Wahnbach catchment (1:50,000) provided by the regional geologic department of North Rhine Westphalia.

Digital landuse map of the Wahnbach River catchment

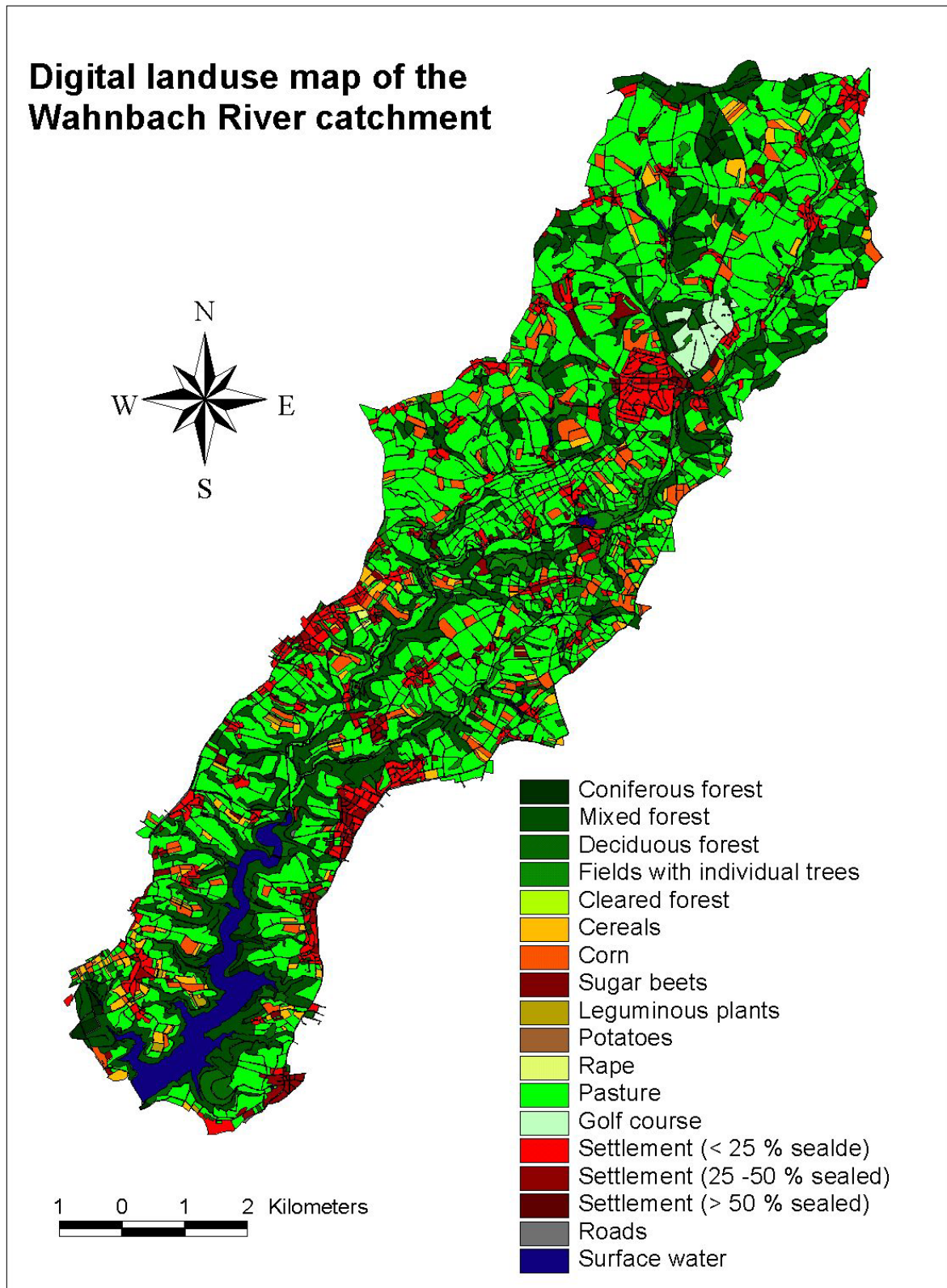


Fig. 84: The digital landuse map of the Wahnbach catchment, own digitization on the basis of landuse mappings (1:5,000) carried out by the association of the Wahnbach reservoir (WTV).

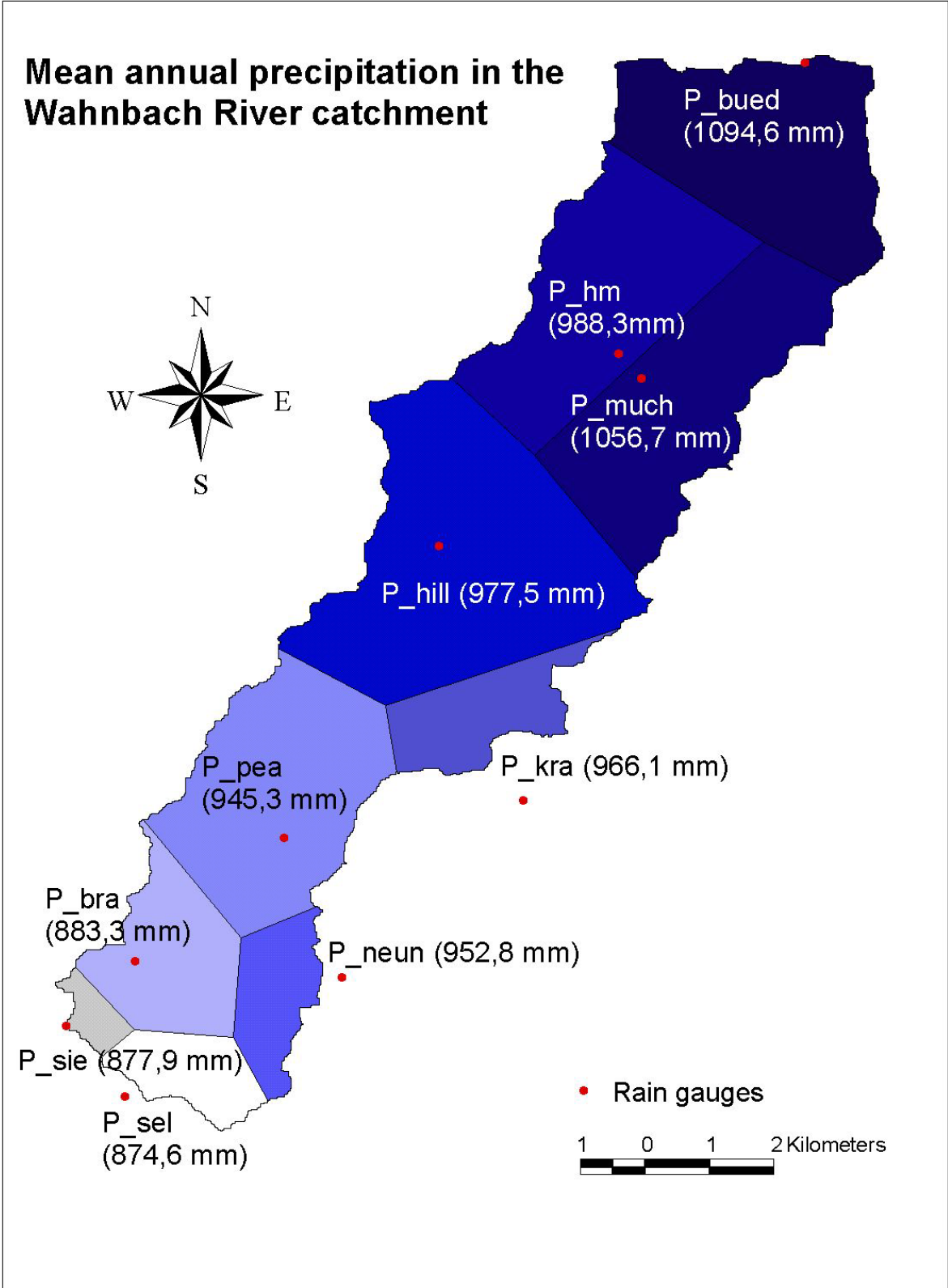


Fig. 85: The rainfall stations in the Wahnbach catchment and mean annual precipitation amounts; rainfall data from the association of the Wahnbach reservoir (WTV); see also Tab. 1 for further informations.

Tab. 24: Weekly measured chloride concentrations [mg/l].

	B	H	Ste	Stu	Sch		B	H	Ste	Stu	Sch
10.08.98	6,2	7,3	16,2	11,4	15,8	25.10.99	6,4	7,2	14,4	15,0	16,3
17.08.98	6,5	6,9	15,7	13,7	16,6	02.11.99	8,0	7,7	14,9	9,7	15,3
24.08.98	6,5	7,1	14,0	10,1	13,0	08.11.99	6,5	8,5	13,8	15,9	15,2
31.08.98	6,3	7,3	18,1	12,2	19,6	15.11.99	7,4	7,7	14,9	16,5	18,5
07.09.98	5,3	6,4	15,3	6,8	11,0	22.11.99	7,3	9,5	17,2	14,1	17,3
14.09.98	5,0	6,2	13,4	6,1	10,3	29.11.99	7,0	8,8	19,8	13,8	17,8
21.09.98	5,0	6,5	15,0	7,3	13,0	06.12.99	7,1	8,6	17,5	14,0	16,3
28.09.98	5,6	7,3	15,7	9,3	13,6	13.12.99	6,0	6,2	15,1	8,6	10,5
05.10.98	5,9	7,7	15,3	11,2	13,4	20.12.99	6,8	7,3	16,9	8,8	14,9
12.10.98	4,6	5,8	12,1	6,5	10,2	29.12.99	8,2	8,8	17,9	8,8	14,8
19.10.98	5,0	6,3	13,5	7,0	11,8	05.01.00	7,4	8,5	14,9	8,8	11,0
26.10.98	4,6	6,2	12,2	7,6	9,2	10.01.00	7,7	8,5	17,3	12,2	14,8
02.11.98	4,3	6,2	11,3	6,6	8,7	17.01.00	7,1	8,2	16,7	10,3	15,9
09.11.98	16,2	5,5	9,1	5,9	4,4	24.01.00	7,4	8,2	15,9	7,9	11,4
16.11.98	4,7	6,5	11,6	6,4	9,0	31.01.00	6,7	6,8	14,7	8,8	10,3
23.11.98	5,3	7,2	13,9	8,1	12,2	07.02.00	7,3	7,8	16,1	8,3	13,1
30.11.98	5,8	7,1	12,9	8,5	12,5	14.02.00	6,4	7,5	16,5	8,1	12,2
07.12.98	5,7	7,2	13,5	9,7	14,4	21.02.00	6,6	7,6	15,5	8,3	12,3
14.12.98	9,0	9,2	15,4	11,1	11,3	28.02.00	6,4	8,1	16,5	7,8	12,3
21.12.98	7,4	9,6	17,9	9,7	13,5	08.03.00	5,5	7,6	13,6	5,0	7,7
28.12.98	7,0	8,6	14,8	9,8	10,5	13.03.00	5,7	7,7	15,1	7,6	11,6
04.01.99	7,2	10,1	14,1	9,1	11,7	20.03.00	7,9	8,2	15,7	9,2	13,5
11.01.99	6,7	8,2	14,9	8,8	12,1	27.03.00	5,5	6,3	12,0	6,8	8,4
18.01.99	7,1	8,9	14,5	8,9	12,7	03.04.00	6,1	7,5	15,1	8,5	12,2
25.01.99	6,9	8,4	14,8	9,5	13,4	10.04.00	6,3	7,5	15,7	9,7	13,9
01.02.99	6,4	8,3	14,8	9,3	13,1	17.04.00	6,4	7,6	16,4	10,5	14,4
08.02.99	6,8	8,7	12,6	8,9	10,5	25.04.00	6,5	7,7	15,7	11,0	14,1
16.02.99	6,7	8,1	15,1	12,7	12,4	02.05.00	6,4	7,8	16,0	11,9	15,4
22.02.99	7,2	8,9	13,8	19,0	13,6	08.05.00	7,5	7,5	16,8	11,8	16,0
01.03.99	8,9	9,8	17,4	12,8	15,8	15.05.00	7,0	7,5	16,3	11,9	16,4
08.03.99	7,6	9,4	15,0	11,2	13,5	22.05.00	7,1	7,9	14,7	11,5	12,6
15.03.99	7,3	9,3	16,3	15,0	14,9	29.05.00	7,2	7,7	15,4	11,9	15,7
22.03.99	7,2	9,9	15,7	10,9	12,0	05.06.00	7,1	7,6	14,6	12,0	15,1
29.03.99	7,6	8,8	16,9	11,4	14,9	12.06.00	6,6	7,2	14,7	11,5	15,9
05.04.99	7,2	9,0	16,6	12,1	15,2	19.06.00	6,3	7,5	15,4	12,1	16,7
12.04.99	7,1	9,4	16,1	10,7	13,7	26.06.00	6,1	7,4	14,8	12,4	15,9
19.04.99	7,0	8,0	15,7	10,2	14,2	03.07.00	6,0	7,1	13,9	12,0	14,0
26.04.99	6,7	8,0	16,1	11,2	15,0	10.07.00	5,8	7,0	12,6	10,9	12,6
03.05.99	6,8	8,1	15,9	12,0	15,3	17.07.00	5,6	5,8	12,5	8,2	12,9
10.05.99	6,8	8,0	16,6	12,3	16,3	24.07.00	5,9	6,3	12,7	7,5	10,0
17.05.99	7,0	7,6	17,0	11,6	16,5	31.07.00	5,3	5,6	12,2	7,3	11,8
25.05.99	6,7	7,5	16,3	11,7	18,1	07.08.00	5,9	6,3	14,3	9,0	15,1
01.06.99	6,8	8,2	16,1	12,9	16,4	14.08.00	5,9	7,0	14,8	9,8	15,5
07.06.99	7,1	8,7	16,6	12,1	16,0	21.08.00	6,0	6,6	14,5	10,1	12,8
14.06.99	6,9	7,9	16,0	12,3	16,7	28.08.00	5,9	6,6	16,7	10,0	12,5
21.06.99	6,6	7,5	15,4	12,7	15,4	04.09.00	5,9	6,3	16,4	9,3	12,7
28.06.99	6,8	7,4	15,4	13,7	15,6	11.09.00	5,9	6,2	16,3	9,0	14,1
05.07.99	6,4	7,3	15,5	13,1	16,7	18.09.00	6,0	6,4	14,8	9,1	12,3
12.07.99	6,3	7,5	15,5	13,0	16,9	25.09.00	6,0	6,1	14,6	7,9	12,7
20.07.99	4,3	6,0	16,1	13,7	15,4	02.10.00	5,5	5,5	13,7	6,9	11,3
26.07.99	6,1	6,4	15,4	13,9	16,8	09.10.00	5,6	5,9	13,7	6,9	11,2
02.08.99	6,2	6,2	16,1	14,4	17,3	16.10.00	5,6	5,7	15,1	8,6	13,4
09.08.99	6,3	6,1	15,8	14,4	17,9	23.10.00	5,9	5,9	15,9	9,1	13,7
16.08.99	6,0	8,7	14,6	13,3	14,1	30.10.00	5,7	5,6	13,7	7,5	11,1
23.08.99	6,3	8,4	17,0	14,8	18,2	06.11.00	5,8	6,1	14,7	8,9	13,2
30.08.99	6,6	7,5	16,1	14,7	17,7	13.11.00	6,3	6,1	15,2	10,3	14,2
06.09.99	6,7	6,9	16,0	17,8	18,0	20.11.00	6,1	6,3	15,6	10,9	14,8
13.09.99	6,4	6,4	16,1	15,3	18,5	27.11.00	5,8	6,0	15,7	9,8	13,9
20.09.99	6,2	5,8	20,5	15,6	18,6	04.12.00	5,7	5,5	14,0	8,6	12,9
27.09.99	6,5	6,1	15,3	20,1	17,5	11.12.00	5,5	5,4	13,5	7,0	11,0
04.10.99	7,3	8,7	14,9	13,7	16,0	18.12.00	5,3	5,3	12,8	6,8	10,5
11.10.99	7,0	9,1	16,0	14,7	16,3	25.12.00	5,5	5,6	14,0	8,7	13,0
18.10.99	7,1	8,0	15,8	15,0	18,2	01.01.01	6,4	8,6	14,7	10,1	11,6

Tab. 25: Weekly measured nitrate-concentrations [mg/l].

	B	H	Ste	Stu	Sch		B	H	Ste	Stu	Sch
10.08.98	24,2	13,6	29,3	13,9	16,4	25.10.99	13,3	6,7	23,3	9,2	10,8
17.08.98	22,9	11,5	27,9	14,5	14,9	02.11.99	10,6	6,0	16,7	6,4	7,1
24.08.98	18,1	16,1	25,4	20,0	22,4	08.11.99	14,4	12,5	19,4	10,4	11,6
31.08.98	19,5	13,0	31,4	13,1	16,1	15.11.99	18,2	12,4	21,9	10,0	11,3
07.09.98	22,9	21,4	37,1	16,6	25,8	22.11.99	19,5	15,0	25,1	12,3	14,9
14.09.98	23,3	21,6	32,3	15,2	24,2	29.11.99	25,5	17,3	27,4	13,5	17,0
21.09.98	23,8	18,2	33,7	16,4	24,9	06.12.99	25,3	17,4	26,9	14,1	17,4
28.09.98	23,0	16,1	30,9	15,2	20,9	13.12.99	29,4	22,7	35,6	18,9	24,4
05.10.98	22,7	15,6	29,9	14,3	19,0	20.12.99	31,3	19,8	37,0	17,3	23,0
12.10.98	22,5	20,4	30,6	13,6	22,4	29.12.99	30,1	19,8	36,0	16,7	22,4
19.10.98	24,4	18,8	33,1	15,5	23,8	05.01.00	28,8	20,8	32,6	16,2	22,5
26.10.98	23,2	19,2	31,6	14,3	21,8	10.01.00	28,7	17,7	34,5	21,2	21,4
02.11.98	20,9	19,0	29,7	16,1	21,8	17.01.00	25,1	15,8	31,5	14,2	19,4
09.11.98	13,2	15,6	21,3	15,0	10,6	24.01.00	28,3	19,9	35,0	15,9	22,4
16.11.98	22,0	18,5	27,3	13,2	20,4	31.01.00	27,4	20,9	34,6	16,1	22,2
23.11.98	23,3	18,1	30,2	15,5	23,1	07.02.00	28,6	18,0	31,8	15,4	20,6
30.11.98	23,4	18,3	27,1	15,4	22,1	14.02.00	26,9	18,8	35,8	15,7	21,8
07.12.98	23,8	17,1	27,5	16,0	21,3	21.02.00	26,2	20,0	36,6	16,0	23,0
14.12.98	24,7	19,1	28,3	15,3	20,1	28.02.00	25,7	18,3	36,2	15,5	22,3
21.12.98	24,7	19,5	29,4	15,8	22,4	08.03.00	20,1	16,3	30,7	9,5	15,5
28.12.98	24,5	19,2	27,8	15,4	21,0	13.03.00	23,6	16,9	34,2	14,5	21,6
04.01.99	21,4	16,9	25,3	13,2	18,5	20.03.00	24,0	17,0	33,3	14,2	21,9
11.01.99	24,2	19,0	29,2	16,1	22,3	27.03.00	21,5	17,6	31,3	13,1	20,1
18.01.99	25,4	18,4	28,1	15,5	21,7	03.04.00	21,8	16,0	32,0	13,5	21,0
25.01.99	23,9	17,7	27,5	16,0	22,1	10.04.00	22,2	15,2	32,2	13,9	20,5
01.02.99	25,4	18,6	27,9	16,7	24,0	17.04.00	20,8	13,5	30,4	13,0	18,8
08.02.99	25,0	18,0	24,4	14,1	20,8	25.04.00	18,8	12,1	28,1	11,9	17,2
16.02.99	21,0	16,6	24,8	15,2	26,8	02.05.00	19,0	11,0	27,6	11,8	15,5
22.02.99	23,0	19,1	23,2	14,5	17,5	08.05.00	19,3	12,8	26,5	10,2	14,0
01.03.99	21,3	18,9	25,8	15,2	23,0	15.05.00	19,1	11,2	25,4	8,8	12,8
08.03.99	20,2	17,5	24,7	14,4	21,3	22.05.00	17,3	11,0	23,0	10,2	13,6
15.03.99	23,1	17,2	27,4	15,0	21,6	29.05.00	19,2	11,4	24,6	11,3	15,4
22.03.99	20,2	16,0	26,2	14,0	19,5	05.06.00	17,9	10,5	22,5	9,5	13,4
29.03.99	24,2	17,0	27,3	15,6	21,8	12.06.00	17,5	10,9	23,1	10,2	12,5
05.04.99	20,7	15,1	26,3	14,6	21,3	19.06.00	17,6	10,4	23,4	9,2	12,0
12.04.99	23,1	16,7	26,6	14,4	20,1	26.06.00	15,9	9,7	23,5	9,5	13,0
19.04.99	24,0	16,8	27,6	15,2	22,1	03.07.00	15,3	8,5	21,0	9,2	12,3
26.04.99	22,8	15,6	27,5	15,0	21,2	10.07.00	18,1	15,2	21,1	14,3	17,3
03.05.99	22,0	14,4	27,8	15,2	19,8	17.07.00		16,8	27,3	14,5	19,2
10.05.99	21,4	12,8	28,0	14,0	18,6	24.07.00	23,6	14,2	25,1	11,1	12,0
17.05.99	20,2	11,4	27,6	14,2	18,2	31.07.00	21,8	15,8	30,6	13,7	19,2
25.05.99	19,8	10,7	27,1	13,1	16,5	07.08.00	22,4	16,3	29,8	12,4	17,0
01.06.99	19,2	10,5	26,5	12,2	15,6	14.08.00	20,6	15,4	28,7	11,1	15,3
07.06.99	18,7	11,1	25,4	12,9	16,6	21.08.00	13,7	14,5	27,8	12,5	16,4
14.06.99	18,3	9,9	25,8	12,0	15,2	28.08.00	15,9	16,0	39,1	14,2	19,1
21.06.99	16,3	10,1	25,7	12,7	15,9	04.09.00	18,2	13,7	33,5	11,1	13,8
28.06.99	16,4	8,4	25,2	11,3	13,0	11.09.00	20,3	15,6	36,0	13,1	17,1
05.07.99	15,4	7,4	24,1	9,9	12,6	18.09.00	21,7	13,1	32,6	13,6	18,0
12.07.99	14,8	6,5	24,0	9,1	11,5	25.09.00	19,2	15,3	35,0	13,3	17,5
20.07.99	9,9	5,4	24,0	8,9	10,1	02.10.00	20,2	16,7	35,7	13,6	19,0
26.07.99	13,3	5,4	24,1	9,4	11,0	09.10.00	22,4	15,6	33,7	12,4	19,1
02.08.99	13,8	4,9	24,4	9,0	10,2	16.10.00	20,0	14,9	32,7	12,3	17,1
09.08.99	12,8	4,2	23,2	8,3	9,3	23.10.00	21,4	14,0	31,1	11,7	16,7
16.08.99	11,3	8,3	22,2	12,0	17,1	30.10.00	20,7	16,7	30,4	12,3	17,3
23.08.99	13,5	7,4	23,4	10,0	13,2	06.11.00	22,8	15,3	30,7	11,9	16,7
30.08.99	12,6	5,2	22,2	9,0	11,7	13.11.00	21,5	13,0	29,1	10,5	14,8
06.09.99	12,4	4,3	22,3	8,8	10,8	20.11.00	19,9	14,4	30,0	11,3	15,6
13.09.99	12,1	4,1	21,1	8,7	9,3	27.11.00	20,2	15,7	29,3	11,8	16,2
20.09.99	12,0	3,4	22,4	8,6	8,9	04.12.00	21,8	15,7	31,2	12,6	17,4
27.09.99	11,7	3,7	21,2	7,7	9,8	11.12.00	22,9	16,3	31,7	12,2	17,9
04.10.99	13,0	12,0	21,5	12,4	15,6	18.12.00	22,8	15,8	32,7	14,2	18,9
11.10.99	13,2	12,4	22,6	12,5	15,9	25.12.00	24,6	13,4	30,9	13,0	17,9
18.10.99	15,5	9,6	23,9	11,3	14,3	01.01.01	22,2	17,6	32,2	14,0	18,4

Tab. 26: Weekly measured sulphate concentrations [mg/l].

	B	H	Ste	Stu	Sch		B	H	Ste	Stu	Sch
10.08.98	13,5	16,2	17,4	24,0	26,5	25.10.99	13,9	13,1	12,6	26,6	25,3
17.08.98	13,0	14,6	16,3	24,9	25,1	02.11.99	14,3	12,5	12,6	16,6	20,0
24.08.98	14,4	14,3	15,4	27,0	26,1	08.11.99	16,9	11,4	14,8	28,9	24,4
31.08.98	13,0	14,5	16,5	23,3	25,5	15.11.99	15,1	14,3	14,1	25,8	25,1
07.09.98	14,9	50,1	19,3	24,2	26,2	22.11.99	15,5	14,5	16,5	25,2	24,8
14.09.98	15,3	15,2	20,5	22,5	27,3	29.11.99	15,2	15,8	20,2	25,2	28,8
21.09.98	15,1	17,5	20,6	23,5	38,4	06.12.99	15,3	15,5	20,7	24,2	27,6
28.09.98	14,2	16,4	18,3	23,9	30,9	13.12.99	14,1	16,0	19,2	23,5	26,3
05.10.98	16,5	18,5	21,5	25,8	39,5	20.12.99	14,5	17,2	19,9	22,8	32,8
12.10.98	17,5	18,2	24,2	25,6	32,8	29.12.99	14,5	17,2	19,4	21,5	31,1
19.10.98	16,7	18,8	21,4	24,5	35,6	05.01.00	14,6	16,7	18,1	21,2	26,2
26.10.98	16,3	19,2	20,2	23,7	29,8	10.01.00	14,9	17,5	19,3	31,0	30,9
02.11.98	16,3	19,0	21,3	26,8	30,8	17.01.00	14,1	16,8	20,1	22,5	28,9
09.11.98	10,5	15,7	14,8	17,6	14,5	24.01.00	14,2	15,8	17,6	20,9	25,6
16.11.98	15,2	18,3	18,7	21,5	27,9	31.01.00	13,8	15,8	16,6	20,4	24,0
23.11.98	15,2	18,9	19,3	23,5	30,6	07.02.00	15,7	17,5	18,5	21,7	27,6
30.11.98	15,3	18,0	18,5	24,2	29,4	14.02.00	14,3	17,4	18,6	22,1	29,6
07.12.98	15,0	18,1	16,9	24,4	28,9	21.02.00	14,6	18,4	18,1	22,1	30,6
14.12.98	15,0	18,0	18,0	23,0	26,5	28.02.00	14,9	19,2	18,9	23,3	30,7
21.12.98	16,3	18,6	19,5	24,7	30,9	08.03.00	13,1	18,7	17,7	15,1	20,5
28.12.98	15,9	18,2	19,0	23,6	27,0	13.03.00	14,8	19,9	19,0	23,9	30,7
04.01.99	13,7	17,1	17,7	21,5	24,0	20.03.00	15,3	19,4	19,4	24,1	30,3
11.01.99	15,9	19,5	19,5	25,1	30,2	27.03.00	14,6	18,1	17,9	21,0	24,4
18.01.99	15,9	19,3	19,9	24,0	29,2	03.04.00	15,3	18,9	19,6	25,4	29,7
25.01.99	15,8	18,8	18,1	25,8	29,1	10.04.00	15,2	19,0	19,6	25,6	30,0
01.02.99	15,2	19,9	20,0	26,1	33,5	17.04.00	14,7	18,3	19,4	25,9	28,8
08.02.99	15,6	19,0	19,6	24,6	28,5	25.04.00	14,2	17,6	18,4	25,6	27,6
16.02.99	14,1	18,0	18,9	23,7	27,4	02.05.00	13,8	17,0	17,3	24,8	26,9
22.02.99	15,0	19,1	19,0	24,1	24,8	08.05.00	13,6	17,7	16,2	22,7	25,5
01.03.99	13,7	19,3	20,6	27,3	33,2	15.05.00	12,7	16,0	15,1	21,4	24,3
08.03.99	15,5	19,9	20,6	26,0	31,7	22.05.00	12,7	15,6	15,8	22,0	21,7
15.03.99	15,7	19,8	21,8	28,0	32,4	29.05.00	13,1	15,8	15,3	22,8	24,7
22.03.99	14,3	18,9	20,5	23,6	27,9	05.06.00	13,1	14,7	14,6	21,6	23,4
29.03.99	15,9	19,8	21,7	29,7	33,9	12.06.00	12,2	14,0	13,7	21,6	23,8
05.04.99	15,1	18,8	20,8	28,2	31,7	19.06.00	11,9	13,4	13,0	21,3	23,2
12.04.99	15,5	19,3	21,1	27,1	30,9	26.06.00	11,8	13,6	13,4	21,9	23,4
19.04.99	16,0	20,1	22,1	28,4	35,4	03.07.00	11,9	13,0	13,3	21,2	22,1
26.04.99	15,7	19,2	21,8	28,7	33,2	10.07.00	14,0	15,4	15,1	27,0	23,1
03.05.99	15,0	18,3	20,2	27,9	30,8	17.07.00	14,3	16,8	17,1	22,6	29,0
10.05.99	12,9	15,4	16,8	24,0	26,9	24.07.00	13,7	15,8	15,5	17,9	20,0
17.05.99	12,6	14,1	16,0	23,1	27,2	31.07.00	14,2	16,8	17,9	20,6	28,5
25.05.99	12,1	13,8	15,3	21,7	25,6	07.08.00	14,2		18,3	21,8	29,1
01.06.99	12,2	13,5	14,7	22,0	24,9	14.08.00	13,6		17,0	21,1	27,5
07.06.99	12,2	14,1	14,4	22,2	24,8	21.08.00	13,4		16,5	23,6	24,4
14.06.99	11,8	13,6	13,6	21,2	24,6	28.08.00	14,1	15,6	17,3	24,6	25,1
21.06.99	12,4	14,0	14,9	22,5	25,2	04.09.00	14,5	14,1	16,9	20,0	22,9
28.06.99	12,0	13,3	14,5	21,9	24,2	11.09.00	14,1	15,8	18,2	21,5	27,5
05.07.99	11,7	12,8	14,3	22,5	24,6	18.09.00	13,0	14,2	16,3	21,7	24,8
12.07.99	11,1	12,4	15,5	21,5	23,1	25.09.00	13,3	14,8	17,1	20,5	26,7
20.07.99	8,5	11,7	16,1	20,8	21,5	02.10.00	13,6	15,5	17,8	19,9	28,0
26.07.99	10,8	11,6	15,4	21,3	22,9	09.10.00	13,7	15,1	17,0	19,5	25,8
02.08.99	10,4	11,6	11,6	21,0	22,7	16.10.00	14,0	15,1	17,1	20,4	26,7
09.08.99	10,2	11,0	11,5	20,6	21,5	23.10.00	13,4	14,8	16,3	20,5	25,6
16.08.99	12,9	11,2	15,6	30,3	24,9	30.10.00	14,7	16,0	16,8	20,1	24,9
23.08.99	11,1	12,6	12,8	25,1	25,4	06.11.00	14,3	15,9	17,3	21,0	26,7
30.08.99	10,7	12,6	11,7	23,1	24,3	13.11.00	13,6	15,1	17,1	20,9	25,2
06.09.99	10,4	11,5	11,4	23,1	23,6	20.11.00	13,9	15,4	16,4	21,2	25,1
13.09.99	10,1	10,8	10,4	21,6	22,5	27.11.00	14,4	15,7	16,7	21,0	24,1
20.09.99	10,0	10,5	11,7	21,3	22,5	04.12.00	15,0	16,4	17,3	21,2	26,7
27.09.99	10,6	9,9	10,7	23,7	21,9	11.12.00	14,8	16,3	17,6	20,3	24,0
04.10.99	15,4	10,2	16,5	29,7	23,9	18.12.00	14,8	18,6	18,2	20,8	28,4
11.10.99	17,4	13,9	16,2	29,2	27,3	25.12.00	14,3	16,7	17,6	21,1	26,7
18.10.99	13,6	14,6	13,2	25,0	26,4	01.01.01	14,9	17,2	17,5	20,2	25,0

Tab. 27: Weekly measured dissolved phosphate concentrations [$\mu\text{g/l}$].

	B	H	Ste	Stu	Sch		B	H	Ste	Stu	Sch
10.08.98	34	15	34	194	176	25.10.99	83	20	92	42	118
17.08.98	28	41	31	128	186	02.11.99	52	18	152	97	105
24.08.98	28	23	49	167	169	08.11.99	66	49	39	18	57
31.08.98	4	8	2	84	124	15.11.99	76	35	44	38	51
07.09.98	6	l.a.m.	8	105	113	22.11.99	44	29	39	36	62
14.09.98	l.a.m.	l.a.m.	5	80	86	29.11.99	59	41	64	71	65
21.09.98	l.a.m.	l.a.m.	l.a.m.	46	137	06.12.99	84	48	64	72	97
28.09.98	l.a.m.	l.a.m.	l.a.m.	28	53	13.12.99	140	30	63	114	97
05.10.98	18	9	16	82	105	20.12.99	57	25	62	91	118
12.10.98	14	1	13	92	88	29.12.99	45	l.a.m.	33	79	93
19.10.98	13	l.a.m.	11	61	64	05.01.00	23	l.a.m.	46	98	97
26.10.98	5	l.a.m.	10	66	84	10.01.00	20	l.a.m.	43	72	92
02.11.98	25	l.a.m.	7	94	171	17.01.00	57	38	59	85	106
09.11.98	146	8	111	280	330	24.01.00	26	l.a.m.	48	78	94
16.11.98	12	4	l.a.m.	100	130	31.01.00	40	l.a.m.	45	l.a.m.	104
23.11.98	l.a.m.	4	l.a.m.	77	73	07.02.00	55	24	43	73	93
30.11.98	l.a.m.	l.a.m.	l.a.m.	54	77	14.02.00	23	l.a.m.	45	84	96
07.12.98	l.a.m.	l.a.m.	l.a.m.	34	69	21.02.00	33	l.a.m.	40	88	95
14.12.98	l.a.m.	l.a.m.	l.a.m.	69	88	28.02.00	66	29	48	82	105
21.12.98	38	17	38	81	80	08.03.00	64	26	72	119	133
28.12.98	34	23	47	99	101	13.03.00	40	25	51	79	90
04.01.99	51	27	59	86	140	20.03.00	32	17	49	78	88
11.01.99	36	24	47	81	94	27.03.00	54	23	44	118	101
18.01.99	31	25	29	69	97	03.04.00	36	18	46	82	89
25.01.99	8	4	26	61	83	10.04.00	34	20	39	73	109
01.02.99	8	l.a.m.	23	63	78	17.04.00	58	25	42	71	99
08.02.99	8	3	54	88	112	25.04.00	56	31	54	74	116
16.02.99	31	18	54	93	199	02.05.00	52	25	57	98	14
22.02.99	48	17	114	118	423	08.05.00	68	22	54	80	118
01.03.99	54	25	76	89	94	15.05.00	45	32	60	112	172
08.03.99	55	51	106	135	170	22.05.00	79	35	64	99	130
15.03.99	72	20	111	70	151	29.05.00	59	57	90	135	149
22.03.99	94	20	110	171	200	05.06.00	49	59	74	149	222
29.03.99	28	12	47	82	105	12.06.00	63	38	83	188	270
05.04.99	20	14	35	77	110	19.06.00	89	55	101	184	252
12.04.99	20	12	40	76	102	26.06.00	99	59	120	200	248
19.04.99	18	12	33	79	31	03.07.00	136	l.a.m.	187	218	398
26.04.99	27	19	69	82	109	10.07.00	82	58	142	198	251
03.05.99	29	19	61	81	107	17.07.00	46	20	66	111	140
10.05.99	31	23	58	100	136	24.07.00	43	27	94	151	201
17.05.99	22	22	77	85	138	31.07.00	65	l.a.m.	54	117	148
25.05.99	47	36	76	101	148	07.08.00	33	22	74	115	158
01.06.99	46	30	90	125	185	14.08.00	36	30	64	155	184
07.06.99	44	27	80	122	163	21.08.00	46	34	96	166	240
14.06.99	66	44	28	138	163	28.08.00	45	22	77	161	217
21.06.99	81	49	120	113	220	04.09.00	36	32	75	175	202
28.06.99	37	11	61	117	160	11.09.00	30	34	69	125	169
05.07.99	22	15	76	125	169	18.09.00	51	17	58	109	169
12.07.99	117	52	114	163	215	25.09.00	18	15	41	89	108
20.07.99	62	49	122	162	268	02.10.00	35	31	36	118	120
26.07.99	70	41	125	163	218	09.10.00	43	26	49	111	130
02.08.99	76	45	141	169	243	16.10.00	21	46	69	67	128
09.08.99	72	43	139	149	195	23.10.00	33	20	46	62	105
16.08.99	61	39	110	169	221						
23.08.99	64	32	87	119	192						
30.08.99	40	35	108	141	205						
06.09.99	83	38	135	149	230						
13.09.99	59	51	145	144	202						
20.09.99	63	44	173	136	185						
27.09.99	68	29	136	118	189						
04.10.99	46	24	100	114	193						
11.10.99	43	18	102	128	175						
18.10.99	44	19	70	72	143						

Tab. 28: Weekly measured calcium concentrations [mg/l].

	B	H	Ste	Stu	Sch		B	H	Ste	Stu	Sch
10.08.98	13,9	12,0	12,0	25,5	25,4	25.10.99	8,2	8,2	16,3	22,1	22,3
17.08.98	14,0	12,1	23,5	26,9	26,6	02.11.99	11,4	8,9	16,8	11,9	18,7
24.08.98	12,8	10,6	19,3	24,3	23,9	08.11.99	10,4	7,6	14,9	27,5	18,6
31.08.98	12,8	11,2	21,9	23,8	24,4	15.11.99	10,3	7,5	14,9	22,7	21,3
07.09.98	12,8	11,0	22,2	20,0	22,1	22.11.99	10,5	8,2	14,9	18,5	19,3
14.09.98	12,9	11,0	19,4	20,0	21,2	29.11.99	9,7	8,1	16,9	17,9	23,1
21.09.98	12,5	10,9	20,9	19,8	24,3	06.12.99	8,8	5,8	11,8	15,6	15,8
28.09.98	12,7	11,2	20,3	21,2	23,4	13.12.99	7,9	7,6	24,0	16,4	20,8
05.10.98	14,1	9,9	19,2	19,3	21,2	20.12.99	8,0	8,1	13,4	16,3	20,8
12.10.98	12,3	10,1	17,2	18,0	21,0	29.12.99	10,6	8,0	10,5	14,5	14,9
19.10.98	12,5	10,3	19,6	20,3	25,9	05.01.00	10,7	4,9	10,0	20,0	12,9
26.10.98	12,6	10,5	18,6	20,1	19,8	10.01.00	6,8	5,2	9,8	16,6	26,1
02.11.98	11,7	10,3	18,0	18,9	19,5	17.01.00	8,0	4,8	15,2	16,8	18,9
09.11.98	10,2	8,9	13,1	14,5	13,6	24.01.00	7,2	6,2	10,8	11,3	22,1
16.11.98	11,6	9,8	15,8	17,9	17,1	31.01.00	9,8	8,5	18,1	19,9	16,8
23.11.98	12,4	10,8	18,3	19,4	21,7	07.02.00	13,4	10,3	20,3	21,9	23,4
30.11.98	12,2	10,6	17,0	20,0	21,3	14.02.00	13,5	10,7	21,0	21,1	25,2
07.12.98	12,2	10,7	16,6	20,6	21,5	21.02.00	12,4	9,2	19,3	19,8	22,5
14.12.98	13,6	10,7	17,4	20,6	19,5	28.02.00	12,8	11,1	20,1	23,8	23,3
21.12.98	10,0	9,5	15,4	19,0	19,0	08.03.00	11,8	10,4	18,2	19,1	15,8
28.12.98	9,1	8,3	15,7	19,0	20,2	13.03.00	10,1	10,6	19,4	12,8	17,6
04.01.99	10,9	9,6	15,1	19,8	19,2	20.03.00	12,6	10,5	19,7	17,5	24,6
11.01.99	7,7	7,2	16,9	15,9	16,7	27.03.00	11,9	10,1	17,4	20,5	19,3
18.01.99	10,6	7,0	13,0	17,0	17,0	03.04.00	10,8	9,5	19,4	20,6	21,2
25.01.99	6,1	6,6	12,7	18,3	17,6	10.04.00	12,4	10,3	20,3	21,1	25,4
01.02.99	11,6	9,8	17,3	20,7	24,0	17.04.00	12,5	10,3	20,1	22,1	25,4
08.02.99	7,8	6,5	11,0	17,0	13,0	25.04.00	12,4	10,1	18,8	22,7	25,3
16.02.99	10,5	9,3	16,1	19,4	17,2	02.05.00	12,2	9,9	19,3	22,8	24,8
22.02.99	11,4	9,8	16,1	21,9	18,1	08.05.00	12,8	9,8	19,1	22,3	25,0
01.03.99	11,8	10,3	19,2	22,7	25,9	15.05.00	12,5	10,1	18,9	22,7	26,1
08.03.99	11,5	10,4	17,0	21,2	22,8	22.05.00	12,4	9,8	18,5	23,1	23,4
15.03.99	11,3	9,4	16,4	18,9	23,3	29.05.00	12,8	7,9	19,1	23,9	24,1
22.03.99	11,8	7,3	13,8	20,6	20,9	05.06.00	13,0	9,9	18,8	23,6	25,3
29.03.99	11,8	9,3	18,4	21,3	24,8	12.06.00	13,0	10,1	18,7	24,2	26,5
05.04.99	11,3	9,2	18,2	22,0	24,8	19.06.00	13,0	10,6	22,0	27,5	24,6
12.04.99	14,4	11,6	21,6	25,4	28,1	26.06.00	12,8	11,8	22,1	27,2	28,6
19.04.99	12,0	9,2	18,8	22,2	25,9	03.07.00	12,3	12,3	20,4	25,7	24,8
26.04.99	13,9	11,4	22,5	26,9	30,9	10.07.00	13,0	11,9	21,0	26,9	26,0
03.05.99	13,0	10,3	19,8	23,2	26,5	17.07.00	12,6	11,5	20,5	22,6	27,7
10.05.99	14,3	11,6	22,9	27,4	29,8	24.07.00	14,7	9,2	19,0	21,0	20,1
17.05.99	12,6	10,1	20,0	23,6	26,7	31.07.00	13,5	11,6	13,6	23,2	24,8
25.05.99	13,1	10,4	20,3	24,3	26,6	07.08.00	18,5	11,5	18,5	24,1	27,2
01.06.99	10,6	10,0	20,8	23,9	22,4	14.08.00	15,5	11,1	20,0	23,7	26,4
07.06.99	11,6	9,7	20,0	24,4	21,4	21.08.00	22,9	9,9	20,8	24,4	21,5
14.06.99	12,3	10,9	20,5	25,4	26,8	28.08.00	15,7	11,0	23,5	27,1	24,4
21.06.99	9,8	9,0	18,5	20,4	25,6	04.09.00	15,3	8,4	22,6	23,9	22,8
28.06.99	12,5	10,3	19,6	24,3	26,4	11.09.00	13,0	8,7	16,3	23,6	29,2
05.07.99	13,3	10,9	20,6	26,8	28,2	18.09.00	16,1	12,3	22,8	25,2	24,0
12.07.99	13,5	11,3	21,4	27,0	30,0	25.09.00	15,8	12,2	23,0	24,6	24,7
20.07.99	14,2	12,3	25,3	30,8	32,7	02.10.00	15,3	9,7	20,5	19,2	24,5
26.07.99	12,6	11,0	22,1	28,8	30,6	09.10.00	14,5	10,5	20,0	22,0	22,6
02.08.99	13,2	11,2	22,1	28,9	30,6	16.10.00	15,8	10,6	19,5	23,1	26,2
09.08.99	12,1	10,5	19,8	25,8	27,0	23.10.00	16,1	10,3	17,3	23,2	26,3
16.08.99	12,6	10,9	20,8	28,1	26,3	30.10.00	15,2	10,4	16,7	21,8	23,8
23.08.99	14,6	12,4	23,7	30,5	31,2	06.11.00	11,9	10,4	20,5	22,6	26,0
30.08.99	13,5	11,1	21,7	29,4	30,9	13.11.00	14,1	10,4	18,9	23,8	26,1
06.09.99	12,9	11,2	20,8	31,4	29,1	20.11.00	13,7	10,4	20,4	24,1	25,9
13.09.99	12,9	11,1	21,0	28,9	30,1	27.11.00	13,1	10,4	20,1	23,8	25,7
20.09.99	10,6	7,3	23,5	26,0	30,5	04.12.00	11,8	9,1	19,8	22,3	23,9
27.09.99	12,2	14,5	23,6	35,2	17,5	11.12.00	13,4	10,4	19,8	21,7	23,3
04.10.99	13,3	11,1	20,4	27,3	26,6	18.12.00	13,3	9,3	19,5	21,3	23,3
11.10.99	12,0	7,8	21,5	24,6	27,9	25.12.00	9,4	10,4	19,3	21,0	24,6
18.10.99	12,9	10,7	20,7	27,9	29,2	01.01.01	13,4	11,3	19,4	19,2	22,0

Tab. 29: Weekly measured potassium concentrations [mg/l].

	B	H	Ste	Stu	Sch		B	H	Ste	Stu	Sch
10.08.98	1,2	0,8	1,4	2,1	3,6	25.10.99	0,7	0,7	1,2	3,0	5,9
17.08.98	1,0	0,8	1,2	2,1	3,3	02.11.99	2,8	1,6	5,9	5,3	6,9
24.08.98	1,9	0,9	1,8	5,0	5,2	08.11.99	1,5	0,8	2,9	4,9	4,7
31.08.98	1,3	0,9	1,3	2,6	3,5	15.11.99	1,3	0,6	1,0	2,9	2,6
07.09.98	1,8	1,0	1,4	3,2	4,7	22.11.99	1,2	0,6	1,1	2,5	2,9
14.09.98	1,7	0,9	1,4	3,0	4,8	29.11.99	0,9	0,7	1,1	2,5	2,4
21.09.98	1,5	0,8	1,3	2,2	5,2	06.12.99	0,9	0,3	1,9	2,2	2,0
28.09.98	1,5	0,9	1,4	2,2	4,1	13.12.99	1,0	0,6	1,3	3,0	3,9
05.10.98	1,8	0,9	1,6	4,6	3,9	20.12.99	0,8	0,6	0,8	2,0	3,4
12.10.98	1,6	0,8	1,3	2,9	4,3	29.12.99	1,1	0,6	1,0	3,1	2,9
19.10.98	1,5	0,8	1,3	2,4	4,0	05.01.00	1,5	0,3	0,7	2,2	2,5
26.10.98	1,3	0,8	1,2	2,7	3,8	10.01.00	0,6	0,2	0,4	1,7	2,9
02.11.98	1,3	0,9	1,2	2,9	4,5	17.01.00	0,9	0,2	0,9	1,9	3,3
09.11.98	14,2	0,7	1,6	4,5	4,6	24.01.00	0,6	0,3	0,4	1,3	2,7
16.11.98	1,2	0,6	0,9	2,7	4,0	31.01.00	0,7	0,3	0,8	2,3	2,2
23.11.98	1,0	0,5	0,8	1,9	3,8	07.02.00	1,5	0,8	1,2	4,0	3,7
30.11.98	1,0	0,4	0,8	2,4	3,5	14.02.00	2,5	1,5	2,8	6,8	3,4
07.12.98	0,8	0,4	0,7	1,9	3,3	21.02.00	1,2	0,7	1,1	2,4	5,1
14.12.98	1,1	0,5	0,9	2,5	1,9	28.02.00	1,5	0,8	1,1	3,7	3,5
21.12.98	1,0	0,7	2,2	6,0	3,6	08.03.00	1,6	0,9	2,2	2,7	7,2
28.12.98	0,9	0,8	2,1	3,5	4,8	13.03.00	1,2	0,8	1,2	3,5	2,7
04.01.99	1,6	0,8	3,2	3,4	4,2	20.03.00	1,9	0,9	1,3	2,2	3,4
11.01.99	0,7	0,6	1,4	2,0	2,8	27.03.00	1,9	1,2	1,7	2,1	4,1
18.01.99	1,1	0,5	1,5	3,0	3,1	03.04.00	1,6	0,7	1,2	14,6	3,4
25.01.99	0,6	0,4	4,5	2,9	3,7	10.04.00	1,3	0,7	1,4	2,9	3,4
01.02.99	1,2	0,7	1,2	2,5	3,5	17.04.00	1,2	0,8	1,2	2,2	3,6
08.02.99	0,8	0,6	1,8	3,4	3,9	25.04.00	1,2	0,8	1,2	2,5	4,4
16.02.99	1,6	0,9	1,7	3,9	5,1	02.05.00	1,2	0,8	1,6	2,5	3,4
22.02.99	1,2	0,7	2,6	5,4	10,0	08.05.00	1,5	0,8	1,4	2,5	3,4
01.03.99	1,5	0,9	3,9	5,6	9,5	15.05.00	1,3	0,8	1,9	2,6	4,2
08.03.99	1,6	1,1	3,0	7,6	7,9	22.05.00	1,4	0,8	1,7	4,2	4,1
15.03.99	1,4	0,9	1,4	1,9	3,8	29.05.00	1,3	0,6	1,3	3,3	3,2
22.03.99	1,7	0,7	2,1	9,2	3,7	05.06.00	1,3	0,8	1,3	4,1	3,9
29.03.99	1,5	0,9	1,9	4,5	5,9	12.06.00	1,2	0,8	1,2	2,9	3,4
05.04.99	1,2	0,8	1,1	5,0	4,7	19.06.00	1,2	0,7	1,0	2,5	3,0
12.04.99	1,2	1,2	1,3	2,9	3,8	26.06.00	0,8	0,8	1,4	2,9	3,4
19.04.99	1,2	0,8	2,3	3,8	3,7	03.07.00	0,9	0,9	1,5	4,1	4,4
26.04.99	1,3	0,9	1,3	2,4	4,1	10.07.00	1,6	0,8	1,8	5,1	4,8
03.05.99	1,2	0,7	1,9	2,4	5,6	17.07.00	1,2	0,7	1,2	2,7	3,7
10.05.99	1,2	0,7	2,2	3,6	3,7	24.07.00	1,0	0,6	1,8	4,1	4,8
17.05.99	1,1	0,8	1,1	2,0	3,4	31.07.00	1,2	0,8	1,0	2,3	3,4
25.05.99	1,3	0,8	1,2	3,3	3,1	07.08.00	1,1	0,8	1,1	2,3	3,3
01.06.99	1,0	0,8	3,4	2,2	3,4	14.08.00	1,0	0,8	1,1	2,1	2,8
07.06.99	1,1	0,8	1,1	4,6	3,1	21.08.00	1,7	0,7	1,4	4,0	3,9
14.06.99	1,0	1,0	2,7	3,7	4,8	28.08.00	2,0	0,7	1,4	4,2	4,6
21.06.99	1,0	0,8	2,5	3,0	4,4	04.09.00	1,6	0,7	1,7	3,8	4,4
28.06.99	1,0	0,7	1,2	5,0	3,6	11.09.00	1,1	0,6	0,8	2,2	3,5
05.07.99	1,6	0,9	1,3	2,6	5,2	18.09.00	1,6	0,8	1,4	3,6	3,1
12.07.99	1,1	1,1	1,8	2,3	4,3	25.09.00	2,0	0,8	1,5	2,5	3,5
20.07.99	0,9	1,0	5,8	3,8	4,3	02.10.00	1,3	0,6	1,3	2,2	3,8
26.07.99	0,7	0,7	1,3	2,1	4,9	09.10.00	1,6	0,8	0,9	2,8	3,7
02.08.99	1,2	0,8	1,6	2,0	3,4	16.10.00	1,4	0,8	1,2	2,4	3,7
09.08.99	0,8	0,8	1,2	2,0	2,9	23.10.00	1,5	0,6	1,0	2,5	3,3
16.08.99	1,0	1,0	1,4	7,5	8,9	30.10.00	1,6	0,6	1,3	2,8	3,6
23.08.99	1,1	1,0	1,2	2,7	3,7	06.11.00	1,5	0,8	1,5	2,4	2,8
30.08.99	0,9	1,0	1,4	2,9	6,4	13.11.00	1,9	1,0	1,5	3,3	3,8
06.09.99	0,9	0,9	7,5	7,5	6,2	20.11.00	1,5	0,9	1,4	2,6	3,2
13.09.99	0,9	0,8	7,0	7,0	7,6	27.11.00	1,2	0,8	1,4	2,6	3,3
20.09.99	0,9	1,1	2,2	2,2	8,5	04.12.00	1,3	0,8	1,1	2,3	3,1
27.09.99	1,5	1,2	4,1	4,1	3,1	11.12.00	1,3	0,7	1,5	2,6	3,5
04.10.99	1,6	1,1	4,0	4,0	4,3	18.12.00	1,3	0,7	1,1	2,3	3,6
11.10.99	1,5	0,6	5,3	5,3	4,1	25.12.00	0,9	0,5	1,3	2,7	3,2
18.10.99	1,1	0,7	1,1	2,9	3,8	01.01.01	1,5	1,1	1,9	2,5	3,6

Tab. 30: Weekly measured sodium concentrations [mg/l].

	B	H	Ste	Stu	Sch		B	H	Ste	Stu	Sch
10.08.98	4,1	4,2	4,0	6,5	8,3	25.10.99	2,6	3,3	4,7	7,0	7,0
17.08.98	4,3	4,3	5,8	7,2	8,2	02.11.99	3,8	3,5	5,6	4,3	6,3
24.08.98	3,9	4,2	5,2	7,3	7,8	08.11.99	3,4	3,2	4,4	7,3	6,0
31.08.98	4,4	4,4	5,6	7,4	9,8	15.11.99	3,6	2,9	4,3	7,1	6,6
07.09.98	3,4	3,7	5,1	5,3	7,1	22.11.99	3,5	3,6	4,7	6,0	7,0
14.09.98	3,1	3,7	4,9	5,4	6,8	29.11.99	2,7	3,4	5,5	5,8	6,4
21.09.98	3,2	3,5	5,1	5,4	7,1	06.12.99	2,4	2,2	3,8	5,5	5,0
28.09.98	3,5	3,9	5,2	6,0	7,4	13.12.99	1,8	2,5	4,2	5,0	5,7
05.10.98	3,9	3,5	5,6	6,1	7,3	20.12.99	1,6	2,9	3,5	4,8	7,4
12.10.98	2,9	3,1	4,6	5,3	7,2	29.12.99	2,8	3,1	2,7	4,5	5,1
19.10.98	3,0	3,1	4,7	5,4	7,9	05.01.00	3,0	1,7	3,0	5,0	4,8
26.10.98	2,8	3,0	4,4	5,4	6,9	10.01.00	1,6	1,8	2,6	5,0	7,2
02.11.98	2,6	2,9	4,2	5,1	6,6	17.01.00	2,4	1,6	4,6	5,5	6,8
09.11.98	2,5	2,9	3,9	4,6	4,0	24.01.00	1,8	2,4	2,8	3,3	6,4
16.11.98	3,2	3,5	4,6	5,2	6,5	31.01.00	1,8	2,1	3,9	4,6	4,5
23.11.98	3,3	3,7	5,0	5,4	7,5	07.02.00	3,9	4,0	5,7	6,3	7,7
30.11.98	3,4	3,8	4,9	5,9	7,4	14.02.00	4,4	4,0	5,6	5,7	9,0
07.12.98	3,3	3,5	4,6	5,8	7,4	21.02.00	3,3	3,1	5,0	5,9	7,5
14.12.98	3,3	3,7	4,6	5,6	6,9	28.02.00	4,3	4,0	5,2	7,9	7,4
21.12.98	2,8	3,8	4,5	7,5	6,2	08.03.00	4,0	3,9	5,4	5,3	11,6
28.12.98	2,5	3,3	4,6	5,2	7,0	13.03.00	3,3	3,8	5,1	4,2	5,7
04.01.99	3,3	4,0	4,6	5,6	6,7	20.03.00	4,5	4,1	5,4	5,1	7,9
11.01.99	2,2	2,9	4,7	4,3	5,4	27.03.00	4,0	3,6	4,7	5,8	6,5
18.01.99	2,9	2,6	3,9	4,9	5,6	03.04.00	4,0	3,6	5,3	5,6	6,8
25.01.99	1,9	2,5	3,6	5,0	5,6	10.04.00	4,0	4,0	5,5	5,9	7,9
01.02.99	3,3	3,6	4,9	5,8	7,9	17.04.00	3,9	4,2	5,4	7,0	8,0
08.02.99	2,3	2,7	3,3	4,8	4,7	25.04.00	4,0	4,1	5,0	7,4	8,2
16.02.99	3,6	4,0	5,2	7,0	9,6	02.05.00	3,9	3,9	5,1	6,3	7,7
22.02.99	3,3	3,8	5,0	9,9	7,3	08.05.00	4,0	3,8	5,1	6,2	7,5
01.03.99	3,9	4,1	5,5	7,5	8,5	15.05.00	4,1	3,8	5,1	6,1	7,8
08.03.99	3,9	4,8	5,9	7,5	9,1	22.05.00	4,2	3,9	5,0	6,9	7,0
15.03.99	3,7	4,2	5,5	6,0	8,3	29.05.00	4,0	3,0	5,3	6,6	7,1
22.03.99	4,3	3,4	4,4	6,2	7,6	05.06.00	4,1	3,8	5,1	6,9	7,6
29.03.99	4,2	4,2	5,6	6,9	9,2	12.06.00	4,2	4,0	5,3	6,7	7,8
05.04.99	3,9	4,3	5,7	7,2	8,8	19.06.00	4,4	3,7	5,8	6,8	6,9
12.04.99	3,9	4,3	5,7	7,0	8,5	26.06.00	4,2	4,1	5,6	7,1	8,1
19.04.99	3,7	3,9	5,6	6,3	8,5	03.07.00	4,3	4,3	5,2	6,7	7,8
26.04.99	4,1	4,4	6,1	7,0	9,2	10.07.00	4,0	4,1	5,3	8,2	8,2
03.05.99	4,3	4,3	6,0	6,7	8,8	17.07.00	3,5	3,7	5,5	5,9	8,2
10.05.99	4,3	4,4	5,9	7,1	8,8	24.07.00	4,8	3,6	6,3	6,8	7,5
17.05.99	4,6	4,8	6,4	7,4	9,6	31.07.00	3,5	3,6	3,5	5,5	7,2
25.05.99	4,2	4,0	5,2	6,0	7,4	07.08.00	3,8	3,8	4,6	5,9	8,0
01.06.99	3,2	3,6	5,6	6,5	6,6	14.08.00	4,1	3,6	5,4	5,9	7,3
07.06.99	3,8	4,3	5,2	6,1	6,2	21.08.00	4,5	3,4	5,0	7,3	6,8
14.06.99	3,8	4,6	5,4	6,9	8,2	28.08.00	4,3	3,5	5,2	7,6	8,1
21.06.99	3,5	4,1	5,2	5,2	7,0	04.09.00	4,1	2,9	5,4	6,6	6,9
28.06.99	3,9	3,9	5,1	6,5	7,2	11.09.00	3,6	3,1	3,6	6,0	8,1
05.07.99	4,6	4,5	5,8	7,3	8,3	18.09.00	4,4	3,9	5,3	6,9	7,7
12.07.99	5,1	4,9	6,2	7,1	8,4	25.09.00	4,1	3,9	5,4	5,9	7,8
20.07.99	5,1	5,0	6,9	8,3	9,4	02.10.00	3,9	3,4	5,5	4,9	8,1
26.07.99	4,2	4,1	5,4	6,8	7,5	09.10.00	4,0	4,0	5,4	5,9	7,1
02.08.99	4,5	4,1	5,8	6,8	7,7	16.10.00	4,2	3,6	5,4	6,2	8,4
09.08.99	4,2	4,0	5,2	6,5	7,2	23.10.00	4,2	3,6	4,5	6,3	8,1
16.08.99	4,5	4,9	5,7	8,7	8,4	30.10.00	3,9	3,4	4,3	5,8	7,3
23.08.99	4,8	4,8	6,1	8,2	8,6	06.11.00	3,4	3,5	5,5	6,2	8,0
30.08.99	5,4	5,3	6,8	8,9	9,6	13.11.00	3,9	3,5	5,0	6,5	7,8
06.09.99	4,7	4,7	5,9	9,9	8,5	20.11.00	4,0	4,0	5,6	6,6	8,0
13.09.99	5,3	5,1	6,8	9,0	9,6	27.11.00	3,5	3,9	5,5	6,5	7,8
20.09.99	4,1	9,5	8,1	15,0	11,0	04.12.00	3,3	3,4	5,5	5,9	7,1
27.09.99	10,4	8,6	7,6	13,1	11,0	11.12.00	3,5	3,6	5,3	5,8	7,3
04.10.99	4,8	5,2	5,9	8,6	8,3	18.12.00	3,6	3,0	5,1	5,5	7,6
11.10.99	4,7	5,6	9,3	13,3	8,5	25.12.00	2,5	4,0	5,4	5,9	7,8
18.10.99	4,7	4,6	5,9	8,3	8,5	01.01.01	3,4	4,3	5,3	5,4	7,3

Tab. 31: Weekly measured magnesium concentrations [mg/l].

	B	H	Ste	Stu	Sch		B	H	Ste	Stu	Sch
10.08.98	4,7	4,7	6,5	5,9	7,0	25.10.99	3,5	4,2	5,5	6,5	6,8
17.08.98	4,8	4,5	6,0	6,7	7,0	02.11.99	4,8	4,6	5,5	3,3	5,9
24.08.98	4,3	4,4	5,7	6,0	6,5	08.11.99	3,7	3,9	5,2	6,4	5,9
31.08.98	4,8	4,7	6,5	6,2	7,5	15.11.99	4,0	3,8	5,4	6,6	7,0
07.09.98	4,1	4,2	6,5	5,2	6,5	22.11.99	4,2	4,1	5,5	5,6	6,2
14.09.98	4,0	4,1	5,8	4,8	6,1	29.11.99	3,5	4,0	5,8	5,4	5,7
21.09.98	4,2	4,1	6,2	4,8	6,6	06.12.99	3,3	2,8	4,3	4,5	4,9
28.09.98	4,5	4,3	6,1	5,4	6,5	13.12.99	2,7	3,4	5,3	4,4	5,0
05.10.98	4,9	4,3	6,2	5,2	6,2	20.12.99	2,9	3,6	4,7	4,4	6,4
12.10.98	4,0	4,0	5,7	4,7	6,1	29.12.99	3,8	3,5	3,7	3,9	4,5
19.10.98	4,1	4,1	6,0	5,2	6,9	05.01.00	3,7	2,3	3,6	4,1	4,2
26.10.98	4,1	4,1	5,7	5,1	5,8	10.01.00	2,6	2,5	3,5	4,6	6,2
02.11.98	3,8	4,0	5,4	4,7	5,5	17.01.00	3,2	2,3	5,5	4,9	5,8
09.11.98	2,7	3,5	4,2	3,6	3,0	24.01.00	2,9	2,9	4,1	3,3	5,5
16.11.98	3,9	3,9	5,0	4,4	5,0	31.01.00	2,8	3,0	5,2	4,2	4,3
23.11.98	4,4	4,4	5,4	4,8	6,4	07.02.00	3,1	3,0	4,4	3,8	4,1
30.11.98	4,2	4,2	5,3	5,0	6,1	14.02.00	3,1	2,9	4,5	3,5	4,9
07.12.98	4,3	4,1	5,0	5,3	6,3	21.02.00	2,8	2,5	4,3	3,4	4,3
14.12.98	4,2	4,2	5,0	4,8	5,5	28.02.00	3,0	3,0	4,5	4,7	4,4
21.12.98	3,5	3,9	4,6	4,7	5,0	08.03.00	2,4	2,8	4,1	3,2	3,1
28.12.98	3,2	4,4	4,9	4,3	5,2	13.03.00	2,5	2,9	4,3	2,0	3,4
04.01.99	3,4	4,0	4,5	4,4	4,8	20.03.00	3,0	2,9	4,5	3,0	4,8
11.01.99	2,8	3,1	5,1	3,7	4,5	27.03.00	2,6	2,8	4,1	3,5	3,7
18.01.99	3,5	3,1	4,1	4,1	4,6	03.04.00	2,5	2,7	4,4	3,1	4,2
25.01.99	2,3	2,9	4,0	4,5	4,8	10.04.00	3,1	3,1	4,5	3,6	4,9
01.02.99	4,0	4,2	5,3	5,0	6,4	17.04.00	3,1	3,0	4,5	3,8	4,9
08.02.99	2,6	2,7	3,5	3,8	3,6	25.04.00	3,2	3,2	4,2	3,9	5,0
16.02.99	3,5	3,7	4,6	4,2	4,0	02.05.00	4,2	4,0	5,2	5,3	6,2
22.02.99	3,4	3,7	4,5	4,2	4,1	08.05.00	4,1	3,9	5,2	5,2	6,3
01.03.99	3,3	3,8	5,2	4,6	6,1	15.05.00	4,2	4,0	5,2	5,3	6,4
08.03.99	3,6	4,3	5,1	4,8	6,0	22.05.00	4,1	3,9	5,1	5,1	5,6
15.03.99	3,9	3,9	4,8	4,5	5,7	29.05.00	3,9	3,2	5,2	5,4	5,9
22.03.99	3,8	3,2	4,4	4,4	5,3	05.06.00	4,0	3,9	5,1	5,4	6,2
29.03.99	4,0	4,0	5,4	5,0	6,3	12.06.00	4,0	4,0	5,2	5,6	6,4
05.04.99	4,3	4,4	6,1	5,7	6,9	19.06.00	4,1	3,8	5,6	5,8	5,7
12.04.99	4,4	4,3	6,1	5,3	6,6	26.06.00	4,1	4,3	5,7	5,8	6,5
19.04.99	4,2	4,1	5,7	5,3	6,8	03.07.00	4,0	4,3	5,3	5,5	6,2
26.04.99	4,2	4,2	5,9	5,5	6,9	10.07.00	3,3	4,0	5,3	5,5	5,9
03.05.99	4,3	4,0	5,6	5,3	6,5	17.07.00	3,7	3,7	5,2	4,7	6,5
10.05.99	4,6	4,4	6,0	5,8	6,8	24.07.00	4,2	3,1	4,9	4,1	4,6
17.05.99	4,2	4,0	5,5	5,2	6,3	31.07.00	3,7	3,7	3,6	4,5	5,7
25.05.99	4,4	4,1	5,5	5,4	6,4	07.08.00	4,1	3,9	4,6	5,0	6,4
01.06.99	3,6	4,0	5,5	5,3	5,3	14.08.00	4,5	3,7	5,4	5,2	6,1
07.06.99	5,7	4,1	5,5	5,2	5,0	21.08.00	4,2	3,4	5,2	5,5	5,5
14.06.99	4,1	4,3	5,2	5,9	5,9	28.08.00	3,9	3,7	6,3	5,6	6,1
21.06.99	3,2	3,6	5,2	4,5	5,7	04.09.00	4,1	2,9	5,9	4,9	5,7
28.06.99	4,2	4,0	5,3	5,2	6,1	11.09.00	3,9	3,3	4,3	4,9	6,7
05.07.99	4,4	4,2	5,5	5,8	6,6	18.09.00	4,4	4,1	5,8	5,2	6,4
12.07.99	4,8	4,5	5,8	6,3	7,0	25.09.00	4,3	4,0	5,9	4,9	6,7
20.07.99	4,5	4,5	6,1	6,5	7,3	02.10.00	4,1	3,5	5,7	4,4	6,6
26.07.99	4,0	4,1	5,6	5,9	6,4	09.10.00	4,0	3,9	5,7	5,0	6,1
02.08.99	4,2	4,1	5,6	6,1	5,5	16.10.00	4,4	3,9	5,5	5,4	6,7
09.08.99	4,3	4,3	5,6	6,3	6,8	23.10.00	4,4	3,9	4,9	5,6	6,9
16.08.99	4,6	4,8	6,2	6,6	6,7	30.10.00	4,2	3,5	4,7	5,2	6,2
23.08.99	5,0	5,1	6,7	7,2	6,7	06.11.00	3,7	3,7	5,7	5,4	6,9
30.08.99	5,2	5,1	6,6	7,3	8,0	13.11.00	4,4	3,8	5,2	5,8	6,7
06.09.99	4,4	4,5	5,9	7,1	6,9	20.11.00	4,3	4,2	5,7	5,8	6,9
13.09.99	4,4	4,4	5,8	6,9	7,2	27.11.00	4,0	4,0	6,0	5,7	6,6
20.09.99	3,8	4,1	6,1	6,3	7,2	04.12.00	3,5	3,5	5,9	5,2	6,2
27.09.99	4,3	5,6	4,9	6,6	5,4	11.12.00	4,0	3,8	6,0	5,1	6,2
04.10.99	4,5	4,6	5,8	6,3	6,4	18.12.00	4,2	3,4	6,0	4,9	6,2
11.10.99	3,8	3,4	5,8	5,9	5,9	25.12.00	3,1	4,1	6,3	5,3	7,0
18.10.99	4,6	4,7	6,1	7,0	7,4	01.01.01	4,2	4,1	6,3	4,9	6,2

Tab. 32: Weekly measured suspensoid concentrations [mg/l].

	B	H	Ste	Stu	Sch		B	H	Ste	Stu	Sch
10.08.98	1,8	2,5	13,8	12,9	55,9	25.10.99	1,9	5,1	13,1	15,1	16,1
17.08.98	29,6	6,7	18,5	19,6	47,5	02.11.99	2,5	10,4	46,3	21,8	21,6
24.08.98	4,0	15,2	13,1	11,6	59,2	08.11.99	2,6	6,1	27,8	8,2	4,8
31.08.98	1,6	7,6	15,9	20,0	30,0	15.11.99	2,4	12,6	6,3	7,2	5,4
07.09.98	20,3	37,3	79,0	34,1	48,4	22.11.99	2,1	5,1	9,1	4,9	5,5
14.09.98	32,5	38,8	145,3	49,9	60,0	29.11.99	3,1	5,8	10,6	6,0	159,6
21.09.98	6,6	13,1	43,5	9,9	44,4	06.12.99	2,4	7,0	21,2	5,6	4,9
28.09.98	5,5	2,8	30,2	5,3	29,9	13.12.99	9,4	10,1	162,3	13,6	18,1
05.10.98	3,9	4,3	25,4	6,0	19,7	20.12.99	2,2	5,0	14,7	7,5	8,1
12.10.98	15,0	12,5	102,4	24,3	71,8	29.12.99	2,6	5,0	24,7	7,5	11,0
19.10.98	7,1	7,2	39,3	6,7	15,4	05.01.00	4,0	5,8	48,0	10,4	17,4
26.10.98	7,8	7,4	57,2	8,0	18,6	10.01.00	2,3	11,8	15,2	8,2	9,8
02.11.98	13,4	8,8	113,6	8,4	23,6	17.01.00	2,3	5,1	11,2	11,7	14,6
09.11.98	78,5	16,5	232,5	128,0	44,4	24.01.00	2,7	4,5	46,2	10,9	10,8
16.11.98	8,1	6,9	25,4	7,8	25,9	31.01.00	5,2	10,5	167,5	13,3	26,1
23.11.98	5,3	6,5	15,8	5,3	13,3	07.02.00	2,4	4,6	20,9	36,4	21,6
30.11.98	5,4	6,8	16,0	6,3	15,8	14.02.00	2,7	4,1	23,2	10,6	14,4
07.12.98	3,5	4,6	21,5	4,4	11,6	21.02.00	2,8	6,1	37,2	8,1	17,6
14.12.98	6,2	8,6	31,5	9,1	21,8	28.02.00	11,1	8,1	23,4	10,0	23,4
21.12.98	7,3	8,1	22,4	10,2	21,5	08.03.00	4,3	7,0	1236,5	108,6	1366,9
28.12.98	6,7	10,1	50,1	7,4	37,9	13.03.00	2,2	3,2	32,0	6,2	19,1
04.01.99	11,8	8,7	43,0	14,2	45,2	20.03.00	1,7	2,0	18,1	4,5	15,8
11.01.99	4,9	6,7	25,2	9,3	21,3	27.03.00	5,4	9,6	271,5	11,7	40,7
18.01.99	5,1	8,2	32,1	7,7	27,5	03.04.00	1,7	4,2	14,9	4,9	21,0
25.01.99	3,9	6,4	20,8	10,6	26,3	10.04.00	1,5	1,5	10,2	4,5	16,6
01.02.99	4,5	5,7	47,4	10,8	25,6	17.04.00	1,8	5,0	9,1	4,6	20,9
08.02.99	3,0	3,8	112,9	8,0	26,8	25.04.00	33,9	54,4	7,9	6,1	28,8
16.02.99	12,6	14,6	169,9	37,2	182,5	02.05.00	1,1	2,2	10,3	6,4	24,3
22.02.99	6,6	12,4		14,6	200,6	08.05.00	1,3	7,7	12,5	8,8	34,7
01.03.99	11,3	6,7	89,3	9,3	89,3	15.05.00	5,9	2,3	20,4	8,5	53,0
08.03.99	4,6	3,6	97,9	8,7	39,6	22.05.00	2,9	4,0	10,8	7,9	33,6
15.03.99	2,0	4,1	31,8	5,8	27,4	29.05.00	1,2	3,8	8,1	6,6	18,9
22.03.99	2,6	3,0	32,9	22,1	46,4	05.06.00	1,7	6,0	11,8	7,8	26,5
29.03.99	5,6	3,5	26,7	7,6	23,7	12.06.00	1,1	2,4	10,4	10,0	32,5
05.04.99	2,2	34,5	22,4	9,0	31,2	19.06.00	1,2	3,1	10,7	11,7	36,5
12.04.99	3,9	13,7	34,9	14,6	46,4	26.06.00	1,1	2,4	5,9	9,9	26,0
19.04.99	3,6	4,6	135,5	7,6	28,3	03.07.00	1,0	2,4	13,2	15,7	47,7
26.04.99	2,1	4,8	71,3	8,4	30,4	10.07.00	3,2	4,7	12,9	13,2	26,5
03.05.99	4,9	5,3	29,2	13,9	30,8	17.07.00	2,5	2,8	20,8	10,7	23,4
10.05.99	2,2	4,0	22,4	9,9	20,9	24.07.00	1,4	2,7	138,4	34,2	383,8
17.05.99	1,7	3,3	28,2	7,7	25,1	31.07.00	2,2	2,8	140,9	14,3	27,8
25.05.99	3,1	6,6	52,2	9,6	25,7	07.08.00	2,3	4,8	16,7	13,0	16,1
01.06.99	1,7	6,8	29,7	10,8	25,5	14.08.00	1,1	4,9	16,2	17,5	23,6
07.06.99	3,8	6,1	27,7	9,7	22,6	21.08.00	2,2	5,6	22,3	17,0	23,6
14.06.99	1,2	57,6	21,9	10,0	40,9	28.08.00	7,3	11,8	66,3	23,0	21,6
21.06.99	2,1	5,5	34,0	14,0	42,1	04.09.00	4,8	31,2	47,0	26,5	51,9
28.06.99	1,8	4,5	28,9	14,3	19,8	11.09.00	2,6	5,6	57,7	25,2	27,2
05.07.99	1,4	5,4	33,3	13,9	35,5	18.09.00	1,4	5,3	33,1	16,4	21,7
12.07.99	1,5	4,7	32,9	30,1	82,9	25.09.00	2,1	7,4	36,0	15,4	25,6
20.07.99	6,5	3,5	43,3	12,7	36,5	02.10.00	13,3	5,7	755,6	14,4	25,8
26.07.99	2,5	3,3	25,1	12,0	44,5	09.10.00	4,4	6,1	30,7	14,9	
02.08.99	2,0	3,3	23,8	11,6	39,1	16.10.00	2,7	5,9	17,1	11,5	25,1
09.08.99	1,3	2,5	45,3	11,8	28,4	23.10.00	2,1		11,6	9,7	11,0
16.08.99	1,9	3,7	28,9	18,7	29,2	30.10.00	5,7		14,9	5,0	6,8
23.08.99	7,2	11,8	23,8	17,2	21,3	06.11.00	2,3		7,3	4,2	3,1
30.08.99	2,1	4,4	26,9	24,1	22,7	13.11.00	2,5		5,2	5,7	3,4
06.09.99	3,2	23,8	44,0	49,6	43,2	20.11.00	2,0		5,5	6,1	9,2
13.09.99	3,3	3,5	44,9	44,6	36,5	27.11.00	2,8		6,6	5,8	3,8
20.09.99	1,4	3,7	109,3	49,3	33,1	04.12.00	3,3		8,9	6,1	5,5
27.09.99	3,2	4,7	31,7	40,1	36,6	11.12.00	6,2		18,0	10,5	8,6
04.10.99	1,6	6,8	21,4	23,5	25,4	18.12.00	5,6		25,5	7,6	9,0
11.10.99	2,1	9,3	46,4	27,8	28,2	25.12.00	2,0		22,4	9,9	10,0
18.10.99	1,6	5,7	16,4	19,1	15,1	01.01.01	10,0		159,6	16,6	14,0

11 Literature

- Abdulla, F.A. and Lettenmaier, D.P., 1997.** Development of regional parameter estimation equation for a macroscale hydrologic model. *Journal of Hydrology*, 197: 230-257.
- Anderson, M.G. and Burt, T.P., 1990a.** Process studies in hillslope hydrology: an overview. In: M.G. Anderson and T.P. Burt (Editors), *Process Studies in Hillslope Hydrology*. John Wiley & Sons, Chichester, pp. 1-8.
- Anderson, M.G. and Burt, T.P., 1990b.** Subsurface runoff. In: M.G. Anderson and T.P. Burt (Editors), *Process Studies in Hillslope Hydrology*. John Wiley & Sons, Chichester, pp. 365-400.
- Anderson, M.G. and Brooks, S.M., 1996.** Hillslope processes: research prospects. In: M.G. Anderson and S.M. Brooks (Editors), *Advances in Hillslope Processes*. John Wiley & Sons, Chichester, pp. 5-32.
- Bennett, J.P., 1974.** Conceptions of mathematical modeling of sediment yield. *Water Resources Research*, 10: 299-303.
- Beven, K., 1985.** Distributed models. In: M.G. Anderson and T.P. Burt (Editors), *Hydrological Forecasting. Landscape Systems*. John Wiley & Sons, Chichester, pp. 405-435.
- Beven, K. and Binley, A., 1992.** The future of distributed models: Model calibration and uncertainty prediction. In: K.J. Beven and I.D. Moore (Editors), *Terrain Analysis and Distributed Modelling in Hydrology. Advances in Hydrological Processes*. John Wiley & Sons, Chichester, pp. 227-246.
- Beven, K., 1995.** Linking parameters across scales: subgrid parameterizations and scale dependent hydrological models. In: J.D. Kalma and M. Sivapalan (Editors), *Scale Issues in Hydrological Modelling*. John Wiley & Sons, Chichester, pp. 265-281.
- Beven, K., 2001a.** How far can we go in distributed hydrological modelling? *Hydrology and Earth System Sciences*, 5(1): 1-12.
- Beven, K.J., 2001b.** *Rainfall - runoff modelling: The primer*. John Wiley & Sons, Chichester, 359 pp.
- Birkinshaw, S.J. and Ewen, J., 2000.** Nitrogen transformation component for SHETRAN catchment nitrate transport modelling. *Journal of Hydrology*, 230: 1-17.
- Blöschl, G. and Sivalapan, M., 1995.** Scale issues in hydrological modelling: A review. In: J.D. Kalma and M. Sivalapan (Editors), *Scale Issues in Hydrologic Modelling*. John Wiley & Sons, Chichester, pp. 9-48.
- Blöschl, G., 1996.** Scale and scaling in hydrology. *Wiener Mitteilungen Wasser - Abwasser - Gewässer*, 132 pp.
- Bogena, H. and Diekkrüger, B., 2000.** Modifizierung des Erosionsmodells OPUS zur Simulation des durch Makroporen induzierten Interflows. *Mitteilungen der deutschen bodenkundlichen Gesellschaft*, 92: 65-68.
- Bogena, H., Diekkrüger, B., Klingel, R., Jantos, K. and Thein, J., 2001.** Analyzing and modelling the solute and sediment transport in the catchment of the Wahnbach River. *Physics and Chemistry of the Earth*, (submitted).
- Bonilla, C.A., Muñoz, J. and Vauclin, M., 1999.** Opus simulation of water dynamics and nitrate transport in a field plot. *Ecological Modelling*, 122: 69-80.
- Bormann, H., 2001.** *Hochskalieren prozeßorientierter Wassertransportmodelle - Methoden und Grenzen*. Herbert Utz Verlag, München, 182 pp.

- Borstel, U., 1993.** Grünlandwirtschaft. In: H.A. Dülmen (Editor), Faustzahlen für die Landwirtschaft und Gartenbau. Landwirtschaftsverlag, Münster-Hiltrup, pp. 477-496.
- Botschek, J., 1999.** Zum Bodenerosionspotential von Oberflächen- und Zwischenabfluss. Bonner Bodenkundliche Abhandlungen, 29, Bonn, 174 pp.
- Briese, D. and Erpenbeck, C., 1986.** Landwirtschaftliche Wege im Rahmen des Boden- und Gewässerschutzes - Probleme und Lösungsmöglichkeiten. Zeitschrift für Kulturtechnik und Flurbereinigung, 27: 158-164.
- Bronstert, A., 1994.** Modellierung der Abflußbildung und der Bodenwasserdynamik von Hängen. Mittellungen des Instituts für Hydrologie und Wasserwirtschaft der Universität Karlsruhe, 192 pp.
- Bronstert, A. and Plate, E.J., 1997.** Modelling of runoff generation and soil moisture dynamics for hillslopes and micro-catchments. Journal of Hydrology, 198: 177-195.
- Brooks, R. and Corey, A., 1964.** Hydraulic properties of porous media. Hydrology Paper, 3. Colorado State University Fort Collins, 27 pp.
- Brown, M.J., 1986.** Use of stream chemistry to estimate hydrologic parameters. Water Resources Research, 22(5): 805-811.
- Bryan, R.B. and Jones, J.A.A., 1997.** The significance of soil piping processes: inventory and prospect. Geomorphology, 20: 209-218.
- Bryan, R.B., 2000.** Soil erodibility and processes of water erosion on hillslopes. Geomorphology, 32: 385-415.
- Burns, D.A. et al., 1998.** Base cation concentrations in subsurface flow from a forested hillslope: The role of flushing frequency. Water Resources Research, 34(12): 3535-3544.
- Collins, A.L., Walling, D.E. and Leeks, G.J.L., 1997.** Source type ascription for fluvial suspended sediment based on a quantitative composite fingerprinting technique. Catena, 29: 1-27.
- Cronshey, R.G. and Theurer, F.D., 1998.** AnnAgNPS - Non-point pollution loading model, Proceedings of the first Federal Interagency Hydrologic Modelling Conference, pp. 20-28.
- De Roo, A.D.J., 1993.** Modelling surface runoff and soil erosion in catchments using geographical information systems; Validity and applicability of the "ANSWERS" model in two catchments in the loess area of South Limburg (the Netherlands) and one in Devon (UK). Netherlands Geographical Studies, 157, 304 pp.
- De Wit, M. and Schmoll, O., 1999.** Emission estimates: rubbish in - rubbish out? In: N. Fohrer and P. Döll (Editors), Modellierung des Wasser- und Stofftransports in großen Einzugsgebieten. Kassel University Press, Kassel, pp. 51-58.
- Deckers, F. and Stroet, C.B.M., 1996.** Use of GIS and database with distributed modelling. In: M.B. Abbott and J.C. Refsgaard (Editors), Distributed Hydrological Modelling. Kluwer Academic, Dordrecht/Boston/London, pp. 215-232.
- DeCoursey, D.G. et al., 1992.** Root zone water quality model, version 1.0, technical documentation. USDA, Agricultural Research Service, Great Plains Systems Research Unit, Fort Collins, Colorado.
- Diekkrüger, B., Smith, R.E., Krug, D. and Baumann, R., 1992.** Validation of the model system OPUS. Catena Supplement, 19: 139-153.
- Diekkrüger, B., 1996.** SIMULAT - ein Modellsystem zur Berechnung der Wasser- und Stoffdynamik landwirtschaftlich genutzter Standorte. In: O. Richter, D. Söndgerath and B. Diekkrüger (Editors), Sonderforschungsbereich 179 "Wasser- und Stoffdynamik in Agrarökosystemen". Landschaftsökologie und Umweltforschung, pp. 30-47.
- Diekkrüger, B., 2001.** Upscaling of hydrological models by means of parameter aggregation technique. In: H.J. Neugebauer: Multiscale Geosystems and their Dynamics. Lecture

- Notes in Earth Sciences. Springer Verlag. In press.
- Erpenbeck, C., 1987.** Über Stoffaustrag mit dem Oberflächen- und Zwischenabfluss von landwirtschaftlichen Flächen verschiedener Nutzungsweise - Ein Beitrag zur Klärung der Gewässerbelastung in Mittelgebirgslagen. Ph.D. thesis, Gießen, 201 pp.
- Esteves, M., Faucher, X., Galle, S. and Vauclin, M., 2000.** Overland flow and infiltration modelling for small plots during unsteady rain: Numerical results versus observed values. *Journal of Hydrology*, 228: 265-282.
- Ewen, J. and Birkinshaw, S.J., 2000.** Modelling nitrate transport in the Slapton Wood catchment using SHETRAN. *Journal of Hydrology*, 230: 18-33.
- Favis-Mortlock, D., 1998.** A self-organizing dynamic systems approach to the simulation of rill initiation and development on hillslopes. *Computer & Geosciences*, 24(4): 353-372.
- Feddes, R.A., Menenti, M., Kabat, P. and Bastiaanssen, W.G.M., 1993.** Is large scale inverse modelling of unsaturated flow with areal average evaporation and surface soil moisture as estimated from remote sensing feasible? *Journal of Hydrology*, 143: 125-152.
- Ferreira, V.A. and Smith, R.E., 1992.** Opus: An integrated simulation model for transport of nonpoint-source pollutants at the field scale: Volume II, User Manual. USDA, Agricultural Research Service, Springfield, 200 pp.
- Flügel, W.-A. and Schwarz, O., 1988.** Beregnungsversuche zur Erzeugung von Oberflächenabfluß, Interflow und Grundwassererneuerung. *Heidelberger Geogr. Arb.*(66): 169-200.
- Flügel, W.-A. and Smith, R.E., 1999.** Integrated process studies and modelling simulations of hillslope hydrology and interflow dynamics using the HILLS model. *Environmental Modelling & Software*, 14: 153-160.
- Fohrer, N., 1995.** Auswirkungen von Bodenfeuchte, Bodenart und Oberflächenbeschaffenheit auf Prozesse der Flächenerosion. *Bodenökologie und Bodengenese*, 19. Technische Universität Berlin, Berlin, 183 pp.
- Folly, A., Quinton, J.N. and Smith, R.E., 1999.** Evaluation of the EUROSEM model using data from the Catsop watershed, the Netherlands. *Catena*, 37: 507-519.
- Foster, G.R., 1982.** Modeling the erosion process. In: C.T. Haan (Editor), *Hydrologic Modeling of Small Watersheds*, St. Joseph, Michigan, USA, pp. 297-388.
- Foster, I., Grew, R. and Dearing, J., 1990.** Magnitude and frequency of sediment transport in agricultural catchments: A paired lake-catchment study in Midland England. In: J. Boardman, I.D.L. Foster and J.A. Dearing (Editors), *Soil Erosion on Agricultural Land*. John Wiley & Sons, Chichester, pp. 153-171.
- Fürchtenich, K.J., Heyn, J., Kuhlmann, H., Laurenz, L. and Müller, S., 1993.** Pflanzenernährung und Düngung. In: H.A. Dülmen (Editor), *Faustzahlen für Landwirtschaft und Gartenbau*. Landwirtschaftsverlag, Münster-Hiltrup, pp. 254-295.
- Garbrecht, J., Starks, P.J. and Martz, L.W., 1996.** New digital landscape parameterisation methodologies, 32nd Annual Conference and Symposium on GIS and Water Resources. Fort Lauderdale, USA.
- Germann, P.F., 1990.** Macropores and hydrologic hillslope processes. In: M.G. Anderson and T.P. Burt (Editors), *Process Studies in Hillslope Hydrology*. John Wiley & Sons, Chichester, pp. 327-363.
- Giertz, S., 2000.** GIS-gestützte Modellierung des Stoffaustrags im Einzugsgebiet der Wahnbachtalsperre. Unpublished diploma thesis, Bonn.
- Gilmanov, T.G., Parton, W.J. and Ojim, D.S., 1997.** Testing the 'CENTURY' ecosystem level model on data sets from eight grassland sites in the former USSR representing a wide climatic/soil gradient. *Ecological Modelling*, 96: 191-210.
- Goodrich, D.C., Woolhiser, D.A. and Keefer, T.O., 1991.** Kinematic routing using finite elements on a triangular irregular network. *Water Resources Research*, 27: 995-1003.

- Göttlicher-Göbel, 1987.** Wasserqualität von Fließgewässern landwirtschaftlich genutzter Einzugsgebiete insbesondere bei Hochwasserwellen. Ph.D. thesis, Gießen, 262 pp.
- Grunwald, S., 1997.** GIS-gestützte Modellierung des Landschaftswasser- und Stoffhaushaltes mit dem Modell AGNPSm. Schriftenreihe zur Bodenkunde, Landeskultur und Landschaftsökologie, 14. Justus-Liebig-Universität, Gießen, 170 pp.
- Grunwald, S. and Frede, H.-G., 1999.** Using the modified agricultural non-point source pollution model in German watersheds. *Catena*, 37: 319-328.
- Haag, D. and Kaupenjohann, M., 2001.** Landscape fate of nitrate fluxes and emissions in Central Europe: A critical review of concepts, data, and models for transport and retention. *Agriculture, Ecosystems and Environment*, 86: 1-21.
- Hangen, E., Lindenlaub, M., Leibundgut, C. and von Wilpert, K., 2001.** Investigating mechanisms of stormflow generation by natural tracers and hydrometric data: A small catchment study in the Black Forest, Germany. *Hydrological Processes*, 15: 183-199.
- Hansen, S., Jensen, H.E., Nielsen, N.E. and Svendsen, H., 1993.** The soil plant system model DAISY. Simulation model for transformation and transport of energy and matter in the soil plant atmosphere system. Basic principles and modelling approach. Jordburgsforlaget. Royal Veterinary and Agricultural University, Copenhagen.
- Hartkamp, A.D., White, J.W. and Hoogenboom, G., 1999.** Interfacing geographic information systems with agronomic modeling: A review. *Agronomic Journal*, 91: 761-772.
- Hasenpusch, K., 1995.** Nährstoffeinträge und Nährstofftransport in den Vorfluter zweier landwirtschaftlich genutzter Gewässereinzugsgebiete. Wissenschaftliche Mitteilungen der Bundesforschungsanstalt für Landwirtschaft, Sonderheft 158, Braunschweig-Vökenrode, 216 pp.
- Herbst, M. and Diekkrüger, B., 2001.** Modeling the spatial variability of soil moisture in a micro-scale catchment. *Physics and Chemistry of the Earth*, submitted.
- ICWE, 1992.** The Dublin statement and report of the conference, International Conference on Water and the Environment: Development issues for the 21st century, Dublin, Ireland, pp. 26-31.
- Inam, B., 1994.** Non-linear uncertainty analysis for multiple criteria natural resource decision support system. Ph.D. thesis, Tuscon.
- Jarvis, N., 1994.** The MACRO Model (Version 3.0) - Technical description and sample simulations. Monograph, reports and dissertations, 19, Department of Soil Science, Swedish University of Agricultural Science, Uppsalla, Sweden.
- Jetten, V., De Roo, A. and Favis-Mortlock, D., 1999.** Evaluation of field-scale and catchment-scale soil erosion models. *Catena*, 37: 521-541.
- Johnes, P.J., 1999.** Understanding lake and catchment history as a tool for integrated lake management. *Hydrobiologia*, 395-396: 41-60.
- Jones, J.A.A., 1997.** The role of natural pipeflow in hillslope drainage and erosion: Extrapolating from the Maesnant data. *Physics and Chemistry of the Earth*, 22(3-4): 303-308.
- Jux, U., 1983.** Erläuterungen zu Blatt 5010 Engelskirchen. Geologisches Landesamt Nordrhein-Westfalen, Krefeld, 148 pp.
- Kasper, F. and Döll, P., 1999.** Modeling of water availability on the global scale: Influences of model structure and uncertainty of precipitation data. In: N. Fohrer and P. Döll (Editors), *Modellierung des Wasser- und Stofftransports in großen Einzugsgebieten*. Kassel University Press, Kassel, pp. 119-126.
- Kirkby, M.J., 1985.** Hillslope hydrology. In: M.G. Anderson and T.P. Burt (Editors), *Hydrological Forecasting. Landscape Systems*. John Wiley & Sons, Chichester, pp. 37-75.

- Kirkby, M., 1988.** Hillslope runoff processes and models. *Journal of Hydrology*, 100: 315-339.
- Klingel, R., Krämer, R., Stoffels, M. and Thein, J., 1997.** Hydrogeochemisches Monitoring im Trinkwasserschutz dargestellt am Einzugsgebiet der Wahnbachtalsperre. *Zeitschrift der deutschen geologischen Gesellschaft*, 148(3-4): 357-367.
- Krämer, R., 2000.** Personal communication.
- Kresser, W., 1964.** Gedanken zur Geschiebe- und Schwebstoffführung der Gewässer. *Österr. Wasserwirtschaft*, 16: 6-11.
- Krysanova, V., Müller-Wohlfeil, D.-I. and Becker, A., 1998.** Development and test of a spatially distributed hydrological/water quality model for mesoscale watersheds. *Ecological Modelling*, 106: 261-289.
- Lamers, M., 2001.** Analyse und Simulation des fluvialen Feststofftransports im Wendbach (Einzugsgebiet Wahnbachtalsperre). Unpublished diploma thesis, Bonn, 118 pp.
- Lane, L.J. and Nearing, M.A., 1989.** USDA - Water erosion prediction project: Hillslope profile model documentation. 2, NSERL, West Lafayette, USA.
- Lane, L.J., Hernandez, M. and Nichols, M., 1997a.** Processes controlling sediment yield from watersheds as functions of spatial scale. *Environmental Modelling & Software*, 12: 355-369.
- Lane, L.J., Nichols, M.H. and Paige, G.B., 1997b.** Modeling erosion on hillslopes: Concepts, theory and data. United States Department of Agriculture.
- Lange, H., 1998.** Are ecosystems dynamical systems? *International Journal Comput. Anticip. System*, 3: 169-186.
- Luxmoore, R.J. and Ferrand, L.A., 1993.** Towards pore-scale analysis of preferential flow and chemical transport. In: D. Russo and G. Dagan (Editors), *Water Flow and Solute Transport in Soils*. Springer Verlag, New York, pp. 45-60.
- Lützen, J., 1999.** Prognose des Stoffaustrags aus dem Einzugsgebiet der Wahnbachtalsperre mit dem Modellsystem AGNPS und dem geographischen Informationssystem ARC/INFO. Unpublished diploma thesis, Bonn.
- Ma, Q.L., Hook, J.E. and Wauchope, R.D., 1999.** Evapotranspiration predictions: A comparison among GLEAMS, Opus, PRZM-2, and RZWQM models in a humid and thermic climate. *Agricultural Systems*, 59: 41-55.
- Martin, W., 1988.** Die Erodierbarkeit von Böden unter simulierten und natürlichen Regen und ihre Abhängigkeit von Bodeneigenschaften, Technische Universität München, München.
- Matheron, G., 1963.** Principles of geostatistic. *Economic Geology and the Bulletin of the Society of Economic Geologists*, 58: 1246-1266.
- McCuen, R.H. and Snyder, W.M., 1975.** A proposed index for comparing hydrographs. *Water Resources Research*, 11(6): 1021-1024.
- McDonnell, J.J., 1990.** A rationale for old water discharge through macropores in a steep, humid catchment. *Water Resources Research*, 26(11): 2821-2832.
- Merz, B. and Bárdossy, A., 1998.** Effects of spatial variability on the rainfall runoff process in a small loess catchment. *Journal of Hydrology*, 212-213: 304-317.
- Merz, B. and Bárdossy, A., 1998.** Effects of spatial variability on the rainfall runoff process in a small loess catchment. *Journal of Hydrology*, 212: 304-317.
- Mollenhauer, K. and Wohlrab, B., 1990.** Strategien zur Reduzierung des bodennutzungsbedingten Stoffeintrags in Trinkwassertalsperren. LWA Schriftenreihe, 46. Landesamt für Wasser und Abfall Nordrhein-Westfalen, Düsseldorf, 24 pp.
- Morgan, R.P.C., 1999.** Bodenerosion und Bodenerhaltung. Enke, Stuttgart, 236 pp.
- Nash, J.E. and Sutcliffe, J.V., 1970.** River flow forecasting through conceptual models: Part I - A discussion of principles. *Journal of Hydrology*, 10: 282-290.

- Nearing, M.A. et al., 1997.** Hydraulics and erosion in eroding hills. *Water Resources Research*, 33(4): 865-876.
- Nicke, H., 1989.** Siefen - Geomorphologische Untersuchungen an einer Sonderform der Talanfänge im Bergischen Land. *Decheniana*, 142: 147-156.
- Panagoulia, D. and Dimou, G., 1997.** Linking space-time scale in hydrological modelling with respect to global climate change Part 1. Models, model properties, and experimental design. *Journal of Hydrology*, 194: 15-37.
- Parton, W.J., Mosier, A.R. and Schimel, D.S., 1988.** Rates and pathways of nitrous oxide production in a shortgrass steppe. *Biogeochemistry*, 6: 45-58.
- Peter, M., 1988.** Zum Einfluss der Abflußkomponenten Q_O , Q_I und Q_G auf den Stofftransport von Wasserläufen aus Einzugsgebieten verschiedener Bodennutzung in Mittelgebirgen mit speziellen hydromorphologischen Verhältnissen, Gießen, 333 pp.
- Refsgaard, J.C. and Abbott, M.B., 1996.** The role of distributed hydrological modelling in water resources. In: M.B. Abbott and J.C. Refsgaard (Editors), *Distributed Hydrological Modelling*. Kluwer Academic, Dordrecht/Boston/London, pp. 1-16.
- Refsgaard, J.C. and Storm, B., 1996.** Construction, calibration and validation of hydrological models. In: M.B. Abbott and J.C. Refsgaard (Editors), *Distributed Hydrological Modelling*. Kluwer Academic, Dordrecht/Boston/London, pp. 41-54.
- Reid, M.R. and Dunne, T., 1996.** Rapid evaluation of sediment budgets. *Catena Verlag*, Reiskirchen, 164 pp.
- Renschler, C.S., Mannaerts, C. and Diekkrüger, B., 1999.** Evaluating spatial and temporal variability in soil erosion risk - rainfall erosivity and soil loss ratios in Andalusia, Spain. *Catena*, 34: 209-225.
- Renschler, C.S., 2000.** Strategies for implementing natural resource management tools - A geographical information science perspective on water and sediment balance assessment at different scales. Ph.D. thesis, University of Bonn, Bonn, 182 pp. Unpublished.
- Richardson, C.W. and Wright, D.A., 1984.** WGEN: A model for generating daily weather variables. USDA, Agricultural Research Service, 83 pp.
- Rijtema, P.E., Roest, C.W.J. and Kroes, J.G., 1991.** Formulation of the nitrogen and phosphate behaviour in agricultural soils, the ANIMO model. 30, DLO Winand Staring Centre, Wageningen, the Netherlands.
- Ritchie, J.T., 1972.** A model for predicting evaporation from a row crop with incomplete cover. *Water Resources Research*, 8: 182-190.
- Robertson, D.M. and Roerish, E.D., 1999.** Influence of various water quality sampling strategies on load estimates for small streams. *Water Resources Research*, 35(12): 3747-3759.
- Salles, C. and Poesen, J., 2000.** Rain properties controlling soil splash detachment. *Hydrological Processes*, 14: 271-282.
- Schachtschabel, P., Blume, H.-P., Brümmer, G., Hartge, K.H. and Schwertmann, U., 1998.** *Lehrbuch der Bodenkunde*. Springer Verlag, Stuttgart, 494 pp.
- Schaub, D. and Rolli, S., 1998.** Bodenerosion kann man berechnen, *Uni Nova - Wissenschaftsmagazin der Universität Basel*, pp. 15-17.
- Schmidt, F., 1993.** Voraussetzungen, Möglichkeiten und Grenzen von Modell-Validierungen anhand empirischer Meßwerte. Expert-N und Wachstumsmodelle. Referat des Anwendungsseminars im März 1993 in Weihenstephan. *Agrarinformatik*, 24. Ulmer Verlag, Stuttgart.
- Schmidt, J., von Werner, M. and Michael, A., 1999.** Application of the EROSION 3D model to the CATSOP watershed, The Netherlands. *Catena*, 37: 449-456.
- Schultz, K., Beven, K. and Bernd, H., 1999.** Equifinality and the problem of robust calibration in nitrogen budget simulations. *Soil Science Society of America Journal*, 63:

1934-1941.

- Schumm, S.A., 1999.** Causes and controls of channel incision. In: S.E. Darby and A. Simon (Editors), *Incised River Channels*. John Wiley & Sons, Chichester, pp. 19-31.
- Schwarze, R., 1999.** Skalenwechsel über Parameter: Grundwasser. In: H.-B. Kleeberg, W. Mauser, G. Peschke and U. Streit (Editors), *Hydrologie und Regionalisierung - Ergebnisse eines Schwerpunktprogrammes (1992-1998)*. DFG-Forschungsbericht. VCH-Wiley, pp. 78-98.
- Schwertmann, U., Vogle, W. and Kainz, M., 1987.** Bodenerosion durch Wasser: Vorhersage des Abtrags und Bewertung von Gegenmaßnahmen. Ulmer, Stuttgart, 64 pp.
- Seibert, J. and McDonell, J., 2001.** Towards a better process representation of catchment hydrology in conceptual runoff modelling., Proc. Int. Workshop on Runoff Generation and Implications for River Basin Modelling.
- Sivapalan, M. and Woods, R.A., 1995.** Scale issues in hydrological modelling: A review. In: J.D. Kalma and M. Sivalapan (Editors), *Scale Issues in Hydrologic Modelling*. John Wiley & Sons, Chichester, pp. 453-473.
- Sklash, M.G., 1990.** Environmental isotope studies of storm and snowmelt runoff generation. In: M.G. Anderson and R.P. Burt (Editors), *Process Studies in Hillslope Hydrology*. John Wiley & Sons, Chichester, pp. 401-435.
- Slutsky, A.H. and Yen, B.C., 1997.** A macro-scale natural hydrologic cycle water availability model. *Journal of Hydrology*, 201: 329-347.
- Smith, R.E. and Parlange, J.-Y., 1978.** A parameter-efficient hydrologic infiltration model. *Water Resources Research*, 14: 533-538.
- Smith, R.E., 1992.** Opus: An integrated simulation model for transport of nonpoint-source pollutants at the field scale: Volume I, Documentation, 1. USDA, Agricultural Research Service, Springfield, 120 pp.
- Smith, R.E., 1995.** Opus simulation of a wheat/sugarbeet plot near Neuenkirchen, Germany. *Ecological Modelling*, 81: 121-132.
- Smith, R.E., Goodrich, D.C. and Unkrich, C.L., 1999.** Simulation of selected events on the Catsop catchment by KINEROS2 - A report for the GCTE conference on catchment scale erosion models. *Catena*, 37: 457-475.
- Sparks, D.L., 1995.** *Environmental soil chemistry*. Academic Press, San Diego, 267 pp.
- Steffen, D., 2001.** Messung und Modellierung der Erosion an einem landwirtschaftlich genutzten Hang im Einzugsgebiet der Wahnbachtalsperre. Unpublished diploma thesis, Bonn, 108 pp.
- Tani, M., 1998.** A concept for runoff processes on a steep forested hillslope. In: K. Sassa (Editor), *Environmental Forest Science*. Forestry Sciences. Kluwer Academic Publishers, Dordrecht, pp. 455-462.
- Thieken, A.H., Lücke, A. and Diekrüger, B., 1997.** Einfluß von Datenqualität und DHM-Analysen auf die Ergebnisse eines Oberflächenabflußmodells, Salzburger geographische Materialien, pp. 153-162.
- Thorsen, M., Feyen, J. and Styczen, M., 1996.** Agrochemical modelling. In: M.B. Abbott and J.C. Refsgaard (Editors), *Distributed Hydrological Modelling*. Kluwer Academic, Dordrecht/Boston/London, pp. 121-142.
- Tim, U.S., 1996.** Coupling vadose zone models with GIS: Emerging trends and potential bottlenecks. *Journal of Environmental Quality*, 25: 535-544.
- Trudgill, S., Ball, J. and Rawlins, B., 1996.** Modeling the solute uptake component of hillslope hydrochemistry: Are flow times and path lengths important during mineral dissolution. In: M.G. Anderson and S.M. Brooks (Editors), *Advances in Hillslope Processes*. John Wiley & Sons, Chichester, pp. 295-324.
- Uhrich, S.L., 1999.** Analyse und Simulation des Stofftransports im Boden im Einzugsgebiet

- der Wahnbachtalsperre. Unpublished diploma thesis, Bonn, 118 pp.
- USACE, 1991.** HEC-6, a one-dimensional model for scour and deposition in rivers and reservoirs. User's manual. Hydrologic Engineering Center, Davis, 163 pp.
- USDA-SCS, 1972.** National engineering handbook, section 4, hydrology. USDA, Soil Conservation Service, 593 pp.
- Vanclooster, M., Viaene, J. and Christians, K., 1994.** WAVE- a mathematical model for simulating agrochemicals in the soil vadose environment. Reference and user's manual (release 2.0). Katholieke Universiteit Leuven, Belgium.
- von Kamp, H., 1983.** Hydrologie. In: U. Jux (Editor), Erläuterungen zu Blatt 5010 Engelskirchen. Geologisches Landesamt Nordrhein-Westfalen, Krefeld, pp. 113-125.
- Walling, D.E., 1990.** Linking the field to the river: Sediment delivery from agricultural land. In: J. Boardman, I.D.L. Foster and J.A. Dearing (Editors), Soil Erosion on Agricultural Land. Symposia Series. John Wiley & Sons, Chichester, pp. 129-152.
- Walther, W., 1999.** Diffuser Stoffeintrag in Gewässer. Teubner-Reihe Umwelt, Stuttgart, 310 pp.
- Whelan, M.J., Kirkby, M.J. and Burt, T.P., 1995.** Predicting nitrate concentrations in a small catchment. In: S.T. Trudgill (Editor), Solute Modelling in Catchment Systems. John Wiley & Sons, Chichester, pp. 165-192.
- Williams, J.R., 1975.** Sediment yield prediction with universal equation using runoff energy factor. ARS-S-40. USDA, Agricultural Research Service, pp. 244-252.
- Willmott, C.J., 1981.** On the validation of models. *Physical Geography*, 2: 184-194.
- Wischmeier, W., 1984.** The USLE - some reflections. *Journal of Soil and Water Conservation*, 39: 105-107.
- Wohlrab, B., Ernstberger, H., Meuser, A. and Sokollek, V., 1992.** Landschaftswasserhaushalt, Verlag Paul Parey Hamburg, 352 pp.
- Woods, R.A., Sivapalan, M. and Duncan, M., 1995.** Investigating the representative elementary area concept: An approach based on field data. In: J.D. Kalma and M. Sivalapan (Editors), Scale issues in hydrologic modelling. John Wiley & Sons, Chichester, pp. 49-70.